

FLOW AND TRANSPORT IN WETLAND DEPOSITS

By
Lana A. Aref

B.S. in Civil Engineering, 1993
Georgia Institute of Technology

Submitted to the Department of Civil and Environmental Engineering
In Partial Fulfillment of the Requirements for the Degree of

Doctor of Science in Civil and Environmental Engineering

At the
Massachusetts Institute of Technology

May, 1999
[June 1999]

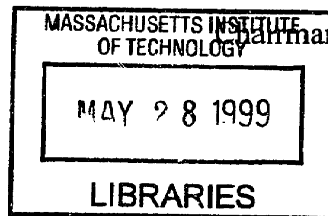
Copyright © Massachusetts Institute of Technology, 1999. All rights reserved.

Signature of Author _____
Department of Civil and Environmental Engineering
May 7, 1999

Certified by _____
Dr. Patricia J. Culligan, Thesis Advisor
Associate Professor, Department of Civil and Environmental Engineering

Certified by _____
Dr. John T. Germaine, Thesis Co-Advisor
Principal Research Associate, Department of Civil and Environmental Engineering

Accepted by _____
Professor Andrew Whittle
Chairman, Departmental Committee on Graduate Studies



ARCHIVES

FLOW AND TRANSPORT IN WETLAND DEPOSITS

By Lana A. Aref

Submitted to the Department Of Civil and Environmental Engineering on May 7th, 1999
In Partial Fulfillment of the Requirements for the Degree of
Doctor of Science in Civil and Environmental Engineering

Abstract

At present, very little is known about the mechanisms that control flow and transport through wetland deposits. Therefore, the objective of this research was to investigate the factors that influenced flow in wetland soils. To accomplish this, Column Experiments, run on a specialized permeameter, were conducted on both re-sedimented and undisturbed wetland soil specimens. During these experiments, sodium chloride (NaCl) tracer was injected into the soil specimen, and its breakthrough was monitored concurrently with other parameters, such as flow velocity and hydraulic gradient. Subsequently, the breakthrough data collected during the Column Experiments were fit using both the One-Region and Two-Region transport models, and the fit results were analyzed and compared to the geotechnical data collected for the soil.

The data collected during the experimental program indicate enormous complexity in the mechanisms controlling flow and transport through wetland soils. From their analysis the following observations were made: First, even though wetland soils are considered to be two-region soils, having both an effective and an immobile porosity, the One-Region model was able to describe Sodium Chloride breakthrough in the soil. This indicates that the NaCl tracer was not interacting with the immobile region of the specimen. Second, the results demonstrated that wetland soil hydraulic conductivity is highly variable and sensitive to volume of flow. In fact, hydraulic conductivity was seen to decrease irreversibly by up to 6% per pore volume of flow. It was also found that hydraulic conductivity was sensitive to increases in pore water salt concentration, and to the flushing out of salts from wetland specimens. Finally, it was observed that, for the most part, large changes in hydraulic conductivity did not correspond to changes in the specimen's effective pore size or pore distribution. In fact, unless salt concentrations were increased drastically, the effective pore space remained invariant over an order of magnitude change in soil hydraulic conductivity. This suggests that changes in soil hydraulic conductivity might be due to increases or decreases in the number of flow channel constrictions in a specimen. From the results of this research it is hypothesized that the number of flow channel constrictions increased when flow and a decrease in salt concentration mobilized organic and mineral particles, which collected and clogged narrow pore throats along the flow channels. It is also hypothesized that the number of flow channel constrictions decreased when increases in pore water salt concentration caused organic fibers along the flow channel walls to coil.

Advisor: Dr. P. J. Culligan

Title: Associate Professor, Department of Civil and Environmental Engineering

Co-advisor: Dr. J. T. Germaine

Title: Principal Research Associate, Department of Civil and Environmental Engineering

ACKNOWLEDGMENTS

Thanks to Professor Culligan, my advisor, for her generous support and input, for her faith in me, for her time, and for being an advisor who cares so much about her students.

Thanks to Dr. Germaine, my co-advisor, for his enthusiastic input and for his sense of humor no matter the circumstance (or disaster).

Thanks to Professors Harvey, Hemond and Ladd, members of my thesis committee, for their interest, time, and valuable contributions.

Thanks to Professor Einstein for his continuous support throughout my stay at MIT, and to Professor Kausel for his help in compiling and setting up my Fortran programs.

Thanks to Alise Kalemekiarian, Mary Elliff, and Carolyn Jundzilo-Comer for their administrative as well as emotional support.

Thanks to my Undergraduate Assistants: Yasmin Rehmanjee, Michelle Evans, and Sylwia Daniszewska for doing so much leg work for this project.

Thanks to Kurt Sjoblom, Laurent Levy, and Doug Cauble my office-mates, past and present, for being generous colleagues and good friends.

Thanks to Erin Wood, Brad Ramsay, Greg Da Re, and Joe Sinfield for their helpfulness in the laboratory. Also, thanks to the rest of the geotechs/dirtballs/labrats for creating a friendly and supportive environment inside and outside of the lab.

Thanks to several people in the Parsons laboratory who helped me with equipment, as well as with Aberjona, and chemistry questions: John Mac Farlane, Chris Schwartz, Dan Brabander, and Jim Gawel.

Thanks to all my friends for sharing in good conversation, laughter, and sympathy throughout my stay, with special thanks to Maya Farhoud, Lisa Moore, Gabrielle Rocap, Cristina Gouveia, and Alejandro Colom. Extra-special thanks to Liz Mann who has been a sister to me.

Thanks to my Mom, Dad, to my brothers, Molham and Karim, and to my extended family for so much support, love, and for never expecting less than my very best.

This project was made possible by the National Institute of Health Sciences, NIH Grant Number P42-ES04675

TABLE OF CONTENTS

1. INTRODUCTION	23
1.1 THE ABERJONA WATERSHED	23
1.2 GOALS AND SCOPE OF THIS RESEARCH	25
1.3 THESIS ORGANIZATION	26
1.4 REFERENCES	27
2. BACKGROUND ON WETLAND SOILS	33
2.1 WETLANDS AND WETLAND DEPOSITS	33
2.1.1 CLASSIFICATION OF WETLAND SOILS	34
2.1.2 INDEX AND COMPRESSIBILITY PROPERTIES OF WETLAND SOILS	36
2.1.3 HYDRAULIC CONDUCTIVITY OF WETLAND SOILS	36
2.1.3.1 Vertical vs. horizontal Hydraulic Conductivity, k	37
2.1.3.2 k vs. Degree of Humification	38
2.1.3.3 k vs. Effective Stress	38
2.1.3.4 k vs. Depth	39
2.1.3.5 Field vs. laboratory tests	40
2.1.3.6 Conclusions	41
2.1.4 MASS TRANSFER IN WETLAND SOILS	41
2.1.4.1 Tracer Experiments	42
2.1.4.2 Imaging Experiments	44
2.1.4.3 Conclusions	44
2.2 MODELING MASS TRANSFER BEHAVIOR IN WETLAND SOILS	45
2.2.1 MATHEMATICAL MODELS IN USE FOR PEAT	45
2.2.2 THE TWO REGION MODEL	46
2.2.3 THE CXTFIT FITTING PROGRAM	48
2.3 PREVIOUS WORK AT THE WELLS G & H SITE	49
2.3.1 STRATIGRAPHY AND ZONE OF INFLUENCE	50

2.3.1.1 Traditional cores and testing wells	50
2.3.1.2 Piezocone testing	51
2.3.2 GEOTECHNICAL ANALYSIS	52
2.3.2.1 Summary of Test Results	52
2.3.2.2 Trends between parameters	53
2.3.3 HYDRAULIC CONDUCTIVITY AND MASS TRANSFER	53
2.3.3.1 The permeameter	54
2.3.3.2 Testing procedures	55
2.3.3.3 Summary of Test Results	55
2.3.3.3.1 Tests on Sand.	55
2.3.3.3.2 Tests on Wetland Deposits	56
2.3.3.3.3 Initial Experimental problems	56
2.3.3.3.3.1 Compressibility of soil	57
2.3.3.3.3.2 Salt loss into system	57
2.4 REFERENCES	58

3. EQUIPMENT AND MODIFICATIONS **93**

3.1 INTRODUCTION	93
3.2 EXPERIMENTAL EQUIPMENT	94
3.2.1 EQUIPMENT OVERVIEW	94
3.2.1.1 The Triaxial Cell	95
3.2.1.2 Manifold Control System	96
3.2.1.3 Flow Control System	96
3.2.1.4 Pedestal	96
3.2.1.5 Data Acquisition	97
3.3 MODIFICATIONS TO EQUIPMENT AND TESTING PROCEDURE	97
3.3.1 SALT LOSS	97
3.3.1.1 Salt Loss Into The Soil	98
3.3.1.2 Salt Loss Through The Membrane	99
3.3.1.3 Salt Loss Into The Equipment	99
3.3.1.3.1 Salt Mass Balance (Tracer) Tests on Sand	99

3.3.1.3.1.1 Interpretation of the data	100
3.3.1.3.1.2 Effluent Sampling	101
3.3.1.3.1.3 Sub-sampled tracer tests on sand	102
3.3.1.3.2 Salt Mass Balance (Tracer) Tests on Wetland Deposits	103
3.3.1.4 Conclusions	103
3.3.2 CONSOLIDATION	104
3.3.2.1 Re-sedimenting Procedure	104
3.3.2.2 Proof Tests on Re-sedimented Wetland deposits	105
3.3.2.3 Conclusions	107
3.3.3 EVALUATION OF END EFFECTS	107
3.3.3.1 Proposed Diffusion Mechanism	108
3.3.3.2 Limiting End Effects	109
3.3.3.3 Conclusions	109
3.3.4 ELIMINATING TRAVEL TIME	109
3.4 REFERENCES	110

4. SOIL CHARACTERIZATION EXPERIMENTS **153**

4.1 INTRODUCTION	153
4.2 SOILS TESTED	153
4.3 WETLAND DEPOSIT SAMPLING AND SPECIMEN PREPARATION	154
4.3.1 UNDISTURBED WETLAND DEPOSIT SAMPLES	154
4.3.1.1 The piston sampler	154
4.3.1.2 Sample transportation, storage and checking	155
4.3.1.3 Sample description	155
4.3.2 RESEDIMENTED WETLAND DEPOSIT SAMPLES	156
4.3.2.1 Re-sedimentation proof tests	157
4.3.2.2 Sample description	157
4.3.3 WETLAND DEPOSIT CLASSIFICATION	158
4.3.4 TESTING ORGANIZATION	159
4.4 SPECIFIC GRAVITY TESTS	160
4.5 SOIL ASH CONTENT	160

4.6 SOIL SIZE DISTRIBUTION	161
4.6.1 PROCEDURE	161
4.6.2 RESULTS	162
4.7 SOIL STRESS HISTORY AND COMPRESSIBILITY (CONSTANT RATE OF STRAIN TESTS)	163
4.7.1 CRS EQUIPMENT	163
4.7.2 CRS PROCEDURE AND DATA ANALYSES	164
4.7.3 RESULTS	165
4.7.3.1 Re-sedimented soil data	165
4.7.3.1.1 Discussion	166
4.7.3.2 Undisturbed soil data	167
4.7.3.3 Conclusions	168
4.8 CHARACTERIZATION OF MINERAL FRACTION OF WETLAND SOIL	168
4.8.1 EXTRACTION METHOD	169
4.8.2 MINERALOGY	169
4.8.3 SIZE DISTRIBUTION	169
4.9 REFERENCES	170
<u>5. COLUMN EXPERIMENTS: PROCEDURES AND DATA ANALYSES</u>	<u>197</u>
5.1 INTRODUCTION	197
5.2 EXPERIMENTAL PROCEDURE	197
5.2.1 SPECIMEN PREPARATION AND SETUP	197
5.2.1.1 Re-sedimented Soil	198
5.2.1.1.1 Obtaining the soil for trimming.	198
5.2.1.1.2 Trimming the specimen	199
5.2.1.1.3 Column setup	199
5.2.1.2 Undisturbed Soil	202
5.2.1.2.1 Obtaining the soil for trimming.	202
5.2.1.2.2 Trimming the specimen and column setup	202
5.2.1.3 Sand	202
5.2.2 TRACER TESTING PROCEDURE & SPECIMENS TESTED	204

5.2.2.1 Tracer Tests	204
5.2.2.1.1 Number of tests per specimen	204
5.2.2.1.2 Tracer concentration	205
5.2.2.1.3 Length of tracer injection pulse	205
5.2.2.2 Continuous Tracer Injection	205
5.2.2.3 Summary of Testing Sequence For all Specimens	206
5.2.3 CONTROL COLUMN EXPERIMENTS	207
5.3 PROCESSING OF DATA ACQUISITION FILES	208
5.3.1 LIST OF DATA COLLECTED	208
5.3.2 DESCRIPTION OF SPREADSHEET CALCULATIONS	209
5.3.2.1 Flow Rate, Effective Stress, and K	209
5.3.2.2 Influent and Effluent Concentration	210
5.3.2.2.1 Temperature Correction	210
5.3.2.2.2 Electrical Conductivity to Concentration	210
5.3.2.2.3 % Recovery	211
5.3.2.3 Effluent Sample Concentration	211
5.3.2.4 Breakthrough Curves (BTCs) for CXTFIT	211
5.3.2.4.1 Normalizing the BTCs	211
5.3.2.4.2 De-sloping and zeroing the BTCs	211
5.3.2.4.3 Adjusting the BTCs for travel time	212
5.4 CXTFIT CURVE-FITS	212
5.4.1 INPUT PARAMETERS	213
5.4.1.1 Block A: Model Description	213
5.4.1.2 Block B: Inverse Problem Parameters	214
5.4.1.3 Block C: Transport Parameters	214
5.4.1.4 Block D: Boundary Value Problem	215
5.4.1.5 Block E: Initial Value Problem	215
5.4.1.6 Block F: Production Value Problem	215
5.4.1.7 Block G: Observed Data for Inverse Problem	216
5.4.1.8 Block H: Position and Time for a Direct Problem	216
5.4.2 OUTPUT DATA	216
5.5 REFERENCES	216

6.1 INTRODUCTION	229
6.2 CXTFIT ANALYSIS	229
6.2.1 FITS FOR ONE-REGION SOILS (SANDS)	230
6.2.2 FITS FOR TWO REGION SOILS (WETLAND SOILS)	231
6.2.2.1 One vs. Two-Region Models	231
6.2.2.2 Fit Results	232
6.2.2.3 Verification of Fit Values	233
6.3 INTERPRETATION OF FIT RESULTS AND OTHER COLUMN EXPERIMENT DATA	234
6.3.1 THE ONE-REGION BEHAVIOR OF THE NaCl TRACER	235
6.3.2 RELATIONSHIP BETWEEN θ_M AND K	2326
6.3.2.1 Effective Stress	236
6.3.2.2 Salt Concentration	237
6.3.2.2.1 Decreasing Background Concentration	237
6.3.2.2.2 10 Minute Salt Injections	238
6.3.2.2.3 Continuous Salt Injections	238
6.3.2.2.4 Constant Salt Concentration	239
6.3.2.2.5 Background Concentration Effect on θ_m	239
6.3.2.2.6 Summary	240
6.3.2.3 Possible Mechanisms at Work	240
6.3.2.3.1 Salt Concentration Related	240
6.3.2.3.1.1 Organic Coiling	241
6.3.2.3.1.2 Colloid Mobilization	241
6.3.2.3.1.3 High Salt Concentrations	242
6.3.2.3.2 Additional Factors	242
6.4 DISCUSSION OF FINDINGS	243
6.4.1 CONNECTING CAUSE AND EFFECT	243
6.4.2 SIGNIFICANCE OF FINDINGS	245
6.4.2.1 Flow and Transport Modeling	245
6.4.2.2 Real World Applications	245
6.5 VERIFICATION OF FINDINGS USING NMR	246

6.6 FUTURE TESTS	247
6.6.1 THE NEXT STEPS	247
6.6.2 LONG TERM GOALS	248
6.7 REFERENCES	248
7. CONCLUSIONS AND RECOMMENDATIONS	279
<hr/>	
7.1 SUMMARY OF FINDINGS	279
7.1.1 EQUIPMENT AND PROCEDURE DEVELOPMENT	280
7.1.1.1 Electrical Conductivity Probes	280
7.1.1.2 Re-sedimented Soil Specimens	281
7.1.1.3 The Limiting of End Effects	282
7.1.2 GEOTECHNICAL ANALYSIS	283
7.1.3 FLOW AND TRANSPORT IN WETLAND SOILS	284
7.2 RECOMMENDATIONS FOR FUTURE RESEARCH	287
7.2.1 RECOMMENDATIONS	287
7.2.2 LONG TERM GOALS	288
7.3 REFERENCES	288
APPENDIX A: SOIL PROPERTIES	289
APPENDIX B: LABORATORY PROCEDURES AND DATA SHEETS	293
APPENDIX C: COMPUTER CODE	331
APPENDIX D: OUTSIDE TEST DATA	357



TABLE OF TABLES

Table 2.1: Partial listing of von Post classification of peat: Degree of humification table (From Bailon, 1995)	63
Table 2.2: Radforth Classification of peat structure (Radforth, 1969b)	64
Table 2.3: Values of wetland deposit Hydraulic Conductivity from the literature	65
Table 2.4: (a) Experimental and (b) fitted data for samples Sand 1 and Sand 2 (Ramsay, 1996)	66
Table 2.5: (a) Experimental and (b) fitted data for samples Peat 1 and Peat 2 (Ramsay, 1996)	67
Table 3.1: (a) Summary of K_d values calculated from Soil-Salt sorption experiments (b) Summary of R values calculated from K_d , bulk density, and void ratio of wetland soil	112
Table 3.2: (a) Summary of testing parameters and salt recovered for Tracer Tests on Sand Specimen 1 (b) Summary of testing parameters and salt recovered for Tracer Tests on Sand Specimen 1 with sub-samples taken	114
Table 3.3: Physical characteristics of re-sedimented (batched) wetland soil as compared to those of undisturbed soil tested by Bailon (1995)	115
Table 3.4: CRS data for re-sedimented wetland soil specimens N1 to N3	116
Table 4.1: Type and number of tests conducted on (a) re-sedimented and (b) undisturbed wetland samples	172
Table 4.2: Summary of Specific Gravity values for wetland soil samples	173
Table 4.3: Summary of Ash Content values for wetland soil samples	174
Table 4.4: Size Distribution data for re-sedimented specimens S4 and S5 and undisturbed specimen N1	175
Table 4.5: Ash Content for the different particle size classes in re-sedimented specimens S4 and S5 and undisturbed specimen N1	176
Table 4.6: CRS data for re-sedimented specimens S1 to S10 (except S2 and S6)	177
Table 4.7: CRS data for undisturbed specimens N1 to N3	178
Table 4.8: Age of soil after re-sedimentation and during testing, and duration of final batching increment	179

Table 5.1: Summary of Column Experiments on wetland deposit specimens	217
Table 5.2: Test sequence and testing parameters for Column Experiments on specimen S9	218
Table 5.3: Test sequence and testing parameters for Column Experiments on specimen S10	219
Table 5.4: Test sequence and testing parameters for Column Experiments on specimen N1	220
Table 6.1: (a) Results of One-Region Model fits for Tracer Tests on Sand Specimen 2 (b) Comparison of One and Two Region Model fits for Tracer Test 3 on Sand Specimen 2	250
Table 6.2: Results of One-Region Model fits for Specimen S9	251
Table 6.3: Results of One-Region Model fits for Specimen S10	252
Table 6.4: Results of One-Region Model fits for Specimen N1	253
Table 6.5: Comparison of CXTFIT and Method of Moments results	254
Table 6.6: Summary of relationships between pore water salt concentration, hydraulic conductivity, and effective porosity	255
Table 6.7: Results of One-Region Model fits for Specimen N5	256

TABLE OF FIGURES

Figure 1.1: Location of Aberjona Watershed (Durant, 1995)	30
Figure 1.2: Location of Wells G and H site in the Aberjona Watershed (Durant, 1995)	31
Figure 2.1: Classification systems used for wetland soils	68
Figure 2.2: Geotechnical properties of wetland soils (a) Specific gravity (b) Organic content (c) Void ratio and (d) Compression Index vs. Water content (MacFarlane, 1969)	69
Figure 2.3: Relationship between Compression Index and Natural Water Content for wetland deposits as compared to those of soft clay and silt deposits (Mesri et al., 1997)	70
Figure 2.4: Log of k_h/k_v vs. Depth. Data from laboratory tests on cores taken at three test sites (Chason and Siegel, 1986)	71
Figure 2.5: Hydraulic conductivity vs. Degree of humification (Rycroft et al., 1979a)	72
Figure 2.6: Log of k vs. Depth at three test sites. Laboratory data are expressed as continuous profiles with depth. Each triangle represents an average of horizontal and vertical k at each depth. No distinction was made for field k_h and k_v values (Chason and Siegel, 1986)	73
Figure 2.7: Log of k from permeameter data vs. Log k from field data (Knott et al., 1987)	74
Figure 2.8: k vs. Time (a) Field test in depletion mode (b) Field test in recharge mode (Rycroft et al., 1979b)	75
Figure 2.9: Vertical distribution of tracer according to electrical conductivity readings at a sampling point, which is 0.45 m from injection point (a) 207 min following tracer injection on July 12 (b) on July 18, 21, 29 and August 4 (Hoag and Price, 1995)	76
Figure 2.10: The six kinds of pore space in peat according to Loxham (1980).	77
Figure 2.11: Model fit using Equations 2.2a and b (—) for experimental breakthrough curve (•), as well as breakthrough predictions using Equations 2.2a and b (---) and the solution to the Advection Dispersion Equation (···) for another experimental breakthrough curve (×) (Loxham and Burghardt, 1983)	78
Figure 2.12: The ratio of the longitudinal dispersion coefficient to the coefficient of molecular diffusion vs. The Peclet number in a uniform sand (Freeze and Cherry, 1979, after Perkins and Johnston, 1963)	79
Figure 2.13: Map of the Wells G and H site in Woburn, Massachusetts showing the monitoring wells used in the USGS study conducted by De Lima and Olimpio (1989)	80

Figure 2.14: Stratigraphy at the Wells G and H site in Woburn, Massachusetts along transect A-A' (See Figure 2.13) (De Lima and Olimpio, 1989)	81
Figure 2.15: Map of the Wells G and H site in Woburn, Massachusetts showing the location of the soil cores sampled and the piezocone explorations conducted by Zeeb (1996)	82
Figure 2.16: Stratigraphy at the Wells G and H site in Woburn, Massachusetts along transects A-A' and B-B' (See Figure 2.15) (Zeeb, 1996)	83
Figure 2.17: Map of the Wells G and H site in Woburn, Massachusetts showing the location of the soil cores sampled and tested by Bailon (1995)	84
Figure 2.18: Schematic of soil profile of Cores 1 and 2 sampled and tested by Bailon (1995)	85
Figure 2.19: Summary of (a) Water content (b) Ash content (c) Specific gravity (d) Void ratio (e) Hydraulic conductivity and (f) C_k vs. Depth (Bailon, 1995)	86
Figure 2.20: Summary of (a) CR (b) RR and (c) σ'_p vs. Depth (Bailon, 1995)	87
Figure 2.21: Summary of (a) Water content (b) Void ratio (c) Hydraulic conductivity and (d) C_k vs. Ash content (Bailon, 1995)	88
Figure 2.22: Summary of (a) Hydraulic conductivity (b) C_k (c) CR and (d) RR vs. Void ratio (Bailon, 1995)	89
Figure 2.23: Breakthrough curve for tracer test on sand (Ramsay, 1996)	90
Figure 2.24: Breakthrough curve for tracer test on wetland soil (Ramsay, 1996)	91
Figure 3.1: (a) Permeameter (Modified standard MIT triaxial cell) (b) Typical rigid wall permeameter (Lambe and Whitman, 1969)	117
Figure 3.2: Diagram of manifold-control system (Ramsay, 1996)	119
Figure 3.3: Diagram of the flow-control system (Ramsay, 1996)	120
Figure 3.4: Specimen setup on permeameter (Cross section)	121
Figure 3.5: Standard MIT volume-control device (Ramsay, 1996)	122
Figure 3.6: Section of the permeameter removable pedestal (Ramsay, 1996)	123
Figure 3.7: Example of NaCl sorption in soil as a function of time for wetland deposit soil (Soil-Salt Sorption Experiment)	124
Figure 3.8: Permeameter membrane leak-testing setup	125
Figure 3.9: Typical breakthrough curves for tracer tests on Sand Specimen 1	126

Figure 3.10: (a) % Salt Recovered vs. Effective Stress in Sand Specimen 1 (b) Mass of Salt Lost vs. Effective Stress in sand specimen	127
Figure 3.11: (a) % Salt Recovered vs. Flow Velocity in Sand Specimen 1 (b) Mass of Salt Lost vs. Flow Velocity in sand specimen	128
Figure 3.12: (a) % Salt Recovered vs. Time Since Setup of Sand Specimen 1 (b) Mass of Salt Lost vs. Time Since Setup of of Sand Specimen 1	129
Figure 3.13: Schematic of 2-pin probe configuration (Ramsay, 1996)	130
Figure 3.14: Breakthrough curve for Tracer Test sb on Sand Specimen 1 after pulsing 10% Micro solution through system	131
Figure 3.15: Effluent sub-sampling tube setup	132
Figure 3.16: Breakthrough curves from Tracer Test sa on Sand Specimen 1. Influent conductivity probe data as well as effluent conductivity probe and sub-sampled data	133
Figure 3.17: Breakthrough curves from Tracer Test sa on Sand Specimen 1. Effluent conductivity probe, sub-sampled, and scaled data	134
Figure 3.18: Duplicate breakthrough curves: one sub-sampled (Tracer Test sc) and one not (Tracer Test sd) for Sand Specimen 1	135
Figure 3.19: Breakthrough curves from Tracer Test sd on Sand Specimen 1. Effluent conductivity probe, sub-sampled, and scaled data. (Sub-samples taken at small intervals)	136
Figure 3.20: Breakthrough curves from Tracer Test sb on Sand Specimen 1. Effluent conductivity probe and sub-sampled data after pulsing 10% Micro solution through system	137
Figure 3.21: Breakthrough curves for re-sedimented wetland deposit specimen (Specimen S7). Effluent conductivity probe and sub-sampled data.	138
Figure 3.22: % Salt recovered for 4 tracer tests on re-sedimented wetland deposit specimen (Specimen S7). Effluent conductivity probe and sub-sampled data.	139
Figure 3.23: Modified oedometer used for re-sedimenting wetland soils	140
Figure 3.24: (a) Two consecutive breakthrough curves for tracer tests on filter stones. Pulses <i>in</i> and <i>out</i> for two flow rates. (b) Superimposed breakthrough curves. Pulses <i>out</i> for tests a and b	141
Figure 3.25: (a) Two consecutive breakthrough curves for tracer tests without filter stones. Pulses <i>in</i> and <i>out</i> for two flow rates. (b) Superimposed breakthrough curves. Pulses <i>out</i> for tests a and b	142
Figure 3.26: Proposed mechanism of Two-Region behavior in filter stones	143
Figure 3.27: Breakthrough curves fit using Two-Region Model for tracer tests on filter stones (a) For fast flow rate (1.43×10^{-3} cm/s) (b) For <i>slow</i> flow rate (6.16×10^{-4} cm/s)	144

Figure 3.28: Schematic of distribution cap	146
Figure 3.29: (a) Two consecutive breakthrough curves for tracer tests on filter stones and distribution caps. Pulses <i>in</i> and <i>out</i> for two flow rates. (b) Superimposed breakthrough curves. Pulses <i>out</i> for tests a and b	147
Figure 3.30: Example of time shift for typical breakthrough curve	148
Figure 3.31: Typical breakthrough curve for Time Shift test. T_5 corresponds to the time it takes for 5% of tracer to break through.	149
Figure 3.32: Compilation of breakthrough curves for Time Shift tests run at <i>slow</i> flow velocities; that is, velocities used in wetland deposit tests.	150
Figure 3.33: T_5 vs. Flow Rate data taken from Time Shift tests.	151
Figure 4.1: Sample locations at the Wells G and H Site, Woburn, MA (Bialon, 1995)	180
Figure 4.2: Manually operated, portable Piston Sampler. (a) Piston and threaded rod. (b) Shelby Tube connected to Steel Tube and Handle Bars.	181
Figure 4.3: Example of Sample X-ray (Cores taken 4/96)	182
Figure 4.4: Organization of re-sedimentation batches and samples.	183
Figure 4.5: Particle Size Distribution for Batches 4 and 5, and Natural Sample N1.	184
Figure 4.6: Ash Content vs. Particle Size Fraction: Batches 4 and 5, and Natural Sample N1.	185
Figure 4.7: Schematic of Wissa CRS Device (Wissa et al., 1971)	186
Figure 4.8: (a) Example of CRS data and constructions: re-sedimented Sample 9) STRAIN VS. STRESS (b) Example of CRS data and constructions: re-sedimented Sample 9) VOID RATIO VS. HYDRAULIC CONDUCTIVITY (c) Example of CRS data and constructions: re-sedimented Sample 9) TOTAL WORK VS. STRESS	187
Figure 4.9: Summary of Void Ratio vs. Effective Stress data from CRS tests on Samples 1 to 10 (except 2 and 6).	190
Figure 4.10: Summary of Void Ratio normalized to $e_{1.5}$ vs. Effective Stress data from CRS tests on Samples 1 to 10 (except 2 and 6).	191
Figure 4.11: Summary of Void Ratio vs. Hydraulic Conductivity data from CRS tests on Samples 1 to 10 (except 2 and 6).	192
Figure 4.12: Summary of Void Ratio vs. Effective Stress data from CRS tests on Samples N1, N2, and N3 compared to tests on Samples 3 to 10 (except 6).	193

Figure 4.13: Summary of Void Ratio normalized to $e_{1.5}$ vs. Effective Stress data from CRS tests on Samples S7, S10, N1, N2, and N3.	194
Figure 4.14: Summary of Void Ratio vs. Hydraulic Conductivity data from CRS tests on Samples N1, N2, and N3 compared to tests on Samples 3 to 10 (except 6).	195
Figure 4.15: Size Distribution of wetland soil mineral fraction determined by the Pipette Analysis Method	196
Figure 5.1: Trimming jig used for preparing wetland deposit specimens for Column Experiments	221
Figure 5.2: Specimen setup on permeameter (Cross Section)	222
Figure 5.3: Membrane stretcher used for Column Experiment specimen setup.	223
Figure 5.4: Breakthrough Curves (BTCs) for 6 consecutive Tracer Tests on Wetland Deposit Specimen S9	224
Figure 5.5: Breakthrough Curve (BTC) 4 for Tracer Test on Specimen S10. Experimental BTC, Line defining BTC slope, and De-sloped, Zeroed BTC.	225
Figure 5.6: Typical CXTFIT Input file for Tracer Test on Wetland Deposit.	226
Figure 5.7: Typical CXTFIT Input file for Tracer Test on Sand.	227
Figure 5.8: Typical CXTFIT Output file for Tracer Test on Sand.	228
Figure 6.1: Breakthrough curves and CXTFIT fits for 6 Tracer Tests on Sand Specimen 2.	257
Figure 6.2: D/D^* vs. Peclet number from literature (Freeze and Cherry, 1979)	258
Figure 6.3: An example of the One Region Model Fit for Tracer Test 4 on specimen S10	259
Figure 6.4: D/D^* vs. Peclet number from results of CXTFIT analysis on Tracer Tests run on specimens S9, S10, and N1	260
Figure 6.5: Effective porosity vs. Effective stress for Tracer Tests run on specimens S9, S10, and N1	261
Figure 6.6: Effective porosity vs. Pore volume for Tracer Tests run on specimens S9, S10, and N1	262
Figure 6.7: Effective porosity vs. Hydraulic conductivity for Tracer Tests run on specimens S9, S10, and N1	263
Figure 6.8: D calculated for Tracer Tests on specimen S10 using CXTFIT and the Method of Moments vs. Hydraulic conductivity	264

Figure 6.9: θ_m calculated for Tracer Tests on specimen S10 using CXTFIT and the Method of Moments vs. Hydraulic conductivity	265
Figure 6.10: D ₂ O and NaCl breakthrough in Column Experiment on specimen N4	266
Figure 6.11: Breakthrough summary for Column Experiment on specimen S10	267
Figure 6.12: Breakthrough and hydraulic conductivity summary for Column Experiment on specimen S10	268
Figure 6.13: Hydraulic Conductivity variations for specimen S10 during Tracer Test 7	269
Figure 6.14: Hydraulic Conductivity of specimen S10 at a steady state effluent concentration of 10 mM NaCl	270
Figure 6.15: Hydraulic Conductivity of specimen N1 relative to variations in pore water salt concentration	271
Figure 6.16: Hydraulic Conductivity of specimen S10 at a steady state effluent concentration of 50 mM NaCl	272
Figure 6.17: Hydraulic Conductivity variations for specimen N5 relative to variations in pore water salt concentration	273
Figure 6.18: Effect of large decrease in pore water salt concentration on k (Specimen N5)	274
Figure 6.19: The influence of tracer salt concentration on organic fiber coiling in wetland soil flow channels	275
Figure 6.20: Schematic of colloid mobilization of clays in wetland soil flow channels	276
Figure 6.21: Measurements of the mobile fraction of the pore space in the peat specimen obtained through NMR imaging (Sinfield, 1998)	277

1. INTRODUCTION

1.1 THE ABERJONA WATERSHED

The Aberjona watershed, located in northeastern Massachusetts, comprises most of the city of Woburn, as well as portions of neighboring cities (Figure 1.1). Due to the watershed's abundant water supply, Woburn became an industrial center starting in the early 1800's. Leather tanning, finishing, and rendering factories, as well as the chemical industries that supported them, thrived there for over 150 years (Durant, 1991). According to the waste disposal methods of the time, industrial wastewater was released into the network of rivers, which drain the watershed. In addition, scrap hides and leather were buried on site. As a result of these practices, large amounts of toxic, heavy metals, used in leather processing and rendering, were input into the watershed over the years. In fact, between 1900 and 1936 alone, 2000 to 4000 tons of Chromium, 65 to 400 tons of Copper, 85 to 175 tons of Lead, and 40 to 45 tons of Zinc were released into the watershed (Durant, 1991). Furthermore, since the industrialization of the area, a total of 200 to 700 tons of Arsenic have also been released (Aurilio, 1992).

Recently, studies have found these heavy metals at elevated levels throughout Aberjona surface waters and sediments. Concentrations of chromium, copper, lead, zinc and arsenic have been measured to be 10 times higher than background levels along most of the Aberjona River (Knox, 1991), the principal river of the watershed (Figure 1.2).

High levels of Volatile Organic Compounds (VOCs), common to most industrialized areas, have also been detected in some of the surface waters in the watershed (Kim, 1995). In the late 1970's, high levels of 1,1,1-trichloroethane, 1,2-trans-dichloroethylene, tetrachloroethylene, chloroform, trichlorotrifluoroethane, and trichloroethene were found in Woburn's municipal drinking water at concentrations ranging from 1 to 400 parts per billion. As a result, in May of 1979, two of Woburn's municipal wells, Wells G and H, were shut down after fifteen years of operation (Myette et al., 1987).

In 1982, the site where Wells G and H are located and another in north Woburn, the Industriplex site, home to large amounts of buried leather wastes, were designated Superfund sites under CERCLA, and were slated for federal cleanup (Figure 1.2). Currently, the Industriplex site is fifth on the National Priority List of Superfund sites, since it poses such an extreme hazard to human health (Durant, 1991).

Since their designation as Superfund sites, it has become necessary to better identify the wastes at these locations, as well as other locations in the watershed, to quantify the risks these wastes pose, and to develop a mitigation or remediation strategy for these sites. To that end, extensive studies of the area were begun first by the USGS in 1985 and then by The Center of Human Health Sciences at the Massachusetts Institute of Technology (MIT) in 1988.

The MIT studies have four broad objectives. The first objective is to locate, name, and quantify different wastes through historical research on the industries of Woburn and through field sampling for different toxic chemicals associated with these industries' wastes (Durant, 1991, Knox, 1991, Aurilio, 1992, Solo-Gabriele, 1995). The second objective is to identify the physical and chemical pathways through which different wastes become accessible to humans. This is done, first, by determining the stratigraphy and the hydrogeology of the different sites (Myette et al., 1987, De Lima and Olimpio, 1989, Bailon, 1995, Ramsay 1996, and Zeeb, 1996). It is also done by studying the chemical and biological transformations that might render different wastes more or less harmful, and/or more or less mobile in the environment (Spliethoff, 1995, Seeman, 1996, Tay, 1997, Newman, 1998). The third objective is to determine the health effect, if any, of the different chemicals that the residents of Woburn have been exposed to. Both epidemiological and toxicological studies have been, and are being conducted to find connections between exposure and disease (Chen and Thilly, 1994). The last objective of these studies is to determine which techniques will be most useful for the remediation of the different sites (Kim, 1996).

The objective of the study described in this thesis, which falls under the second category cited above, is to better understand how contaminated water from the Aberjona River was transported into the aquifer, which supplied drinking Wells G and H. Subsequently, the

primary focus of this study has been to characterize the wetland deposits which form the Aberjona River bed and which separate it from the aquifer below. Studies have already been conducted to determine the stratigraphy of the Wells G and H site, the zone of influence of the wells, and the geotechnical properties of the wetland deposits at the site (Myette et al., 1987, De Lima and Olimpio, 1989, Bailon, 1995, Zeeb, 1996). The results of these studies are discussed in Section 2.3.

This thesis reports the results of an experimental program that further explores the hydrogeologic properties of these wetland deposits. That is, it focuses on the relationship between the hydraulic conductivity, and porosity of these deposits. A more detailed discussion of the goals of this thesis follow.

1.2 GOALS AND SCOPE OF THIS RESEARCH

Organic soils like those that comprise the Aberjona River bed have been established as a dual porosity medium (Loxham, 1980, Loxham and Burghardt, 1983, Price and Woo, 1986). That is, they are made up of flow channels through which tracer advects, as well as immobile pores into and out of which tracer diffuses. As a result of this, the mechanics of flow as well as the chemical interaction between solutes and the different regions of the soil can't be affected. This makes the understanding of contaminant flow through these soils more difficult. Therefore, a goal of this study is to define what complications the dual porosity of these soils presents for the modeling of flow and transport of contaminants. It is also the goal of this study to understand other wetland soil characteristics that might affect flow and transport in wetland soils.

To meet these goals, specific steps must be taken.

1. The existing One and Two Region models must be examined to see if either model is adequate in describing solute breakthrough at steady state flow in an organic soil.
2. Second, once the proportion of mobile to immobile space is known, the hypothesis that soil hydraulic conductivity, k , is dependent on effective porosity, θ_m , must be tested.
3. The factors that affect the $k - \theta_m$ relationship must be explored.

1.3 THESIS ORGANIZATION

An experimental program was developed to address these points. It consisted of three parts: (1) equipment and procedure development; (2) characterization of the geotechnical properties (water content, G_s , ash content, size distribution, compressibility, and stress history) of the soil; and (3) characterization of the hydro-geologic properties (hydraulic conductivity, dispersivity, effective porosity) of the soil. Each of these three parts is described in detail in this thesis, which is organized as follows.

In Chapter 2, the relevant literature is reviewed in order to give a context for the goals and approaches of this research. A discussion of wetlands and the important geotechnical and hydro-geological properties of their soils is included in Section 2.1. The theoretical framework used in describing flow and mass transfer in wetland soils is summarized in Section 2.2, and, finally, research specific to the wetland deposits at the Wells G and H site is reviewed in Section 2.3.

Chapter 3 is divided into two principal sections. The specifications for the design of the permeameter developed by Ramsay (1996) are presented in Section 3.2, and the permeameter and all relevant testing components are described and evaluated. Modifications to the equipment and to the experimental procedure since the equipment was first built and tested are discussed in Section 3.3. These modifications were necessary to mitigate problems of incomplete recovery of the sodium chloride tracer in the breakthrough curves, the extreme variability in field specimens, and the diffusion of the tracer in the apparatus itself.

Chapter 4 includes the procedures as well as the results of the geotechnical analysis conducted on these soils. This chapter begins with a description of the soils tested (Section 4.2), the soil sampling program, and the testing scheme (Section 4.3). Then, it continues by describing the procedures and the results of the geotechnical tests. These include Specific Gravity (Section 4.4), Ash (Mineral) Content (Section 4.5), Particle Size Distribution (Section 4.6), and Constant Rate of Strain consolidation (Section 4.7), which were run on soil samples that were also tested in the permeameter. Also in this chapter, the mineralogy and size distribution of the wetland deposit mineral fraction is discussed (Section 4.8).

The permeameter Column Experiment, during which the hydraulic conductivity, k , of the soil is measured and the breakthrough of a sodium chloride tracer is monitored, are discussed in Chapter 5. The testing procedures and the data analysis are outlined in the following manner. Section 5.2, includes a detailed description of specimen setup and testing sequence. Section 5.3 includes an explanation of the spreadsheet used to manipulate the electronically acquired data, and, finally, Section 5.4 includes an explanation of how the breakthrough curves are fitted using CXTFIT (Parker and van Genuchten, 1984).

The results of the Column Experiments conducted on undisturbed and re-sedimented wetland deposit specimens are analyzed in Chapter 6. First, the results of the CXTFIT analysis on the Tracer Test breakthrough curves are presented in Section 6.2. Second, an interpretation of these results is given and the influence of effective stress, tracer concentration, and specimen age on the specimen hydraulic conductivity, k , is evaluated in Section 6.3. Third, a conceptual model that takes into account the results of the analyses is developed and the significance of the results are discussed in Section 6.4. Fourth, Nuclear Magnetic Resonance (NMR) imaging is presented in Section 6.5 as a means of validating the Column Experiment results, and finally, future goals are listed in Section 6.6.

The results of all tests are summarized and their significance discussed in Chapter 7. Also, recommendations are made for future tests that will help in the understanding of flow and transport through wetland media.

1.4 REFERENCES

- Aurilio, A.C., *Arsenic in the Aberjona Watershed*. M.S. Thesis. Massachusetts Institute of Technology, Cambridge, MA, 1995.
- Bialon, J.L. *Characterization of the Physical and Engineering Properties of the Aberjona Wetland Sediment*. M.S. Thesis. Massachusetts Institute of Technology, Cambridge, MA, 1995.

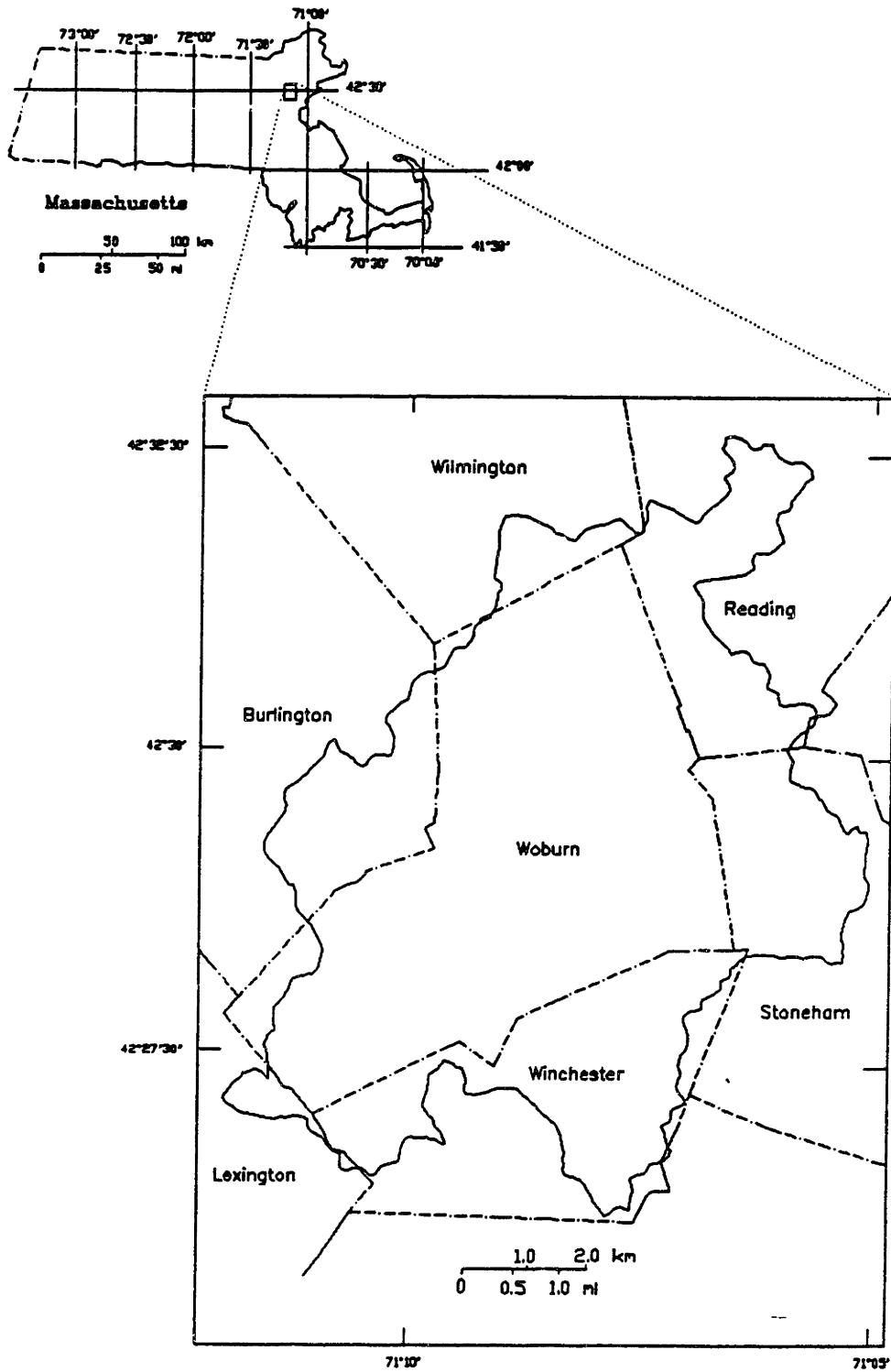
- Chen, J. and Thilly, W.G., *Mutational Spectrum of Chromium (VI) in Human Cells*. Mutation Research, 323, 1994: 21-27.
- De Lima, V. and Olimpio, J.C. *Hydrogeology and Simulation of Groundwater Flow at Superfund Site Wells G and H, Woburn, Massachusetts*. U.S. Geological Survey, Water-Resources Investigation Report 89-4059, Boston, MA. 1989.
- Durant, J.L. *Industrial History, Mutagenicity, and Hydrologic Transport of Pollutants in the Aberjona Watershed*. MS Thesis, Massachusetts Institute of Technology, Cambridge, MA. 1995.
- Kim, H. *Discharge of Volatile Organic Compounds From a Contaminated Aquifer and Their Fate in a Stream*. Ph.D. Thesis. Massachusetts Institute of Technology, Cambridge, MA, 1995.
- Kim, H. *When is it Best Not to Remediate? Mid-Course Corrections for Superfund*. MS Thesis. Massachusetts Institute of Technology, Cambridge, MA, 1996.
- Knox, M.L., *The Distribution and Depositional History of Metals in Surface Sediments of the Aberjona River Watershed*. M.S. Thesis. Massachusetts Institute of Technology, Cambridge, MA, 1991.
- Myette, C.F., Olimpio, J.C., Johnson, D.G. *Area of Influence and Zone of Contribution to Superfund Site Wells G and H, Woburn, Massachusetts*. U.S. Geological Survey, Water-Resources Investigation Report 87-4100, Boston, MA. 1987.
- Newman, D. *Microbial Respiration and Precipitation of Arsenic*. Ph.D. Thesis. Massachusetts Institute of Technology, Cambridge, MA, 1998.
- Ramsay, W.B. *A Modified Triaxial Permeameter for Physical Characterization of Parameters Affecting Contaminant Transport through Wetland Deposits*. MS Thesis, Massachusetts Institute of Technology, Cambridge, MA. 1996.
- Seeman, H.B., *Temporal Variability of Arsenic Transport into the Upper Mystic Lake*. M.S. Thesis. Massachusetts Institute of Technology, Cambridge, MA, 1997.

Spliethoff, H.M. *Biotic and Abiotic Transformations of Arsenic in the Upper Mystic Lakes*. MS Thesis. Massachusetts Institute of Technology, Cambridge, MA, 1995.

Solo-Gabriele, H., *Metal Transport in the Aberjona River System: Monitoring, Modeling, and Mechanisms*. Ph.D. Thesis. Massachusetts Institute of Technology, Cambridge, MA, 1995.

Zeeb, P.J. *Piezocone Mapping, Groundwater Monitoring, and Flow Modeling in a Riverine Peatland: Implications for the Transport of Arsenic*. Ph.D. Thesis. Massachusetts Institute of Technology, Cambridge, MA, 1996.

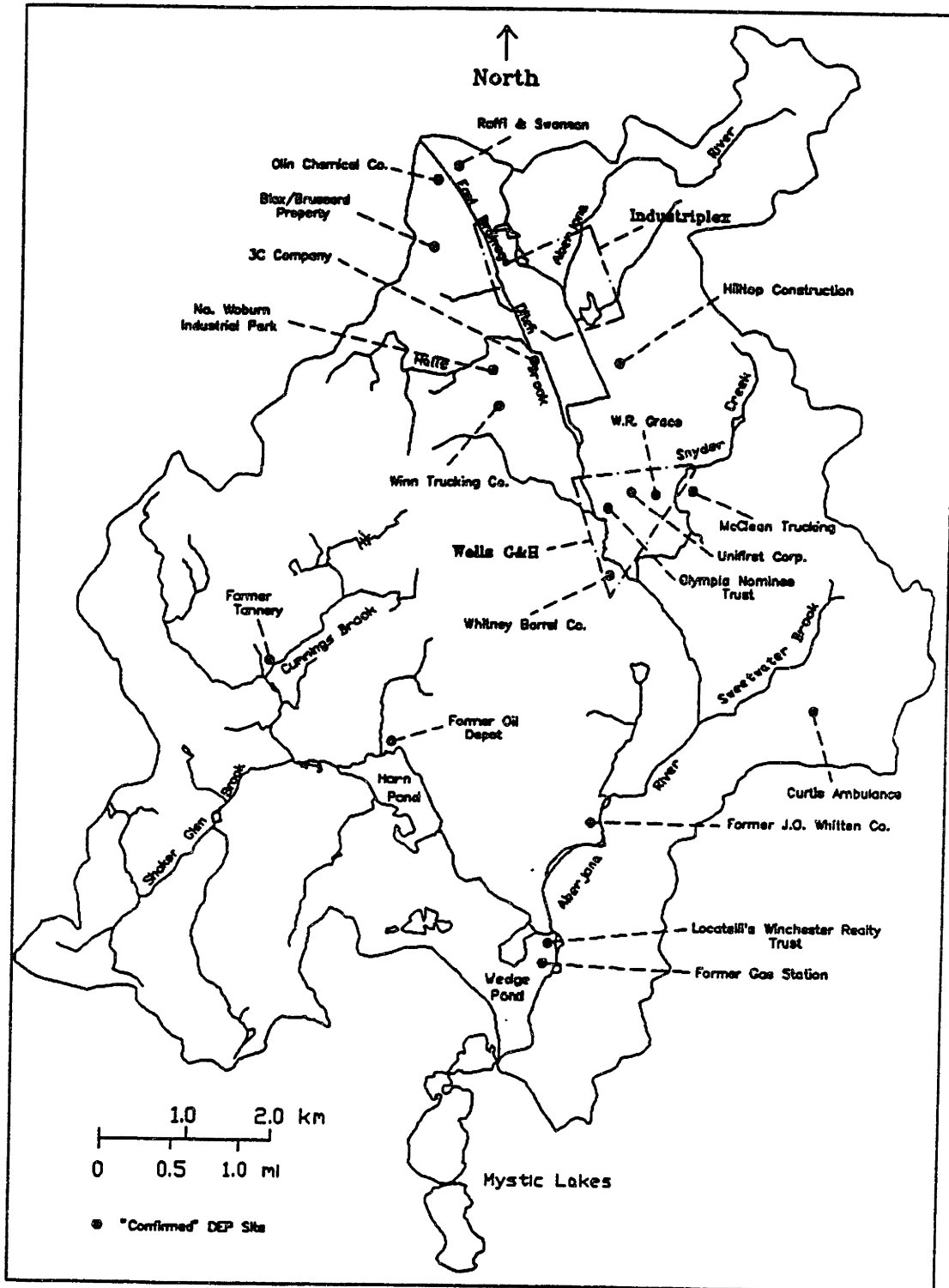
Figure 1.1: Location of Aberjona Watershed (Durant, 1995)



Key

- Watershed Boundary
- - - Town Boundary

Figure 1.2: Location of Wells G and H site in the Aberjona Watershed (Durant, 1995)



2. BACKGROUND ON WETLAND SOILS

Wetlands have been studied in the past by, first, ecologists who wish to understand the agricultural, engineering, and environmental role of these complex ecosystems and to quantify the diversity of plants and animals that characterize them (e.g. Mitsch and Gosselink, 1993). They have also been studied by agricultural scientists who drain and reclaim their nutrient rich soils for farmland and fuel (e.g. Chow et al, 1992), and by civil engineers who build on them (e.g. Radforth, 1969a). Most recently, they have been studied by environmental engineers who are increasingly investigating the potential of wetlands as natural filters or repositories for waste water and other sources of pollution (e.g. Viraraghavan and Ayyaswami, 1986, Hammer, 1989, Couillard, 1994).

This diversity of interest in wetlands and their characteristic soils has lead to a variety of approaches to studying them and has made available a range of information. In this chapter, the relevant literature is reviewed in order to center the goals and approaches of this research. A discussion of wetlands and the important geotechnical and hydrogeological properties of their soils is included in Section 2.1. The theoretical framework used in describing flow and mass transfer in wetland soils is summarized in Section 2.2, and, finally, research specific to the wetland deposits at the Wells G and H site is reviewed in Section 2.3.

2.1 WETLANDS AND WETLAND DEPOSITS

Wetlands are transition zones between terrestrial and aquatic ecosystems. They are characterized, first, by a high water table which coincides with or is near the ground surface; second, by hydrophilic plants, which have adapted to these wet conditions; and, third, by unique soils which usually have a large organic component. The organics result when the decay of wetland vegetation is slowed by the anoxic conditions often present in these saturated systems (Mitsch and Gosselink, 1993).

Wetlands occur in all types of climate and in coastal and inland regions. They can be flooded permanently or in cycles, and they support a diverse number of hydrophilic plants. Wetlands are classified according to whether the saturating water is saline or fresh. They are often sub-classified by the types of plant they support and by their hydrology. However, due to the diversity in conditions, locations, and ecology, wetland ecologists often find it difficult to define and classify all wetlands in a consistent manner (Mitsch and Gosselink, 1993).

2.1.1 CLASSIFICATION OF WETLAND SOILS

It is difficult to classify wetland deposits because of the possible variations in their plant makeup and in their depositional history, and because these soils can exist at different degrees of plant decomposition and can have a small to large mineral component. Moreover, because wetland deposits have different uses, wetland ecologists, as well as civil, environmental, and agricultural engineers need different criteria for classifying these soils.

In general, the broad term *organic soils* is used to define wetland soils which are characterized by high organic content, high water content, large void ratios, and high compressibility. Different terms such as *peat* and *muck* are also used, but exact definitions of all three terms vary considerably from source to source.

Since organic soils have both an organic component, made up of decaying wetland plants, and a mineral component, made up of wind or water deposited materials, most classification systems either use Percent Organic Content or Percent Ash, or Mineral, Content as a criteria for distinguishing between soil types. Most engineering classification systems use the measure of ash content of a soil, not the measure of organic content, as a criteria for classification. This is because the value of ash content, found by burning a soil sample at temperatures in excess of 440 °C, is easier to find than the value of organic content, which requires more complex chemical extraction procedures. It is often assumed, though it may not be always correct to do so, that values of organic and ash content are uniquely related.

Mitsch and Gosselink (1993) use the US Soil Conservation Service guidelines to define *organic soil* as a soil that has at least 12 to 20 % organic content (the exact percentage depends on saturation conditions). They go on to define *muck* as an organic soil with plant

material which is more than two thirds decomposed or indistinguishable, *peat* as an organic soil with plant material which is less than one third decomposed or indistinguishable, and *mucky peat* and *peaty muck* as transition terms.

The ASTM standard D4427 makes the distinction between *peat*, a soil with an ash content of less than 25%, and *muck* or *organic sediments*. soils with an ash content greater than 25%. Landva, et al (1983) propose a new, four category classification system, also based on ash content, but which emphasizes the geotechnical properties associated with each of the four soil categories. They suggest that the term *peat* correspond to soils having less than 20% ash content, the term *peaty organic soil* correspond to soils having between 20 and 40% ash content, the term *organic soil* correspond to soils having between 40 and 95% ash content, and finally the term *soil with organic content* correspond to soils having between 95 and 99% ash content. For each of the four terms, likely values for specific gravity, water and fiber content are given. These values are listed in Figure 2.1, which summarizes the three classification systems discussed above.

Landva et al, 1983, also recommend the use of two, more detailed classification systems, the von Post (After Landva et al, 1983, von Post, 1922) and Radforth (Radforth, 1969) systems, as supplements to the one that they propose. The von Post classification system defines soils according to their botanical content and is more pertinent to agriculturists and ecologists (See Table 2.1). The Radforth system defines soils according to plant structure, and condition and is more relevant to civil engineers (See Table 2.2). Landva et al, state that, unlike the von Post system, which can be used to classify soils with any range of mineral content, the Radforth system can only be used to classify peat, or soils with minimal mineral content. However, in a publication by Radforth (1969) on the classification of peat, no specific ash content was given to define peat. Moreover, Radforth reviews engineering values found for peat in the literature, and the listed values of ash content ranged from 0.6 to 74.5%. In any case, for this work, it was found that Radforth's system was still useful in describing the significant organic component of the soil studied (the ash content of this soil is roughly 40%).

Since the definition of *peat* is still somewhat ambiguous, the more general terms *organic soils* and *wetland deposits* will be used to refer to the soils tested in this work. However, for the literature reviewed below, the term *peat* will be used when the term is used by the author(s), even though perhaps, the classification of their soil is not necessarily in keeping with any of the systems cited above.

2.1.2 INDEX AND COMPRESSIBILITY PROPERTIES OF WETLAND SOILS

Highly organic soils and peat have been considered ‘problem’ soils by geotechnical engineers due to their characteristic high compressibility, low strength and modulus (Ladd, 1997).

In 1969, MacFarlane, an expert on *muskeg* or peaty terrain, compiled a manual as an aid to civil engineers designing for, and building on, this type of terrain. He collected data from the literature and formulated relationships between water content and other geotechnical properties including specific gravity (Figure 2.2a), organic content (Figure 2.2b), void ratio (Figure 2.2c), and compressibility (Figure 2.2d). Those relationships show that specific gravity decreases with increased water content whereas void ratio, organic content, and compressibility increase with increased water content.

Mesri et al (1997) found a log-log correlation between water content and compressibility (Figure 2.3). Mesri conducted extensive research on the secondary compression behavior of peat (Mesri and Castro, 1983; and Mesri et al, 1997), since secondary compression of these soils can play a large role in the settlements of civil engineering structures. Mesri found that peat behaves according to the general C_α/C_c concept of compressibility. For an explanation of this concept refer to Mesri and Choi (1981) and for an in depth discussion of these findings, refer to the papers cited above.

2.1.3 HYDRAULIC CONDUCTIVITY OF WETLAND SOILS

There is an increasing number of studies aimed at defining the hydraulic conductivity, k , of wetland soils, since there is an increasing interest in draining wetlands for use as agricultural land, or for harvesting their soil for fuel. There is also an expanding movement to use wetlands and organic soils for the storage and/or the treatment of contaminated water since

the organic component of these soils has been found to sorb, isolate, or facilitate the biodegradation of different pollutants (Couillard, 1994).

2.1.3.1 VERTICAL VS. HORIZONTAL HYDRAULIC CONDUCTIVITY, K

A review of the literature shows that organic soils manifest a wide range of hydraulic conductivity. This variation reflects the wide range of plant types that are found in these soils, their depositional history, their degree of decomposition, as well as the amount of organics and the overall effective stress on the soil. For example, plant type can lead to significant differences in the values of vertical (k_v) and horizontal (k_h) hydraulic conductivity (Radforth, 1969). Mosses, for example, can leave behind small, tough stems that are preserved upright (Rycroft, 1975a), creating vertical channels in the soil, which increases k_v relative to k_h ; whereas grasses fall and lie horizontally, creating lateral channels in the soil, which increases k_h relative to k_v . Chason and Siegel (1986) found up to a two orders of magnitude difference between k_h and k_v for soil specimens tested in a laboratory rigid wall permeameter (Figure 2.4). The ratio of k_h to k_v varied over the length of the 2 to 3 meter profiles taken in three locations within the Lost River Peatland in Northern Minnesota. The authors cited a range of moss, sedge, and wood layers at this site, but they made no comparison between the soil profile and the k_h/k_v profile. Also, horizontal and vertical hydraulic conductivity tests were conducted on separate specimens sub-sampled in the core, so comparisons between k_h and k_v were for nearest neighbor specimens. Therefore, not surprisingly, considering the possible variability found in different layers of wetland deposits, there was no trend between k_h/k_v , and depth. Typically, k_h and k_v were within an order of magnitude of each other with some exceptions where k_h was an order of magnitude, sometimes two, higher than k_v , and some where k_v was an order of magnitude higher than k_h . Boelter (1965) conducted vertical and horizontal hydraulic conductivity tests both in the field and in the laboratory. His test site was a bog in the Marcell Experimental Forest, also in Northern Minnesota, and he found that, due to side-wall leakage, the laboratory rigid wall tests gave inaccurate, high results. However, he did not find a significant difference between the results of the field horizontal and vertical piezometer tests, suggesting a ratio of k_h to k_v equal to unity.

Knott et al (1987) in a study of salt marsh peat, did not find a significant difference between k_h (found using field piezometers) and k_v (found using laboratory rigid wall tests), except at low values of k (less than 10^{-4} cm/s). This difference, however, could be accounted for by the reduction of the spatial heterogeneity in the smaller laboratory specimen as compared to what is found in the field (See Section 2.1.3.3 for more on laboratory vs. field results).

2.1.3.2 K VS. DEGREE OF HUMIFICATION

In a review of the literature, Rycroft et al (1975a) collected data which show that, hydraulic conductivity of peat decreases with increased decomposition (humification) of the plant remains (See Figure 2.5). Rycroft et al (1975a) as well as others (Landva and Pheeney, 1983) have used the von Post scale, a descriptive scale which matches certain visual properties to numbers, as a guideline for determining degree of humification (Table 2.2).

2.1.3.3 K VS. EFFECTIVE STRESS

There have been some studies that have investigated the direct influence of effective stress on hydraulic conductivity. The first was conducted by Hanarahan (1955) a civil engineer interested in understanding road embankment settlements. This study found that, for a partly humified peat under a load of 56 kPa, hydraulic conductivity changed from 4×10^{-4} cm/s ($e = 12$) to 2×10^{-6} cm/s ($e = 6.75$) after two days, and to 8×10^{-9} cm/s ($e = 4.5$) after 7 months. A similar study by Lea and Brawner (1963) cited in MacFarlane (1969) showed that, for a peat under an embankment of 1.83 to 2.44 m of fill, hydraulic conductivity underwent a change from $10^{-2} - 10^{-4}$ cm/s to $10^{-8} - 10^{-9}$ cm/s

In another type of study, Chow et al, 1992, who were interested in finding the ideal compaction of organic soils for successful crop production, also found that changes in effective stress led to significant changes in hydraulic conductivity. They found that a compactive effort that changed the bulk density of a sphagnum peat from 0.1 to 0.24 g/cm³, led to a three order of magnitude decrease in hydraulic conductivity.

2.1.3.4 K VS. DEPTH

Decomposition of organic soil, depending on water table height and oxidation levels, usually increases with depth, depth being synonymous with soil age. Effective stress also increases with depth, that is, increased overburden, although these increases are typically small due to the low unit weight of organic soils. Nonetheless, it is usually seen that the hydraulic conductivity of organic soil decreases with depth (Boelter, 1965, Knott, et al, 1987, Hoag and Price, 1995 and 1997).

Nonetheless, Chason and Siegel, 1986, maintain that this is not always true. In the same study cited in Section 2.1.3.1, they suggest that the decrease of hydraulic conductivity with depth is seen only in the upper 50 cm of most peat deposits (Boetler tested to 0.8 m, Knott et al, 1987, to 1.6 m, and Hoag and Price, 1995, to 1.2 m). They ran a combination of field piezometer bail tests and laboratory rigid wall permeameter tests at three locations within the Lost River Peatland in Northern Minnesota. Their data showed that, although k varied over the depth of the 2 to 3 meter profiles, there was no distinct relationship between k and depth beyond the first 50 cm (See Figure 2.6).

It is worth noting that none of these studies attempt to separate the influences of effective stress and degree of decomposition on the value of hydraulic conductivity. Hoag and Price (1997) do point out that the decrease in hydraulic conductivity with depth at their test site is due to a combination of increased humification and increased load with depth, but they do not quantify the contributions of either of the two variables.

Indeed, with the field and laboratory tests used in these studies, it is not possible to distinguish between their separate contributions. This is because, although the field tests, by default, take into account, the *in situ* stress conditions, they do not measure effective stress. As a result, there is no measure of what direct influence effective stress has on the overall hydraulic conductivity of the different layers. Furthermore, laboratory rigid wall permeameters, do not recreate the *in situ* stress conditions, because the soil specimen is unconfined at top and bottom of the column. In fact, since these tests do not control the vertical swelling of the specimen during testing, they may give a value for hydraulic conductivity that is too high. Finally, the von Post scale used for defining degree of

humification is subjective, and quantifying the absolute contribution of humification to changes in hydraulic conductivity would be impossible.

2.1.3.5 FIELD VS. LABORATORY TESTS

Despite the deficiencies of laboratory rigid wall permeameters, the results of the laboratory tests conducted by Chason and Siegel (1986) were typically the same as, or lower than, the results of their field tests (Figure 2.6). However, the laboratory tests showed more scatter. Also, as mentioned in Section 2.1.3.1, Knott et al (1987) noted that, for low hydraulic conductivity samples, that is deeper samples, laboratory tests gave lower values of k relative to field tests (Figure 2.7). The scatter and relatively low k in laboratory measurements demonstrate that, due to the small sub-sample size and the bias towards easy to trim materials, laboratory tests do not average out field heterogeneity, such as cracking and piping within the soil, as do field tests.

There is an ongoing debate as to which tests, field or laboratory, are more reliable or useful. In fact, both types of test can have their limitations. As discussed in Section 2.1.3.1, results of laboratory tests reported by Boelter (1965) were much higher than those of field tests unlike what was seen by Chason and Siegel (1986) and by Knott et al (1987). Boelter attributes this to side-wall leakage in the rigid wall permeameter, and dismisses the data.

Rycroft et al (1975b) demonstrate some limitations of field-testing. They ran both falling head and bail piezometer tests in the field, which showed that, not only did k values decrease with time during the test, but that the equilibrium k values of the two tests differed by one order of magnitude (Figure 2.8). Baird and Gaffney (1994) explain that matrix compressibility during piezometer tests on peat affect the results given by these tests, and that a more sophisticated analysis of test results is required to interpret the data correctly.

Germaine (1996) summarizes the limitations of both types of tests by saying that field tests are difficult to interpret and have poorly defined boundary conditions, whereas laboratory tests are limited by scaling problems. However, he goes on to say that laboratory tests can be more useful in answering specific questions about a soil by defining boundaries and by limiting such variables as temperature, and water/solute inflow and outflow. Thus,

laboratory tests help in the fundamental understanding of how specific variables, such as effective stress and type of solute, affect the hydrogeology of a soil.

2.1.3.6 CONCLUSIONS

A review of the literature did not show consistent behavior for the hydraulic conductivity of organic soil and peat. First, vertical and horizontal hydraulic conductivity are often similar (Boelter, 1965, Knott, 1989), but can sometimes vary up to two orders of magnitude (Chason and Siegel, 1987). Second, hydraulic conductivity usually decreases with depth (Rycroft et al, 1975, Knott et al, 1987, Hoag and Price, 1995.), but not always (Chason and Siegel, 1987). Finally, field and laboratory tests can give different results depending on the types of tests used (Rycroft et al, 1975), the depth of the soil tested (Knott et al, 1989), and the method of data analyses (Baird and Gaffney, 1994). A summary of the values of k found in the literature (Table 2.3) shows the diversity in hydraulic conductivity for these soils, which can be as permeable as coarse sand (10^{-3} cm/s) or as impermeable as clay (10^{-7} cm/s).

This variability in hydraulic conductivity emphasizes the need for engineers to formulate a physical model for these porous, compressible soils on the macroscopic, or laboratory, scale. This model should define the relationship between hydraulic conductivity and some basic parameters such as pore distribution, stress-strain behavior, and water-soil interaction. Once this relationship is better understood in the laboratory, researchers will be better equipped to understand the processes that affect the overall transport of water and contaminants in the field.

2.1.4 MASS TRANSFER IN WETLAND SOILS

Due to the variability in hydraulic conductivity and the geotechnical properties of wetland soils, mass transfer in these materials is very complex. Several researchers have conducted tracer experiments in wetland soils in order to understand the mechanisms governing mass transfer. The important results of these works are summarized below.

2.1.4.1 TRACER EXPERIMENTS

The following laboratory tests were conducted on peat by Price and Woo (1986). First, peat was added to a chloride and water solution. The concentration of free chloride ions was measured before the peat was added to the solution and after, when the system came to equilibrium. It was found that the concentration of chloride in the water remained constant, and Price and Woo deduced that chloride ions do not sorb to peat.

Second, a pulse of chloride was injected into a peat column at two different flow rates. The chloride concentration of the effluent was measured, and the breakthrough curves analyzed using the solution to the one-dimensional advection-dispersion equation (Freeze and Cherry, 1979):

$$\frac{C}{C_o} = \frac{1}{2} \left[\operatorname{erfc} \left(\frac{x - V_R t}{2 \sqrt{D_R t}} \right) + \exp \left(\frac{V_R t}{D_R} \right) \operatorname{erfc} \left(\frac{x + V_R t}{2 \sqrt{D_R t}} \right) \right] \quad (2.1)$$

Where C is solute concentration; C_o is source concentration; x is distance along the column; V_R is V/R , where V is the pore velocity and R is the retardation factor; D_R is D/R , where D is the dispersion coefficient; t is time; and erfc is the complementary error function. From an analysis of their data, Price and Woo (1986) found that the value of R , the retardation factor, was greater than 1 for both experiments. Furthermore, the slower flow experiment gave a higher value of R .

Column experiments of this nature were also conducted by Ours et al (1997). A constant head test was run on each of two peat columns to determine the hydraulic conductivity of the soil. Then, several chloride tracer experiments were run on 1 meter high columns. The breakthrough of the chloride was measured using a chloride selective probe located 30 cm downstream of the influent. Also, bulk effluent samples were taken at the end of the column. The initial breakthrough of chloride at the effluent end of the column was faster than predicted by the flow velocity calculated from the breakthrough curves measured by the probe. Also, the measured breakthrough curve showed extreme tailing.

The results of both these sets of experiments indicate that peat and organic soils are dual porosity media. That is, these soils contain interconnected pore spaces through which advective flow takes place, as well as dead end pores into and out of which molecules can only diffuse.

The existence of these two types of pores, or of these two regions, one mobile and one immobile, can explain the behavior of the solute transport found in the experiments discussed above as follows. When a non-reactive tracer is injected into a dual porosity medium, the bulk of the tracer flows through the interconnected pores, the mobile region, at a flow velocity equivalent to the Darcy flux divided by the effective (mobile) porosity of the material. This velocity is higher than the average pore water velocity usually estimated by dividing the Darcy flux by the total (mobile + immobile) porosity, and this accounts for the 'early' breakthrough at the effluent observed by Ours et al (1997).

As the bulk of the tracer passes through the material, however, some of the tracer, diffuses into the dead end pores, the immobile region, because of the gradient in concentration across the two regions. Once the bulk of the tracer has moved through the system, the concentration gradient reverses, and the tracer begins to diffuse back out into the mobile region. This mechanism is responsible for the tailing in the breakthrough curves, or retardation, seen in both experiments above. This process is also velocity dependent (Price and Woo, 1986, Loxham and Burghardt, 1983). For example, a slower flow velocity would allow for more of the tracer to diffuse into the dead end pore spaces, and would result in increased retardation.

This type of behavior has also been documented in field tests on peat. Hoag and Price, 1995, conducted a large scale, 30 day, tracer experiment in a Newfoundland peat bog. Two hundred liters of 2.6 M NaCl solution were injected into a well, and the migration of the salt was subsequently measured in several sampling wells downstream of the injection point. Within the first three hours of the test, they found, at an observation well 0.45 meters from the injection point, that concentrations of NaCl were traveling quickly through the top 0.28 meters of the bog (Figure 2.9a). Samples taken at the same point, several days later, show that the bulk of the plume had passed, and that relatively high concentrations of NaCl, which dissipated over the following two and a half weeks, were present in the less permeable peat

layer, 0.2 to 0.45 meters deep (Figure 2.9b). These observations indicate that, initially, the NaCl tracer diffused into the lower, less permeable, peat layer, but then diffused out again, once the bulk of the salt had passed above.

It is necessary to point out, at this point, that in the tracer experiments conducted by Ours et al (1997) and by Hoag and Price (1997) introduction of the tracer into the soil column increased the hydraulic conductivity of the soil by up to 8 times. Ours et al (1997) propose that the ionic interaction between the tracer and the organic portion of the soil, cause soil pores to dilate. This effect of tracer on hydraulic conductivity has serious implications for solute transport in organic soils, and these must be considered.

2.1.4.2 IMAGING EXPERIMENTS

The physical existence of two regions has been documented in studies by Loxham (1980) Hoag and Price (1997) and McBrierty et al (1996). Loxham used Direct Transmission Photomicroscopy to identify 6 different kinds of pore space in peat (See Figure 2.10). His interpretation of the pore size distribution shows that for a range of North German peats, the dead pore volume accounts for 28 to 46 % of the total pore space.

Hoag and Price (1997) used acetone displacement and resin impregnation to define the active pores in peat thin-sections. The area of active pore space was then counted using a magnified image of these thin-sections. They found that the *active* pore space ranged from 16 to 42% of the total pore space, and that the proportion of active pore space decreased with depth in the soil profile.

McBrierty et al (1996) used a different approach to documenting this phenomena. They used Differential Scanning Calorimetry, Thermogravimetric Analysis, and Proton Nuclear Magnetic Resonance to identify 4 different types of water in peat. They defined tightly bound water, two types of loosely bound water, and bulk water by the temperature ranges in which the different water types froze. They also found that the proportion of the different types of water changed for different water contents.

2.1.4.3 CONCLUSIONS

The mass transfer of solute into the immobile regions of wetland soils can potentially explain some important mechanisms of contaminant transport at the Wells G and H site. The goal of this thesis is, in part, to explore how the mobile and immobile regions interact in wetland soils, and how that interaction, along with changes in effective stress, affects hydraulic conductivity. To be able to explore the concept of mass transfer, however, a mathematical model that describes the process is needed. Different models have been applied in some studies on the two region behavior of peat. These are discussed in Section 2.2.1. Another model, the Two-Region Model, which has been applied to studies on other geologic materials, is discussed in Section 2.2.2.

2.2 MODELING MASS TRANSFER BEHAVIOR IN WETLAND SOILS

2.2.1 MATHEMATICAL MODELS IN USE FOR PEAT

In 1983, Loxham and Burghardt collected breakthrough curves from several Sodium Chloride tracer experiments on peat in rigid wall columns. These experiments were conducted at several flow velocities. They used the following equations to fit and predict the breakthrough of a non-reactive solute in the peat column:

$$\frac{\partial C_m}{\partial t} = \frac{1}{R_m} \left(\theta_m D \frac{\partial^2 C_m}{\partial x^2} - \theta \cdot \theta_m \frac{\partial C_m}{\partial x} + 2 \frac{D^*}{\theta_m} \cdot \frac{\partial C}{\partial z} \Big|_{z=0} \right), \quad (2.2a)$$

$$\frac{\partial C_m}{\partial t} = \frac{1}{R_{im}} \left(D^* \frac{\partial^2 C_m}{\partial z^2} \right); \quad (2.2b)$$

Where the subscripts *m* and *im* refer to the mobile and immobile regions, respectively; *C* is solute concentration [ML⁻³]; *t* is time [T]; *R* is the retardation factor; θ is volumetric water content [L³L⁻³]; *D* is the dispersion coefficient [L²T⁻¹]; *x* and *z* are longitudinal and lateral distance, respectively [L]; and *D*^{*} is the molecular diffusion coefficient [L²T⁻¹].

Loxham and Burghardt calculated a value of θ_m from a curve fit on a *fast* tracer experiment using equations 2.2a and b (Figure 2.11). They then used this value of θ_m , which was found to be 14%, to predict the breakthrough of NaCl pulsed at lower flow velocities, and this

prediction was compared to that of the typical solution to the advection-dispersion equation (ADE), 2.1. It is clear, from Figure 2.11, that the ADE is inadequate in describing the tracer flow through organic soils.

Siegel and Glaser (1987) and Ours et al (1997) use a much simpler approach to model flow through peat. They assumed a value for θ_m of 10%, and calculate flow velocity using:

$$V = q / \theta_m \quad (2.3)$$

Where q is the Darcy flux, given by:

$$q = Q / a = ki \quad (2.4)$$

Where Q is volumetric discharge [M^3T^{-1}], a is the specimen cross-sectional area [M], k is hydraulic conductivity [MT^{-1}], and i is hydraulic gradient [LL^{-1}].

Or, conversely, they calculated V from tracer experiments by dividing the soil column length by the time it took for the breakthrough concentration at the effluent to reach 50% of the influent concentration. They then used Equation 2.3 to find a value for θ_m .

Unfortunately, the value of flow velocity, V , calculated from Equation 2.3, describes the flow velocity of the water in peat, and is not necessarily equal to the flow velocity calculated from the breakthrough curves, which describes the often slower flow velocity of the tracer. Hoag and Price (1997) accounted for this by defining V_R as follows:

$$V_R = V / R \quad (2.5)$$

Moreover, Hoag and Price (1997) calculated θ_m , as discussed in 2.1.4.2, by measuring the area displaced by resin in thin-sections of peat. They were then able to quantify R since they knew the value of V_R from the breakthrough curves in the tracer experiments, and they knew V from their independent measurements of θ_m and q .

2.2.2 THE TWO REGION MODEL

Though the equations used by Hoag and Price are useful in finding comparisons between V and V_R , they require an a priori knowledge of θ_m . A useful model which has been used to describe flow in stratified soil (Li et al, 1994), partially saturated soils, and aggregated porous media (Griffioen et al, 1998) is the Two Region Model (TRM) formulated by Coates and Smith (1965). This model is useful in describing flow through peat since it takes into account the two regions of the soil, the rate of transfer of a tracer from one region to the other, the tracer diffusivity, and its retardation due to the dead pore space.

The TRM is written as:

$$(\theta_m + f \rho_b K_d) \frac{\partial C_m}{\partial t} + (\theta_{im} + (1-f) \rho_b K_d) \frac{\partial C_{im}}{\partial t} = \theta_m D \frac{\partial^2 C_m}{\partial x^2} - \theta_m V \frac{\partial C_m}{\partial x}, \quad (2.6a)$$

$$(\theta_{im} + (1-f) \rho_b K_d) \frac{\partial C_{im}}{\partial t} = \alpha (C_m - C_{im}); \quad (2.6b)$$

Where the subscripts m and im refer to the mobile and immobile regions, respectively; θ is volumetric water content [$L^3 L^{-3}$]; f is the fraction of adsorption sites that equilibrate with the mobile liquid phase; ρ_b is bulk density [ML^{-3}]; K_d is the distribution coefficient for linear adsorption [$M^{-1} L^3$]; C is solute concentration [ML^{-3}]; t is time [T]; D is the dispersion coefficient [$L^2 T^{-1}$]; x is distance [L]; V is pore water velocity [LT^{-1}]; and α is the first-order mass transfer coefficient [T^{-1}].

For a non-sorbing solute, the TRM simplifies to:

$$\theta_m \frac{\partial C_m}{\partial t} + \theta_{im} \frac{\partial C_{im}}{\partial t} = \theta_m D \frac{\partial^2 C_m}{\partial x^2} - \theta_m V \frac{\partial C_m}{\partial x}, \quad (2.7a)$$

$$\theta_{im} \frac{\partial C_{im}}{\partial t} = \alpha (C_m - C_{im}); \quad (2.7b)$$

The left hand sides of Equations 2.6a and 2.7a describe the net rate of mass increase within a unit of soil whereas the right hand sides describe the net fluxes into and out of the soil unit.

Equations 2.6b and 2.7b describe the rate of solute transport into the immobile region of the soil. This rate is proportional to the concentration gradient across the two regions.

The TRM can be used to calculate values for θ_m , D , the dispersion coefficient, and α , the mass transfer coefficient. The dispersion coefficient, D , takes into account the effects of chemical diffusion and the effects of mechanical dispersion, and, for a uniform soil, is given by (Freeze and Cherry, 1979):

$$D = \gamma V + \tau D^* \quad (2.8)$$

Where γ is the longitudinal dispersivity specific to the soil [L], τ is the tortuosity specific to the soil [LL⁻¹], and D^* is the molecular diffusion coefficient specific to the tracer in solution [L²T⁻¹].

D varies for different flow conditions and can be described by a curve similar to the one given in Figure 2.12, which plots D , normalized to D^* , vs. the Peclet number, Pe , which is the ratio of the advective flow component, normalized to D^* , the diffusive transport component. It should be noted that this type of curve is unique for a given soil and solute, but all curves of this type have a similar shape and can be divided into five regions. The first region describes a flow regime governed by molecular diffusion only; the second region is a transition zone, where the contribution of mechanical diffusion becomes significant; the third region is governed primarily by mechanical dispersion, and the fourth, not shown on this graph, is governed completely by mechanical dispersion. The flow regime in the final region, also not shown on this graph, is outside the range of Darcy's Law (Fried, 1975).

There is some discussion as to which physical parameters control the value of α . Li et al (1994) prefer the relationship that defines α as D^*/a^2 (a is the characteristic aggregate size) that van Genuchten put forth in 1985. However, it has been observed that α is proportional to pore velocity, albeit on a log-log scale (Griffioen et al, 1998).

2.2.3 THE CXTFIT FITTING PROGRAM

Parker and van Genuchten (1984) wrote a computer program, CXTFIT, which uses a least squares inversion method and the TRM to fit the parameters of steady, one-dimensional

transport to breakthrough curves taken during laboratory and field tracer experiments. Toride and van Genuchten updated this program in 1995. CXTFIT 2.0, the new version, can be used to fit parameters for equilibrium and non-equilibrium transport using the One Region and Two Region models, respectively, as well as for field scale transport using a stream tube model.

For this research, the non-equilibrium transport model embedded in CXTFIT 2.0 is used to solve for values of D , R , β , and ω , a dimensionless form of the mass transfer coefficient, α . Input data include transport parameters such as flow velocity and the retardation factor; boundary conditions such as input type, pulse length, and tracer concentration; initial value parameters such as initial concentration; and breakthrough data either for a fixed time at multiple locations, or for a fixed location at multiple times. A comprehensive description of these parameters, and example input and output files are included in Section 5.4. A copy of the program is included in Appendix C2.

2.3 PREVIOUS WORK AT THE WELLS G & H SITE

In Chapter 1, the wetlands underlying the Aberjona River in Woburn, Massachusetts were introduced as possible conduits of contaminated river water into nearby municipal drinking wells (See Section 1.1). In order to understand if and how the contaminated water flowing in the Aberjona River was transported into drinking Wells G and H, an investigation was launched to explore the interaction between the contaminated water and the wetland deposits underlying the river. This investigation took on three principal forms.

First, two studies by De Lima and Olimpio (1989) and Zeeb (1996) delineated the geological makeup, or stratigraphy of the site so that the relative position and scale of the river, the wetland soil, the aquifer, and the wells were quantified. Included within the first study was a general water balance, which gave information on the site water table and flow patterns. Both studies are summarized in Section 2.3.1.

Second, since very little is known about wetland soils, a geotechnical analyses was undertaken so that the engineering properties of the Aberjona wetland soils could be

quantified. Bailon (1995) conducted several classification, compressibility, and hydraulic conductivity tests and the results of his work are summarized in Section 2.3.2.

Third, a hydrogeologic study was begun in order to understand the fundamentals of contaminant transfer and hydraulic conductivity at the site, and how these are influenced by effective stress. This study was started by Ramsay (1996). His work is summarized in Section 2.3.3. However, this study, is ongoing, and its progress is documented in this thesis. The goals of this portion of the work were outlined in Section 1.2.

2.3.1 STRATIGRAPHY AND ZONE OF INFLUENCE

2.3.1.1 TRADITIONAL CORES AND TESTING WELLS

In 1985, the Environmental Protection Agency (EPA) commissioned the United States Geological Survey (USGS) to conduct a study in which the stratigraphy of the Wells G and H site was determined, and in which the zone of influence of the two wells was delineated. This study was done in two parts. In the first part, historical, geological and hydrological data were collected, cores were taken, and observation wells were drilled. These were used to determine the history of well usage, and to find the stratigraphy and current water table levels at the site. Also, a thirty-day pumping test was conducted in which water was drawn from the two wells at pumping rates comparable to those used historically. The drawdown was measured at the different observation wells and this information was used to determine the zone of influence of the Wells G and H (Myette, et al, 1987). In the second part of this study, a computer model was developed to simulate water flows at the site. The model was calibrated using historical usage data, and the results of the thirty-day pumping test. It was found to be accurate in predicting flows into and out of the Aberjona River under different pumping conditions (De Lima and Olimpio, 1989).

The results of this study showed that, at the Wells G and H site (Figure 2.13), the Aberjona River is underlain by, on average, 2 to 7 feet, and in some areas up to 26 feet, of organic soil (Figure 2.14). This organic layer is in turn underlain by a layer of sand, silt and clay, and then, by the sand and gravel aquifer into which Wells G and H were tapped. This study also found that when Wells G and H are not in use, all regional groundwater flows into the wetland and

river. When Wells G and H are being pumped, however, the zone of influence comprises 1.5 square miles of the surrounding area, with water coming mostly from the surface water, wetlands and aquifer in that region. This reverses the groundwater flow pattern, and the Aberjona River becomes a water source for the wells. The study also showed that, at average pumping rates for Well G and H, 40% of the water drawn originates from the contaminated river.

2.3.1.2 PIEZOCONE TESTING

Zeeb (1996) built a piezocone specifically for use in the soft wetland deposits at the Wells G and H site. This piezocone was designed to sense and measure the excess pore pressure, sleeve friction, and tip resistance created as it is being driven into the ground. Differences in pore pressure, friction, and resistance measurements indicate differences in soil strata. For example, if a piezocone is driven into a sand layer, excess pore pressures would be minimal, whereas the sleeve friction and tip resistance would be high. If the piezocone was driven into a clay layer, the inverse would be true, the excess pore pressures would be high, and the sleeve friction and tip resistance would be relatively low. It follows then, that the combination of pore pressure, sleeve friction, and tip resistance values found for a given soil layer, give that layer its piezocone signature. This signature can be calibrated by taking core samples at the same location as the piezocone profile, and by matching the core information to the piezocone data.

The advantage of using a piezocone to determine site stratigraphy is that many piezocone profiles can be taken in the same time and effort it takes to drill one core. While it's still important to take core samples in order to calibrate the piezocone signals, ultimately, fewer have to be taken, reducing the cost of characterizing the site.

To test out the performance of his piezocone, Zeeb collected extensive piezocone data along two transects at the site (Figure 2.15). He also took some traditional cores along those same transects to interpret the piezocone data. He found that the piezocone signal could differentiate between successive peat layers, as well as sand, and organic silt layers. From this, Zeeb was able to formulate a more detailed soil profile of the top 7 meters at the site

(See Figure 2.16, and compare to top 20 feet of the profile in Figure 2.14). The piezocone profiles show that there are two peat layers, the top one, P1, is approximately 50 cm thick and is a combination of typha and sedge peat. The second layer, P2, is also approximately 50 cm thick, and is a woody swamp peat. The profile also shows that a sand lens separates the two peat layers directly under the river, and that the peat is underlain, by a diatomaceous silt layer, which, in turn, is underlain by glacial outwash.

2.3.2 GEOTECHNICAL ANALYSIS

In an effort to characterize the geotechnical properties of the wetland soil at the Wells G and H site, Bailon (1995) ran 35 constant rate of strain consolidation tests to find the stress history and compressibility of the soil. He also ran two cylindrical specimen triaxial tests to find the vertical hydraulic conductivity of the soil, and four cubical specimen triaxial tests to find and compare the vertical and horizontal hydraulic conductivity of the soil.

The soil specimens he tested were sub-sampled from cores taken from three locations at the site (Figure 2.17, locations B1, B2, B3). Core 1 was taken from the surface to a depth of 2.6 meters. Core 2 was taken from the surface to a depth of 1.8 meters, and Core 3 was taken from the surface to a depth of 3.0 meters. However, it was found that Core 3 was too disturbed to test. The soil profiles for Core 1 and 2 are included in Figure 2.18, and show that, in Core 1, the peat layer starts at the surface and ends at 1.7 meters below the surface, and that, in Core 2, the peat layer starts at the surface and ends at 1.4 meters below the surface. Only the engineering properties found for the peat layers will be reported here.

2.3.2.1 SUMMARY OF TEST RESULTS

During testing, Bailon found values for water content, ash content, and unit weight for specimens in both cores. The values of water contents ranged from 300% to 890% (Figure 2.19a). Values of ash content ranged from 4% to 50% (Figure 2.19b), and the values of unit weight ranged from 0.94 to 1.48 g/cm³ (Figure 2.19c). There were slight trends for water content, and ash content with depth, with water content increasing, and ash content decreasing slightly with depth. However, the trend for unit weight, which decreased with depth, is more visible.

Bailon also found values for void ratio using an average value of specific gravity which he calculated from specimen volume and water content (assuming 100% saturation). Void ratio values increased with depth and ranged from 4.8 to 13.8 (Figure 2.19c).

Values of hydraulic conductivity ranged from 5×10^{-6} to 4×10^{-4} . There were no trends in hydraulic conductivity with depth, and no significant difference between vertical and horizontal hydraulic conductivity (Figure 2.19e). The values of the coefficient of hydraulic conductivity, C_k , which is the slope of the void ratio vs. log of hydraulic conductivity curve, ranged from 0.55 to 1.8. C_k increased slightly with depth (Figure 2.19f).

Values for the Compression Ratio, CR, and the Re-compression Ratio, RR, ranged from 0.275 to 0.5 and from 0.013 to 0.12, respectively (Figure 2.20a and b). And values for the pre-consolidation pressure ranged from 16 to 60 kPa (Figure 2.20c). There were no trends for these parameters with depth.

2.3.2.2 TRENDS BETWEEN PARAMETERS

Bailon also analyzed the data summarized above in order to explore any relationships between organic content, moisture content, void ratio, hydraulic conductivity, and the compressibility ratios, CR and RR, in each of the peat layers. For all, three peat layers, he found that water content, void ratio, and C_k increased with decreased ash content (Figure 2.21a,b and d), although the relationship between C_k and ash content was weak for the sedge and red woody peat. He found that C_k also increased with increased void ratio (Figure 2.22b), but there was no real relationship between k and ash content (Figure 2.21c) or k and void ratio (Figure 2.22b). There were also no apparent trends between CR, RR and void ratio (Figure 2.22c and d).

2.3.3 HYDRAULIC CONDUCTIVITY AND MASS TRANSFER

Since Bailon did not find any relationship between hydraulic conductivity and other geotechnical parameters, a new plan to characterize the Aberjona wetland deposits was devised. This plan took into account the fact that wetland deposits are a dual porosity medium. It also took advantage of the existence of CXTFIT, a model that is able to fit tracer

test breakthrough curves, and that can calculate values for the effective porosity of a specimen, and for the mass transfer parameters such as tracer diffusivity and rate of transfer (See Section 2.2.2). This type of analysis should, therefore, allow for a better understanding of water, contaminant, and soil interaction.

To collect tracer breakthrough curves for a soil specimen, a special permeameter was needed. The effort to build such a permeameter was begun by Ramsay in 1994. Ramsay, 1996) built a permeameter that would allow for measurements of a salt tracer as it passed through a soil specimen. He used the CXTFIT program to fit the breakthrough curves and to see whether the Two-Region Model gives better fits than the standard One-Region Model. From initial tests on wetland deposits, he found that, indeed, the Two-Region Model does fit wetland soil breakthrough curves better than the One-Region Model (See Section 2.3.3.3). However, these initial tests also showed that improvements in the experimental equipment and procedure were required (Ramsay, 1996). His work is summarized below.

2.3.3.1 THE PERMEAMETER

Different permeameter designs were considered to meet the experimental requirements. A flexible-wall permeameter in a modified triaxial cell (Figure 3.1a) was eventually chosen over a rigid wall permeameter (Figure 3.1b), because the flexible wall design allows control of confining pressure, allows free deformation of the enclosed specimen, and eliminates side-wall leakage. Furthermore, changes in specimen dimensions, which can be related to changes in soil porosity, can be monitored by measuring the volume change of the cell fluid in response to an applied change in effective stress. For flow induction, a flow-controlled system (i.e. a system where the flow through the specimen is constant, and the gradient across the specimen is measured) was selected over a gradient-controlled system (i.e. a system where the gradient across the specimen is constant, and the flow through the specimen is measured). This provides better flow stability in a shorter period of time (Olson, 1985). Flow in Ramsay's system is induced using a flow pump, while pressure transducers measure the imposed hydraulic gradient and effective stress. Sodium chloride was chosen as the conservative tracer, and electrical conductivity probes were chosen to monitor variations in the tracer influent and effluent concentrations. In order to avoid

running wires into the specimen, which would cause sample disturbance, the electrical conductivity probes were placed in the tubing before the top cap, and in the pedestal within the base (See Figure 3.2). The flow system was designed with two influent reservoirs, each with air-water interfaces (See Figure 3.3). These are connected to the same air-pressure regulator and to the top cap via a three-way valve. The system maintains constant pressure and a supply of influent at the up-gradient end of the specimen, while a flow pump at the down-gradient end controls the effluent flow rate. The test data, including effluent electric conductivity, pressure, temperature, and displacement of the piston, are recorded using an electronic acquisition system. Using independent calibration curves, the measured electrical conductivity data are converted to concentration data. The tracer concentrations observed with time at the base of the soil specimen are entered into the CXTFIT model to obtain fitted estimates for the hydraulic properties of the specimen, specifically, θ_m , θ_{im} , D , V , and α (See Section 3.2.1 for more details on the equipment).

2.3.3.2 TESTING PROCEDURES

This apparatus was used to test both wetland deposits and sand. Since the effective porosity of sand is, theoretically, the same as its total porosity, the results of the experiments on sand were used to evaluate the model as well as the equipment. The sand used for these experiments was selected because it has been studied extensively and its properties are well known. The experiments on the organic soil were conducted to evaluate the compatibility of the equipment to wetland deposits.

2.3.3.3 SUMMARY OF TEST RESULTS

Results were obtained from five experiments performed on two sand specimens and five on two wetland deposits specimens (Ramsay, 1996). The results of these tests gave an indication of where improvements in the equipment and procedure were necessary. These are discussed in Section 2.3.3.3.3.

2.3.3.3.1 Tests on Sand.

Tests were conducted on two sand specimens, S1 and S2. Two pulses, Pulse 1 and Pulse 2, were injected into S1, and three pulses, Pulses 1, 2 and 3, were injected into S2. The breakthrough curves were measured at the effluent end of the specimen. Influent data was also measured for the tests on specimens S2. No influent data was measured for tests on specimen S1, which was setup before an electrical conductivity probe was placed at the influent. The test conditions (effective stress, flow rate, etc.) are listed for each pulse in Table 2.4a (After Ramsay, 1996).

The curve fits using both the One- and Two-Region Model were good, with an R^2 value ranging from 0.996 to 0.999 (Figure 2.23). Parameter results are included in Table 2.4b (See Equations 2.6a and 2.6b); an in-depth discussion of their values can be found in Ramsay (1996).

2.3.3.3.2 Tests on Wetland Deposits

Two pulse tests were conducted on each of two wetland deposit specimens, P1 and P2, with the conditions varying dramatically from test to test. The flow velocities varied from 9×10^{-6} to 5×10^{-5} cm/s, and the effective stresses varied from 14 to 147 kPa (See Table 2.5a). Since a value of the specific gravity for these wetland deposits was unavailable, there was no accurate information as to the porosity of the two peat specimens. The specific gravity was estimated using the specimen mass, volume and moisture content, assuming 100% saturation. The porosity was then calculated using the initial specimen volume and moisture content. The values for specific gravity, porosity, and water content for each specimen, as well as the specifications and the results of each test are shown in Table 2.5a.

The fits of the breakthrough curves measured in the pulse tests on the wetland deposits were not as good as those for the sand specimens, but the Two-Region Model gave better results than the One-Region Model as was expected for this dual porosity medium (Figure 2.24). For the Two-Region Model, the R^2 values ranged from 0.960 to 0.993. Parameter results are included in Table 2.5b (See Equations 2.6a and 2.6b); an in depth discussion of their values can be found in Ramsay (1996).

2.3.3.3.3 Initial Experimental problems

Two significant problems in the experimental apparatus and procedure were discovered during the proof testing of the permeameter. These are outlined below.

2.3.3.3.3.1 Compressibility of soil

During a preliminary test on a wetland deposit specimen, it was observed that consolidation in the specimen occurred to such a large degree during testing, that the specimen gradually became impermeable. This was due to the nature of the test itself and the high compressibility of these soils.

For flow to occur in a specimen in any given test, the pore pressure at the bottom of the specimen is reduced by the suction created in the flow pump. As a result, the effective stress at the bottom of the specimen is increased, and consolidation occurs. This causes porosity, as well as hydraulic conductivity, to decrease at the base of the specimen. Therefore, with the flow rate constant, the gradient across the specimen increases, further reducing the pore pressure at the base. This created a cycle of consolidation, which eventually leads to an impermeable specimen. Not only is this phenomenon a drawback from a practical testing point of view, it is a drawback in general, since the very parameter being measured, k , is altered during testing.

2.3.3.3.3.2 Salt loss into system

A mass balance calculation for specimen S2, Pulses 1, 2 and 3 found that 81, 86, and 96% of the sodium chloride was recovered after each test, respectively. On further calculation, it was found that 0.027, 0.049, and 0.048 g were lost, respectively, for each pulse. Since the input of salt mass was 0.14g, 0.42g, and 1.18g for Pulses 1, 2, and 3, respectively, these data indicate that there was, perhaps, a finite sink for the salt either in the equipment, or on the surface of the sand grains.

Mass balance calculations for specimen P1 indicated that only 49 and 59% of the salt was recovered for Pulse 1 and Pulse 2, respectively. The same calculations for specimen P2 indicated that only 81 and 52% of the salt was recovered for Pulse 1 and Pulse 2,

respectively. The reason for the large recovery for specimen P2, Pulse 1 is that water was not pushed through the specimen before the pulse was started as was done for specimen P1, Pulse 1; therefore, it is likely that there was salt in the system initially. From the two tests on specimen P1, it would seem that salt disappeared more or less in proportion to the amount of salt put into the system. This indicates a linearly varying sorption constant for this soil.

2.4 REFERENCES

- Andrejko, M.J., Fiene, F., and Cohen, A.D. *Comparison of Ashing Techniques for Determination of the Inorganic Content of Peats*. Testing of Peats and Organic Soils, ASTM STP 820. P.M. Jarrett, Ed. American Society for Testing and Materials, 1983: 5-20.
- The Book of ASTM Standards, Part 19. D4427: 1987.
- Baird, A.J., Gaffney, S.W., *Cylindrical Piezometer Responses in a Humified Fen Peat*. Nordic Hydrology, 25, 1994: 167-182.
- Bialon, J.L. *Characterization of the Physical and Engineering Properties of the Aberjona Wetland Sediment*. M.S. Thesis. Massachusetts Institute of Technology, Cambridge, MA, 1995.
- Boelter, D.H. *Hydraulic Conductivity of Peats*. Soil Science, 100.4, October, 1965: 227-231.
- Chason, D.B. and Siegel, D.I. *Hydraulic Conductivity and Related Physical Properties of Peat, Lost River Peatland, Northern Minnesota*. Soil Science, 142.2, August, 1986: 91-99.
- Chow, T.L., Rees, H.W., Ghanem, I., Cormier, R., *Compactibility of Cultivated Sphagnum Peat Material and its Influence on Hydrologic Characteristics*. Soil Science, 153.4, April, 1992: 300-306.
- Coates, K.H., and Smith, D.B. *Dead-end Pore Volume and Dispersion in Porous Media*. Society of Petroleum Engineering Journal, 4, 1964: 73-84.

- Couillard, D. *The Use of Peat in Wastewater Treatment*. Water Research, 28:6, 1994:1261-1274.
- Culligan-Hensley, P.J. *Physical Characterization of Parameters Effecting Subsurface Contaminant Transport in the Aberjona Watershed, with Emphasis on G and H Site*. Research Proposal, Massachusetts Institute of Technology, Cambridge, MA, 1995.
- De Lima, V., Olimpio, J.C. *Hydrogeology and Simulation of Groundwater Flow at Superfund Site Wells G and H, Woburn, Massachusetts*. U.S. Geological Survey, Water-Resources Investigation Report 89-4059, Boston, MA. 1989.
- Durant, J.L. *Industrial History, Mutagenicity, and Hydrologic Transport of Pollutants in the Aberjona Watershed*. MS Thesis, Massachusetts Institute of Technology, Cambridge, MA. 1995.
- Freeze, R.A. and Cherry, J.A. Groundwater, Prentice Hall, Inc.: Englewood Cliffs, NJ. 1979.
- Fried, J.J. Groundwater Pollution, Elsevier Scientific Publishing Co.: NY. 1975.
- Germaine, J.T. Personal Communication. June 27, 1996.
- Hammer, D.A. Constructed Wetlands for Wastewater Treatment: Municipal, Industrial, and Agricultural. Lewis Publishers, Inc.: Chelsea, MI. 1989.
- Hanrahan, E.T. *An Investigation of Some Physical Properties of Peat*. Geotechnique, 4:3, 1954: 108-123.
- Hoag, R.S. and Price, J.S. *A Field Scale, Natural Gradient Solute Transport Experiment in Peat at a Newfoundland Blanket Bog*. Journal of Hydrology, 172, 1995: 171-184.
- Hoag, R.S. and Price, J.S. *The Effects of Matrix Diffusion on Solute Transport and Retardation in Undisturbed Peat in Laboratory Columns*. Journal of Contaminant Hydrology, 28, 1997: 193-205.
- Knott, J.F., Nuttle, W.K., Hemond, H.F., *Hydrologic Parameters of Salt Marsh Peat*. Hydrological Processes, 1, 1987: 211-220.

- Lambe, T.W. and Whitman, R.V. Soil Mechanics, John Wiley & Sons, 1969.
- Landva, A.O., Korpijaakko, E.O., and Pheeny, P.E. *Geotechnical Classification of Peats and Organic Soils. Testing of Peats and Organic Soils, ASTM STP 820*. P.M. Jarrett, Ed. American Society for Testing and Materials, 1983: 37-51.
- Lea N.D. and Brawner C.O., *Highway Design and Construction over Peat Deposits in Lower British Columbia*. Highway Res. Board, Res. Rec. No. 7, Washington DC, 1963:1-33.
- Li, L., Barry, D.A., Culligan-Hensley, P.J., and Bajracharya, K. *Mass Transfer in Soils with Local Stratification of Hydraulic Conductivity*. Water Resources Research, 30.11, November 1994: 2891-2900.
- Loxham, M. *Theoretical Considerations of Transport of Pollutants in Peats*. Proceedings of the 6th Annual Peat Congress, Dulluth, 1980: 600-606.
- Loxham, M. and Burghardt, M. *Peat as a Barrier to the Spread of Micro-contaminants to the Groundwater*. Proceedings of the International Symposium on Peat Utilization, Bemidji State University, Bemidji, MN, 1983: 337-349.
- MacFarlane, I.C. *Engineering Characteristics of Peat*. Muskeg Engineering Handbook. I.C. MacFarlane, Ed. Muskeg Subcommittee of the NRC Associate Committee on Geotechnical Research, 1969: 78-126.
- McBrierty, V.J., Wardell, G.E., Keely, C.M., O'Neill, E.P., and Prasad, M. *The Characterization of Water in Peat*. The Soil Science Society of America Journal, 60, 1996: 991-1000.
- Mesri G. and Choi, Y.K., *Settlement Analysis of Embankment on Soft Clays*. Journal of Geotechnical Engineering, 111.4, April 1985: 441-464.
- Mesri, G., Stark, T.D., Ajlouni, M.A., Chen, C.S., *Secondary Compression of Peat with or without Surcharging*. Journal of Geotechnical and Geoenvironmental Engineering, May 1997: 411-421.

- Mitsch, W. J., Gosselink, J. G., *Biogeochemistry of Wetlands*. Wetlands, 2nd Edition. Van Nostrand Reinhold, New York, 1993: 114-188.
- Myette, C.F., Olimpio, J.C., Johnson, D.G. *Area of Influence and Zone of Contribution to Superfund Site Wells G and H, Woburn, Massachusetts*. U.S. Geological Survey, Water-Resources Investigation Report 87-4100, Boston, MA. 1987.
- Newman, D. *Microbial Respiration and Precipitation of Arsenic*. Ph.D. Thesis. Massachusetts Institute of Technology, Cambridge, MA, 1998.
- Olson, R.E. and Daniel, D.E. *Measurement of the Hydraulic Conductivity of Fine Grained Soils*. Permeability and Groundwater Contaminant Transport, ASTM STP 746, 1981: 18-64.
- Ours, D.P., Siegel, D.I., Glaser, P.H. *Chemical Dilation and the Dual Porosity of Humified Bog Peat*. Journal of Hydrology, 196, 1997: 348-360.
- Parker, J.C., van Genuchten, M.T. *Determining Transport Parameters from Laboratory and Field Tracer Experiments*. Virginia Agricultural Experiment Station Bulletin 84-3, 1984.
- Price, J.S. and Woo, M. *Wetlands as Waste Repositories? Solute Transport in Peat*. Proceedings of the National Student Conference on Northern Studies. Ottawa: Ontario, 1986.
- Radforth, N.W., *Muskeg as an Engineering Problem*. Muskeg Engineering Handbook. I.C. MacFarlane, Ed. Muskeg Subcommittee of the NRC Associate Committee on Geotechnical Research, 1969a: 3-30.
- Radforth, N.W., *Classification of Muskeg*. Muskeg Engineering Handbook. I.C. MacFarlane, Ed. Muskeg Subcommittee of the NRC Associate Committee on Geotechnical Research, 1969b: 31-52.

- Ramsay, W.B. *A Modified Triaxial Permeameter for Physical Characterization of Parameters Affecting Contaminant Transport through Wetland Deposits*. MS Thesis, Massachusetts Institute of Technology, Cambridge, MA. 1996.
- Ratnam, S., *Geotechnical Centrifuge Modeling of the Behavior of Light Nonaqueous Phase Liquids (LNAPLs) in Sand Samples Under Hydraulic Flushing*. Sc. M. Thesis, Massachusetts Institute of Technology, Cambridge, MA. 1996.
- Rycroft, D.W., Williams, J.A., and Ingram, H.A.P. *The Transmission of Water Through Peat: I. Review*. Journal of Ecology, 63, 1975a: 535-556.
- Rycroft, D.W., Williams, J.A., and Ingram, H.A.P. *The Transmission of Water Through Peat: II. Field Experiment*. Journal of Ecology, 63, 1975b: 557-568.
- Siegel, D.I. and Glaser, P.H. *Groundwater Flow in a Bog-Fen Complex, Lost River Peatland, Northern Minnesota*. Journal of Ecology, 75, 1987: 743-754.
- Toride, N., Leij, F.J., van Genuchten, M.T. *The CXTFIT Code for Estimating Transport Parameters from Laboratory or Field Tracer Experiments, Version 2.0*. U.S. Salinity Laboratory, Agricultural Research Service, U.S. Department of Agriculture, Research Report 137, August 1995.
- Viraraghavan, T., Ayyaswami, A., *Use of Peat in Water Pollution Control: a Review*. Canadian Journal of Civil Engineering, 14, 1987: 230-233.
- Zeeb, P.J. *Piezocone Mapping, Groundwater Monitoring, and Flow Modeling in a Riverine Peatland: Implications for the Transport of Arsenic*. Ph.D. Thesis. Massachusetts Institute of Technology, Cambridge, MA, 1996.

Table 2.1: Partial listing of von Post classification of peat: Degree of humification table (From Bailon, 1995)

Degree of Humification	Decomposition	Plant Structure	Content of Amorphous Material	Material Extruded on Squeezing (passing between fingers)	Nature of Residue
H1	None	Easily identified	None	Clear, colorless water	
H2	Insignificant	Easily identified	None	Yellowish water	
H3	Very slight	Still identifiable	Slight	Brown, muddy water; no peat	Not pasty
H4	Slight	Not easily identified	Some	Dark brown muddy water; no peat	Somewhat pasty
H5	Moderate	Recognizable, but vague	Considerable	Muddy water and some peat	Strongly pasty
H6	Moderately strong	Indistinct (more distinct after squeezing)	Considerable	About one third of peat squeezed out; water dark brown	
H7	Strong	Faintly recognizable	High	About one half of peat squeezed out squeezed out; any water very dark brown	
H8	Very strong	Very indistinct	High	About two thirds of peat squeezed out; also some pasty water	Plant tissue capable of resisting decomposition
H9	Nearly complete	Almost not recognizable		Nearly all the peat squeezed out as a fairly uniform paste	
H10	Complete	Not discernable		All the peat passes between the fingers; no free water visible	

Table 2.2: Radforth Classification of peat structure (Radforth, 1969b)

Predominant Characteristic	Category	Description
Amorphous-granular	1	Amorphous-granular peat
	2	Non-woody, fine fibrous peat
	3	Amorphous-granular peat containing non-woody fine fibers
	4	Amorphous-granular peat containing woody fine fibers
	5	Peat, predominantly amorphous-granular, containing non-woody fine fiber, held in a woody, fine-fibrous framework
	6	Peat, predominantly amorphous-granular, containing woody fine fiber, held in a woody, fine-fibrous framework
	7	Alternate layering of non-woody, fine fibrous peat and amorphous-granular peat containing non-woody fine fibers
Fine-fibrous	8	Non-woody, fine fibrous peat containing a mound of coarse fibers
	9	Woody, fine fibrous peat held in a woody, coarse-fibrous framework
	10	Woody particles held in non-woody, fine-fibrous peat
	11	Woody and non-woody particles held in a fine-fibrous peat
Coarse-fibrous	12	Woody, coarse-fibrous peat
	13	Coarse fibers criss-crossing fine-fibrous peat
	14	Non-woody and woody fine-fibrous peat held in a coarse fibrous framework
	15	Woody mesh of fibers and particles enclosing amorphous-granular peat containing fine fibers
	16	Woody, coarse-fibrous peat containing scattered woody chunks
	17	Mesh of closely applied logs and roots enclosing woody coarse-fibrous peat with woody chunks

Table 2.3: Values of wetland deposit Hydraulic Conductivity from the literature

Reference	Permeability (E-5 cm/s)	
	Laboratory Tests	Field Tests
Bailon, 1995	0.8 - 31	-
Boelter, 1969	3.86 - 15000	0.75 - 6200 ⁽¹⁾
Chasson and Spiegel, 1986	0.3 - 1600	10 - 10000 ⁽²⁾
Knott et al., 1987	1 - 32	10 - 32
Hoag and Price, 1995	-	0.001 - 2000 ⁽³⁾
MacFarlane, 1969 (Review of Papers)	0.01 - 1000	-
Olson and Daniel, 1981 (Review of Papers)	0.02 - 5	0.2 - 30
Rycroft, 1979a (Review of Papers)	-	0.006 - 10000

- (1) Horizontal and Vertical hydraulic conductivity were on the same order of magnitude. Permeability decreased with increased humification.
- (2) Horizontal permeability was 2 to 3 orders of magnitude higher than the vertical. There was no trend in k with depth.
- (3) There was a distinct relationship between permeability and depth.

Table 2.4: (a) Experimental and (b) fitted data for samples Sand 1 and Sand 2 (Ramsay, 1996)

Table 2.4a

EXPERIMENT	Effective Stress (kPa)	V (cm/s)	C _s	θ	Gradient	k (cm s ⁻¹)	% NaCl Recovered
Sand 1 P1	25	0.011	2.66	0.46	2.02	-	-
Sand 1 P2	25	0.011	2.66	0.46	1.07	-	-
Sand 2 P1	23	0.001	2.66	0.42	-0.17	-	81
Sand 2 P2	23	0.003	2.66	0.42	0.21	1.10E-02	86
Sand 2 P3	24	0.007	2.66	0.42	1.68	8.10E-03	96

Table 2.4b

EXPERIMENT	V (cm/s)	D (cm ² s ⁻¹)	Pulse Duration (s)	β	ω	R ²	θ _m
Sand 1 P1	0.011	2.1E-04	600	0.72	1.8	0.998	0.5
Sand 1 P2	0.011	1.3E-06	604	0.72	1.8	0.999	0.5
Sand 2 P1	0.0015	3.2E-05	467	0.77	2.1	0.999	0.48
Sand 2 P2	0.004	7.0E-05	530	0.73	3.1	0.997	0.44
Sand 2 P3	0.0097	1.0E-05	585	0.75	2.0	0.996	0.46

β: the ratio of the mobile region porosity to total porosity.

ω: a normalized coefficient describing the rate of contaminant transport between the mobile and immobile regions.

Table 2.5: (a) Experimental and (b) fitted data for samples Peat 1 and Peat 2 (Ramsay, 1996)

Table 2.5a

EXPERIMENT	Effective Stress (kPa)	V (cm/s)	w _c (%)	θ	Gradient	k (cm s ⁻¹)	% NaCl Recovered
Peat 1 P1	18	0.000009	573	0.87	66.8	1.20E-07	49
Peat 1 P2	147	0.000005	285	0.77	1283	2.90E-08	59
Peat 2 P1	14	0.000001	548	0.88	34.73	2.60E-07	81
Peat 2 P2	69	0.000004	322	0.8	531.64	5.80E-08	53

Table 2.5b

EXPERIMENT	V (cm/s)	D (cm ² s ⁻¹)	Pulse Duration (s)	β	ω	R ²	θ _m
Peat 1 P1	0.000027	1.0E-05	398	0.09	9.4	0.993	0.085
Peat 1 P2	0.000079	2.3E-05	482	0.37	2.1	0.97	0.398
Peat 2 P1	0.000024	8.7E-06	786	0.42	5.4	0.96	0.525
Peat 2 P2	0.000077	4.6E-06	486	0.31	3.6	0.984	0.33

β: the ratio of the mobile region porosity to total porosity.

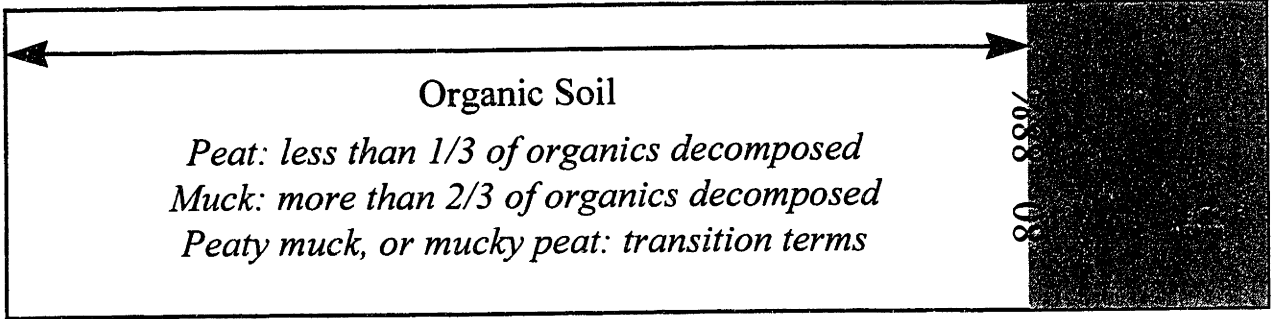
ω: a normalized coefficient describing the rate of contaminant transport between the mobile and immobile regions.

Figure 2.1: Classification systems used for wetland soils

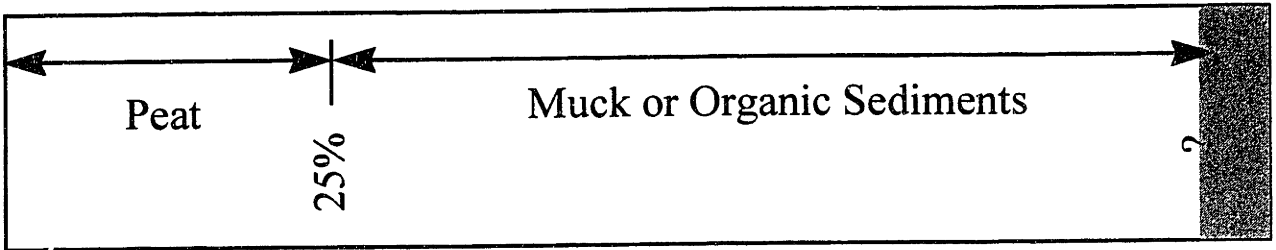
0% Ash Content 100%



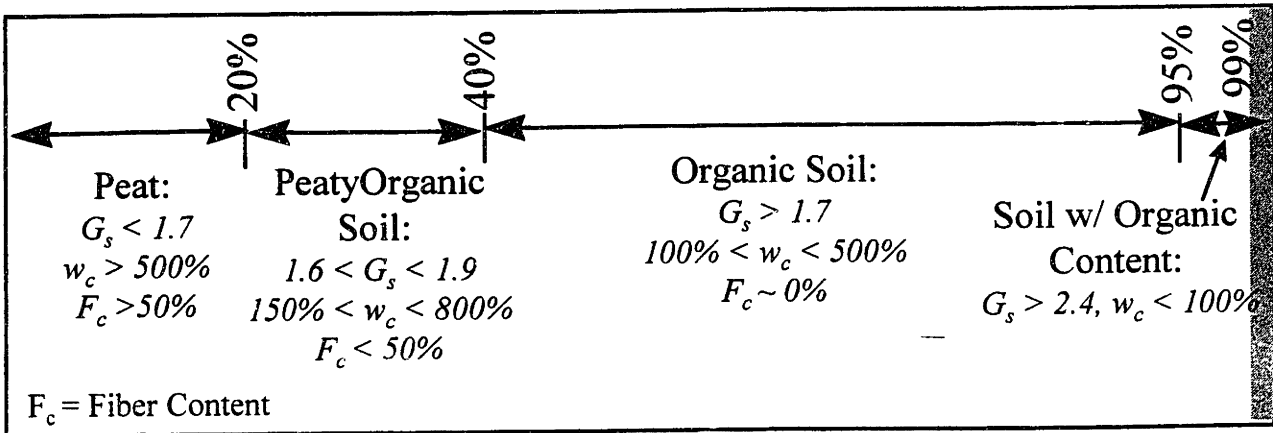
Mitsch and Gosselink, 1993



ASTM D4427



Landva et al., 1983



Mineral soil

Figure 2.2: Geotechnical properties of wetland soils (a) Specific gravity (b) Organic content (c) Void ratio and (d) Compression Index vs. Water content (MacFarlane, 1969)

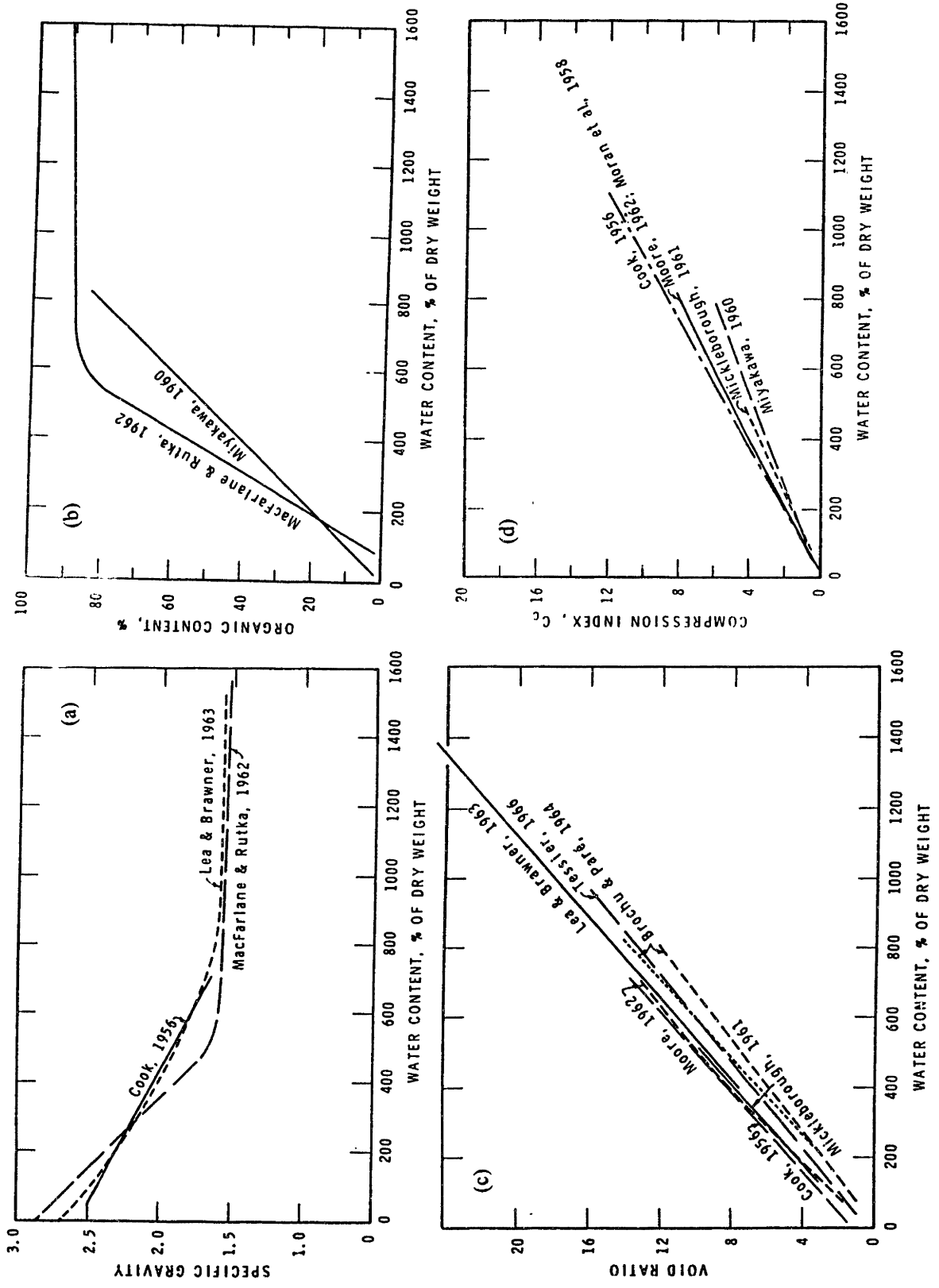


Figure 2.3: Relationship between Compression Index and Natural Water Content for wetland deposits as compared to those of soft clay and silt deposits (Mesri et al., 1997)

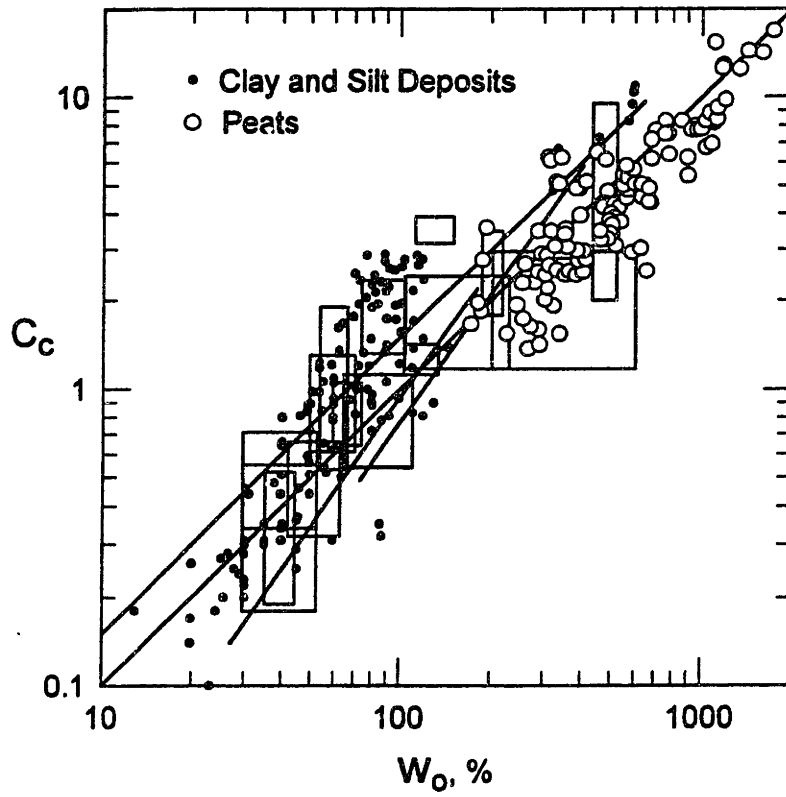


Figure 2.4: Log of k_h/k_v vs. Depth. Data from laboratory tests on cores taken at three test sites (Chason and Siegel, 1986)

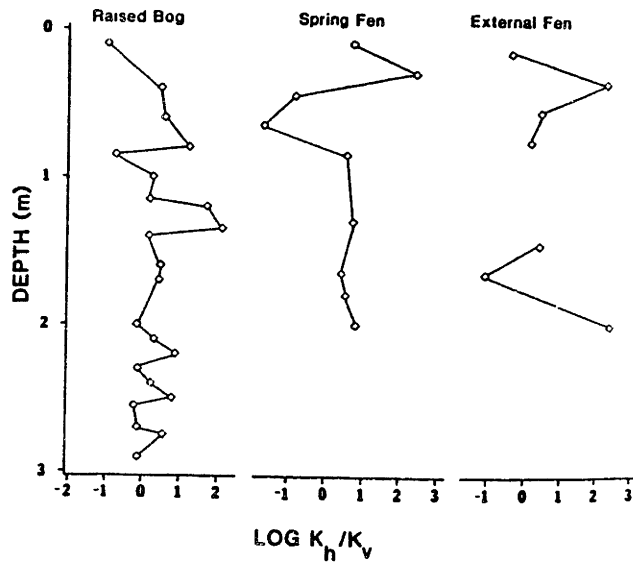


Figure 2.5: Hydraulic conductivity vs. Degree of humification (Rycroft et al., 1979a)

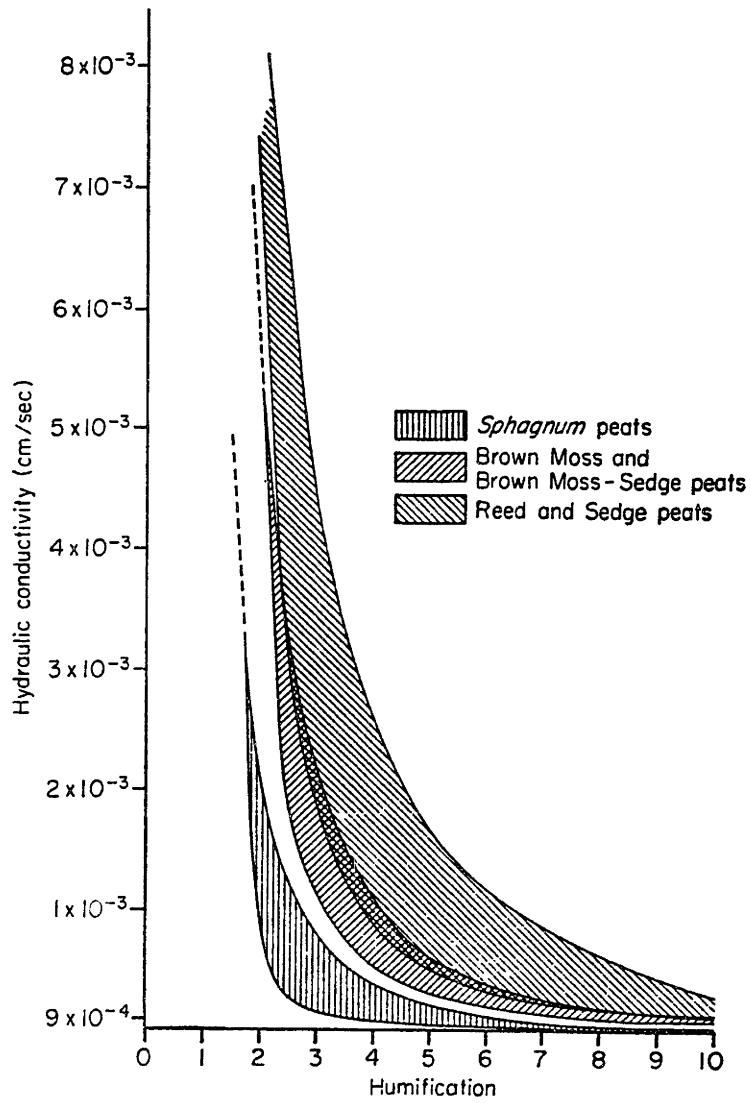


Figure 2.6: Log of k vs. Depth at three test sites. Laboratory data are expressed as continuous profiles with depth. Each triangle represents an average of horizontal and vertical k at each depth. No distinction was made for field k_h and k_v values (Chason and Siegel, 1986)

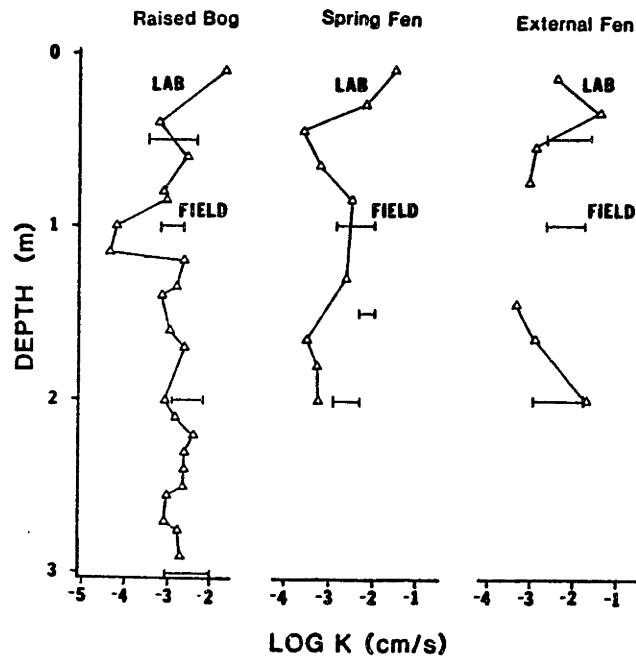


Figure 2.7: Log of k from permeameter data vs. Log k from field data (Knott et al., 1987)

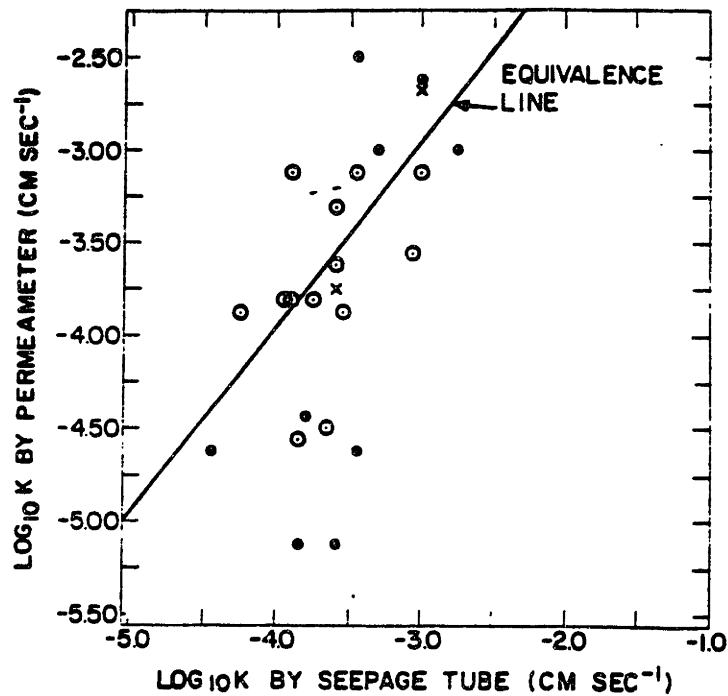


Figure 2.8: k vs. Time (a) Field test in depletion mode (b) Field test in recharge mode (Rycroft et al., 1979b)

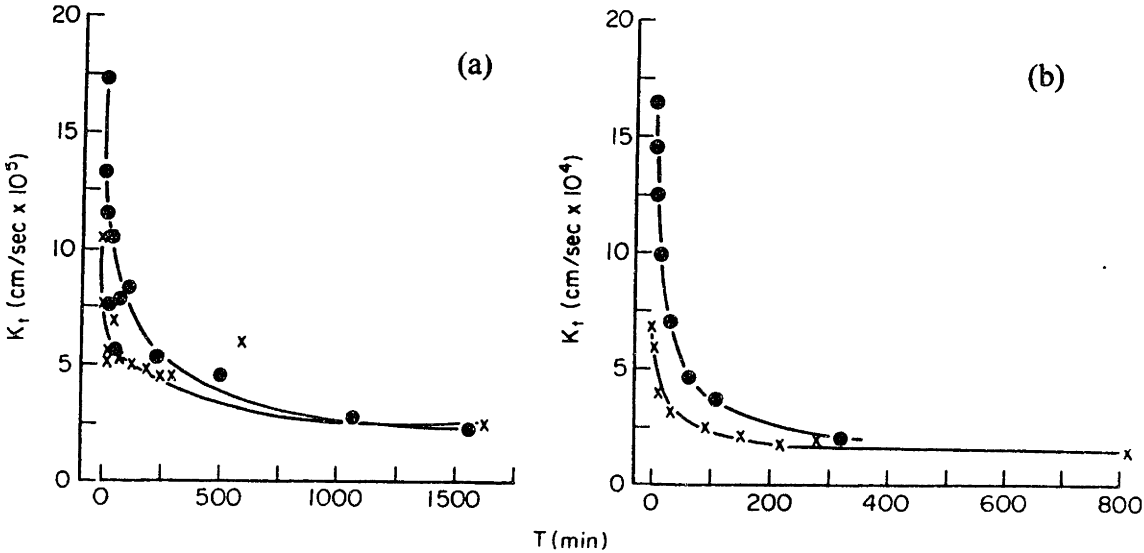


Figure 2.9: Vertical distribution of tracer according to electrical conductivity readings at a sampling point, which is 0.45 m from injection point (a) 207 min following tracer injection on July 12 (b) on July 18, 21, 29 and August 4 (Hoag and Price, 1995)

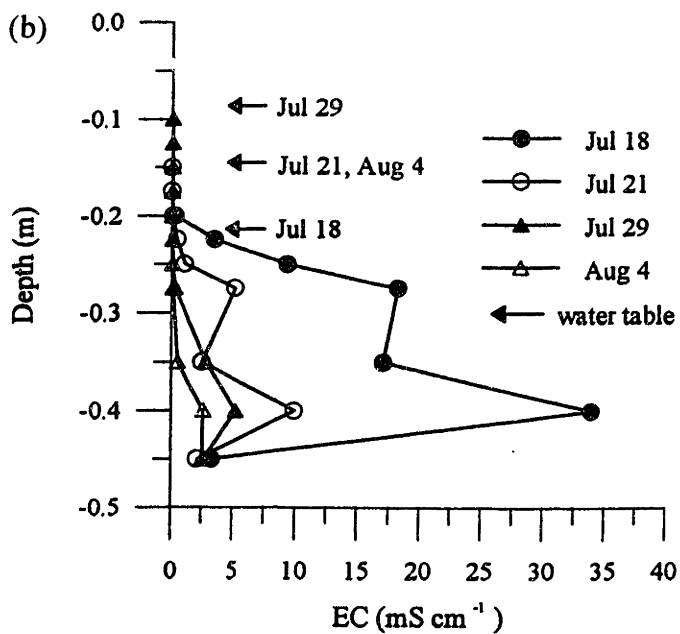
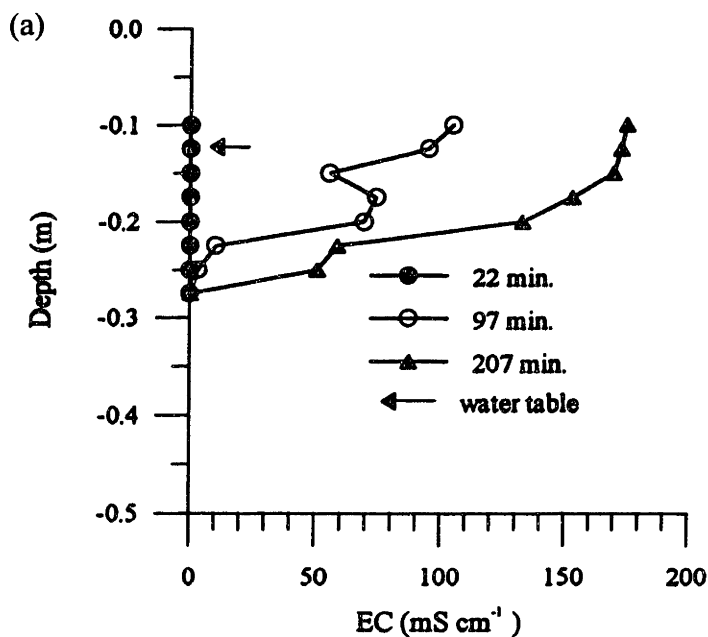
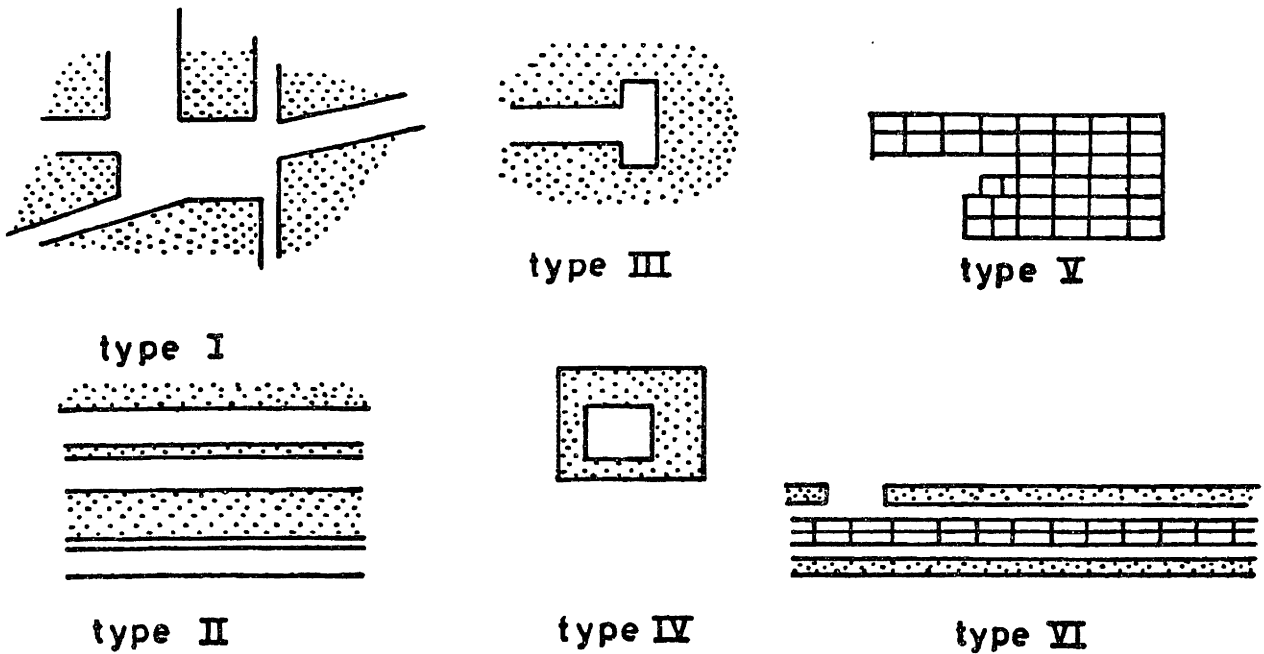


Figure 2.10: The six kinds of pore space in peat according to Loxham (1980).



- TYPE I: Large multiply connected open pores
- TYPE II: Simply connected slit type pores
- TYPE III: Closed end pores
- TYPE IV: Completely isolated pores
- TYPE V: Remains of cells with the walls more or less intact
- TYPE VI: Pores in massive wood structures, roots etc.

Figure 2.11: Model fit using Equations 2.2a and b (—) for experimental breakthrough curve (●), as well as breakthrough predictions using Equations 2.2a and b (---) and the solution to the Advection Dispersion Equation (···) for another experimental breakthrough curve (×) (Loxham and Burghardt, 1983)

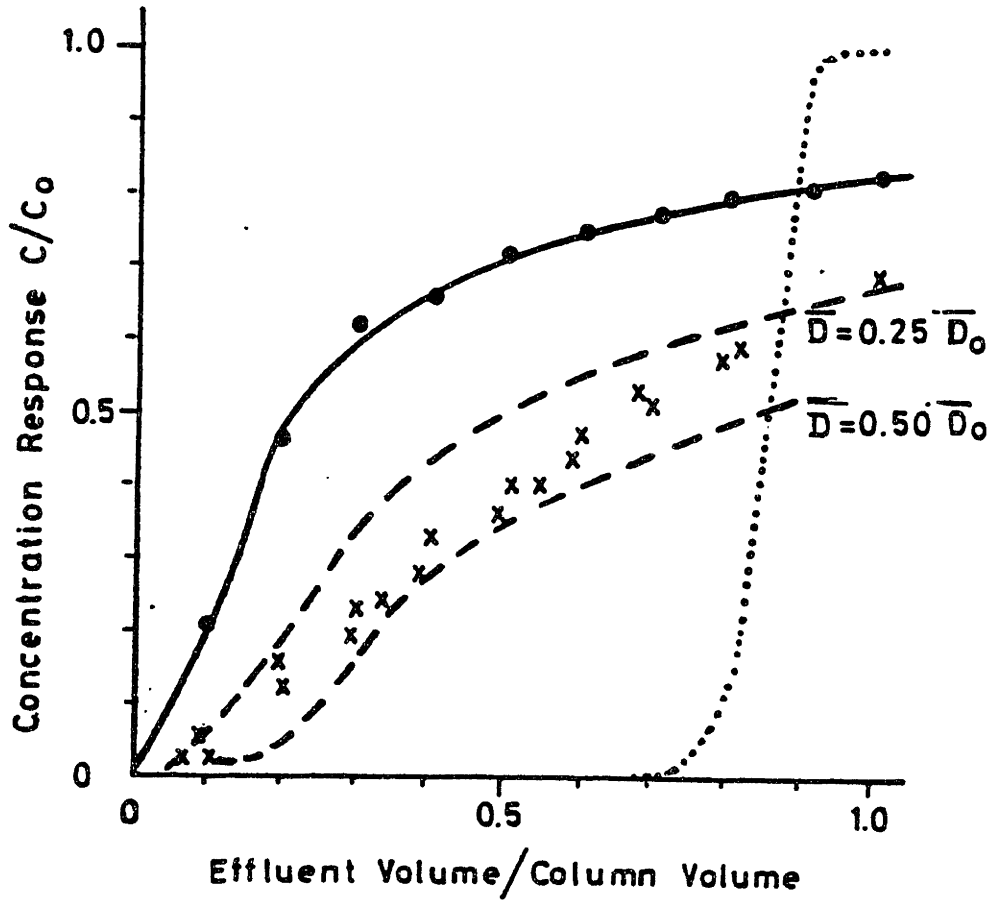


Figure 2.12: The ratio of the longitudinal dispersion coefficient to the coefficient of molecular diffusion vs. The Peclet number in a uniform sand (Freeze and Cherry, 1979, after Perkins and Johnston, 1963)

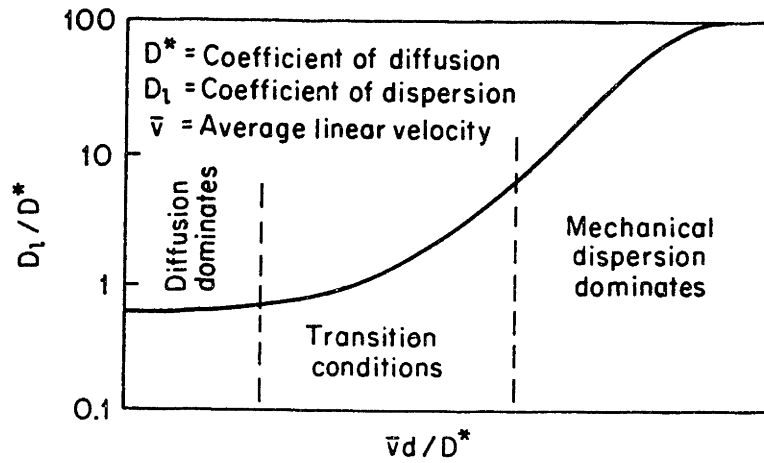
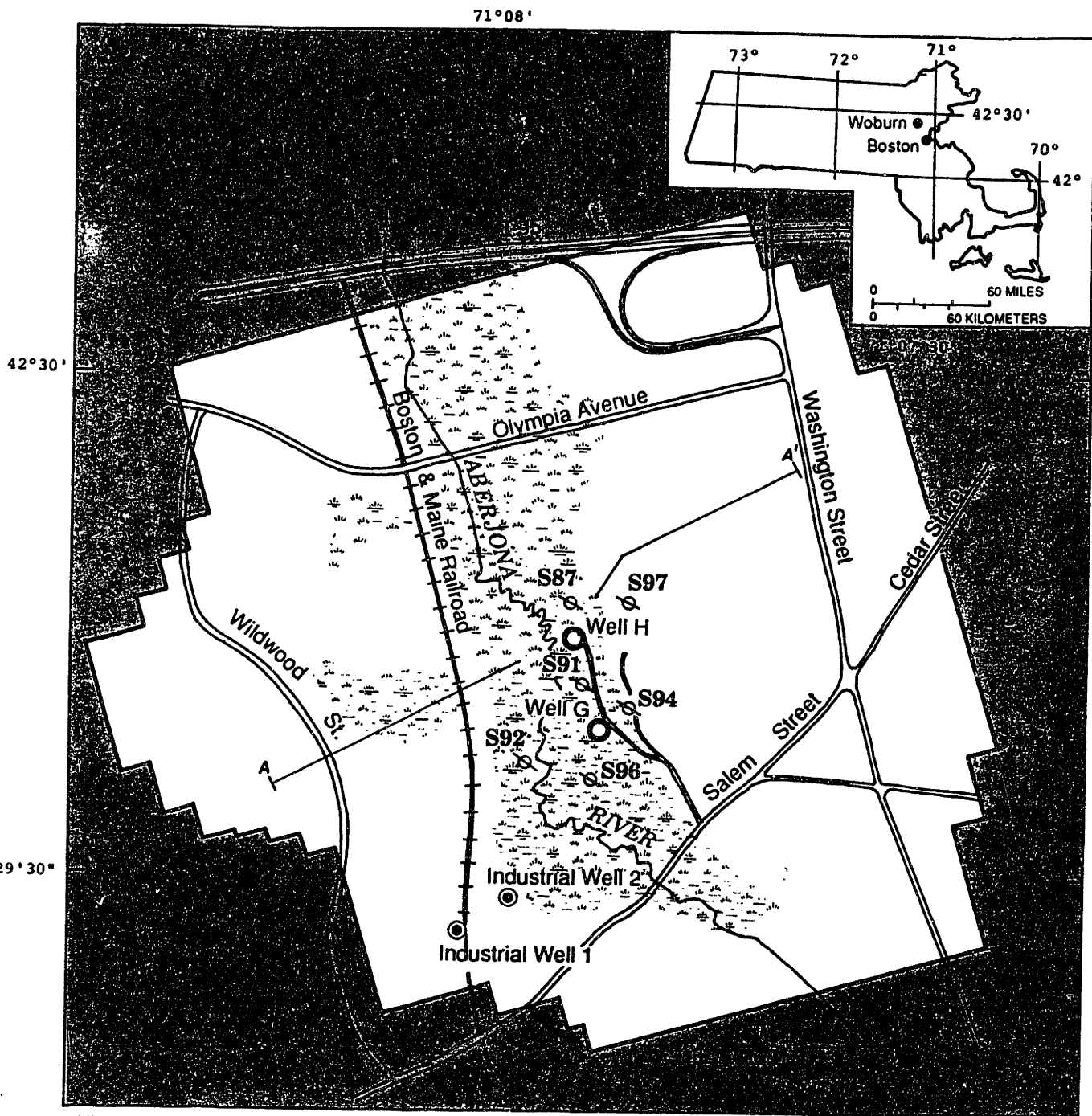


Figure 2.13: Map of the Wells G and H site in Woburn, Massachusetts showing the monitoring wells used in the USGS study conducted by De Lima and Olimpio (1989)



BASE MAP MODIFIED FROM TOPOGRAPHICAL MAPS T-12, 13, 16, 17, 21, 22, CITY OF WOBURN, MASSACHUSETTS

EXPLANATION





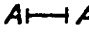

- | | |
|--|--|
|  Wetland |  Industrial supply well |
|  Active model boundary. |  Observation well |
|  A-A' Geologic section |  Public supply well |

Figure 2.14: Stratigraphy at the Wells G and H site in Woburn, Massachusetts along transect A-A' (See Figure 2.13) (De Lima and Olimpio, 1989)

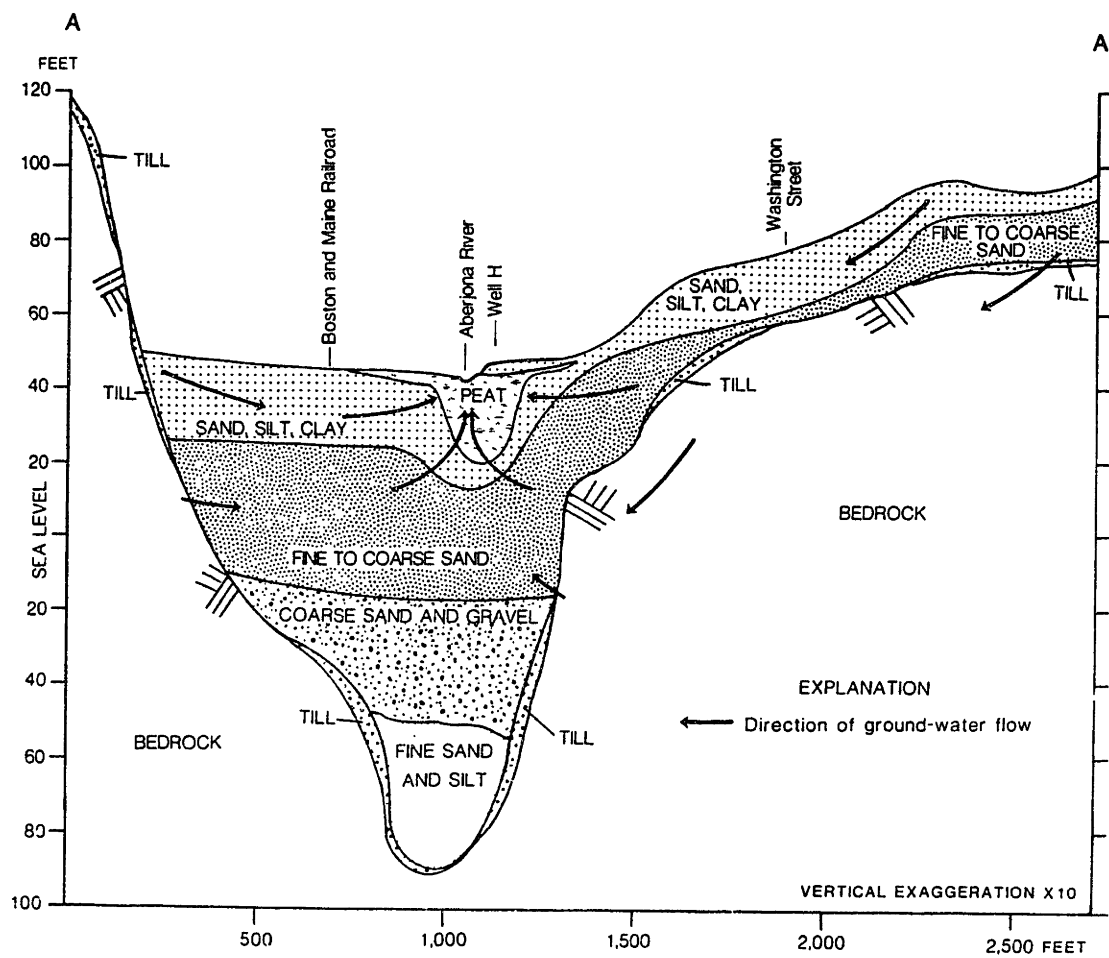


Figure 2.15: Map of the Wells G and H site in Woburn, Massachusetts showing the location of the soil cores sampled and the piezocone explorations conducted by Zeeb (1996)

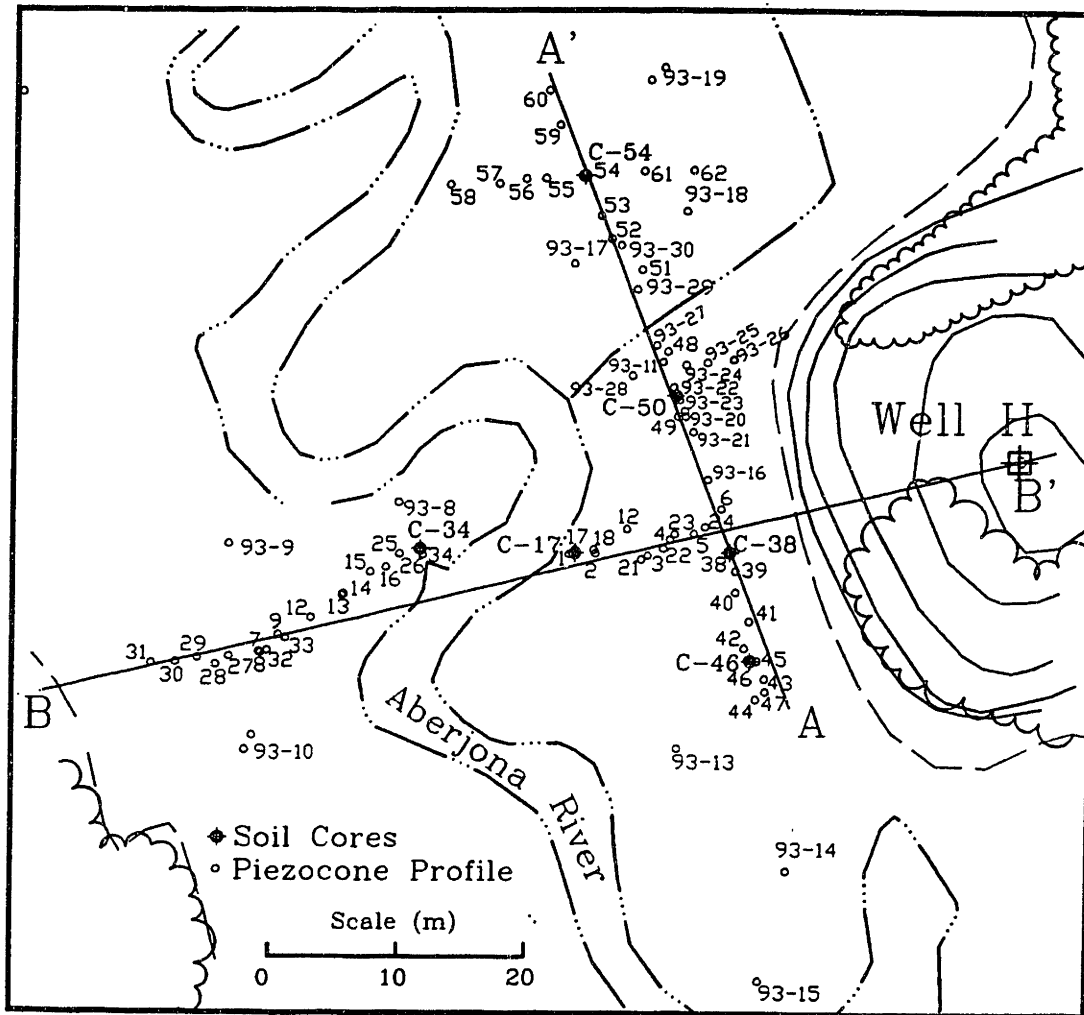


Figure 2.16: Stratigraphy at the Wells G and H site in Woburn, Massachusetts along transects A-A' and B-B' (See Figure 2.15) (Zeeb, 1996)

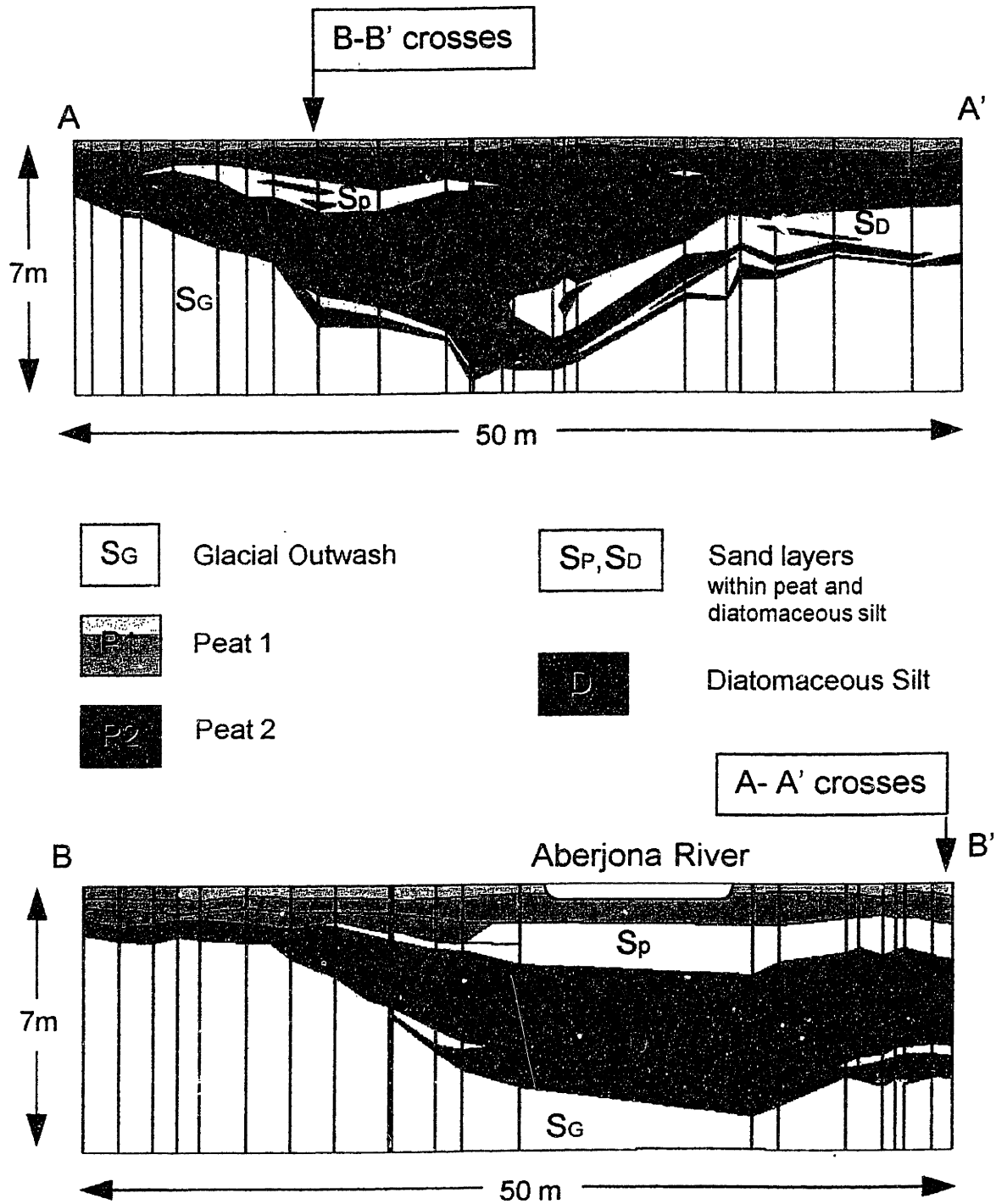


Figure 2.17: Map of the Wells G and H site in Woburn, Massachusetts showing the location of the soil cores sampled and tested by Bailon (1995)

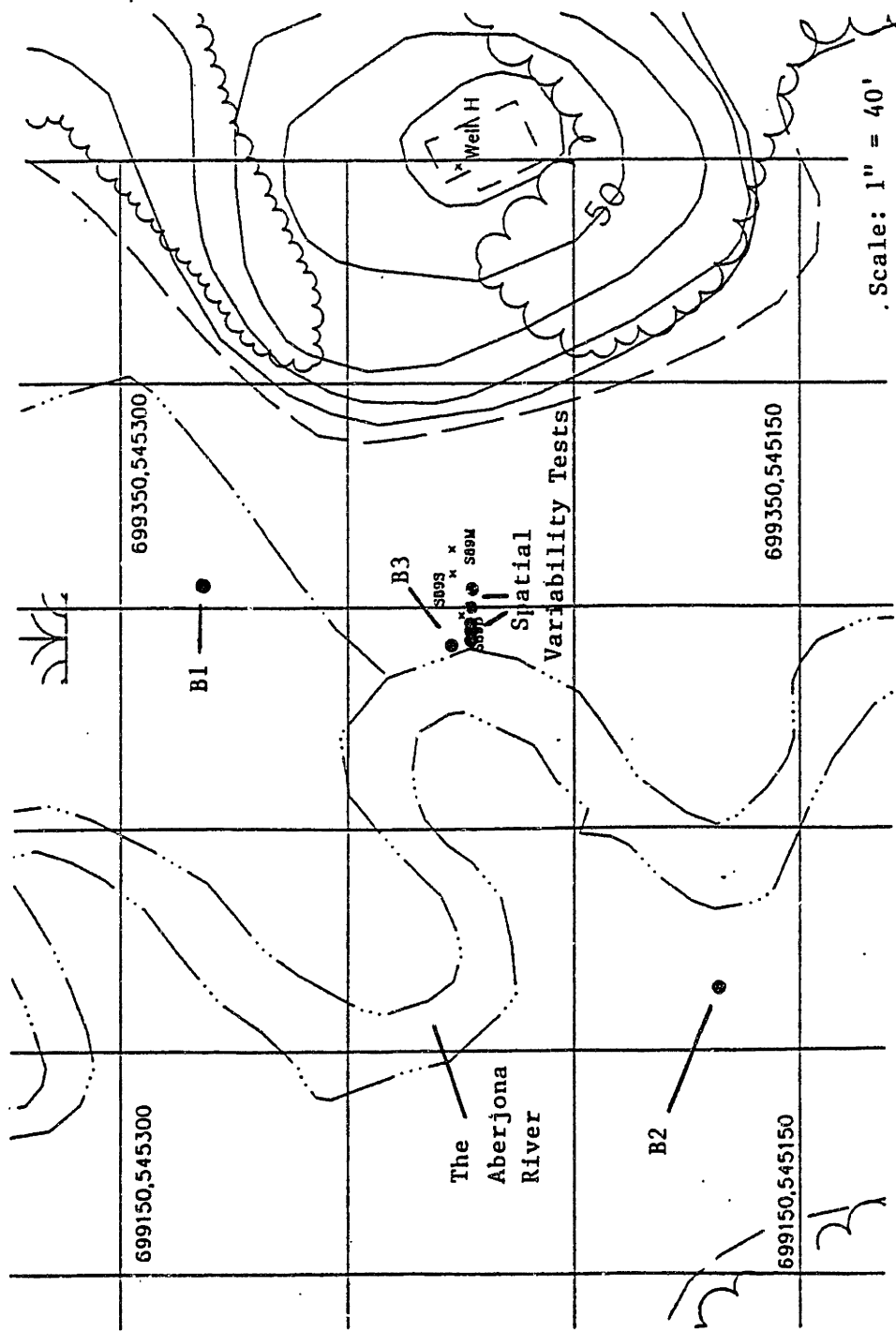


Figure 2.18: Schematic of soil profile of Cores 1 and 2 sampled and tested by Bailon (1995)

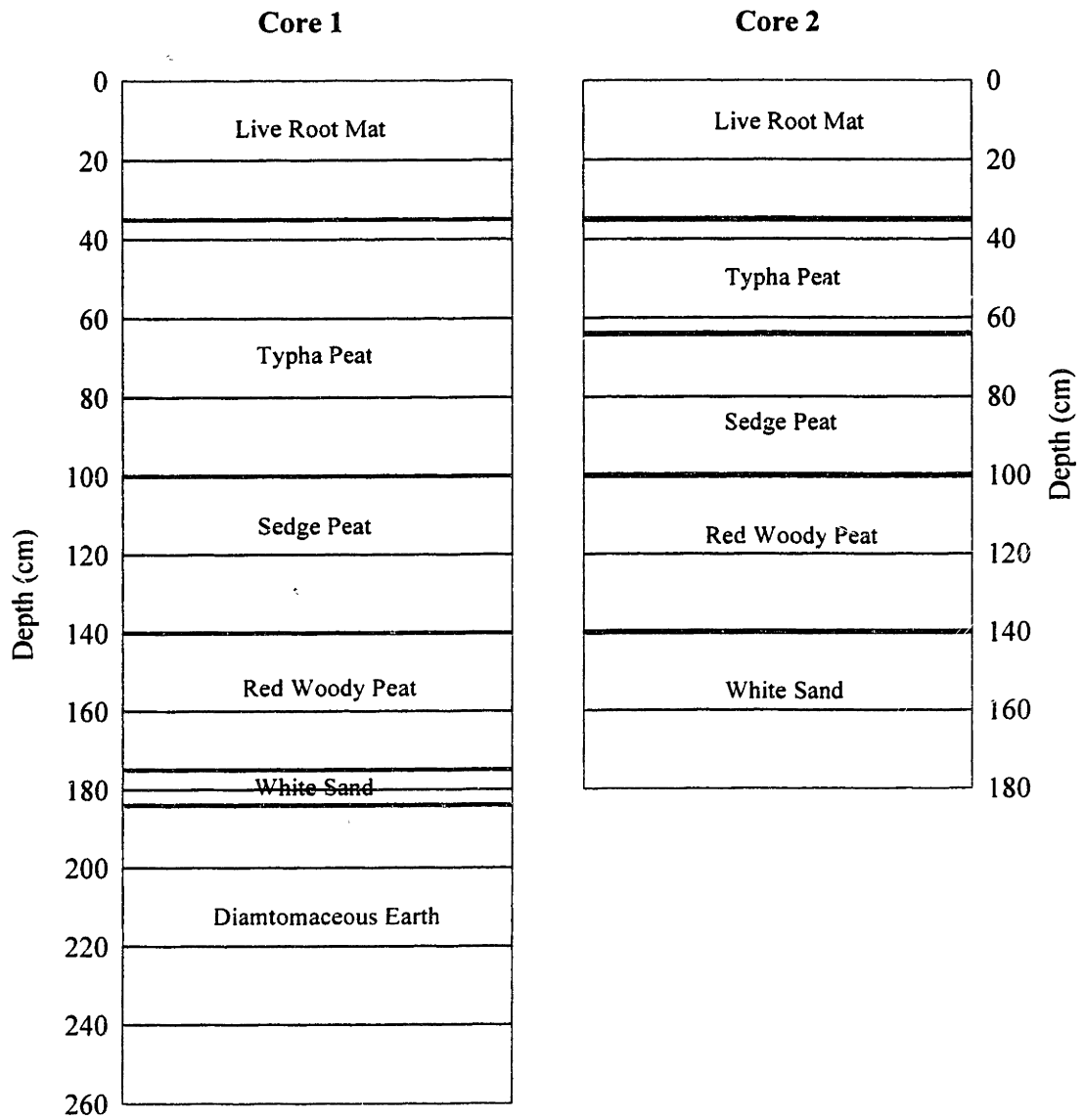


Figure 2.19: Summary of (a) Water content (b) Ash content (c) Specific gravity (d) Void ratio (e) Void ratio (f) C_k vs. Depth (Bailon, 1995)

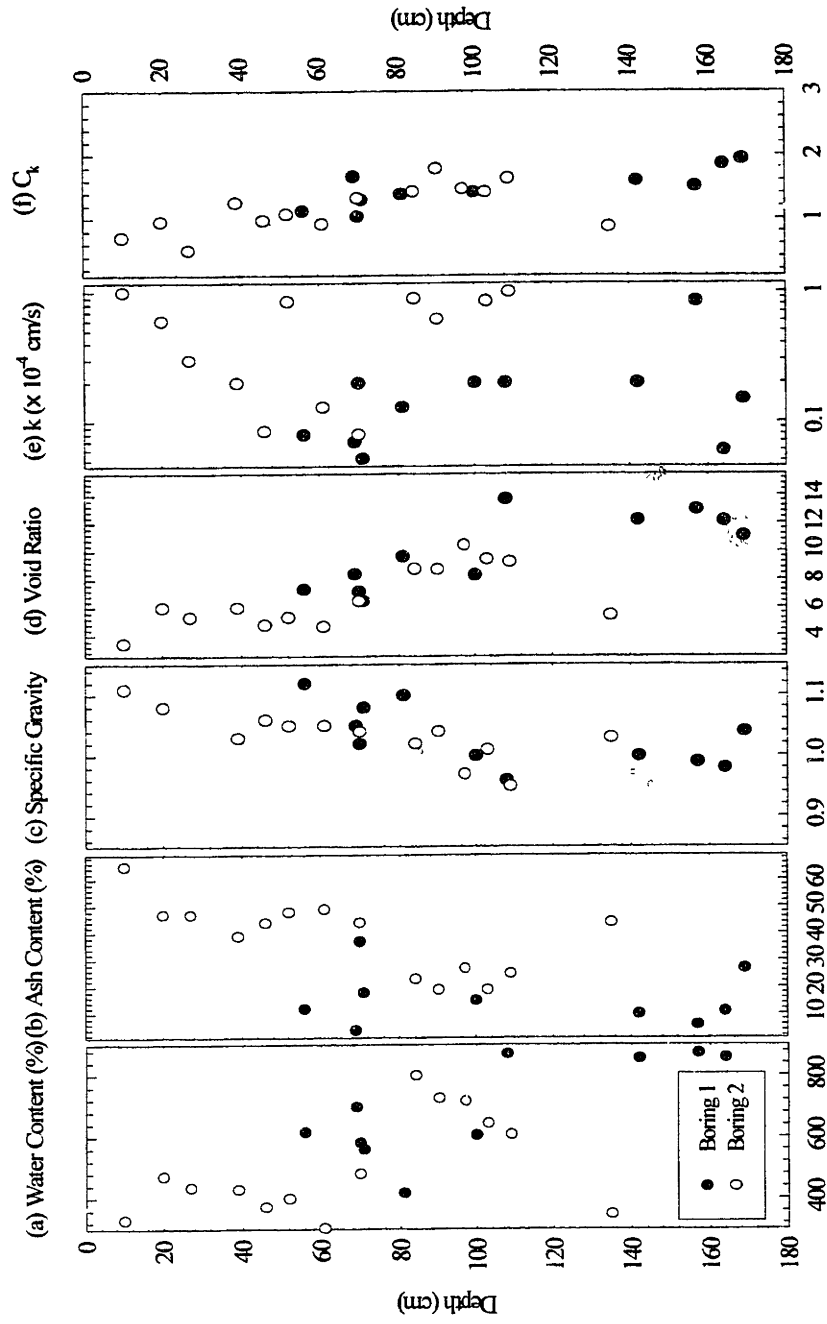


Figure 2.20: Summary of (a) CR (b) RR and (c) σ'_p vs. Depth (Bailon, 1995)

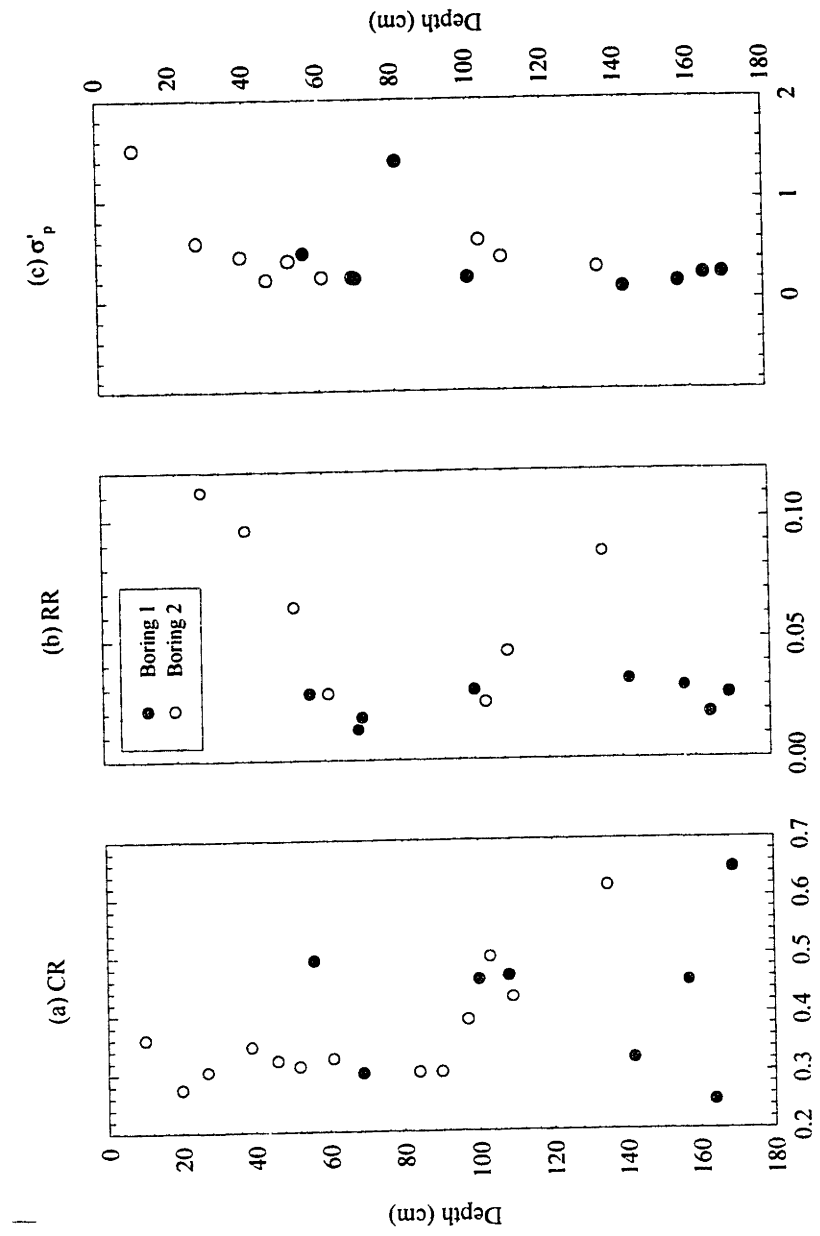


Figure 2.21: Summary of (a) Water content (b) Void ratio (c) Hydraulic conductivity and (d) C_k vs. Ash content (Bailon, 1995)

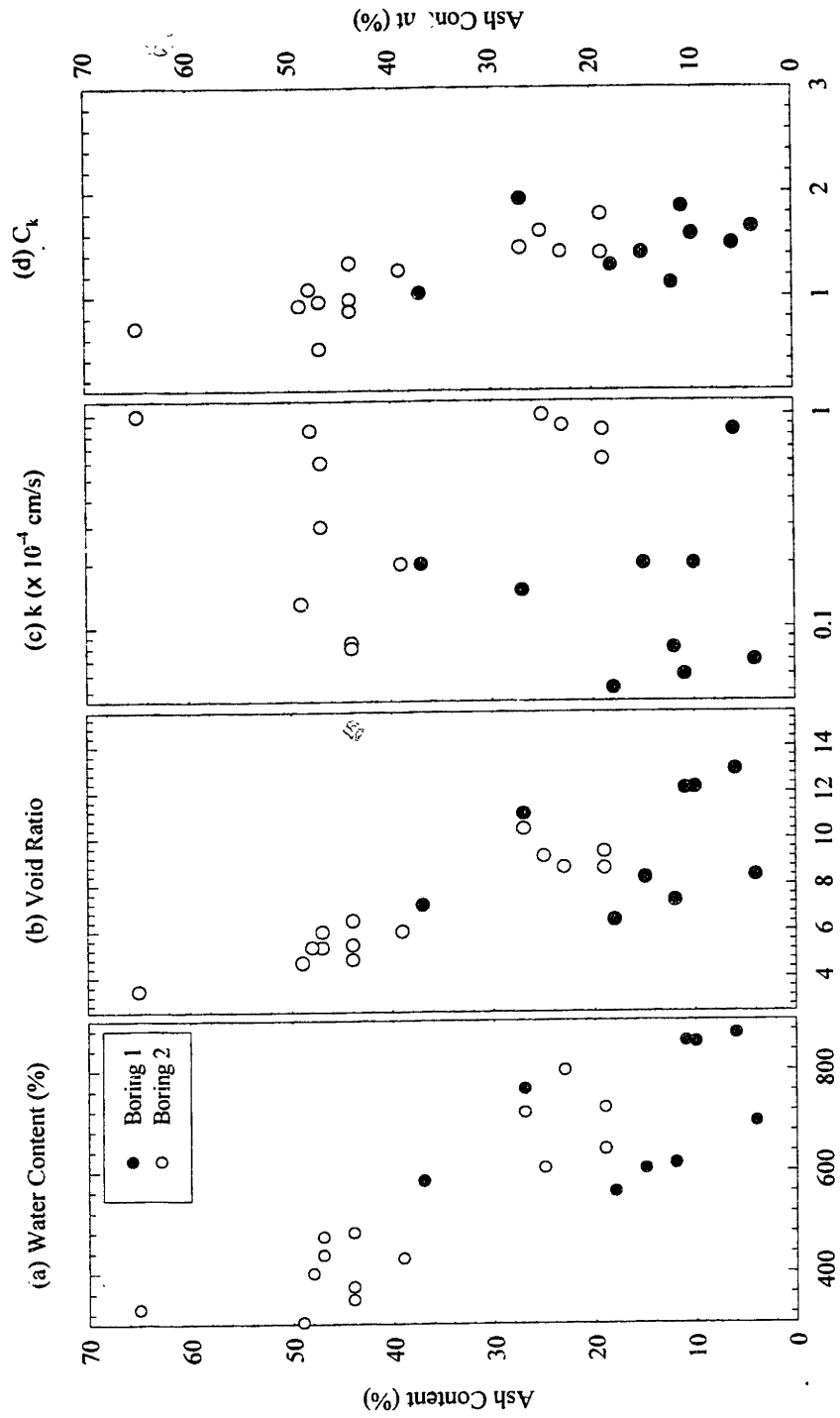


Figure 2.22: Summary of (a) Hydraulic conductivity (b) C_k (c) CR and (d) RR vs. Void ratio (Bailon, 1995)

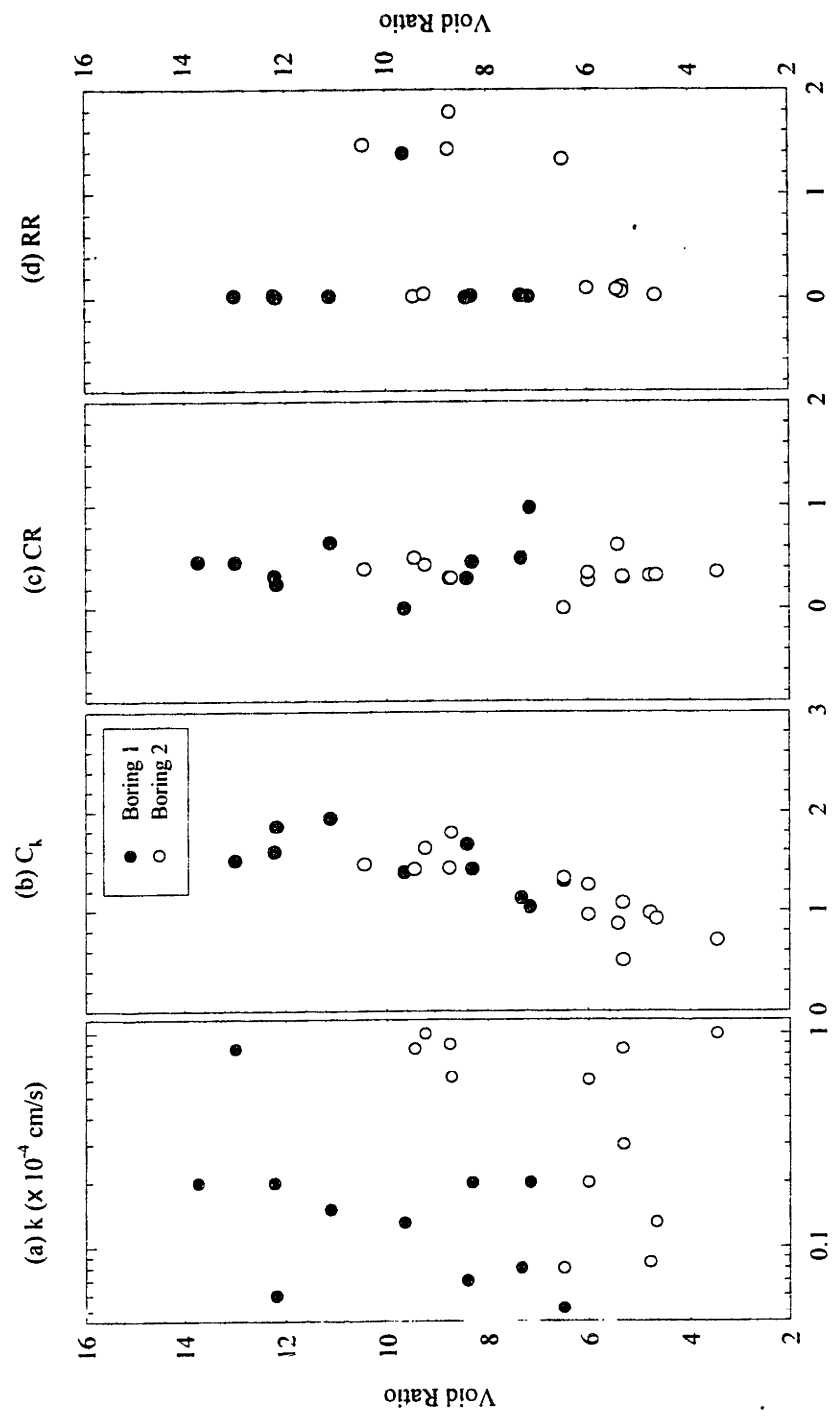


Figure 2.23: Breakthrough curve for tracer test on sand (Ramsay, 1996)

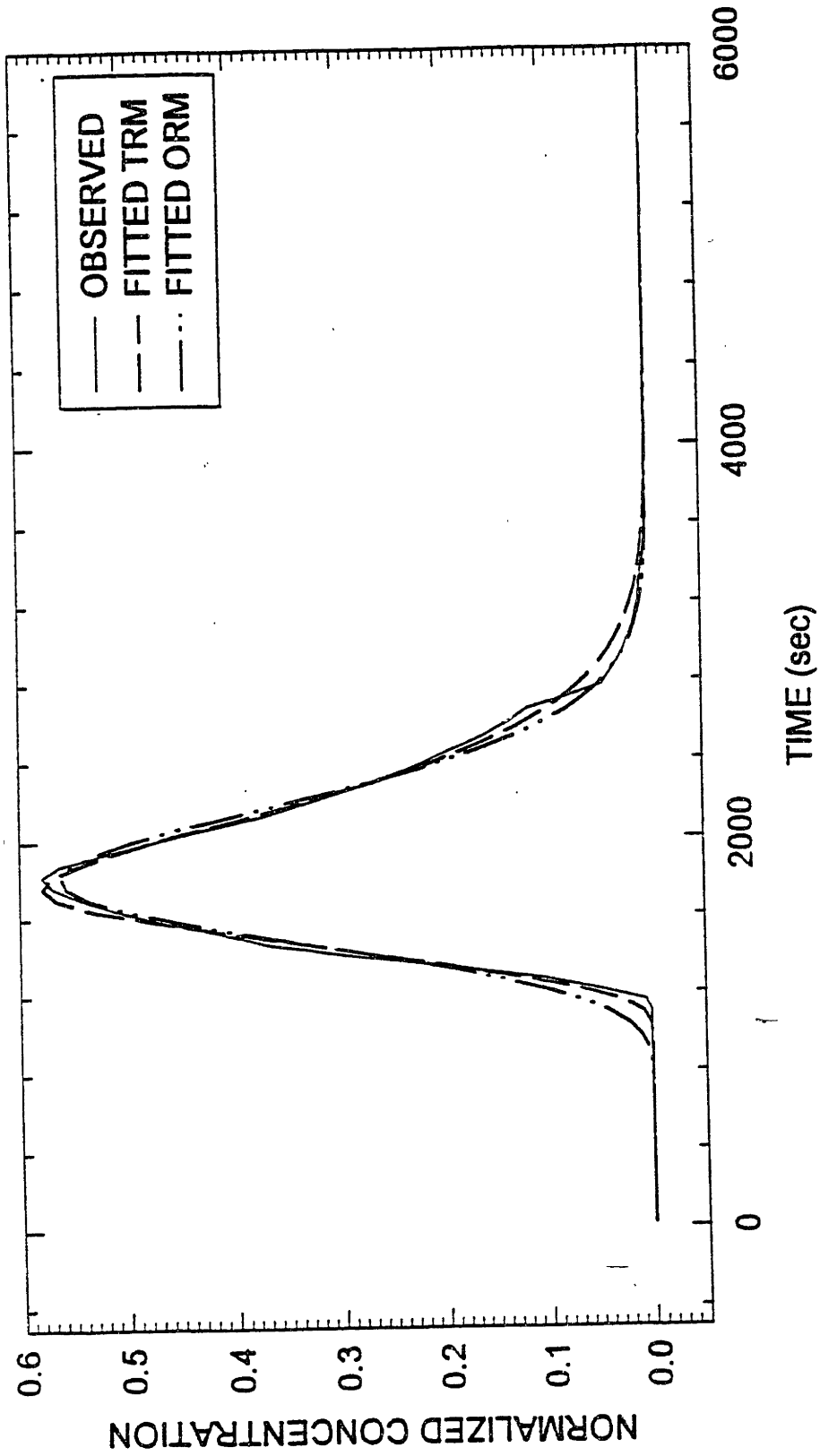
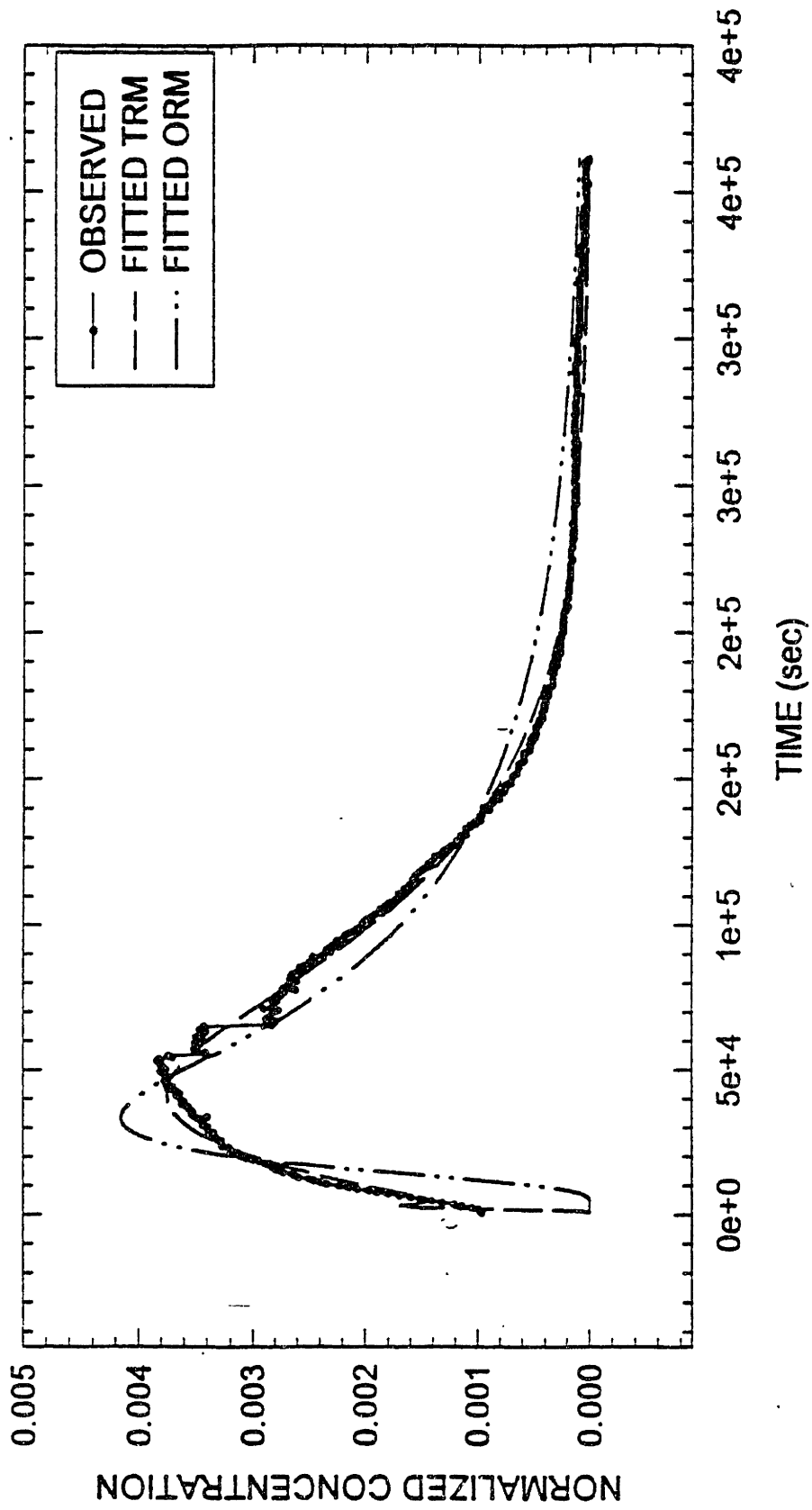


Figure 2.24: Breakthrough curve for tracer test on wetland soil (Ramsay, 1996)



3. EQUIPMENT AND MODIFICATIONS

3.1 INTRODUCTION

To better understand contaminant flow through wetland deposits, a specialized permeameter was built. Previous work (Bialon, 1995) had found that the direct relationship between porosity and hydraulic conductivity, which exists, in theory, for inorganic soils (see discussion in Lambe and Whitman, 1968, Chapter 19), does not hold for peat and highly organic soils, which constitute wetland deposits. Thus, a standard laboratory permeameter was modified to enable the determination of the hydrogeologic properties of a soil specimen, including its hydraulic conductivity, effective porosity, and dispersivity. The objective of measuring these parameters is to better understand the mechanics of flow through wetland deposits. Furthermore, since these soils are highly compressible, and their hydrogeological parameters are sensitive to changes in effective stress, the permeameter was also modified for two purposes: first, to allow for testing over a range of soil stress conditions, and second, to make accurate measurement of flow and stress within the testing system.

This chapter is divided into two principal sections. In Section 3.2 the specifications for the design of the permeameter developed by Ramsay in 1996 are presented, and the permeameter and all relevant testing components are described and evaluated. In Section 3.3, modifications to the equipment and to the experimental procedure since the equipment was first built and tested are discussed. The problems, discussed in Section 2.3.3.3, of incomplete recovery of the sodium chloride tracer in the breakthrough curves, of the extreme between field specimens, and of the diffusion of the tracer in the apparatus itself are also considered and addressed.

Tests discussed in this chapter were conducted on two types of soil: wetland deposits and sand. Details on the sources and properties of these soils are included in Chapter 4.

3.2 EXPERIMENTAL EQUIPMENT

3.2.1 EQUIPMENT OVERVIEW

To meet the experimental requirements, different permeameter designs were considered. A flexible-wall permeameter in a modified triaxial cell (Figure 3.1a) was eventually chosen over a rigid wall permeameter (Figure 3.1b), because the flexible wall design allows control of confining pressure, allows free deformation of the enclosed specimen, and eliminates side-wall leakage. Furthermore, changes in specimen dimensions, which can be related to changes in soil porosity, can be monitored by measuring the volume change of the cell fluid in response to an applied change in effective stress. For flow induction, a flow-controlled system (i.e. a system where the flow through the specimen is constant, and the gradient across the specimen is variable) was selected over a gradient-controlled system (i.e. a system where the gradient across the specimen is constant, and the flow through the specimen is variable) in order to provide better flow stability in a shorter period of time (Olson, 1985). Flow is induced using a flow pump, while the imposed hydraulic gradient and effective stress are measured by pressure transducers. Sodium chloride was chosen as the conservative tracer, and electrical conductivity probes were chosen to monitor variations in the tracer influent and effluent concentrations. In order to avoid running wires into the specimen, which would cause sample disturbance, the electrical conductivity probes were placed in the tubing before the top cap, and in the pedestal within the base (See Figure 3.2). The flow system was designed with two influent reservoirs, each with air-water interfaces (See Figure 3.3). These are connected to the same air-pressure regulator and to the top cap via a three-way valve. The system maintains constant pressure and a supply of influent at the up-gradient end of the specimen, while the effluent flow rate is controlled by a flow pump at the down-gradient end. The test data, including effluent electric conductivity, pressure, temperature, and displacement of the piston, are recorded using an electronic acquisition system. Using independent calibration curves, the measured electrical conductivity data are converted to concentration data. The tracer concentrations observed with time at the base of the soil specimen are entered into the CXTFIT model to obtain fitted estimates for the

hydraulic properties of the specimen, specifically, θ_m , θ_{im} , D , V , and α (see Section 5.4 and Chapter 6).

3.2.1.1 THE TRIAXIAL CELL

To take advantage of existing equipment and parts, a standard MIT triaxial cell with a removable pedestal (Again, see Figure 3.1a) was chosen as the basis of the special permeameter. The cell manifold and pedestal were modified as outlined below. In addition, the fixed top cap was replaced with an independent top cap to facilitate the application of hydrostatic stresses. The triaxial cell was designed for a cylindrical specimen 3.56 cm in diameter and of variable length (2 to 8 cm). The specimen was confined at the top and bottom by filter fabric, porous stones, distribution caps (See Section 3.3.3.2) and the top cap and pedestal, respectively. The circumference of the specimen was confined by two prophylactic membranes, sealed to the top cap and pedestal by o-rings (See Figure 3.4). Hydrostatic stresses are applied to the specimen via the cell fluid (distilled water). The cell itself was made of clear acrylic to allow visual inspection of the specimen, which helps to detect problems during testing. The acrylic cylinder is clamped between the base and top plate assembly as indicated in Figure 3.1a. The valve on the top plate allows venting during filling or draining of the cell.

The top cap drainage line was connected, via a three way valve, to two influent reservoirs, one containing distilled water, and the other NaCl solution. The pedestal drainage line was connected, also via a three way valve, to the effluent reservoir, as well as to the influent reservoir containing distilled water, to permit back pressure saturation.

To prevent corrosion and reaction, all metal components in contact with the permeant were made of stainless steel. Non-metallic components include the acrylic top cap, the pedestal epoxy, Teflon tubing, Buna-N O-rings, the carborundum porous stones, and the nylon filter fabric.

To induce downward flow in the specimen, the cell pressure must be equal to or greater than the pore pressure at the top cap (to prevent ballooning of the membrane), and the pore pressure at the pedestal must be less than that at the top cap. Thus, the effective stress in the

specimen increases linearly, if hydraulic conductivity is constant, from the top cap to the pedestal, reflecting the gradient in the specimen.

3.2.1.2 MANIFOLD CONTROL SYSTEM

The manifold control system and its various valves are illustrated in Figure 3.2. The pressures of the influent and cell fluid were established at the air-fluid interface of each reservoir. Air pressures were controlled by Fairchild regulators, shown in Figure 3.2. To eliminate pressure fluctuations when changing influent solutions, both of the influent reservoirs were connected to the same air pressure regulator. The pressure gauges in the system provided a continuous, qualitative indication of the cell and pore fluid pressures in the specimen.

3.2.1.3 FLOW CONTROL SYSTEM

The flow control system is illustrated in Figure 3.3. The pressure at the influent end of the specimen was maintained via the manifold system, while the flow-control device drew pore fluid from the effluent end of the specimen at a constant rate. Steady state flow was established when the pore pressure at the pedestal reached a constant value (i.e., when the gradient became constant). The flow pump was similar to the standard pressure/volume control devices used in the MIT triaxial systems (Figure 3.5). It was modified to allow a wider range of flow rates (approximately 10⁻⁵ cc/s to 10⁻¹ cc/s), as well as a larger total volume of flow (approximately 270 cc). The larger range of flow rates was obtained with a transmission system driven by an electric DC motor. The range of flow rates could be altered through a selection of gears in the drive system. A manual rheostat was then adjusted until the desired speed had been reached. The displacement of the piston at the core of the flow pump was measured using a linear variable differential transducer, LVDT, which was attached to the flow-control device by an aluminum mounting block (Figure 3.5).

3.2.1.4 PEDESTAL

A section of the removable pedestal is shown in Figure 3.6. The seating area rests on the base of the triaxial cell, and the narrow gap between the pedestal and the base was sealed

with o-rings. The pedestal is held in place by the cell pressure; it has a threaded port in the bottom for the o-ring fitting on the end of the drainage line. The stainless steel component of the pedestal is a continuous machined piece. Two 2-pin electrical conductivity probes, a pH probe, an oxidation-reduction potential probe, and a temperature probe were fit into a machined epoxy tube that held them in place in the pedestal while epoxy was cast around them. The epoxy tube now serves as the pedestal drainage path.

One other electrical conductivity probe similar to the 2-pin probes located in the pedestal was placed in the influent line between the top cap valve and the cell base plate to measure the mass of the tracer solution introduced into the specimen. A diagram indicating the location of all the electrical conductivity probes is provided in Figure 3.2.

3.2.1.5 DATA ACQUISITION

Data from the experiments were recorded using a central data acquisition system used in the Geotechnical laboratory at MIT. This was used to measure influent, effluent, and cell pressures, temperature, piston displacement, and influent and effluent electrical conductivity.

3.3 MODIFICATIONS TO EQUIPMENT AND TESTING PROCEDURE

3.3.1 SALT LOSS

Preliminary tests conducted by Ramsay (1996) showed incomplete recovery of the Sodium Chloride tracer (See Section 2.3.3). For tests on sand, the loss in tracer ranged from 81 to 96% and this loss increased with decreased flow rates through the specimen. For tests on wetland deposits, the loss in tracer ranged from 49 to 81% and this loss did not have any apparent relationship with flow rate (See Table 2.3). Initially, it was hypothesized that there were three possible salt sinks. First, salt might be lost through sorption onto the solid phase of the soil. Second, salt might be diffusing out of the prophylactic membranes encasing the soil in the cell fluid, or third, the salt might be lost through an internal leak in the equipment. Tests were conducted to determine which, if any, of these possible sinks was responsible for the salt loss.

3.3.1.1 SALT LOSS INTO THE SOIL

To test whether sorption could be a permanent sink for the salt, soil-salt interaction experiments were conducted on wetland deposits sampled from the Wells G and H site (See Section 3.3). These tests gave an indication of the time it takes for sorption to occur, and whether this sorption is reversible. These tests also gave a value for the coefficient of linear equilibrium sorption, K_s , which, in turn, gave a value for the retardation factor, R , to be used in the two-region model.

In these experiments, a wetland deposit sample was passed through a meat grinder so that the soil particles had a maximum size of 4 mm. Next, the soil was rinsed twice with distilled water to remove any salt that might be sorbed onto the solid phase of the soil or dissolved into the liquid phase (See Appendix B1 for the exact procedure). Then, a known amount of the rinsed soil was added to several bottles containing a range of sodium chloride solutions of known concentrations. The fluid from the bottles was sampled before the soil was added and several times over the course of 24 hours after the soil was added. The samples were analyzed for overall salt concentration using an electrical conductivity probe, then for chloride alone and sodium alone using ion specific probes. See Appendix B1 for a more detailed description of the procedure, for a mathematical explanation of the different parameters, and for an example calculation of the Freundlich Isotherms used in deriving values for K_s .

Two of these soil-salt experiments were conducted before, and one during, the hydraulic conductivity testing. The sorption coefficient, K_s , was first calculated from the electric conductivity data, and it ranged from 6.15 to 7.62 (See Table 3.1). The value of R was calculated for re-sedimented samples 9 and 10 and undisturbed sample N1 (See Sections 2.3.2, 4.3, and 5.2). For the coarse grained, re-sedimented S9 and S10 (Maximum particle size = 9 mm, Bulk density, $\rho_b \sim 0.31$, and Volumetric water content, $e \sim 6$) the retardation factor, R , was calculated to be 1.4. For the undisturbed sample N1, (Maximum particle size > 9 mm, Bulk density, $\rho_b = 0.21$, and Volumetric water content, $e = 9.2$) R was calculated to be 1.2. The sorption coefficient and the retardation factor were also estimated from the chloride specific sorption data and the sodium specific sorption data. The retardation factor

for chloride was calculated for both re-sedimented and undisturbed samples to be unity, which means that chloride is a conservative tracer in these soil systems. For sodium, R was calculated to be 2.60 and 2.43 for S9 and S10, respectively, and 1.60 for N1. These higher values of R indicate that sodium is highly sorptive in this soil.

In all of these experiments, it was shown that the sorption of sodium chloride was instantaneous since samples taken immediately after the soil was added to the bottles showed the same decrease of salt concentration as subsequent samples (See Figure 3.7). Also, sorption was reversible since the salts could be rinsed from the soil and the experiment repeated on the same soil.

3.3.1.2 SALT LOSS THROUGH THE MEMBRANE

The prophylactic membranes used to seal off the soil specimen from the cell fluid in the permeameter were tested to see whether Sodium Chloride might diffuse through them. The membrane was filled with 0.1 M Sodium Chloride solution, which is the equivalent concentration injected into the specimen during hydraulic conductivity tests. The membrane was then placed in a 500 ml bottle filled with distilled water (Figure 3.8). The electrical conductivity of the bottle and membrane fluids was measured, then both bottle and membrane were sealed. Two weeks later, the electrical conductivity of the two fluids was measured again. There was no detectable change in the electrical conductivity of either fluid. The experiment was duplicated with the same result.

3.3.1.3 SALT LOSS INTO THE EQUIPMENT

3.3.1.3.1 Salt Mass Balance (Tracer) Tests on Sand

Ramsay, 1996, had found that the percentage of salt lost during the hydraulic conductivity tests he conducted decreased with increasing flow rates. A calculation of the net salt loss for his three tests showed that approximately the same amount of salt was lost during each test ($0.041 \pm 0.012\text{g}$). As a result, Ramsay theorized that there was a finite salt sink, that is, a finite volume in the system into which salt was being lost.

To test Ramsay's theory that there was such a leak in the equipment, a sand sample was setup according to the procedure discussed in Chapter 5 (Also see Appendix B8), but without the distribution caps discussed in Section 3.3.3. A series of Tracer tests were conducted on the sand specimen. The effective stress and the flow velocity were varied from test to test to see what factors affected salt loss. Duplicate tests were run at each setting to show whether results were repeatable. The flow rates were changed for every other set of duplicate tests and ranged from 1.5×10^{-4} to 3.2×10^{-3} cm³/s. The effective stresses were also changed alternatively with the flow rates, and they ranged from 1.1 to 73.4 kPa.

Initially, ten minute pulses of 0.1 Molar sodium chloride solution were injected into the system. During the tracer tests, the electrical conductivity of the influent and effluent pulses were recorded. A typical influent pulse was square, whereas, a typical effluent pulse was roughly bell shaped, with a tail at the end. Duplicate tests, Tests **a** and **b**, showed that the results were repeatable (Figure 3.9).

The area under the influent and effluent curves was calculated to determine the percentage of salt recovered. The first tests run on the specimen, Tests **a** through **f**, showed a salt recovery of about 90%. However, the percentage of salt recovered varied over time with minimum recoveries as low as 72% (See Table 3.2a). Some 20 minute pulses were also injected into the system to see what effect, if any, a larger amount of salt injected had on the results, but no meaningful effect on percentage of salt lost was noted.

3.3.1.3.1.1 Interpretation of the data

There were no trends observed between effective stress and percent of salt recovered or mass of salt lost (Figure 3.10). Neither was there any apparent trend between flow velocity and percent of salt recovered (Figure 3.11a). However, the mass of salt lost increased with increased flow velocity (Figure 3.11b). This is due to the fact that, for 10 minute pulses, an increased mass of salt is input into the system when the flow rate is increased, and, when more salt is put into the system, more salt is lost.

The first eighteen tests (Tests **a** through **t**) on the sand specimen were run over the course of twenty four days, and there was a very clear trend observed between salt loss and the time

lapsed since the setup of the sand specimen. The longer the time lapsed since the first test, the lower the salt recovery (Figure 3.12). Thus, it appeared that the effluent probe was becoming less sensitive with time. Under ideal operating conditions, the probe measures the electrical resistance of the fluid between its two electrodes, or pins (Figure 3.13). However, it may be, that after many days of use without cleaning, impurities in the effluent are deposited on these pins, causing the probe to read a higher resistance than is actually given by the fluid. This higher resistance (lower conductance), translates into a lower concentration of salt, and in turn, suggests recoveries lower than 100% when compared to what the influent electrical conductivity probe was reading. It is important to note that the influent pulse was always square with a maximum concentration of 0.1 M which indicated that the influent probe was not becoming less sensitive with time (Figure 3.14).

3.3.1.3.1.2 Effluent Sampling

To determine how much the pedestal electrical conductivity probe readings differed from the actual concentration of the effluent, two sampling tubes with the same inner diameter as the effluent tubing, and 30 cm in length, were spliced into the effluent tubing. These tubes were placed into the effluent line, in parallel, using two three-way Whitney valves (Figure 3.15). These Whitney valves can both be opened to one of the two sampling tubes, such that the effluent flows through and fills it. To sub-sample the effluent, the Whitney valves are switched, simultaneously, to the other sampling tube, and the first tube is removed. The sub-sample is drained into an air-tight container, and the sampling tube is rinsed with distilled water and reattached to the effluent line. The sub-sampled fluid is then diluted and its electrical conductivity, chloride and sodium concentration measured.

This in-line system for sub-sampling the effluent during tracer experiments, not only gives a measure of the effluent concentration independently of the effluent probe, but the in-line Whitney valves allow for sampling without stopping the experiment, and without extreme reductions in the pore pressure in the soil, which would cause excess consolidation of the specimen.

3.3.1.3.1.3 Sub-sampled tracer tests on sand

When the data from the sub-sampled effluent were superimposed on the data measured by the effluent probe, it became clear that the effluent electrical conductivity probe was reading too low (Test **sa**). Figure 3.16 presents a comparison of the influent and effluent concentrations measured by the two techniques. A calculation of the percentage of salt recovered, given by the area under each of the curves, showed that for the readings based on the electrical conductivity probe, recovery was 74.2 %, whereas, for the sampled data, it was 94.2%.

To see whether a simple scaling rule could be followed to adjust the probe data, the breakthrough curve was normalized to the percentage of salt recovered, 74.2%. With this simple adjustment, the sampled data points coincided very well with the electrical conductivity probe data (Figure 3.17).

Another test, Test **sb**, was performed to see if cleaning the effluent electrical conductivity probe in mid-testing would be an effective way of improving recovery of salt. This test was run after three 10 minute pulses of 10% Micro solution were injected into the system and allowed to rinse through. The recovery was 102.0% according to the effluent electrical conductivity probe and 97.0% according to the sampled effluent (Figure 3.18). This further proves that the apparent salt loss in the system is due to the clogging of the effluent probe. Unfortunately, for the test run the day following the injection of the 3 Micro pulses, the salt recovered according to the probe was only 80.1%, which shows that re-clogging was occurring rapidly (See Table 3.2b). However, at this point, the sand specimen had been set up and tested for 38 days. In any case, intermittent cleaning with Micro during a test on wetland deposits would be impossible, since the Micro would damage the organic component of the specimen. So it was necessary to also find out how the apparatus behaves when organic soils are tested (See Section 3.3.1.3.2).

An additional test, Test **sc**, was run where samples were taken at the shortest practical interval to see how much, if at all, sampling during testing disturbed the progress of the breakthrough curve. A duplicate test, Test **sd**, was run at the same flow rate and effective stress without any samples being taken. The measurements show that, although sampling causes local irregularities in the breakthrough curve where samples were taken, overall, the

two data sets agree very well (Figure 3.19). These data were also normalized to the percentage of salt recovered, and the scaled and sampled data matched very well (Figure 3.20).

3.3.1.3.2 Salt Mass Balance (Tracer) Tests on Wetland Deposits

To see whether scaling of the breakthrough curves using the percentage of salt recovered would work for tests on wetland deposits, tests similar to those done on the sand specimen were conducted. A wetland deposit specimen was set up according to the procedure in Chapter 4 (Also see Appendix 4.2), but without the distribution caps discussed in Section 3.3.3. The effective stress and flow rates were kept constant during this test, and only three 10 minute and one 20 minute pulses were injected into the system since tests on wetland deposits run on the order of days and weeks, not hours as for sand. Samples taken during the course of these tests show that the probes are reading correctly (Figure 3.21), and that, in fact, the recoveries for the last three pulses averaged at $98.1 \pm 3.3\%$ according to the effluent probes. The salt recovery according to the samples was in fact lower, at $82.2 \pm 4.4\%$ (Figure 3.22). This low recovery was due to the fact that samples were taken at infrequent intervals, and that important parts of the curves, such as their peaks, were missing, thus giving a lower value for the area under the curve.

The improved recovery of Sodium Chloride may be attributed to the effluent electrical conductivity probe reaching a static equilibrium. That is, the two pins might have become saturated, or completely plated, and so gave stable readings over time. In fact, the effluent probe was re-calibrated after the experiment on the wetland deposit specimen, and the new calibration data used to interpret the test data, since with the old calibration curves, the effluent probe was reading higher than 0.1M for that concentration of salt solution. The slope and intercept of the new calibration curve were slightly lower than those for the previous calibrations, indicating that the probe had become less sensitive with use.

3.3.1.4 CONCLUSIONS

During the initial tests on sand and wetland deposits conducted by Ramsay, 1996, not all the Sodium Chloride used as a tracer in the experiments was recovered. Measurements indicated

that a finite amount of salt was lost in each of the tests conducted on sand specimens. By sampling the influent and effluent during experiments on sand and wetland deposit specimens, it was determined that no salt was actually lost to the system, but that plating of the effluent electrical conductivity probe suggested lower values of Sodium Chloride concentration than was actually present. This problem was solved by plating the effluent probe through repeated use to saturation, and then re-calibrating it. Frequent sampling during experiments ensured that the effluent electrical conductivity probe was reading accurately.

3.3.2 CONSOLIDATION

Ramsay's initial tests on wetland deposits showed that due to pore pressure differences across a specimen needed to induce flow, specimen consolidation was extreme (See Section 2.3.3). Extreme consolidation decreased the hydraulic conductivity during testing to a degree that made experiments prohibitively long. Even after decreasing the specimen height, the consolidation problem still occurred. To reduce this problem, it was proposed that re-sedimented (batched) wetland deposit specimens be used. Re-sedimented specimens would have three distinct benefits. First, the soil could be over-consolidated to a desired stress level that would reduce flow induced consolidation. Second, the stress history of the soil would be known, and third, the large, inherent heterogeneity within a natural specimen and between different natural specimens would be significantly decreased. This would allow for a better understanding of how size distribution affects the relationship between effective stress and hydraulic conductivity.

3.3.2.1 RE-SEDIMENTING PROCEDURE

Re-sedimenting wetland deposits requires three steps. First, soil is sampled in large quantities from the field. Soil for these experiments was sampled directly from the Wells G and H site in Woburn. The fixed piston sampler described in Bailon, 1995, was used to extract cores from the first meter of the wetland deposit within 3 meters of the flooded, east bank of the Aberjona River. The soil was extruded from the sampler immediately and collected in a large bucket, and several kilograms were taken back to the laboratory. There, it was mixed well, and all woody pieces larger than two centimeters removed. The soil was

then placed in air tight container with roughly 5 cm of water over it, and the air was removed from the head-space with a vacuum pump. The container was then covered with opaque plastic and placed in a humid room. All these measures were taken to prevent excessive oxidation and degradation of the material.

The second step in re-sedimenting wetland deposits is the processing step. Roughly one kilogram of soil is sub-sampled from the reserve, and distilled water is added to it until it is at a water content of 400%. Next, the soil is passed through a meat grinder which has several size settings, the largest setting producing a soil with a maximum particle size of 9 mm, and the smallest setting producing a soil with a maximum particle size of 4 mm. After the soil is processed, it resembles a wet, uniform looking slurry.

The last step is to re-sediment the slurry. The batching apparatus is a modified oedometer which has an extended collar, roughly 12 cm high (Figure 3.23). The slurry is spooned into the oedometer ring until the ring is full. Initially, only the filter paper and stone are placed on the slurry. This corresponds to a minimal load of 300 Pa. After the soil has settled a little, and the stone has partially entered the ring, the top cap, which is a brass cylinder that fits into the ring perfectly, is placed above the stone. The batch is left alone for one day before it is placed in a triaxial frame. This frame has a free moving piston and a displacement transducer attached, which allow for uni-axial loading and the measurement of consolidation, respectively. Load is added every other day for 8 days, at a Load Increment Ratio of 1, and the maximum stress on the batch does not exceed 50 kPa. For a more detailed procedure for processing and re-sedimenting of wetland deposits see Appendix 3.3.2.

3.3.2.2 PROOF TESTS ON RE-SEDIMENTED WETLAND DEPOSITS

Three tests were conducted to determine whether re-sedimented samples were sufficiently similar to field samples, and to show whether tests within one batch and between batches gave the same results for compressibility, stress history, specific gravity, void ratio, ash content and hydraulic conductivity. Specific gravity, ash content and constant rate of strain consolidation tests were run and their results compared to the same tests on field samples done by Bailon, 1995. These results showed that both the compressibility and hydraulic

conductivity behavior of re-sedimented wetland deposits fell within the range of those for field samples (See Table 3.3). The compression, CR, and re-compression, RR, ratios for the re-sedimented samples ranged from 0.32 to 0.40 and from 0.15 to 0.17, respectively. For the field samples, they ranged from 0.28 to 0.5 and from 0.015 to 0.3, respectively. The pre-consolidation stress for re-sedimented samples fell within the range of 29 to 88 kPa, which is a little higher than the range of those of the field samples which was 15 to 60 kPa.

Furthermore, C_k , the slope of the void ratio vs. hydraulic conductivity curve, had a range of 0.75 to 0.80 for the re-sedimented soil, and 0.75 to 1.7 for the field samples. However, the range of hydraulic conductivity values for the re-sedimented wetland deposits, at 2×10^{-6} to 8×10^{-6} cm/s, was narrower than, and at the lower extreme of, that of the field samples, at 1×10^{-1} to 7×10^{-6} cm/s. This is to be expected, since the re-sedimented samples have less large irregularities, are finer and are more uniform than the field samples.

Also, the water content values of the re-sedimented samples are lower than those of the field samples, and their void ratios, and ash contents are in a narrow range at the low extreme of the those of the field samples. The specific gravity, on the other hand, is higher. These low values of water content and of void ratio, and the high value of specific gravity are most likely reflecting the elimination of large woody pieces during processing, which would contribute to larger pore size, and to an increase in the portion of less dense material in the soil. Overall, however, the re-sedimented samples seemed to duplicate the engineering and physical properties of the field samples, while eliminating the variability within and between samples.

This is shown by comparing the CRS results for specimens from the same batch and between batches (Table 3.4). Although the data for the first specimen tested in Batch 2 was lost, a comparison between the two specimens tested from Batches 1 and 3 show that for a given batch, values of CR and C_k are all within 5%. Values for RR are within 8.8%, and values of e_0 are uniform within a batch. However, there is a larger difference between values of pre-consolidation pressure. Also, the measured pressure is consistently lower than the actual pressure imposed on the sample. These pre-consolidation pressures are so low, however....

For specimens in all three batches, the average values of CR, RR, and C_k are $0.348 \pm 8.5\%$, $0.16 \pm 6.8\%$, and $0.78 \pm 3.2\%$, respectively. This shows that the re-sedimentation procedure gives the desired repeatability from batch to batch. It should be noted that values for e_o have a larger scatter since the pre-consolidation pressure was different for the different batches. Subsequent batches were loaded to the same pressure.

3.3.2.3 CONCLUSIONS

Consolidation of the specimen during testing was extreme for wetland deposits. This caused the specimen to become virtually impermeable as the tests progressed. This problem was avoided by using re-sedimented soil specimens which were pre-consolidated to pressures at the higher end of the of field sample range. These re-sedimented samples also proved to be less variable from one sample to the next and less heterogeneous than field samples while maintaining the compressibility, the consolidation histories, and the hydraulic conductivity range of field samples.

3.3.3 EVALUATION OF END EFFECTS

Some tracer experiments on the permeameter were conducted without any specimen. This was done in order to check the effect, if any, of the experimental setup on the breakthrough of the tracer. The permeameter was setup with only nylon filter paper and the two carborundum filter stones (4 mm high and 3.556 cm in diameter) that are used to distribute the influent and effluent at either end of the specimen. Then, a 10 minute pulse of 0.1 M NaCl solution was injected into the system.

Even though the influent pulse was square, the resultant breakthrough curve was bell shaped with some tailing at its end (Figure 3.24). Furthermore, when the flow rate was decreased and another 10 minute pulse injected, the resultant breakthrough curve was flatter and wider, and showed more pronounced tailing. This apparent retardation of the sodium chloride tracer is indicative of two region flow. That is, this data shows that there is an *immobile* region in the system into which NaCl is diffusing, initially, and then out of which it is diffusing when the system is flushed with fresh water.

In an effort to locate this immobile region, the permeameter was setup without the filter stones and paper, and the tests were repeated. In this configuration, the resultant breakthrough curves were slightly rounded, but basically square no matter what the flow rate (Figure 3.25). This pinpointed the filter stones as the source of the observed two region behavior.

3.3.3.1 PROPOSED DIFFUSION MECHANISM

Since the carborundum filter stones do not react with sodium chloride, and since the pore spaces within the stones are uniform and evenly distributed, it was theorized that the two region behavior was a result of the geometry of the setup. It seems likely that, since the salt water solution was injected into the stones at a single point, and since it was also removed from the stones at a single point, that not all the pore spaces in the stone were directly serviced by the salt water. That is, there is probably a direct path between the injection and collection points, through the center of the stones, which extends radially in proportion to the flow rate (Figure 3.26), and that the higher the flow rate, the narrower the path, and vice versa. This action divides the stones into two regions, the 'mobile' region, in which the tracer stream is flowing, and the 'immobile' region, into and out of which the tracer can only diffuse.

To test this theory, the breakthrough curves (BTCs) collected for the tracer tests on the filter stones were fitted using the CXTFIT program in the One Region Model mode (See Section 2.2.4). The fit for the 'fast' breakthrough ($q = 1.48 \times 10^{-3}$ cm/s) showed that the model-calculated effective porosity is 4% less than the actual, measured effective porosity of the filter stones (See Figure 3.27a). Though the difference in the θ_m for the 'fast' case is not significant, the Two-Region transport in the stones becomes more pronounced for the 'slow' breakthrough ($q = 6.16 \times 10^{-4}$ cm/s). In fact, it was no longer possible to use the One-Region Model to fit this breakthrough curve which had significant tailing, which implies Two-Region flow (See Figure 3.27b). This indicates that, as flow velocities decreased, there was more time for the sodium chloride to flow into the 'immobile' region of the stones. Also, dispersion of the NaCl tracer increased causing the injected plug to spread more. These

effects would become more problematic at the low flow velocities used in tracer tests on wetland deposits.

3.3.3.2 LIMITING END EFFECTS

It was assumed that if the inlet and collection points could be distributed across the stones, the two region problem would be minimized. To that end, 'distribution' caps were made. These caps were made from plexi-glass cylinders having the same diameter (3.556 cm) as the top cap and pedestal of the permeameter. These cylinders were drilled such that holes were started from a single point at one end of the cylinder and angled so that they emerged in concentric circles at the other end (Figure 3.28). Thirteen 1 mm diameter holes were drilled in total. To test the performance of these caps, the permeameter was setup with the caps, filter stones and the tracer tests were repeated. The resultant breakthrough curves showed tremendous improvement as the breakthrough curves were almost square (Figure 3.29). Though these improvements are significant, additional improvements are perhaps possible with even more flow paths in the caps. The number of flow paths are limited, however, by the number and size of holes that are practical and possible to drill into these small cylinders.

3.3.3.3 CONCLUSIONS

Tracer tests on the permeameter alone showed that there was apparent two region behavior, or an immobile region, in the equipment itself. Further tests showed that this immobile region was created in the filter stones when the tracer was injected into and collected from them at a single point, limiting the advective flow of the tracer to the center of the stones. This problem was reduced by placing flow distribution caps at the top cap and pedestal of the permeameter. These caps translate the single injection and collection points into 13 points which service more of the specimen directly.

3.3.4 ELIMINATING TRAVEL TIME

Since the permeameter's tracer injection point is at a significant distance upstream of the electrical conductivity probe in the pedestal (See Figure 3.2), during tracer experiments, the tracer travels a considerable distance before reaching the top of the soil specimen. Since

breakthrough data is collected from the instant that tracer is injected into the system, the resultant breakthrough curves include the time it takes for the tracer to travel from the injection point to the top of the specimen (See Figure 3.30).

Therefore, it is necessary to remove the initial portion of all breakthrough curves. That is, it is necessary to shift the breakthrough curve by the amount of time it takes for the tracer to travel from the injection point to the top of the soil specimen. Since the actual distance from the injection point to the top of the pedestal is unknown, it was necessary to find values for the tracer travel time at different flow rates experimentally.

To find the equation defining tracer travel time from the injection point to the pedestal electrical conductivity probe as a function of flow rate, the following experiment was conducted. Tracer experiments were conducted on the permeameter which was set up with the distribution caps and the filter stones and paper, but without any specimen. Tracer was injected into the system at a constant flow velocity, and its breakthrough measured. The time for 5% of the tracer to break through, T_5 , was determined from the breakthrough curve (See Figure 3.31). Similar tracer tests were conducted at a wide range of flow velocities (Figure 3.32). A value of T_5 was determined for each value of flow velocity. These data is plotted in Figure 3.33. The equation defining T_5 as a function of flow velocity, q , was determined from the linear regression on these data. This equation is: $T_5 = -0.975q - 0.247$.

3.4 REFERENCES

- Bialon, J.L. *Characterization of the Physical and Engineering Properties of the Aberjona Wetland Sediment*. M.S. Thesis. Massachusetts Institute of Technology, Cambridge, MA, 1995.
- Lambe, T. W., Whitman, R. V., *Soil Mechanics*, Wiley and Sons, New York. 1968.
- Olsen, H. W., Nichols, R. W., and Rice, T. L., *Low Gradient Permeability Measurements in a Triaxial System*, *Geotechnique*, 35.2, 1985: 145-157.

Ramsay, W. B., *A Modified Triaxial Permeameter for Physical Characterization of Parameters Affecting Contaminant Transport Through Wetland Deposits*. M.S. Thesis, Massachusetts Institute of Technology, Cambridge, MA. 1996.

Ratnam, S., *Geotechnical Centrifuge Modeling of the Behavior of Light Nonaqueous Phase Liquids (LNAPLs) in Sand Samples Under Hydraulic Flushing*. M.S. Thesis, Massachusetts Institute of Technology, Cambridge, MA. 1996.

Table 3.1a: Summary of K_d Values Calculated from Soil-Salt Sorption Experiments on wetland soils

K_d			
Trial Number	Sodium Chloride	Chloride	Sodium
1	6.15	0.12	31.05
2	7.63	-	-
3	7.58	0.12	27.78
Average	7.12	0.12	29.41

Table 3.1b: Summary of R Values Calculated from K_d , Bulk Density and Void Ratio of Soil

R			
Soil Type	Sodium Chloride	Chloride	Sodium
S9	1.39	1.01	2.60
S10	1.35	1.01	2.43
N1	1.16	1.00	1.67
Average	1.30	1.00	2.23

Table 3.2a: Summary of testing parameters and salt recovered for Tracer Tests on Sand Specimen 1

Days Since Setup of Specimen	Test Name	Pulse Duration (min)	σ' (kPa)	Flow Velocity (cm/s)	Area Under Influent Pulse Curve	Area Under Effluent Breakthrough Curve	% Recovered	Average Recovered per Duplicate	Error in Average per Duplicate
1	a	10	19.9	0.00223	59.68	54.16	90.7%	91.1%	0.48%
1	b	10	20.0	0.00207	60.91	55.65	91.4%		
2	c	10	44.8	0.00221	60.73	53.90	88.7%	89.4%	1.05%
2	d	10	45.1	0.00209	60.64	54.61	90.1%		
3	e	10	44.8	0.00051	57.55	52.82	91.8%	90.5%	1.97%
5	f	10	44.5	0.00055	59.86	53.43	89.3%		
9	i	10	70.8	0.00126	59.40	47.85	80.6%	78.9%	2.96%
9	j	10	73.4	0.00128	61.08	47.19	77.3%		
15	k	10	50.4	0.00153	60.62	51.53	85.0%	84.3%	1.13%
15	i	10	51.8	0.00153	60.07	50.25	83.6%		
18	m	10	1.1	0.00138	60.38	44.78	74.2%	74.2%	0.10%
18	n	10	3.6	0.00141	60.50	44.94	74.3%		
21	o	20	6.3	0.00106	123.00	89.77	73.0%	72.3%	1.33%
21	p	20	8.3	0.00114	125.52	89.90	71.6%		
22	q	20	13.2	0.00112	119.95	92.91	77.5%	76.6%	1.51%
22	r	20	15.0	0.00110	123.40	93.55	75.8%		
24	s	20	10.6	0.00016	109.89	91.97	83.7%	84.7%	1.71%
24	t	20	16.1	0.00015	114.05	97.79	85.7%		

Table 3.2b: Summary of testing parameters and salt recovered for Tracer Tests on Sand Specimen 1 with Sub-Samples Taken

Days Since Setup of Specimen	Test Name	Pulse Duration (min)	Effective Stress (kPa)	Flow Velocity (cm/s)	Area Under Influent Pulse Curve	Area Under Effluent Breakthrough Curve	% Recovered (Effluent Probe)	% Recovered (Subsamples)
36	sa	10	2.5	0.00200	59.97	44.48	74.2%	94.3%
37	sb	10	2.5	0.00200	59.90	61.09	102.0%	97.0%
39	sc	10	3.3	0.00086	59.73	47.28	79.1%	no sub-sam.
39	sc'	10	3.3	0.00086	59.56	47.72	80.1%	96.8%

Table 3.3: Physical Characteristics of re-sedimented (batched) wetland soil as Compared to those of undisturbed soil tested by Bailon (1995)

Property	Batches	Undisturbed Soil
CR	0.319 - 0.362	0.28 - 0.5
RR	0.02 - 0.184	0.015 - 0.3
σ'_p (kPa)	18 - 76	15 - 60
C_k	0.91 - 1.89	0.75 - 1.7
k_o (cm/s)	2E-7 - 2E-6	1E-4 - 7E-6
w_c (%)	251 - 279	300 - 800
e_o	5.1 - 6.14	4.5 - 10*
Ash Content (%)	56 - 60	50 - 95
G_s	1.9 - 2.1	0.98 - 1.48*

*back calculated to give S = 100%

Table 3.4: CRS data for re-sedimented wetland soil specimens N1 to N3

Property	S1		S2 a	S3		Averages*
	a	b		a	b	
CR	0.331	0.348		0.342	0.325	0.337 +/- 3.1%
RR	-	-		0.162	-	
C_k	1.05	0.91	0.96	1.15	1.10	1.03 +/- 9.6%
e_o	5.89	5.84		5.44	5.73	5.73 +/- 3.5%
W_c	285%	278%		256%	261%	2.70 +/- 5.1%
S_o	95.3%	93.7%		95.5%	92.5%	94.3% +/- 1.5%
σ'_p (kPa, measured)	30	37	78	44	30	-
σ'_p (kPa, applied)		55	88		48	-

Figure 3.1: (a) Permeameter (Modified standard MIT triaxial cell)

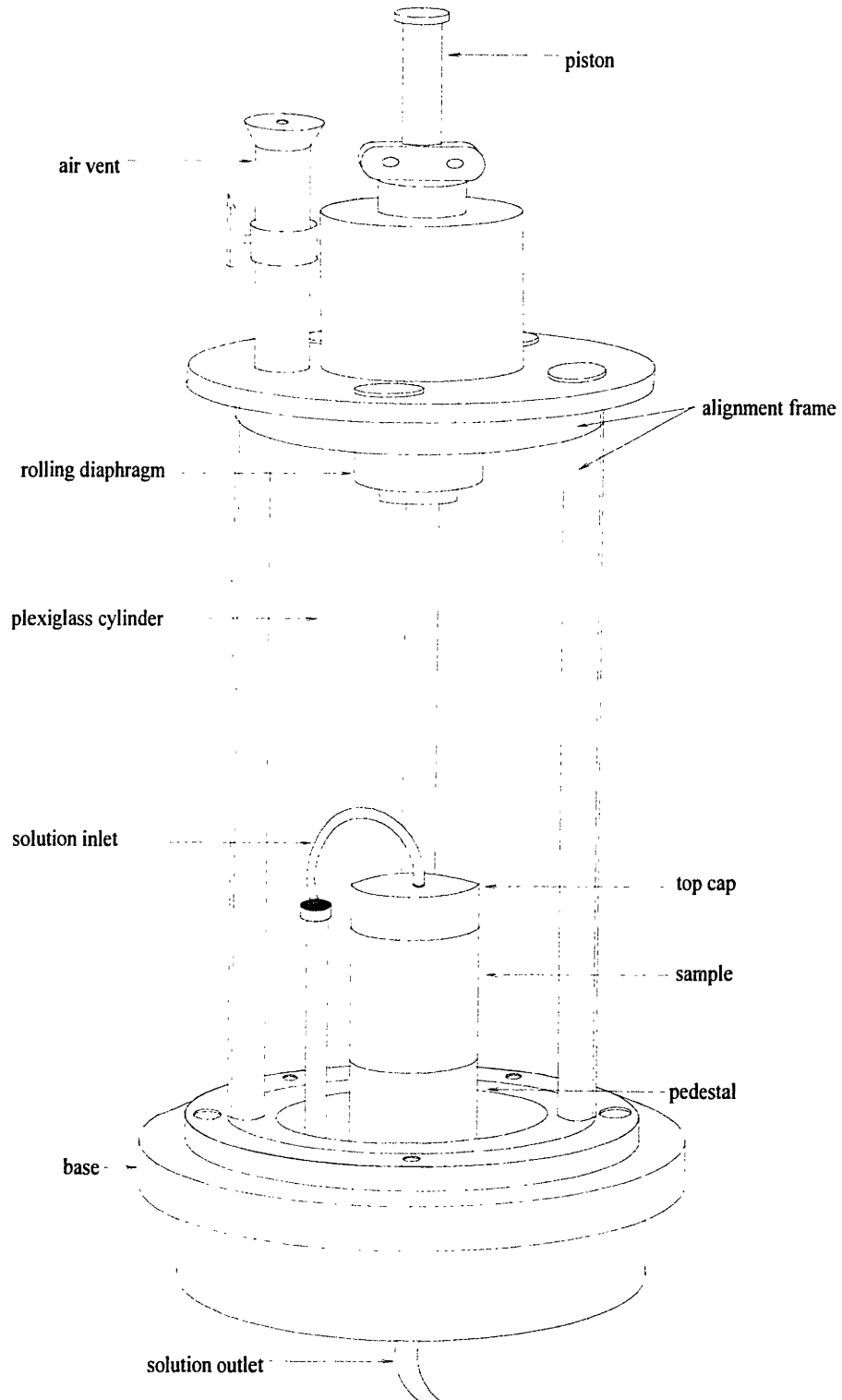


Figure 3.1: (b) Rigid wall permeameter (Lambe and Whitman, 1968)

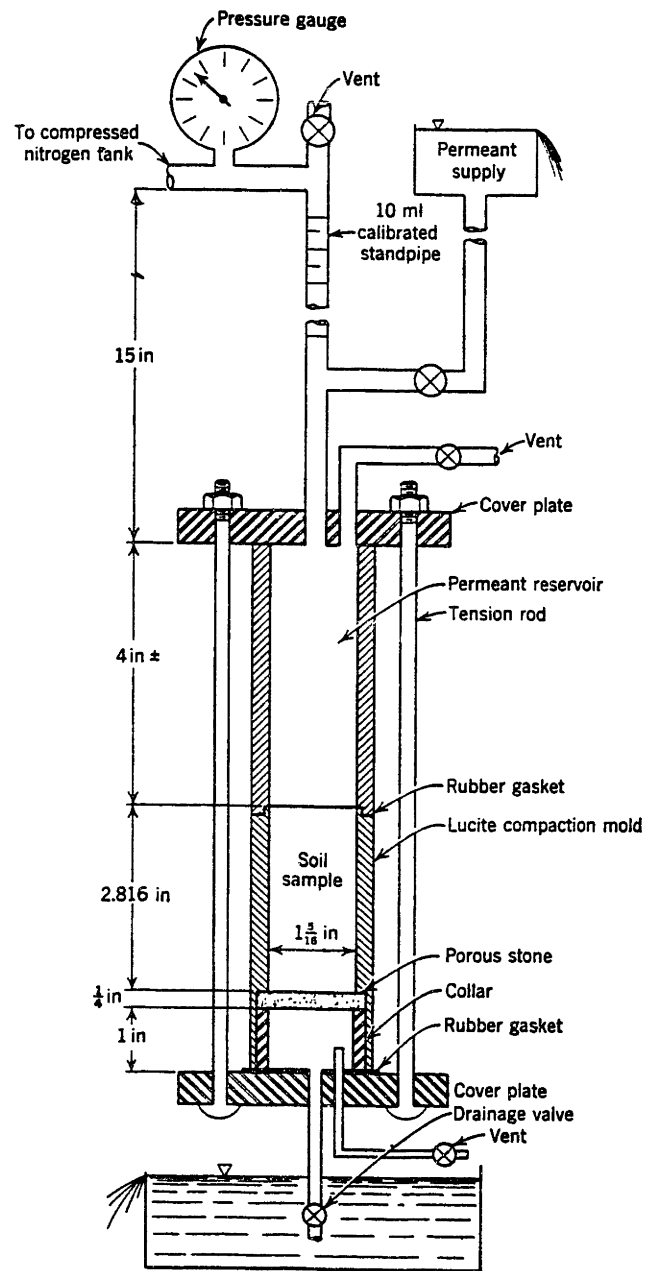


Figure 3.2: Diagram of manifold-control system (Ramsay, 1996)

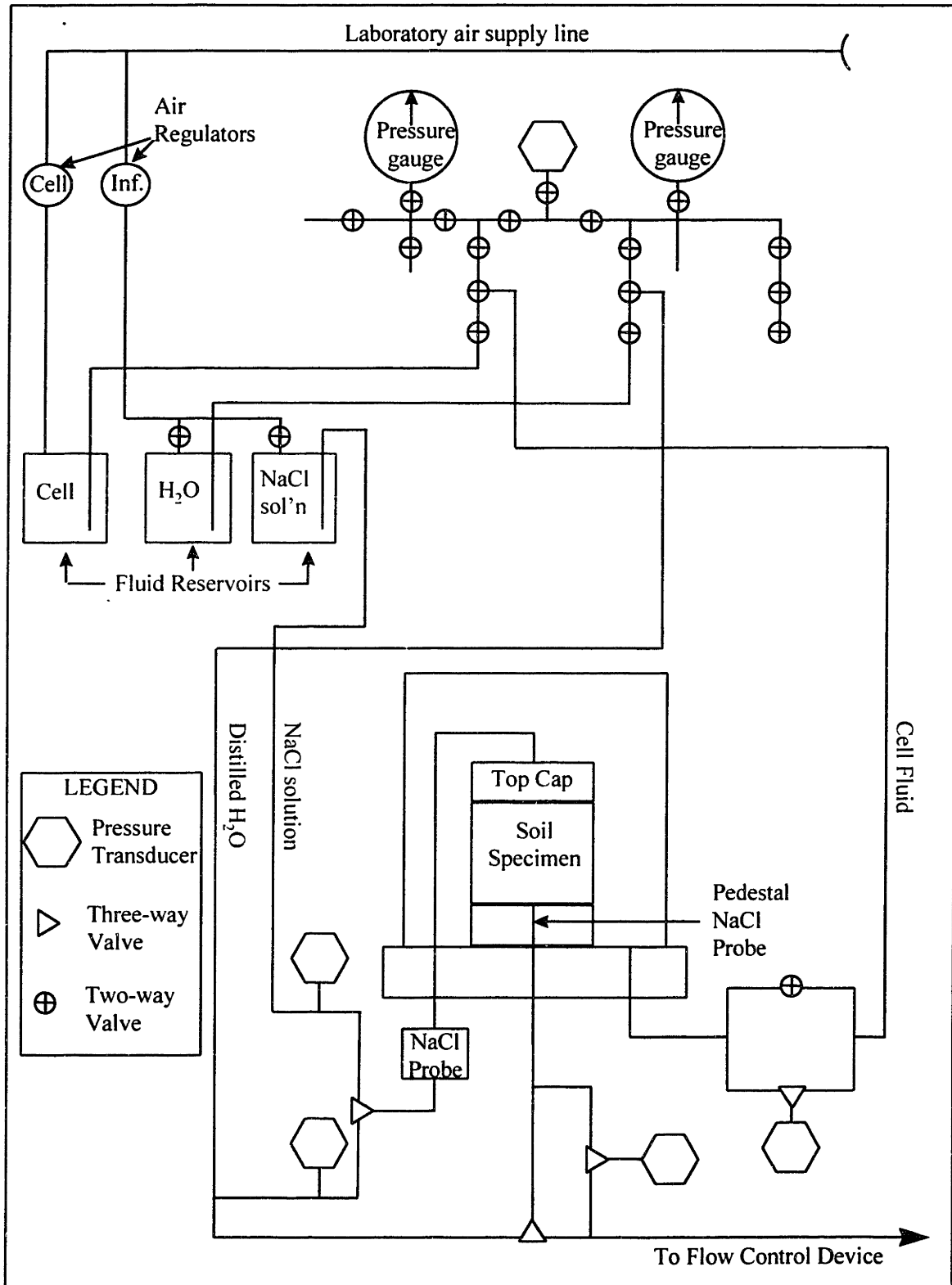


Figure 3.3: Diagram of the flow-control system (Ramsay, 1996)

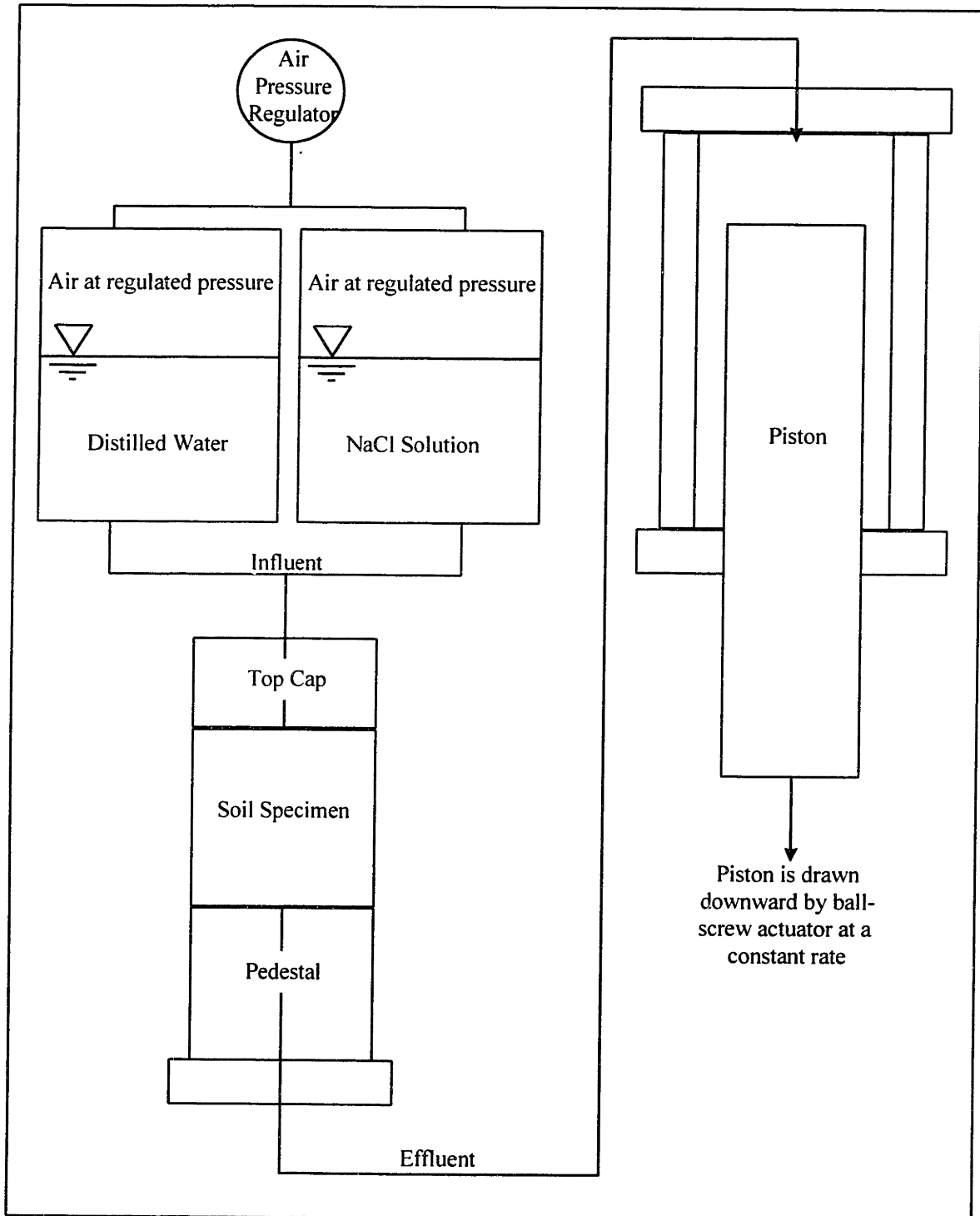


Figure 3.4: Specimen setup on permeameter (Cross section)

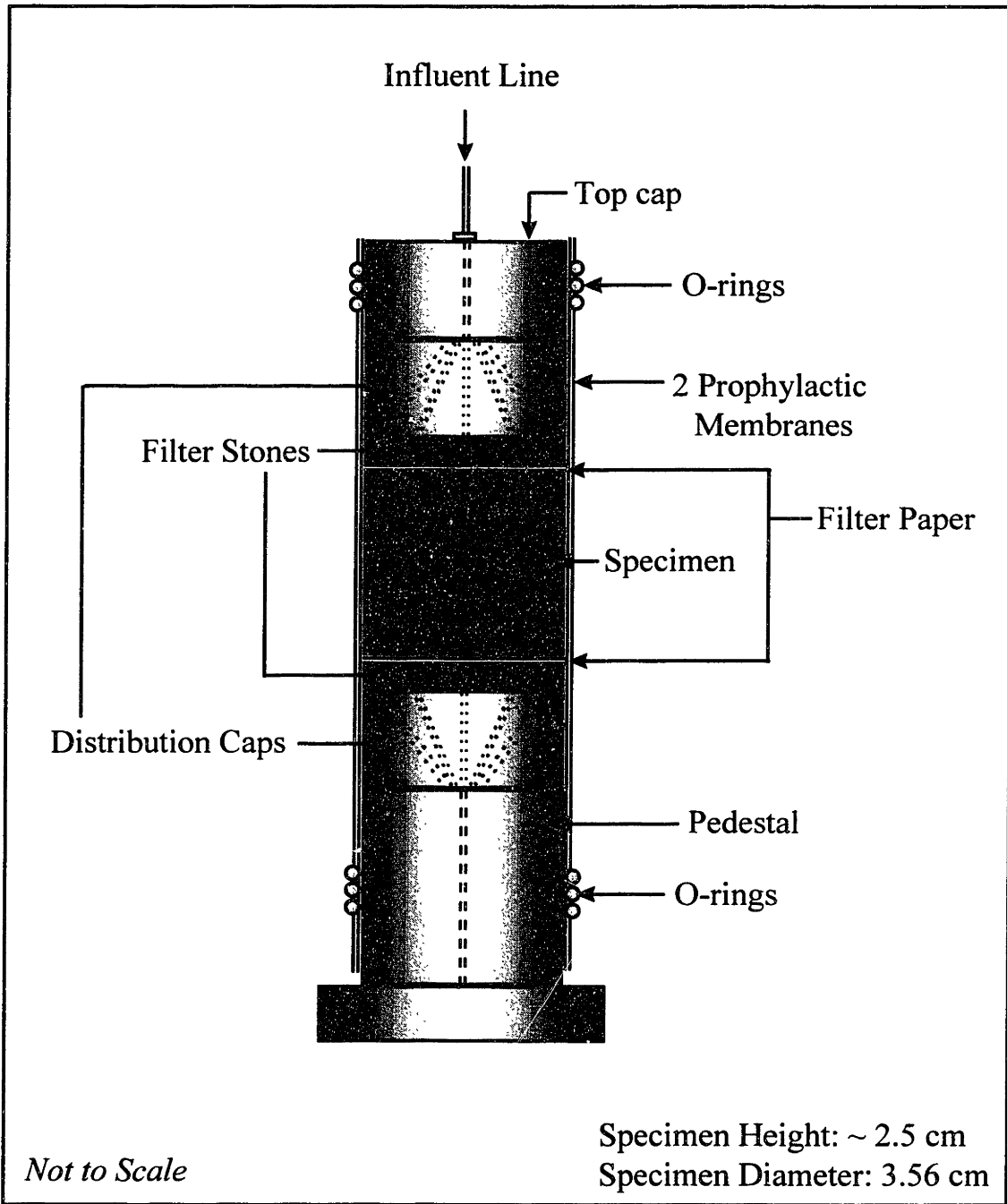


Figure 3.5: Standard MIT volume-control device (Ramsay, 1996)

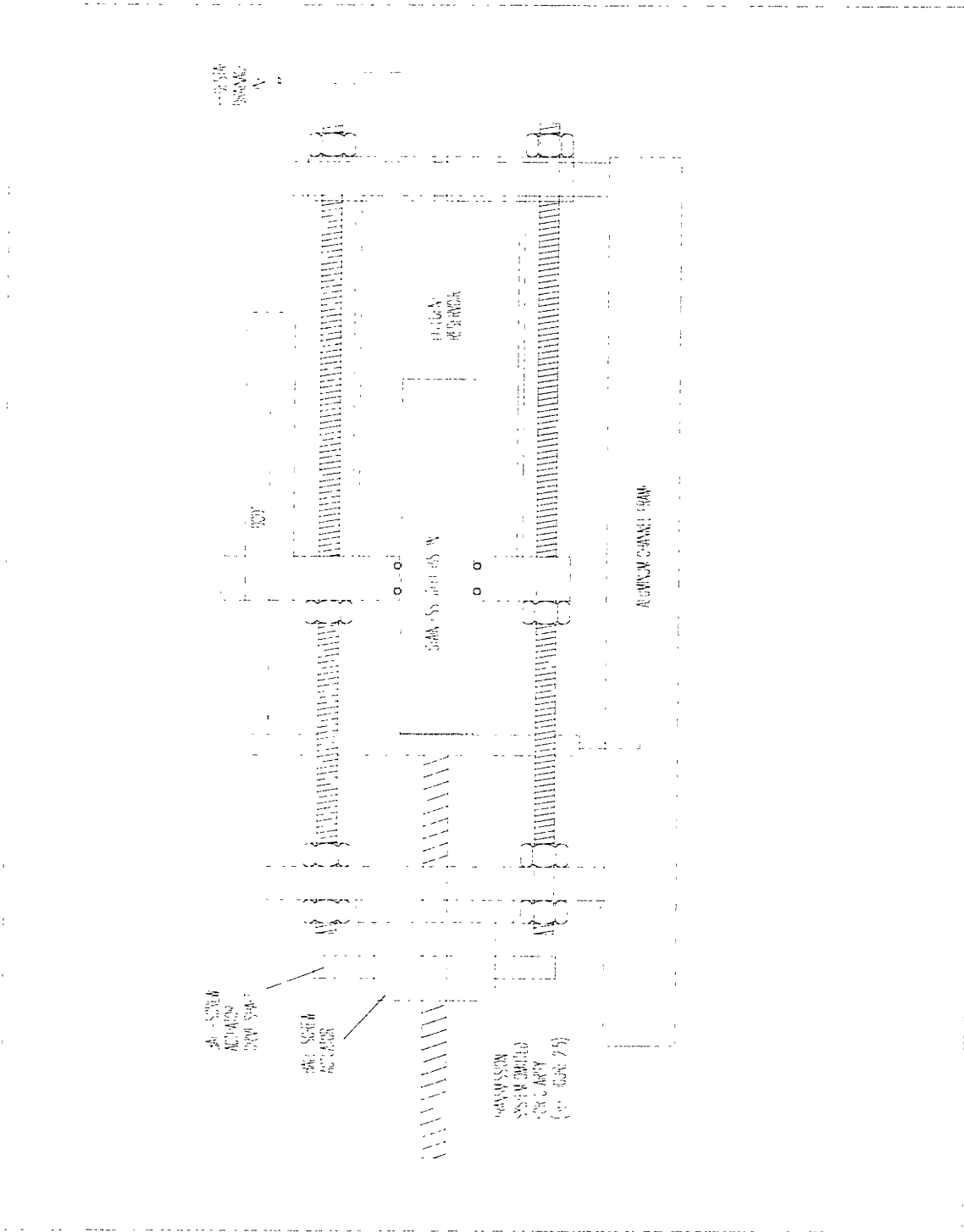


Figure 3.6: Section of the permeameter removable pedestal (Ramsay, 1996)

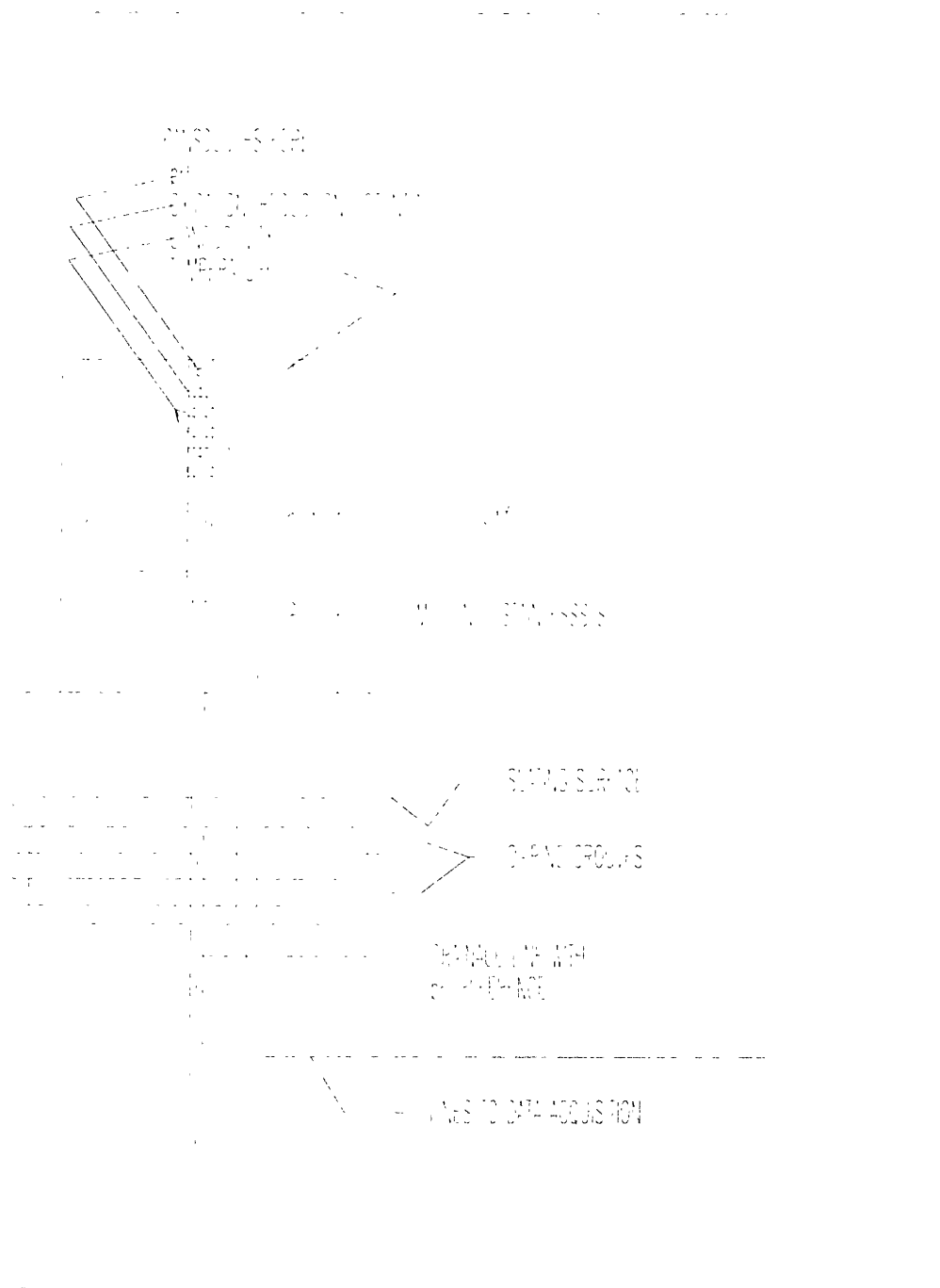


Figure 3.7: Example of NaCl sorption in soil as a function of time for wetland deposit soil (Soil-Salt Sorption Experiment)

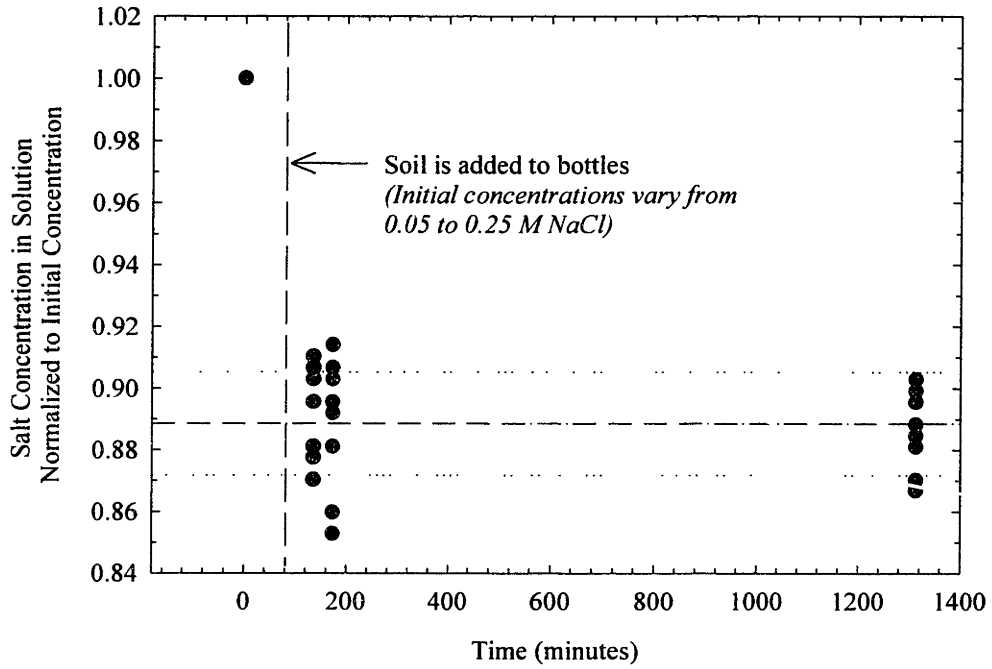


Figure 3.8: Permeameter membrane leak-testing setup

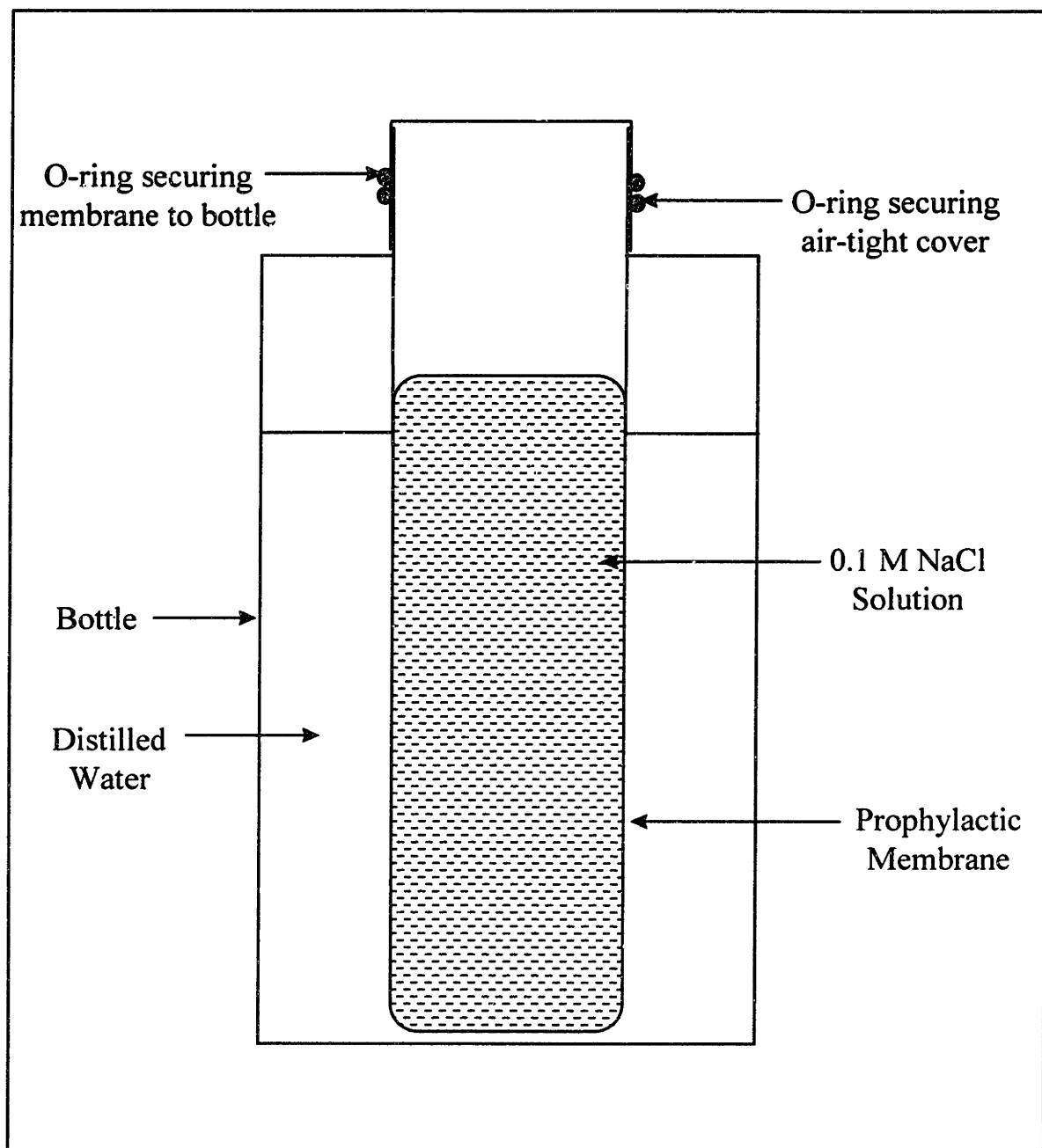


Figure 3.9: Typical breakthrough curves for tracer tests on Sand Specimen 1
Tracer Tests **a** and **b**

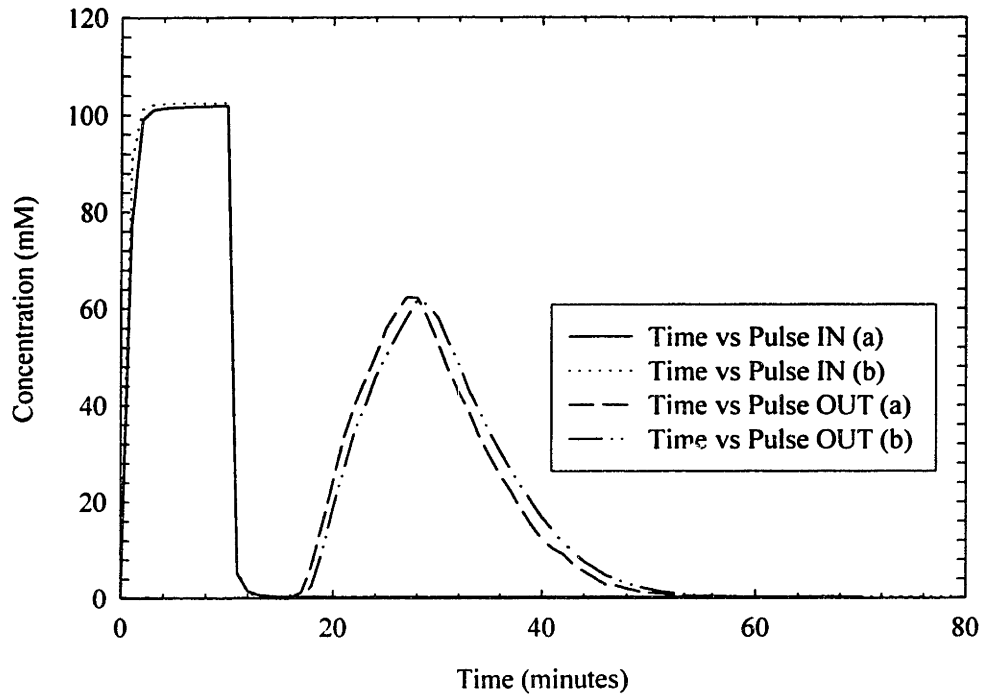


Figure 3.10: (a) % Salt Recovered vs. Effective Stress in Sand Specimen 1 (b) Mass of Salt Lost vs. Effective Stress in sand specimen

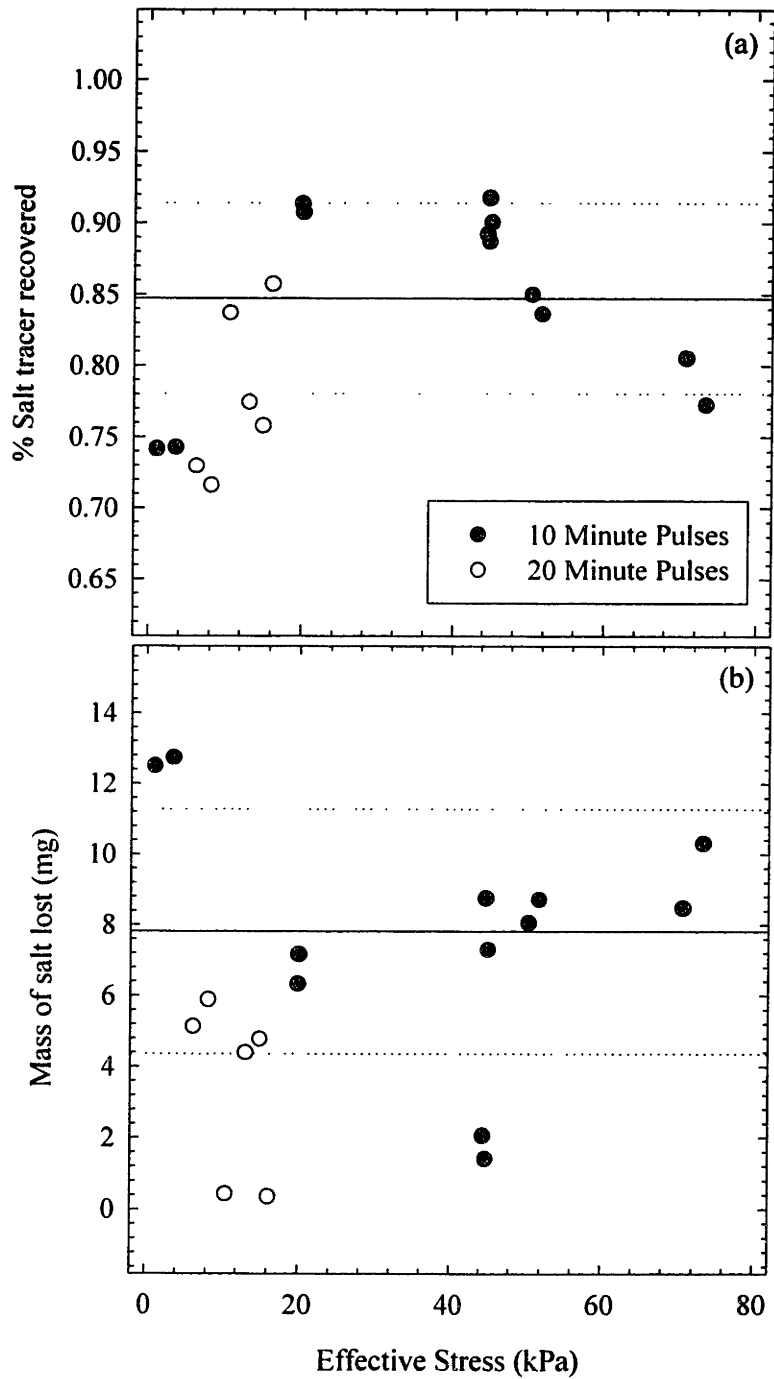


Figure 3.11: (a) % Salt Recovered vs. Flow Velocity in Sand Specimen 1 (b) Mass of Salt Lost vs. Flow Velocity in sand specimen

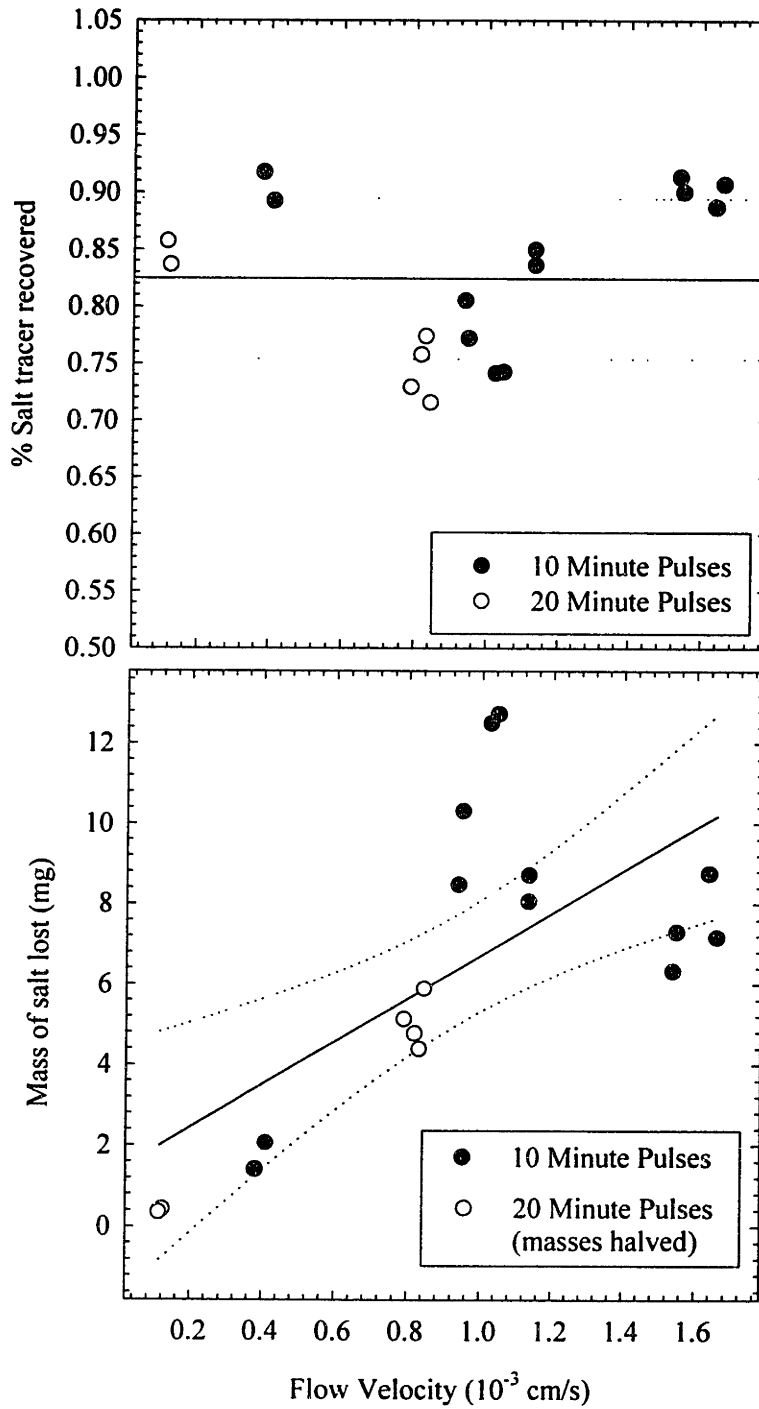


Figure 3.12: (a) % Salt Recovered vs. Time Since Setup of Sand Specimen 1 (b) Mass of Salt Lost vs. Time Since Setup of of Sand Specimen 1

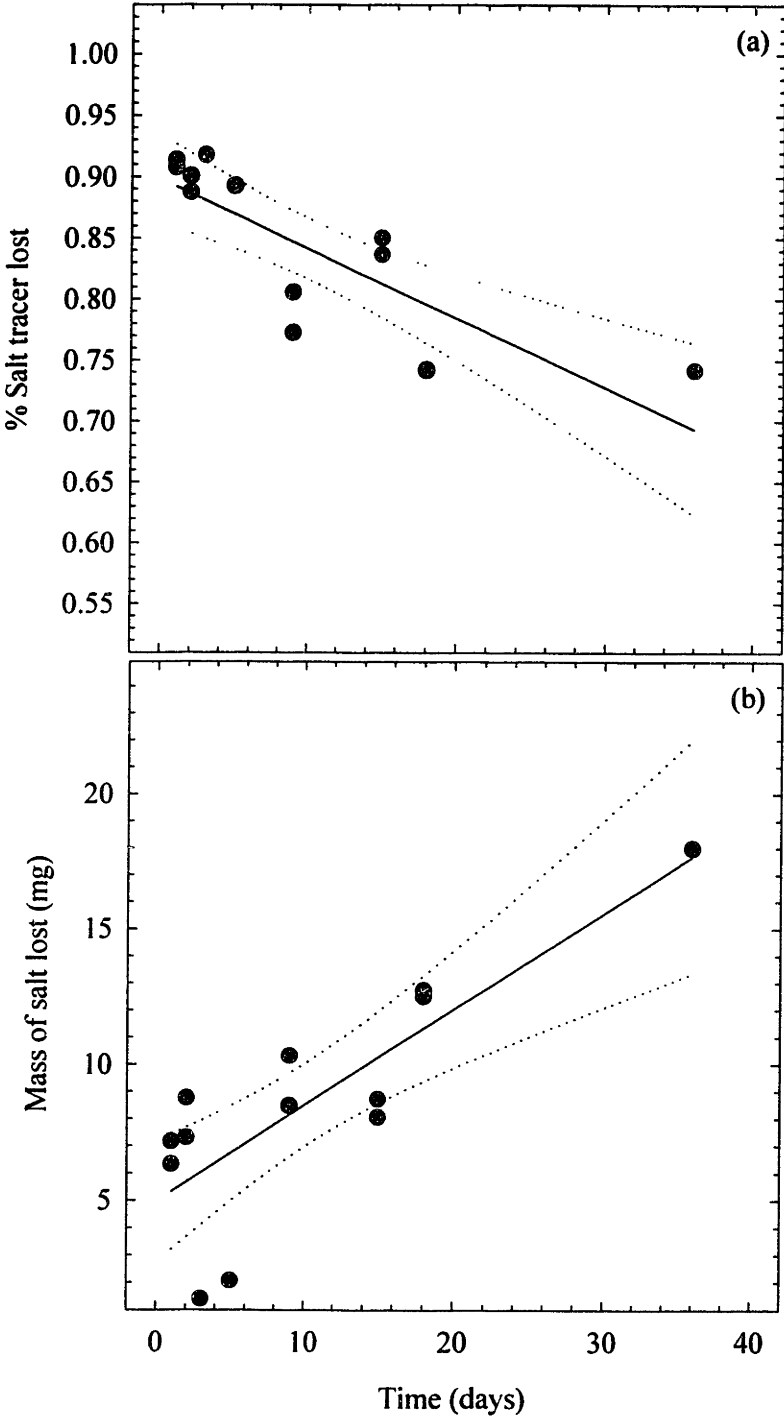


Figure 3.13: Schematic of 2-pin probe configuration (Ramsay, 1996)

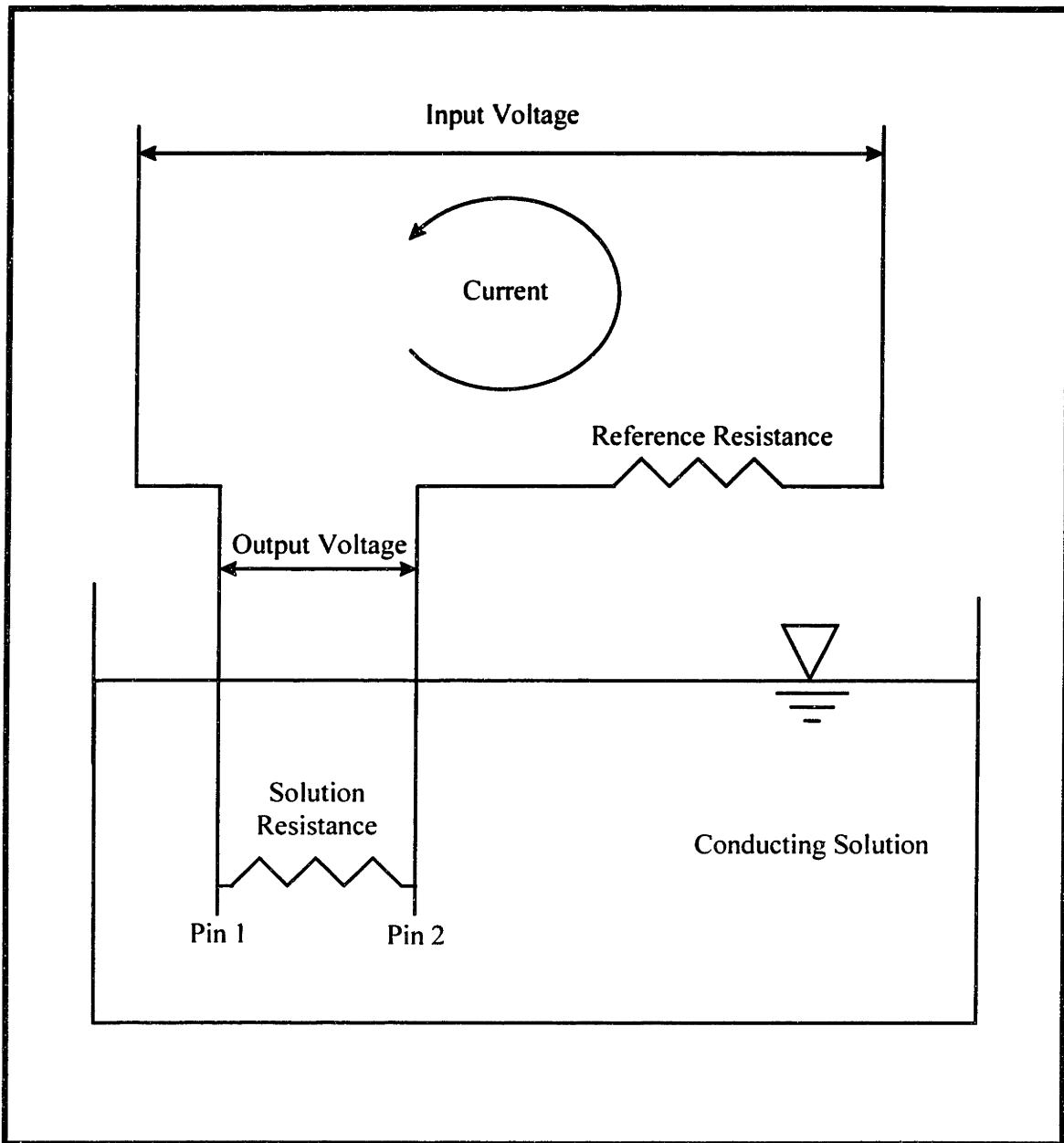


Figure 3.14: Breakthrough curve for Tracer Test **sb** on Sand Specimen 1 after pulsing 10% Micro solution through system

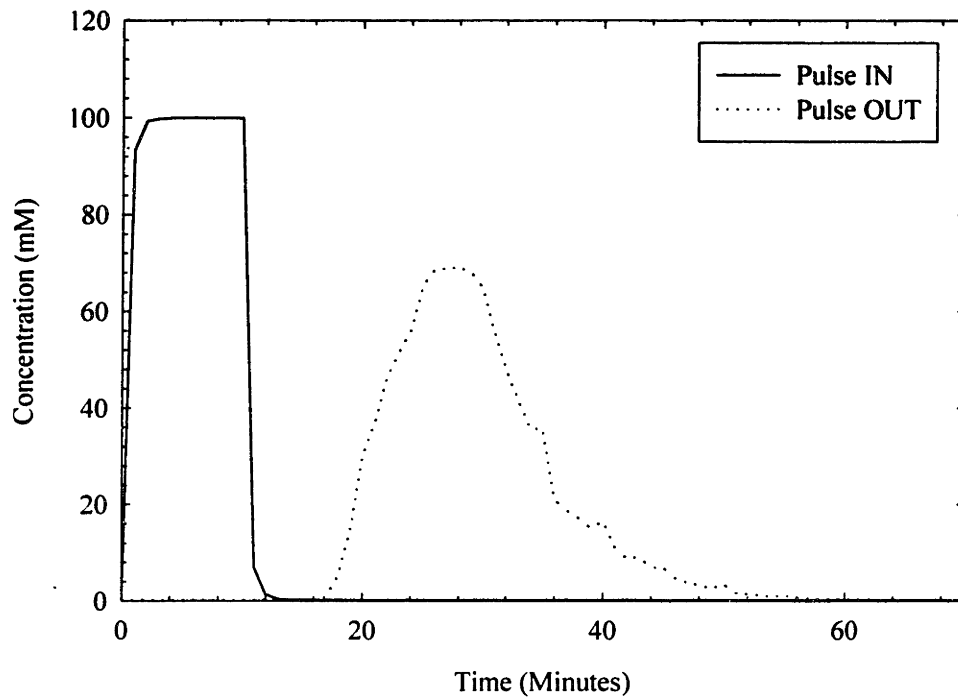


Figure 3.15: Effluent sub-sampling tube setup

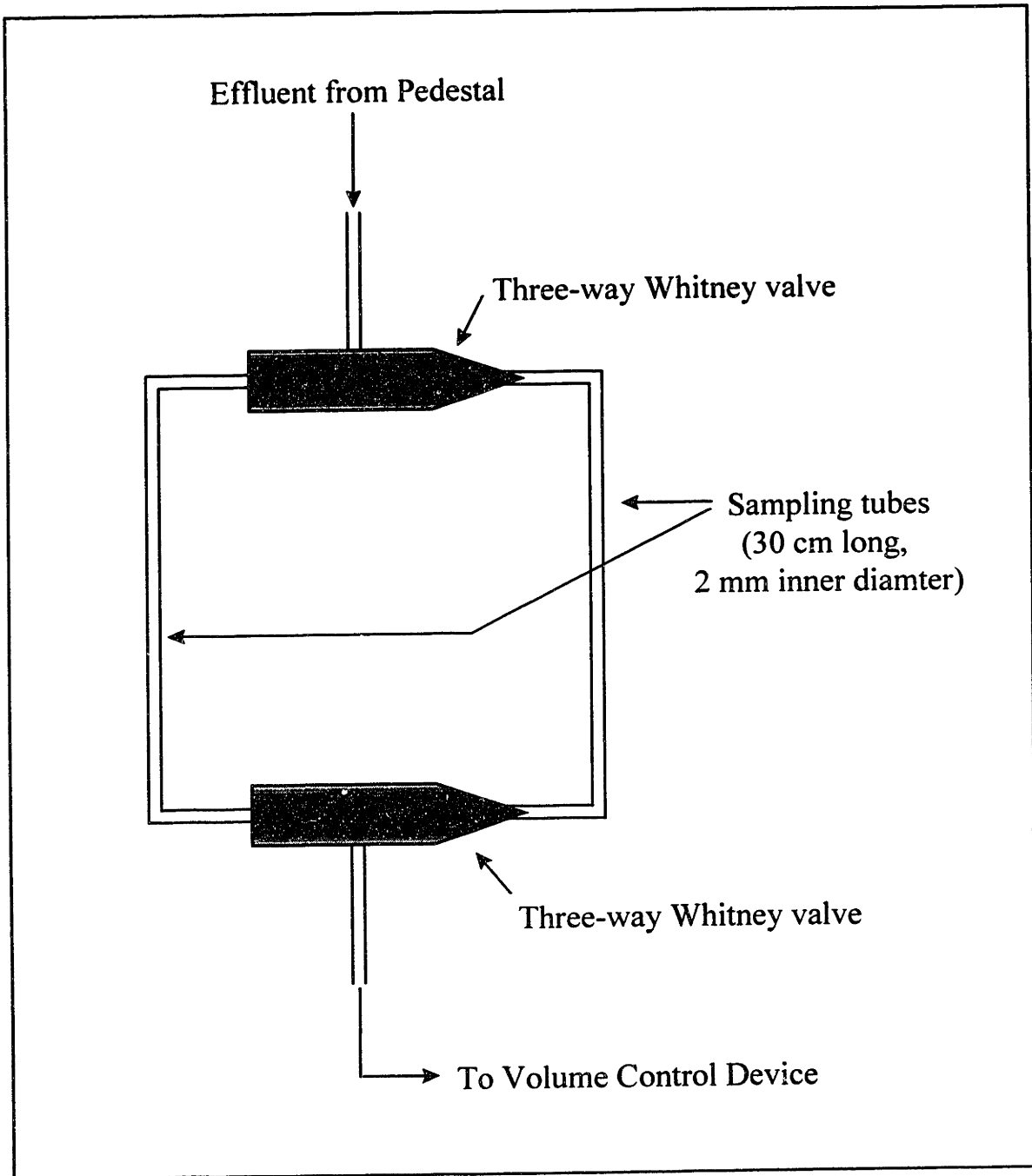


Figure 3.16: Breakthrough curves from Tracer Test sa on Sand Specimen 1. Influent conductivity probe data as well as effluent conductivity probe and sub-sampled data

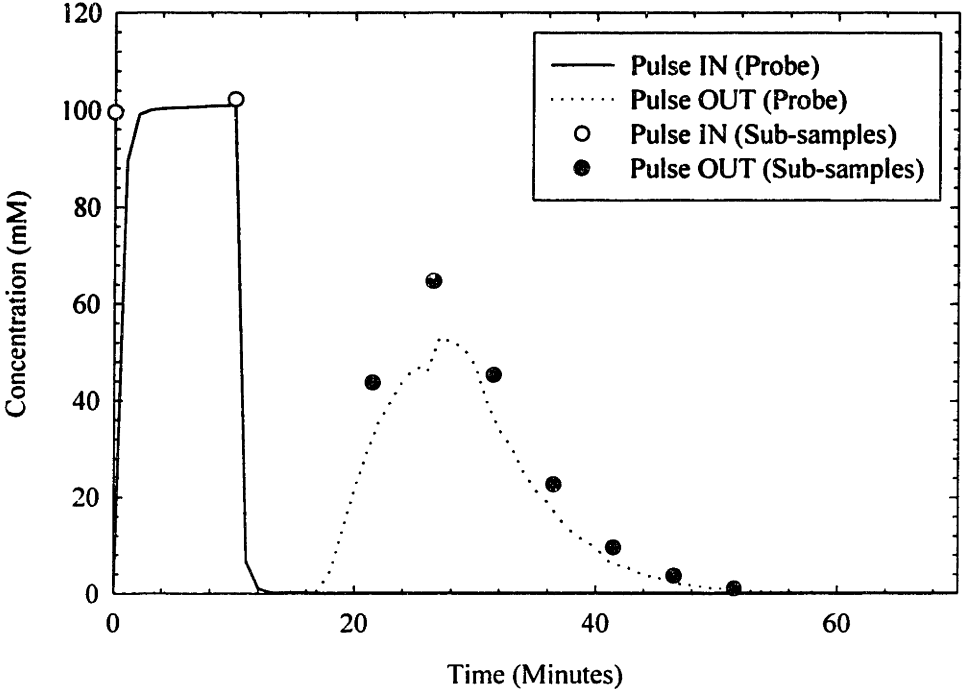


Figure 3.17: Breakthrough curves from Tracer Test *sa* on Sand Specimen 1. Effluent conductivity probe, sub-sampled, and scaled data

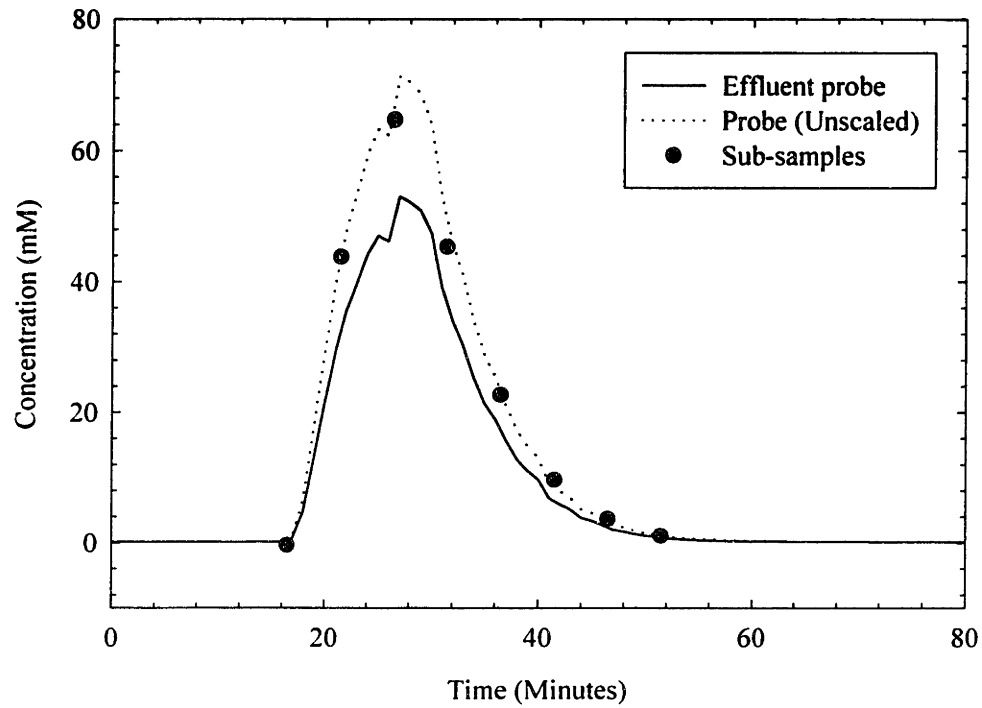


Figure 3.18: Duplicate breakthrough curves: one sub-sampled (Tracer Test *sc*) and one not (Tracer Test *sd*) for Sand Specimen 1

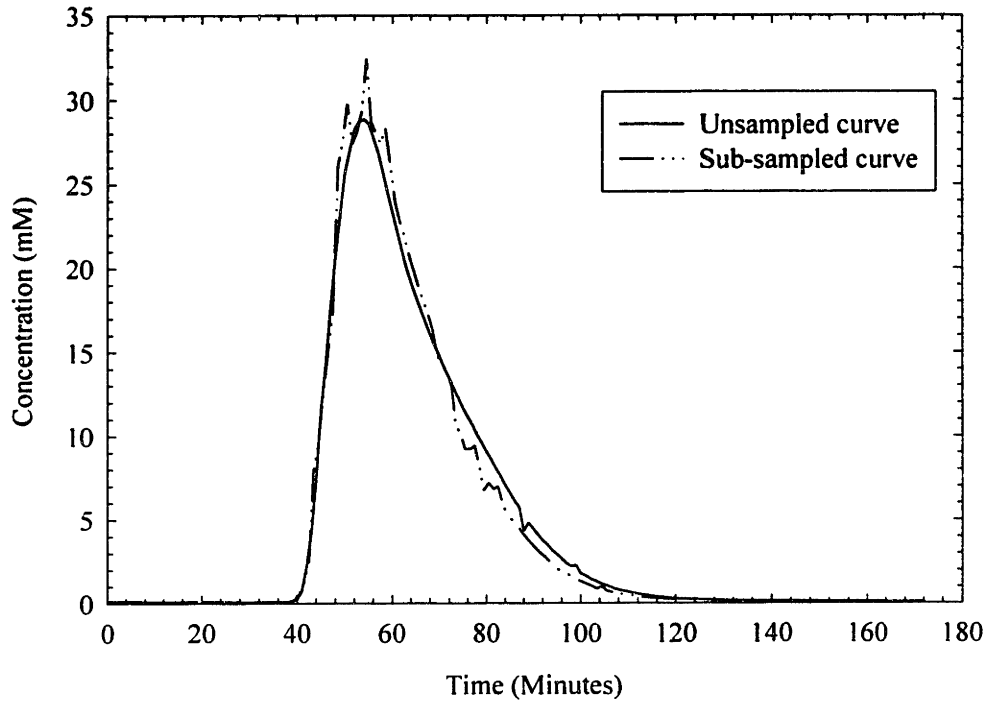


Figure 3.19: Breakthrough curves from Tracer Test sd on Sand Specimen 1. Effluent conductivity probe, sub-sampled, and scaled data. (Sub-samples taken at small intervals)

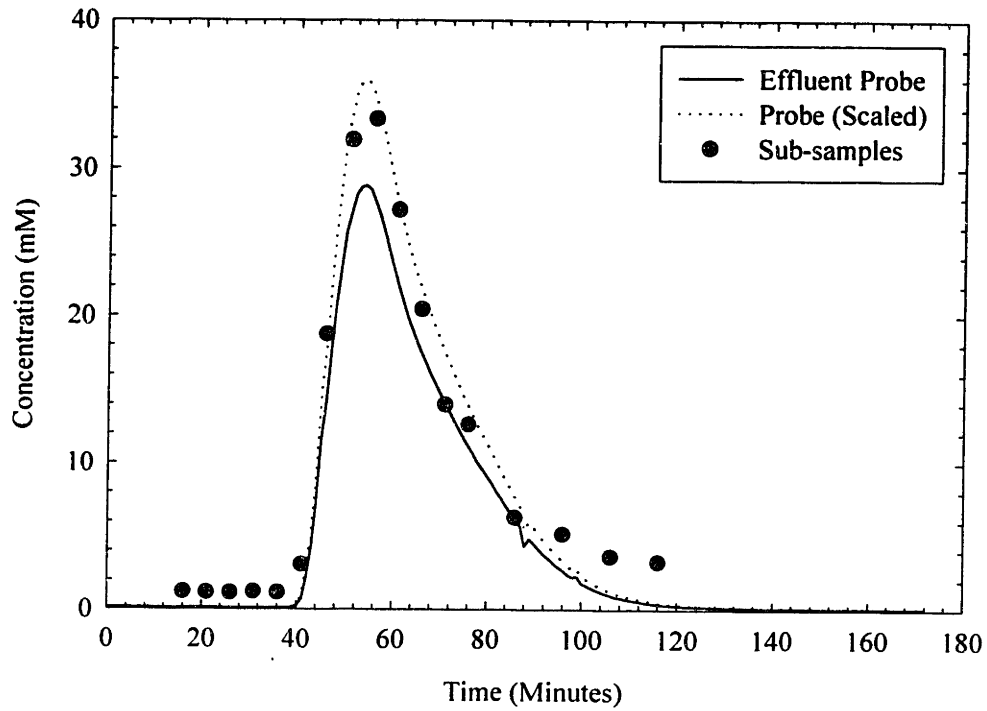


Figure 3.20: Breakthrough curves from Tracer Test **sb** on Sand Specimen 1. Effluent conductivity probe and sub-sampled data after pulsing 10% Micro solution through system

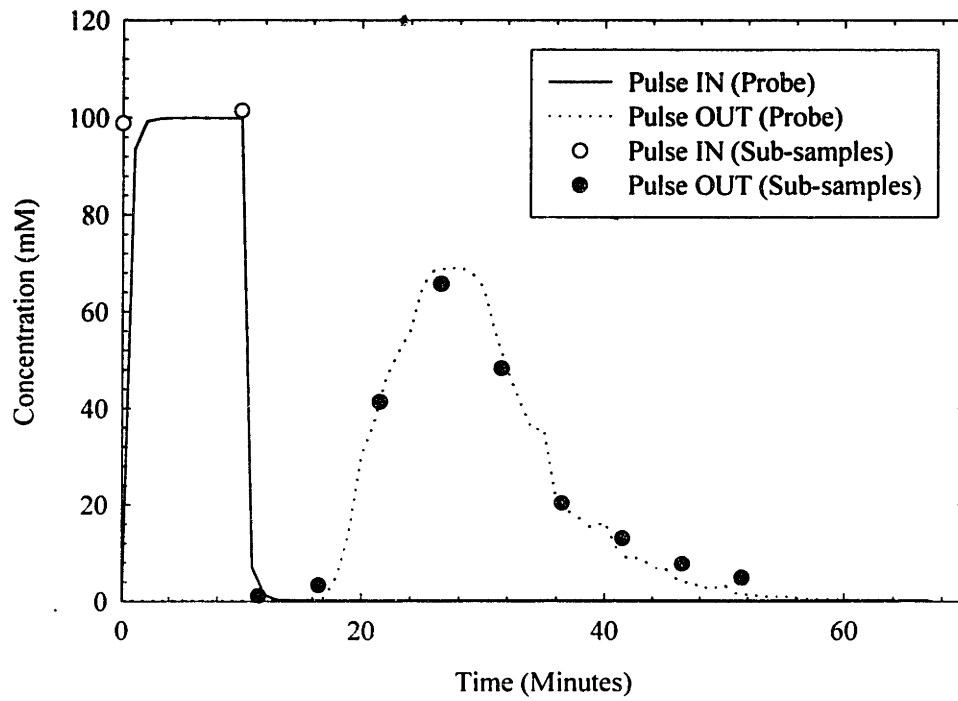


Figure 3.21: Breakthrough curves for re-sedimented wetland deposit specimen (Specimen S7). Effluent conductivity probe and sub-sampled data.

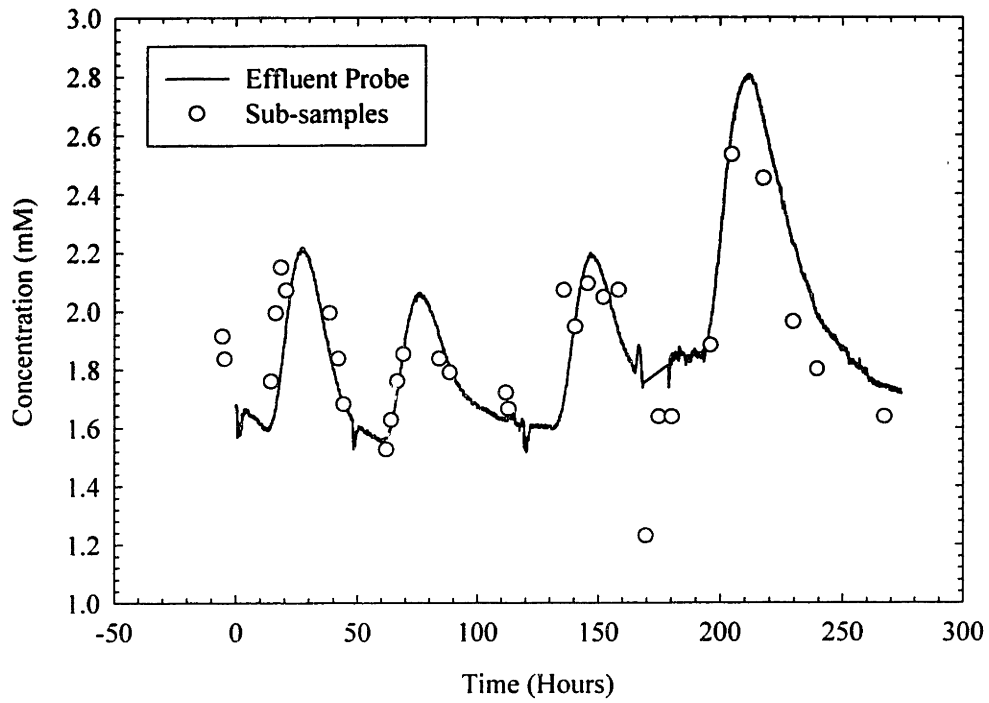


Figure 3.22: % Salt recovered for 4 tracer tests on re-sedimented wetland deposit specimen (Specimen S7). Effluent conductivity probe and sub-sampled data.

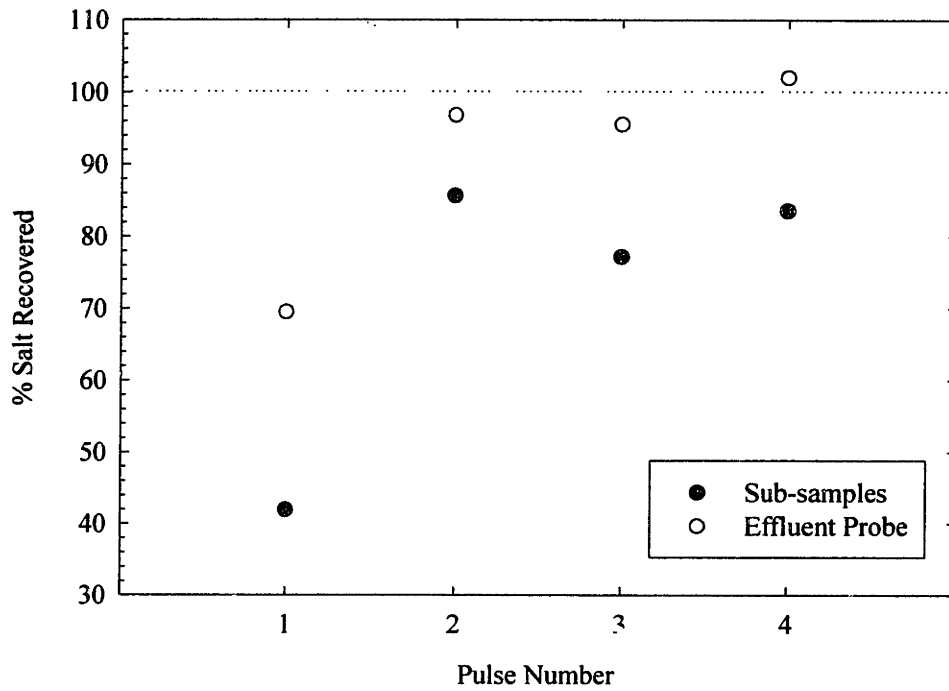


Figure 3.23: Modified oedometer used for re-sedimenting wetland soils

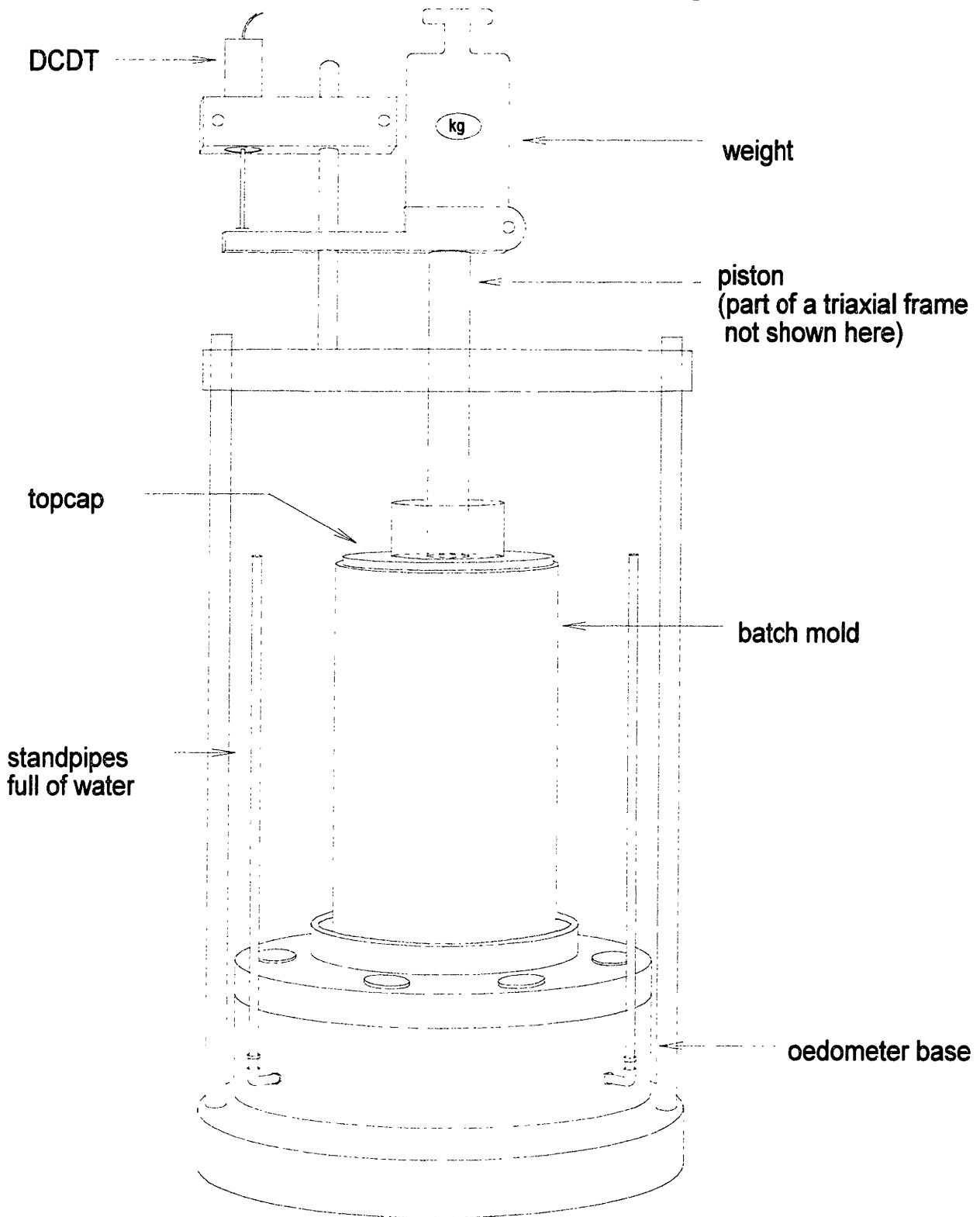


Figure 3.24: (a) Two consecutive breakthrough curves for tracer tests on filter stones. Pulses *in* and *out* for two flow rates. (b) Superimposed breakthrough curves. Pulses out for tests a and b

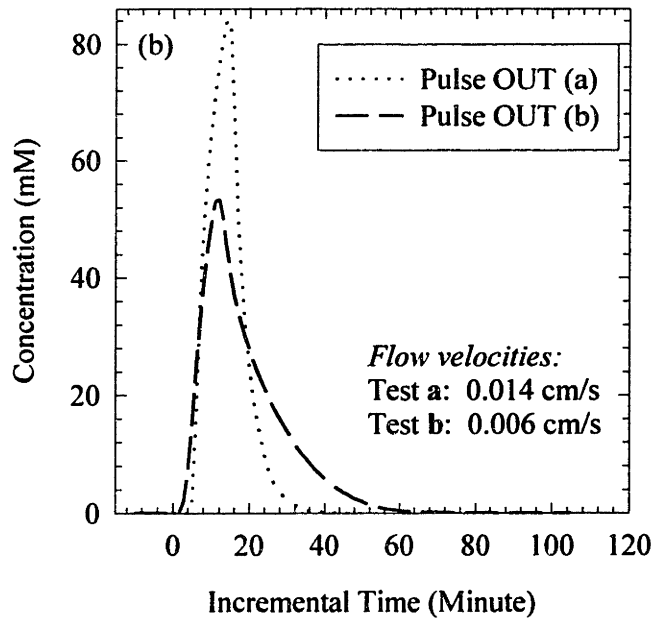
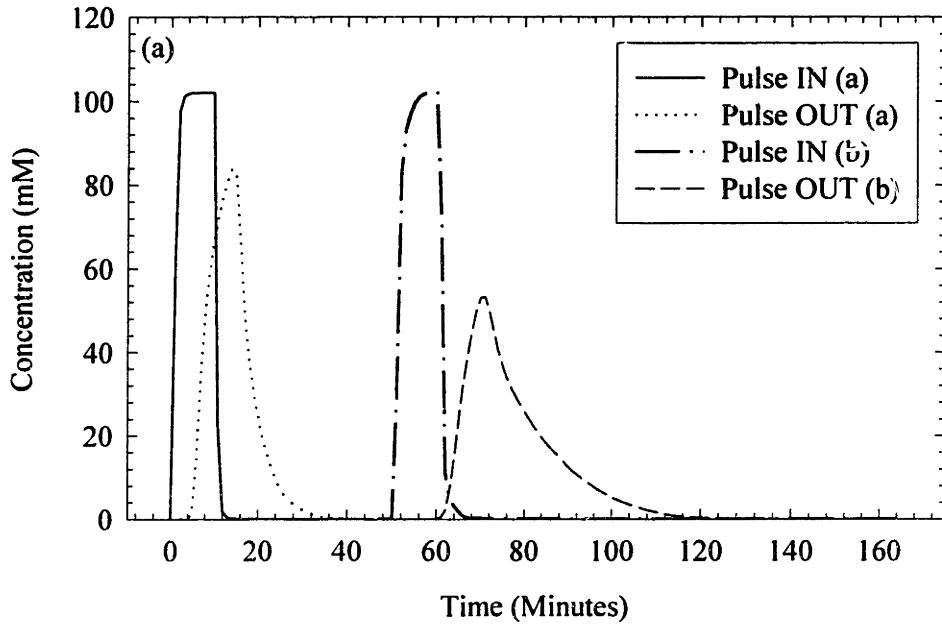


Figure 3.25: (a) Two consecutive breakthrough curves for tracer tests without filter stones. Pulses *in* and *out* for two flow rates. (b) Superimposed breakthrough curves. Pulses out for tests **a** and **b**

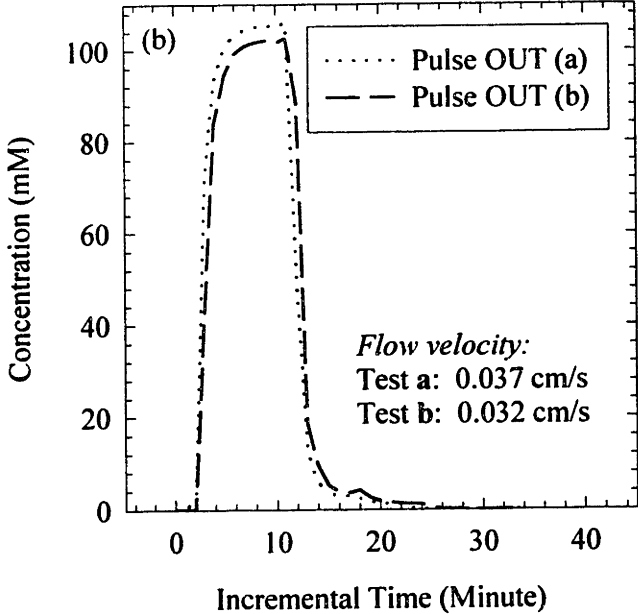
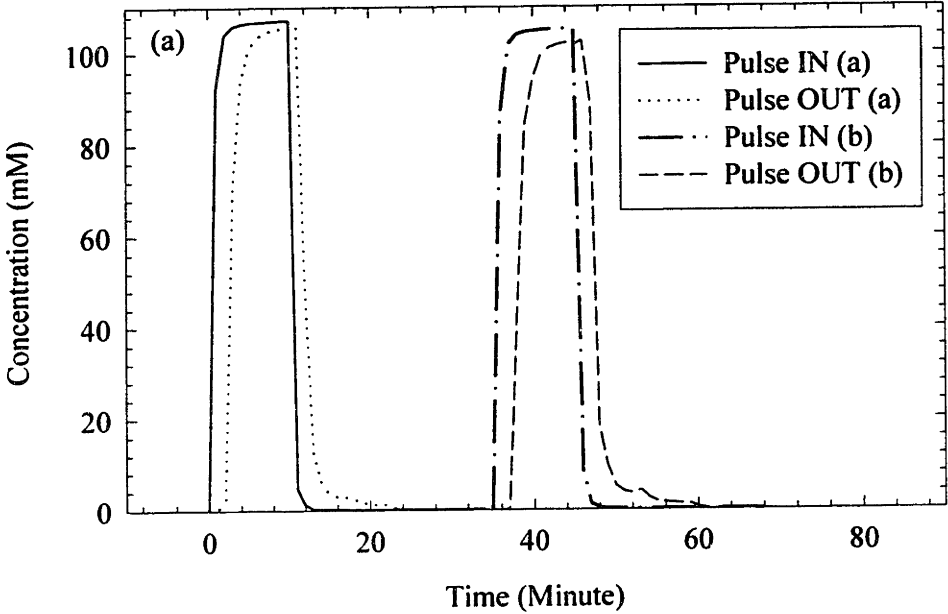


Figure 3.26: Proposed mechanism of Two-Region behavior in filter stones

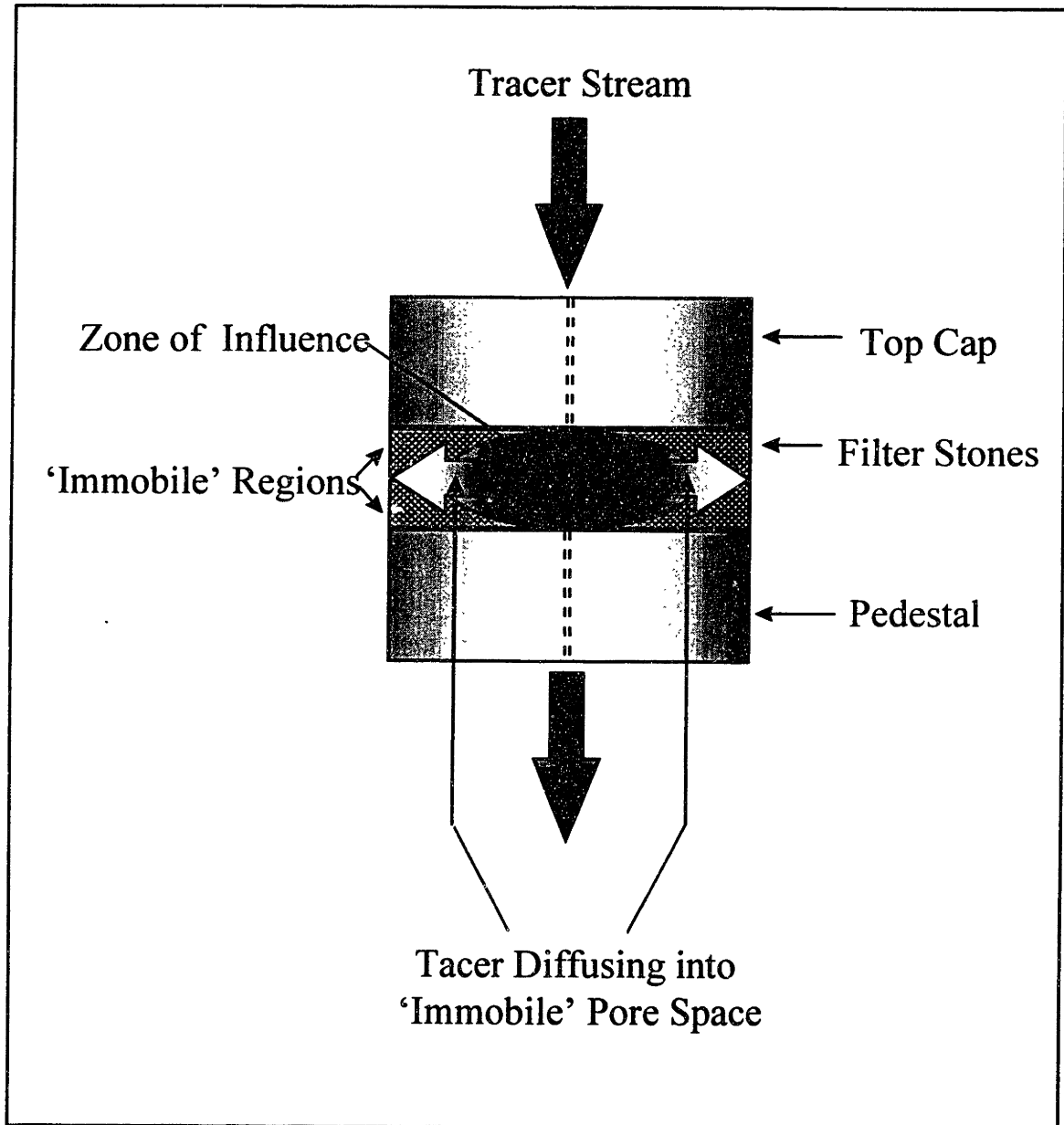


Figure 3.27: Breakthrough curves fit using Two-Region Model for tracer tests on filter stones (a) For fast flow rate (1.43×10^{-3} cm/s)

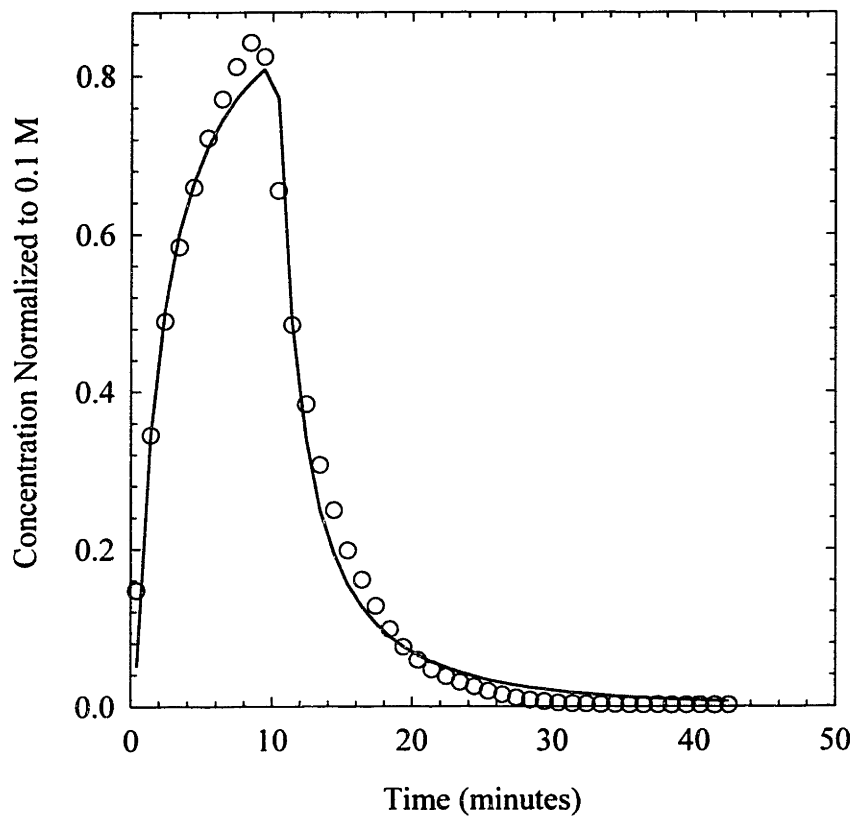


Figure 3.27: Breakthrough curves fit using Two-Region Model for tracer tests on filter stones (b) For *slow* flow rate (6.16×10^{-4} cm/s)

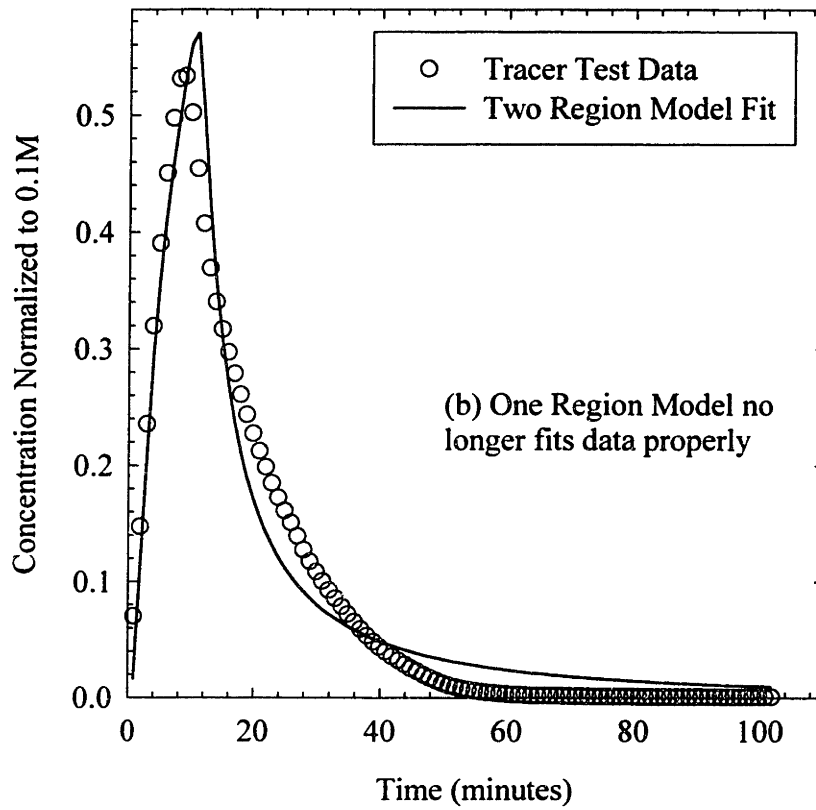


Figure 3.28: Schematic of distribution cap

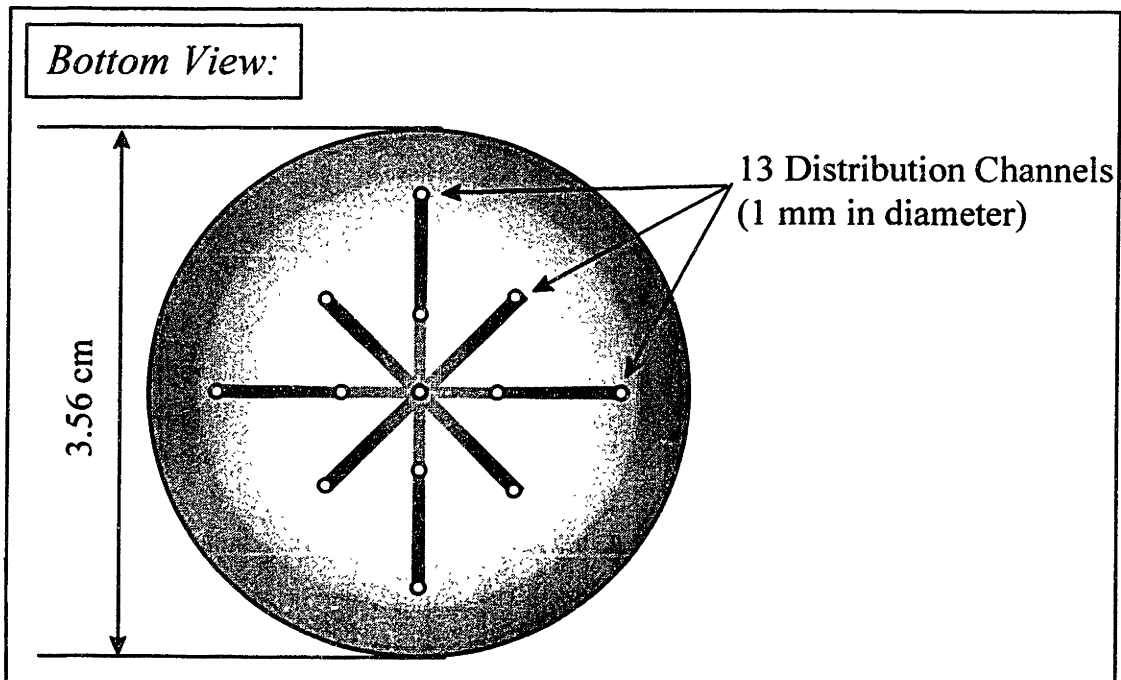
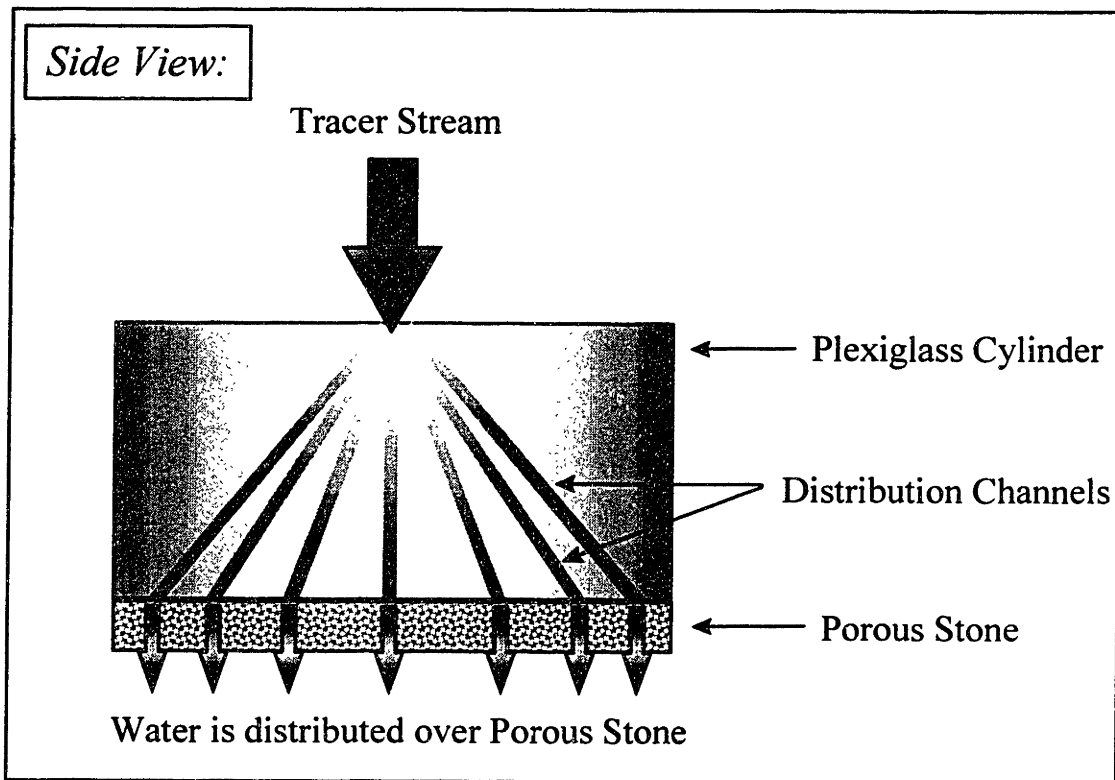


Figure 3.29: (a) Two consecutive breakthrough curves for tracer tests on filter stones and distribution caps. Pulses *in* and *out* for two flow rates. (b) Superimposed breakthrough curves. Pulses *out* for tests a and b

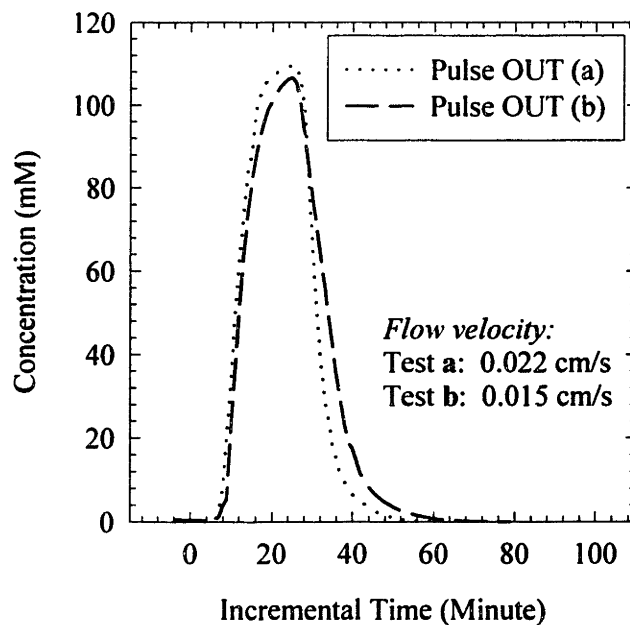
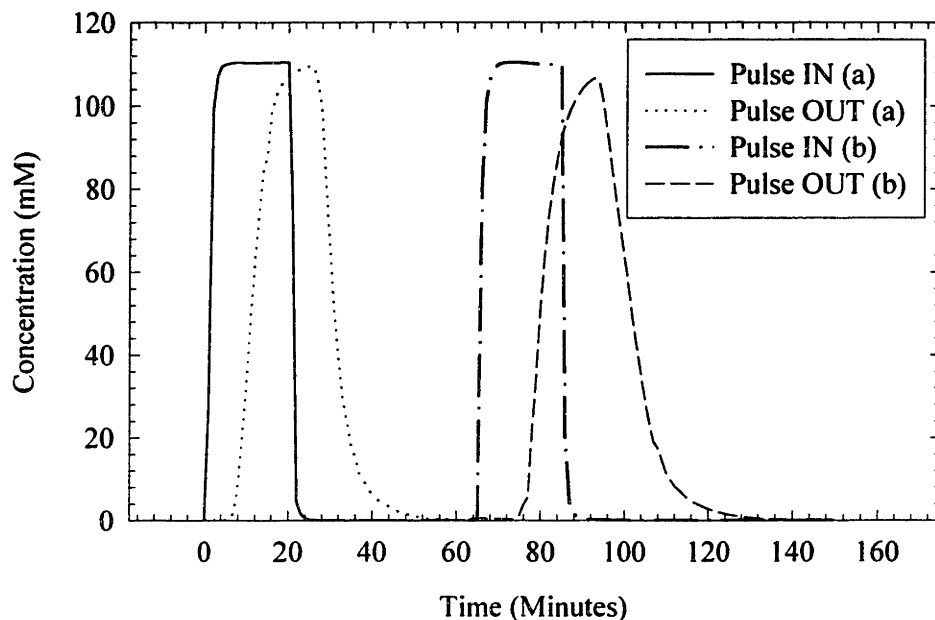


Figure 3.30: Example of time shift for typical breakthrough curve

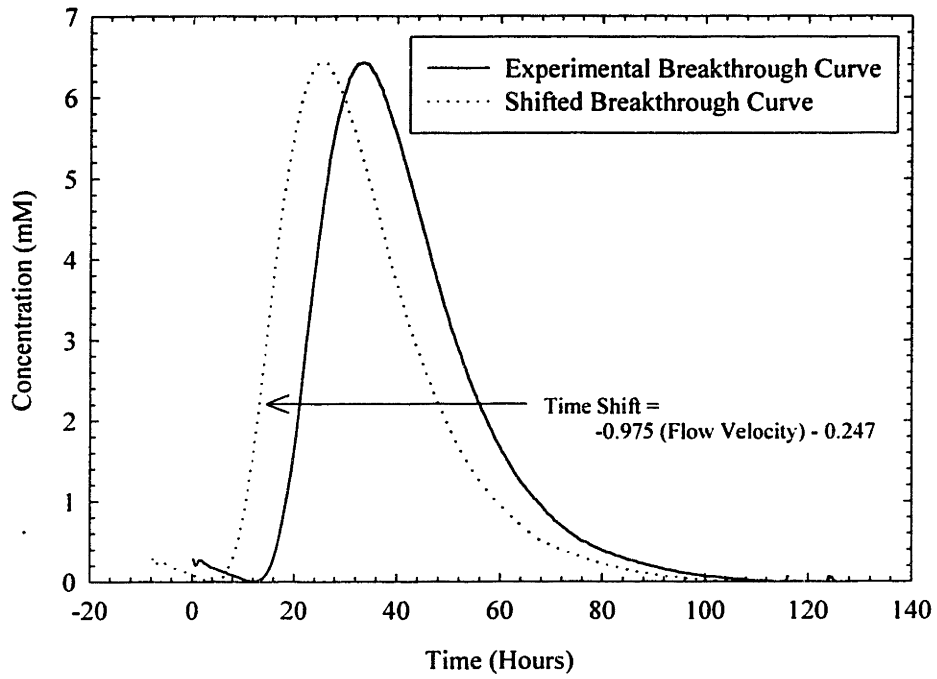


Figure 3.31: Typical breakthrough curve for Time Shift test. T_5 corresponds to the time it takes for 5% of tracer to break through.

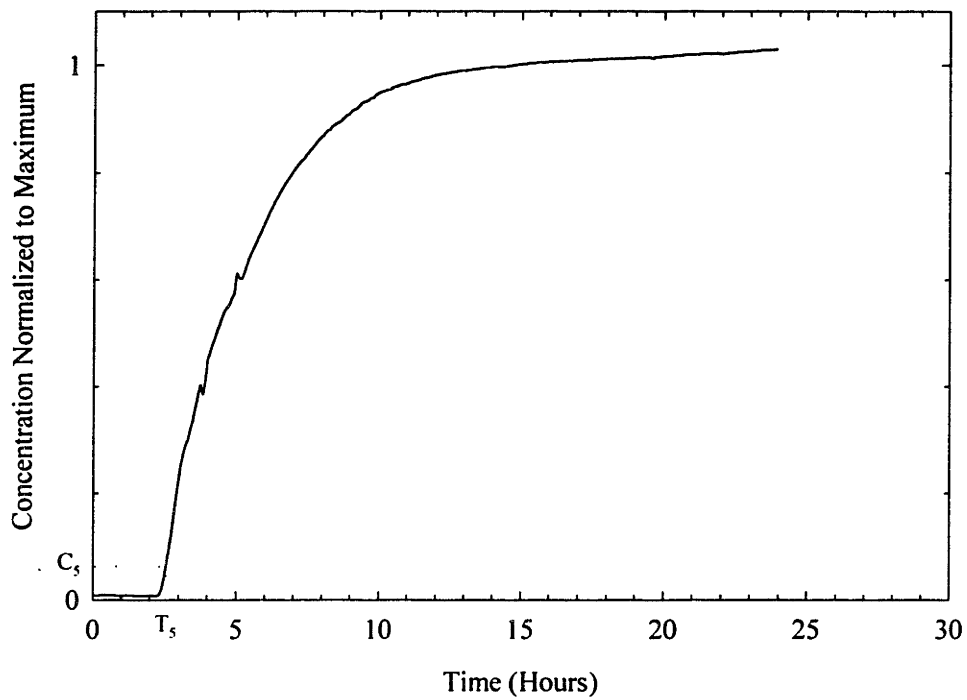


Figure 3.32: Compilation of breakthrough curves for Time Shift tests run at *slow* flow velocities; that is, velocities used in wetland deposit tests.

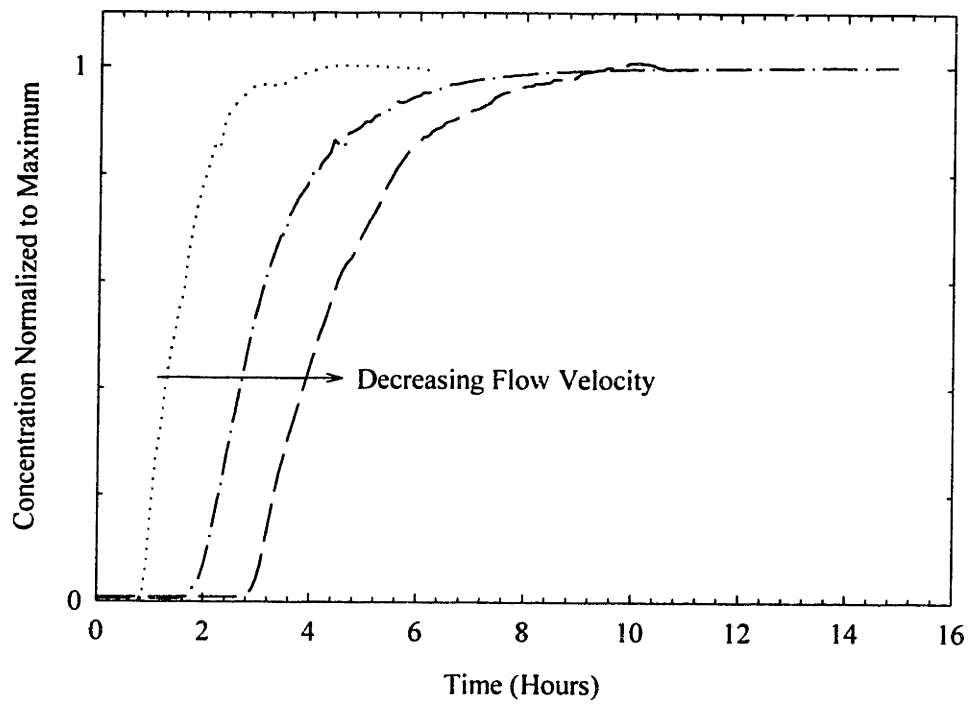
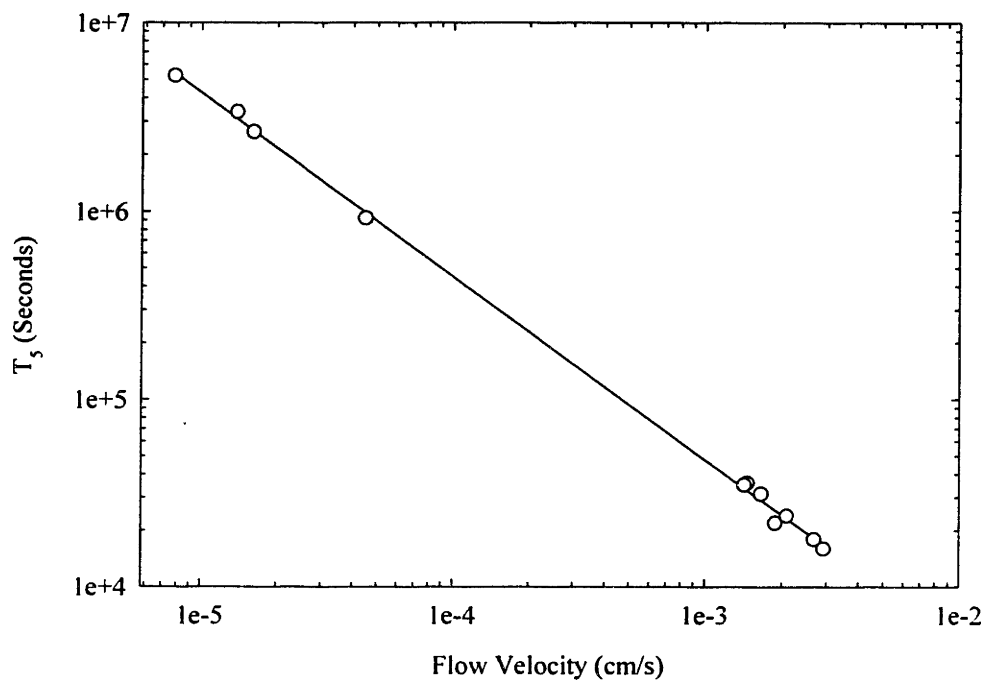


Figure 3.33: T_s vs. Flow Rate data taken from Time Shift tests.



4. SOIL CHARACTERIZATION EXPERIMENTS

4.1 INTRODUCTION

Several geotechnical properties of the wetland deposits tested in this study were investigated to better understand the physical parameters that control the hydraulic conductivity of these soils. Geotechnical tests, including Specific Gravity (Section 4.4), Ash (Mineral) Content (Section 4.5), Particle Size Distribution (Section 4.6), and Constant Rate of Strain (Section 4.7), were run on soil samples that were also tested on the permeameter. Also, the mineralogy and size distribution of the wetland deposit mineral fraction is discussed (Section 4.8). The results of these tests can be compared to indicate whether any trend exists between void ratio, organic content, particle size, compressibility, mineral type, and hydraulic conductivity.

This chapter begins with a description of the soils tested (Section 4.2), the soil sampling program, and the testing scheme (Section 4.3). Then, the procedures and the results of the characterization tests are discussed. Comparisons between the data from these tests and the data from the Column Experiments, outlined in Chapter 5, are given in Chapter 6.

4.2 SOILS TESTED

Even though wetland deposits are the primary focus of this study, Column Experiments were also conducted on a uniform sand for two reasons. First, salt tracer tests were run, to better understand the problem of salt loss into the system (See Section 3.3.1). Tracer tests were also run to form a comparison between the data for wetland deposits, which are dual porosity materials, and for uniform sands, which are not. The sand used in these experiments has been used in several prior projects at MIT and its properties are well characterized (Ratnam, 1996). A summary of these properties is given in Appendix A. The primary focus of this chapter is the characterization experiments conducted on the wetland deposits themselves.

Comparisons between the hydraulic conductivity data for the sand and for wetland deposits are given in Section 6.2.2.

4.3 WETLAND DEPOSIT SAMPLING AND SPECIMEN PREPARATION

The wetland deposits used in this study were all sampled from the Wells G and H site, Woburn Massachusetts (See Figure 1.2). Two types of samples were taken: undisturbed cores and bulk samples, which were then processed and re-sedimented in the laboratory. Both types of samples were taken within 1 meter of the wetland ground surface on the eastern bank of the Aberjona River (Figure 4.1). Below, the sampling procedures and locations are described and a visual classification of the soil is given.

4.3.1 UNDISTURBED WETLAND DEPOSIT SAMPLES

4.3.1.1 THE PISTON SAMPLER

A portable, manually operated, fixed-piston sampler (Figure 4.2) designed and built by Bailon (1995) was used to retrieve undisturbed samples from the site (See ASTM D1587-94). This sampler consists of six basic components: (1) a cylindrical, brass piston with an acrylic base, (2) a threaded rod which threads into the top of the piston (Figure 4.2a), (3) a thin-walled, stainless-steel Shelby tube (3" inner diameter, 30" long), (4) steel tubing, (5) a stainless-steel fitting which connects the steel tubing to the Shelby tube, and, finally, (6) handle bars which tighten around the steel tubing and which allow the apparatus to be pushed into the ground (Figure 4.2b).

To use the sampler, the Shelby tube and the steel tubing are connected together (Figure 4.2b), and the threaded rod is attached to the piston (Figure 4.2a). The piston and rod are then inserted into the Shelby tube, and moved such that the bottom of the piston is flush with the sharpened edges at the bottom of the Shelby tube. Next, the piston is placed flat on the ground surface, and the handle bars are tightened around the steel tubing. Pressure is applied to the handle bars to push the Shelby tube straight into soil while the inner, threaded rod remains fixed in place by the sampler operator. As the Shelby tube is driven into the ground, the soil displaces the piston so that the piston remains at the ground surface. Since the piston

fits snugly into the Shelby tube, a vacuum is created in the Shelby tube when the piston moves up relative to the Shelby tube walls. This vacuum keeps the soil inside the tube when the apparatus is pulled out of the ground. Before the Shelby tube is pulled out, however, the apparatus is allowed to sit for 5 minutes to allow the soil to swell against the Shelby tube walls, and then the handle bars are used to rotate the apparatus $3 \times 360^\circ$ so that the soil at the bottom of the tube is sheared away from the soil in the ground. This allows for a more complete retrieval of the sample.

The relative difference in distance between the threaded rod and the steel tubing ends gives the length of the sample core. This distance is measured and recorded. Additional, deeper samples can also be cored provided the bore hole stays open. This can be done with this sampler by extending the threaded rod and steel tubing with the proper attachments.

Since the Aberjona Wetland deposits are relatively soft, wooden planks are laid under the sampler operators to distribute their mass. However, the root mat at the wetland ground surface made pushing the sampler into the ground difficult (Figure 2.16), and large suction pressures made pulling it out difficult as well. Two operators were, therefore, required to drive the sampler into the ground (up to 2 meters), and to pull it out again.

4.3.1.2 SAMPLE TRANSPORTATION, STORAGE AND CHECKING

After the Shelby tube is disassembled from the rest of the sampling apparatus, it is sealed at both ends using tightly fitting plastic plugs with rubber o-ring seals. All sampling tubes are kept upright and transported back to the lab immediately. They are stored upright in large bins in a 100% humid room. Before the tubes are sub-sampled, they are X-rayed to check for sampling disturbance and anomalies (See Figure 4.3).

4.3.1.3 SAMPLE DESCRIPTION

Cores were taken from two bore holes within a foot of each other, located within 5 meters of the eastern bank of the Aberjona River (Location A, Figure 4.1) in April, 1996. Cores 1 and 3 (Surface to a 146 cm depth) were taken from the first bore hole, Bore Hole 1, and Cores 2

and 4 (Surface to a 138 cm depth) were taken from the second, Bore Hole 2. The bore holes were subsequently filled with bentonite pellets, and marked with wooden stakes.

Tests were conducted on two sub-samples, N1 and N2, taken from the bottom 20 cm of Core 1, the top core from Bore Hole 1. This corresponds to an approximate depth of 50 to 70 cm below the surface. Tests were also conducted on two sub-samples, N3 and N4, taken from the bottom 20 cm of Core 2, the top core from Bore Hole 2. This also corresponds to an approximate depth of 50 to 70 cm. One CRS and one Column Experiment were run on specimens from each sub-sample (except N4). The trimmings from these specimens were used for the Specific Gravity experiments (Section 4.4) and for the Particle Size Distribution experiments (Section 4.6). The dried specimens themselves were burned to find their ash content.

One additional sub-sample, N5, was taken from Core 3, the bottom core taken from Bore Hole 1. This corresponds to a depth of 140 to 146 cm. The last column experiment was run on this specimen.

4.3.2 RESEDIMENTED WETLAND DEPOSIT SAMPLES

Bulk samples, which were taken from the site and re-sedimented in the laboratory, were tested in addition to the undisturbed samples described above, since tests on undisturbed samples can be difficult to perform and to interpret.

In fact, natural wetland deposit samples can exist at such low pre-consolidation pressures and high water contents that they tend to be extremely difficult to trim and to setup. Furthermore, natural samples can vary extremely from one core to the next, and within a single core, due to different environmental and depositional factors. This means that comprehensive testing is required to understand even the most fundamental physical relationship for this type of soil (See Sections 2.2.1 and 3.3.2).

On the other hand, when re-sedimented samples are used, the problems associated with testing natural samples can be minimized. First, re-sedimented samples are more uniform than natural ones. Second, there is less variability between different samples; and third, the pre-consolidation pressure of these samples can be designed such that it is at the upper limit

of the range of pre-consolidation pressures found in the field, and the water content at the lower limit. Tests run on such samples are not only easier to perform, but they allow for an easier comparison between geotechnical and hydrological parameters with fewer tests, since there are fewer variables to consider. If relationships between these parameters are established for re-sedimented samples, it will be easier to interpret the tests on the undisturbed samples. In this chapter, as well as in Chapters 6, comparisons are given for tests performed on undisturbed and re-sedimented samples.

4.3.2.1 RE-SEDIMENTATION PROOF TESTS

The characterization tests described in this chapter (specific gravity, ash content, particle size distribution, and constant rate of strain) showed that the stress history, compressibility, and other geotechnical properties of the re-sedimented samples compared well with those of the undisturbed samples tested by Bailon (1995). See Section 3.3.2. These tests also showed that the re-sedimentation process is repeatable, and that the physical properties within one sample were relatively uniform (Also see Sections 4.4 to 4.7).

4.3.2.2 SAMPLE DESCRIPTION

The re-sedimented soil was made from the same surface layer of wetland deposits at the Wells G and H site as the undisturbed samples. Several cores were collected from within one meter of the surface (Location B, Figure 4.1) in February, 1997, using the same fixed piston sampler used to retrieve the undisturbed samples. However, the cores were extruded on site, into a five gallon bucket. The soil was taken back to the laboratory where it was mixed and cleared of all large woody pieces and reeds larger than 5 mm in diameter. It was then placed under at least an inch of water in a covered container, from which the air was evacuated. The evacuated container was enclosed within opaque plastic and stored in a 100% humid room. All these measures were taken to minimize chemical (oxidation) or biological (degradation) processes that might change the soil structure and fabric.

This soil stock was sub-sampled as needed, then processed and re-sedimented according to procedures described in Section 3.3.2 and Appendices B2 and B3. The soil stock was sub-sampled, processed, and batched on 5 separate occasions. For each Batch, 1 to 5, two

samples were made. All Samples, 1 to 10, were roughly 6.4 cm in diameter and 8 cm high. Samples 1 to 6 (Batches 1 to 3) and 9 to 10 (Batch 5) were processed on the 'Coarse' setting. That is, the maximum particle size was set at 1 cm. Samples 7 and 8 (Batch 4), were processed on the 'Fine' setting. That is, the maximum particle size was set at 4 mm. See Figure 4.4 for an outline of the re-sedimented sample organization.

There was enough soil in each Sample for two of the 1" high specimens required for either the CRS or the Column Experiments. The trimmings from these specimens were used in the specific gravity experiments, and the dried specimens themselves were burned to find their ash content. Left over soil from each batching procedure was reserved for either the Peat-Salt Interaction experiments (Section 3.3.1) or for the Particle Size Distribution experiments (Section 4.6).

4.3.3 WETLAND DEPOSIT CLASSIFICATION

Both the undisturbed and bulk soils sampled from the site are similar in composition. They are highly organic, dark colored (dark brown to black), with a large fine grained, amorphous component. The macroscopic component is primarily made up of partially decomposed grasses (sedge), with some wood and typha pieces that are larger than 5 mm in diameter. The macroscopic pieces constitute about one third of the overall volume of the soil.

Since the organic content of these samples is on average 58% (See Section 4.5), they are classified as 'organic soils' according to most classification systems (See Section 2.1.1), and as 'peat' according to some. In most classification systems, there is a spectrum of terms associated with the value of organic or mineral content, a *mineral soil* having the smallest organic fraction, an *organic soil* having an intermediate organic fraction, and *peat* having the largest organic fraction. For example, according to ASTM Standard D4427, a soil has to have less than 25% ash content to be considered a peat. On the other hand, according to Mitsch and Gosselink (1993), any soil with an organic content higher than 25 to 30% is considered an *organic soil*. This organic soil can be further subdivided into a *peat*, if more than two thirds of the plant material is identifiable, or, into a *muck*, if less than one third of the plant material is identifiable. According to this classification system this soil is a *muck*,

since less than one third of the plant material is identifiable. On the other hand, according to the Radforth classification system also discussed in Section 2.1.1, the sampled sediments classify as No. 7 peat (Radforth, 1969).

4.3.4 TESTING ORGANIZATION

Since both re-sedimented and undisturbed samples were tested, it was necessary to develop a simple nomenclature to help keep the different samples apart. A suite of tests was run on all ten re-sedimented samples and on small portions of undisturbed Cores 1 and 2. For the sake of simplicity, the re-sedimented samples are referred to by their number, S1 to S10, and the undisturbed or natural sub-samples, of which there were five, are referred to as N1 to N5, sub-samples N1 and N3 corresponding to a depth of 60 to 70 cm, sub-samples N2 and N4 corresponding to a depth of 50 to 60 cm, and sub-sample N5 corresponding to a depth of 140 to 146 cm.

Samples S1 to S3 were used for proof tests to ascertain that the geotechnical properties of the re-sedimented soil were comparable to those of the undisturbed samples characterized by Bailon (1995), and to show whether tests within one sample and between samples gave the same results for compressibility, stress history, specific gravity, void ratio, ash content and hydraulic conductivity (Section 3.3.2).

Sample S6, which was preconsolidated to a low 18 kPa, was used to test whether the two CRS devices at the MIT geotechnical facilities gave comparable data. At the time, there was a possibility that a newly acquired Trautwein CRS device would have to be used, and since all previous tests had been conducted on an older, Wissa device (Wissa, 1971), a comparison was necessary. In the end, however, all remaining CRS tests were conducted on the older device.

Both CRS and Column Experiments were conducted on the remaining Samples S4, 5, and 7 to 10. Also, both CRS and Column Experiments were conducted on the undisturbed sub-samples N1 to N3. Specific Gravity and Ash Content were found for each of the re-sedimented and undisturbed samples. Table 4.1 summarizes all tests conducted on both re-sedimented and undisturbed samples, as well as the tests conducted on the soil left over from

the re-sedimentation procedure or trimmed from the core samples. Only Column Experiments were run on undisturbed sub-samples N4 and N5.

4.4 SPECIFIC GRAVITY TESTS

Due to the potential variability between organic soil samples, obtaining an accurate value of the specific gravity (G_s) for each sample is important. The value of G_s is necessary to calculate the void ratio, e , of the soil, and the void ratio is used to interpret CRS data and to calculate the initial and final porosity of a specimen tested on the permeameter. The specific gravity was determined according to ASTM standard D854. The fluid used in the experiments was kerosene since some components of wetland deposits are less dense than water. For a detailed procedure see Appendix B4.

All results for the re-sedimented samples were consistent, and the average value for G_s was $2.04 \pm 4\%$ (Table 4.2). The results for the undisturbed samples were lower, and the spread between the different values was a little larger. For these samples, the average value for G_s was $1.68 \pm 12.7\%$. The lower value of G_s is to be expected since the ash content for the undisturbed specimens was lower (See Section 4.5, below). The difference in G_s values from sample to sample is due to the variability found in natural samples. Table 4.2 shows a summary of all the G_s results for the different samples tested.

4.5 SOIL ASH CONTENT

The ash or mineral content of a wetland deposit is a parameter used to better classify wetland deposits. According to most classification systems, soil with an organic fraction larger than 50% is considered to be a peat, and soil with an organic fraction between 25 and 50% is considered to be an organic soil (See Section 2.1.1). The mineral content of a soil is also a physical parameter that may, or may not, influence the other hydrogeological properties of that soil. For this study, the ash content of the specimens tested was determined so that any relationships between the organic content, porosity, and ultimately, hydraulic conductivity could be investigated. The ASTM standard D2974 was followed, and each specimen was burned at 440 °C, then at 750 °C. For a more detailed procedure see Appendix B5.

Except for the tests on Samples S1 to S3, all results for both the re-sedimented and the undisturbed samples were consistent. The results of tests on the first three re-sedimented samples were discarded, since, for these tests, the soil was not oven dried before ashing. For the remaining re-sedimented samples, the average value for ash content was $58.3\% \pm 1.8\%$ when the soil was burned at $440\text{ }^{\circ}\text{C}$, and $56.7\% \pm 1.6\%$ when the soil was burned at $750\text{ }^{\circ}\text{C}$. For the undisturbed samples, the average value for ash content was $46.9\% \pm 16.8\%$ when the soil was burned at $440\text{ }^{\circ}\text{C}$, and $45.2\% \pm 18.1\%$ when the soil was burned at $750\text{ }^{\circ}\text{C}$. The ash content for the re-sedimented soil is higher, as expected, since large, organic fragments were removed during processing. Also, the spread between the ash content values measured for the undisturbed samples reflects the high variability in natural samples. Table 4.3 shows a summary of all the ash content results for the different specimens tested.

4.6 SOIL SIZE DISTRIBUTION

In order to see what sizes of particle are represented in these wetland deposits, and to see how well or poorly sorted these sizes are, the different size components of the soil have to be separated, and these sizes quantified. Not only does this type of size distribution analysis allow for some quantification of the differences between the processed, re-sedimented samples and the undisturbed, natural samples tested in this study, but it might also help evaluate how particle size affects the void ratio of the soil. This might eventually lead to a better understanding of how particle size affects the hydraulic conductivity of these highly variable, sediments.

4.6.1 PROCEDURE

Because a large component of wetland deposits is organic, it is not possible to determine their size distribution using the methods that have been established for inorganic soils. First, organic material shrinks when it is dry and is more likely to break, so any separation technique must be conducted wet. As a result, the mechanical sieving technique used for coarse, inorganic sands and silts is inappropriate, since shaking the sieves would not necessarily be sufficient to separate wet particles. Second, due to the fact that organic soil can contain elements of different densities, and since some organic material is less dense than

water, a hydrometer, used for determining the size distribution of fine grained clays and silts, would also not be useful. Therefore, a procedure had to be developed to separate the particles into different size categories while keeping the soil saturated. To that end, the sieving technique was modified to accommodate a wet soil.

The modified procedure is as follows: a wetland deposit slurry is made by adding distilled water to roughly 400 grams of soil at a water content of 400%. This slurry is poured into a stack of sieves stacked in descending aperture size. The soil is then washed through the sieves with copious amounts of water. After each sieve is cleared of all smaller particles, it is dried in a 110 °C oven. When all the sieves are dry, they are massed to determine the mass of each size fraction. Finally, The Percent Of Soil Passing each sieve is plotted against Sieve Size.

To determine the error in the procedure, a portion of the slurry is reserved for a water content measurement, and, using this measurement, the wet mass of each size fraction is calculated. These wet masses are summed and the total calculated mass is compared to the measured mass of the original slurry. For a detailed procedure see Appendix B6.

4.6.2 RESULTS

Three size distribution experiments were conducted, the first, on soil processed on the ‘fine’ setting, that is, with a maximum particle size of 0.4 cm , the second, on soil processed on the ‘coarse’ setting, that is, with a maximum particle size of 1 cm, and third, on a sub-sample of the undisturbed cores. The three Size Distribution Curves are plotted in Figure 4.5 and the data tabulated in Table 4.4.

As expected, the unprocessed, natural soil had larger particles and more particles in the large size fractions. On the other hand, the ‘finely’ processed soil had a narrower range of particle size with the maximum particle size, as designed, being 4mm. The Size Distribution Curve for the ‘coarsely’ processed soil fell in between those of the unprocessed and fine soils.

Values for D_{10} and D_{60} were used to calculate the Uniformity Coefficient (C_u), the ratio of D_{60} to D_{10} , for each soil. According to the Unified Soil Classification System, all three soils are well graded, that is, C_u is greater than 2 (Lambe and Whitman, 1969).

After the soils were sieved, it was noted that the coarser size fractions contained mostly organic material and that the finer size fractions contained mostly mineral material. To investigate this, each size fraction was ashed and this trend confirmed. See Table 4.5 and Figure 4.6. The ash content for the processed soil was consistently higher for each size fraction than for the unprocessed soil. This corresponds to the total ash content being higher for the processed soil (See Section 4.5).

However, the ashing of the size fractions demonstrates that there is substantial error in the size separation technique. The coarser size fractions should contain very little ash since there are no visible mineral particles. Yet they contain 20% ash or more. This must be due ineffective washing of clay particles away from the organic particles during the sieving process.

4.7 SOIL STRESS HISTORY AND COMPRESSIBILITY (CONSTANT RATE OF STRAIN TESTS)

Constant Rate of Strain (CRS) tests were conducted to better understand the compressibility behavior and the stress history of the soil samples. These strain-controlled tests have several advantages over the traditional oedometer tests used to find these parameters. First, CRS tests are automated, and give continuous compression data. Second, the excess pore pressure data which is gathered also gives a continuous, direct measure for hydraulic conductivity. Third, the CRS tests are faster than the oedometer tests. For these organic soils, a CRS test takes 2 days to complete, whereas, the oedometer test takes at least one week. Finally, data analysis, which involves graphical interpretation is done by hand and can be somewhat tedious for the oedometer tests, is done by direct calculation by computer program and spreadsheet for the CRS tests and, is subsequently less labor intensive.

4.7.1 CRS EQUIPMENT

The MIT CRS equipment was based on the design by Wissa et al. (1971). Some changes in the original design include the removal of the inner diaphragm separating the specimen from the cell fluid, and the addition of an electronic pore pressure transducer at the base of the cell, an electronic cell pressure transducer connected to the cell water, an electronic load cell to

measure the axial load, and a Linear Variable Displacement Transducer (LVDT) to measure changes in the sample height.

The equipment consists of a stainless steel cell with a ceramic, porous stone at the base which is connected to the pore pressure transducer (See Figure 4.7). The cell itself is connected to a manifold containing the cell pressure transducer and a pressure gauge. The cell pressure is applied through a system of mercury pots that can be elevated until the desired cell pressure is reached. The cell platform can be moved up or down and is either powered by hand or by a motor which is attached to a variable gear box. The load frame is equipped with an air jack, which, when connected to an air compressor, can maintain a constant load on the specimen to measure secondary compression.

4.7.2 CRS PROCEDURE AND DATA ANALYSES

First, the specimen is trimmed to fit the testing ring, which is 2.36 cm high and 6.35 cm in internal diameter. Then, the specimen and ring are placed on the base of the cell, directly over the porous stone, and fixed in place by a brass ring with an o-ring seal at the base, which screws into the base. The cell itself is then screwed into place, and the piston seated. After the specimen is back-pressure saturated to 400 kPa, it is loaded at a constant strain rate, and the variable gears are set such that the strain rate creates an excess pore pressure of 2 to 5% of the total stress on the specimen. The specimen can be loaded up to 2,300 kPa, but these organic soils are never taken beyond 1,000 kPa. The maximum load is then maintained until the excess pore pressure in the specimen is dissipated (usually overnight), then the specimen is unloaded and the cell disassembled. For a complete description of the testing procedure, refer to Appendix B7.

The displacement, load, and pore and cell pressure data are reduced with a computer program written by Dr. J. T. Germaine. This program uses the Linear Theory developed by (Wissa et al., 1971) to calculate values for the effective stress, the void ratio, e , the hydraulic conductivity, k , and the total work (Becker, et al., 1987). These parameters are used to calculate: (1) the Compression Ratio (CR), the slope of the Virgin Compression Line in the Stress vs. Strain Curve; (2) the Re-compression Ratio (RR), the slope of the re-compression

line in the Stress vs. Strain Curve, (3) the Hydraulic Conductivity Index (C_k), the slope of the e vs. $\log k$ curve; and (4) the Pre-consolidation pressure (σ'_p), the stress corresponding to the break in the Stress vs. Total Work Curve. See Figure 4.8 for example data and constructions. A copy of the computer program and a more detailed description of the data analyses can be found in Appendices C2 and B7, respectively.

4.7.3 RESULTS

The results of the first CRS tests run on Specimens S1 and S3 were used to verify the re-sedimentation process and are discussed in Section 3.3.2.2 (Tables 3.3 and 3.4). The results of these CRS tests as well as the tests run on Specimens S4, S5 and S7 to S10 (S6 is excluded since it was consolidated to a lower effective stress), and undisturbed specimens N1 to N3 are included in Table 4.6 and 4.7, respectively and are discussed below.

4.7.3.1 RE-SEDIMENTED SOIL DATA

The values for CR are consistent for all the specimens, ranging from 0.319 to 0.362, with an average value of $0.338 \pm 4.4\%$. The Virgin Compression Lines (VCL) for each test are plotted in Figure 4.9 and 4.10. This figure shows, however, that despite the similarity in slope, the VCLs for Specimens 9 and 10, though they coincide with each other, have a much higher intercept. Possible reasons for this difference are discussed below.

The values for RR are more scattered than those for CR. This is due to the fact that Specimens 1 through 7 were unloaded at a much faster rate (0.07% per second) than Specimens 8 through 10 (0.009% per second). The different unloading rate affected the values of RR almost seven fold. RR values average $0.168 \pm 7.4\%$ for S3 to S7, and $0.025 \pm 22.5\%$ for S8 to S10.

Values of e_o and W_c , S_o are comparable from batch to batch with the overall averages being $5.73 \pm 4.9\%$, $268\% \pm 4.0\%$ and $95.3\% \pm 2.2\%$ respectively. C_k is far more variable with an average of $1.26 \pm 24.3\%$. A plot of e vs. $\log k$ for each specimen shows a similar trend between tests as for the VCLs. The e - $\log k$ lines (Figure 4.11) for Specimens 9 and 10 have a

considerably higher intercept than the those of the other specimens, and the *e-log k* line for Specimen 8 has an intermediate intercept.

In order to understand the difference between the placement of the VCLs and the *e-log k* lines for Specimens 8, 9 and 10 relative to the other specimens', a comparison between the following properties of the specimen were made: measured σ'_p , e_o , S_o , duration of the final increment on specimen during batching (a measure of the 2^o compression the sample has experienced), age of peat at batching (time soil was taken from the field to time it was batched), age of the specimen at time of testing (time soil was batched to time it was tested), and, finally, the total age of the soil at time of testing (time soil was taken from field to time it was tested). These data are included in Table 4.8.

4.7.3.1.1 Discussion

The difference in the *e-log k* behavior of Specimen 8 can be explained by the fact that, during the re-sedimenting process, the Batching apparatus (See Section 3.3.2) was leaking, and the sample was subjected to several wetting-drying cycles. According to Rycroft, et al (1975), colloidal particles in organic soils can undergo irreversible physical changes if the soil is dried beyond a certain point. It is possible that such a physical change occurred in Sample 8, altering its hydraulic conductivity. If, for example, colloidal particles settled out of the pore water and onto the pore walls, the porosity of the sample would decrease, causing the hydraulic conductivity of the sample to decrease. Despite the actual decrease in pore volume, there would be no difference in the measured value of void ratio, since the mass and volume of the sample would remain the same.

The difference in the *stress-strain* and *e-log k* behavior of Specimens 9 and 10 are harder to explain. It is clear that these differences are age related, since these specimens were by far the oldest at the time of testing. The actual mechanisms by which the specimens become relatively less compressible and less permeable given the same void ratio are unclear. It is possible that bacterial growth over time lead to the clogging of pores and the stiffening of the soil. It is also possible that the clay portion of these organic soils are susceptible to the same soil aging mechanism, thixotropy, found to affect inorganic, re-sedimented clay specimens.

Thyxtropy has been well documented in re-sedimented Boston Blue Clay specimens (Zreik, 199x), and was found to cause the strengthening and stiffening of these soils.

4.7.3.2 UNDISTURBED SOIL DATA

As was expected, the differences between the results of the CRS tests on the three undisturbed specimens were larger than for the re-sedimented specimens (See Table 4.7). The values for CR measured for the undisturbed specimens were over 20% lower than was measured for the re-sedimented specimens, and they ranged from 0.240 to 0.299, with an average value of $0.277 \pm 11.6\%$. The Virgin Compression Lines (VCL) for each test are plotted along with the re-sedimented specimen VCLs in Figure 4.12 and 4.13. In Figure 4.12, the graph shows that, despite the fact that the specimens were taken from within 10 to 20 cm from each other, the VCLs for the three specimens do not coincide. For Specimen N2, which was taken from a depth of 55 cm, the VCL almost coincides with the VCLs measured for S9 and S10, the aged re-sedimented specimens. For Specimens N1 and N3, which were taken from a depth of 65 cm, but from Bore Holes set 20 cm apart, the VCLs cross, with their slopes differing by 25%.

The values for RR are more scattered than those for CR. The RR value of 0.030 that was measured for N3, was significantly lower than the RR values measured for N1 and N2, which averaged $0.188 \pm 6.7\%$. The three RR values averaged $0.135 \pm 67.4\%$.

Values of e_0 and W_c , S_0 were relatively less scattered than the values of RR. The average void ratio value for the undisturbed specimens was $9.67 \pm 13.0\%$, which is significantly higher than the average void ratio value measured for the re-sedimented specimens. Also, the average water content value for the undisturbed specimens was higher than was measured for the re-sedimented specimens. It was $416\% \pm 14.1\%$. On the other hand, the average degree of saturation value for the undisturbed specimens was $89.7\% \pm 0.8\%$, which is lower than the average value calculated for the re-sedimented specimens.

Like for the re-sedimented specimens, C_k was variable for the undisturbed specimens, averaging at $1.56 \pm 29.7\%$. A plot of e vs. $\log k$ for each specimen showed that the e - $\log k$ curve for N1 crosses the e - $\log k$ curve for S9 and S10 (Figure 4.14). Also, the e - $\log k$ curve

for N2, which has a lower intercept and higher slope than the one for N1, is similar to the e - $\log k$ curve for S8. The e - $\log k$ curve for N3 has a significantly higher intercept and slope than the curves measured for all other specimens, meaning that, for the same void ratio, this specimen has a lower hydraulic conductivity than the other specimens.

It should be noted that for the re-sedimented Specimens S9 and S10, both the VCL and e - $\log k$ curve were set apart from the curves measured for the other specimens, and it was reasonable to assume that the same physical mechanism, thixotropy, was causing these differences. In the case of the undisturbed specimens, however, there does not seem to be a trend between VCL and C_k . This underscores how trends can become obscured for natural samples since these samples undergo many environmental changes, unlike re-sedimented samples.

4.7.3.3 CONCLUSIONS

A comparison between the CRS data for the re-sedimented and undisturbed specimens shows that CR, RR and σ'_p for the re-sedimented soil are consistently higher than for the undisturbed soil. However, the void ratio and water content values are significantly higher for the undisturbed specimens. C_k values are variable for both soils, with the re-sedimented specimens forming the lower limit of the range of values, and the natural specimens forming the upper limit.

The values measured for the three undisturbed specimens show more variability, despite the fact that they were sampled from within 20 cm from each other. This underscores the usefulness of the re-sedimented specimens, which can potentially be used to differentiate between the effect of different physical, chemical and biological mechanisms.

4.8 CHARACTERIZATION OF MINERAL FRACTION OF WETLAND SOIL

The mineralogy and the size distribution of the mineral fraction of the wetland deposits was determined in order to better understand how this fraction might affect overall flow and transport mechanisms. The mineral extraction procedure, the mineralogy assessment, and the size distribution tests, are discussed below:

4.8.1 EXTRACTION METHOD

The mineral fraction of the soil was extracted from the wetland deposit according to the Peroxide Oxidation Method outlined in Head, 1980. In this method, dilute H_2O_2 is added to a soil slurry, mixed, then left overnight. The following day, the slurry is boiled to insure that the H_2O_2 reacts completely with the organic material. This procedure is repeated until all organic material has been digested. The organics-free slurry is oven dried and the remaining minerals are ready to be tested.

The minerals extracted from the re-sedimented sample S10 trimmings were used for the tests described below.

4.8.2 MINERALOGY

The procedure to determine soil mineralogy was carried out in three steps. First, the mineral portion extracted via the procedure discussed above was sieved through a number 325 sieve. This part of the procedure required that the mineral soil be placed in 5 cm diameter sieve, which had a fitted cap and bottom plate. The sieve was tapped onto a rubber surface 30 to 40 times. The soil retained on the sieve was broken down using a mortar and pestle, then re-sieved. This procedure was repeated until all the soil had passed through the sieve.

In the second step of this procedure, the sieved soil was taken to the X-ray diffraction laboratory in the Material Engineering department at MIT. X-ray diffraction images of the soil were taken by Joseph Adario according to the standard described by Mitchell (1993).

In the third step of this procedure, the X-ray diffraction images were read by Dr. Robert Martin, formerly of the Geotechnical Laboratories at MIT. Dr. Martin concluded that the mineral fraction of these wetland soils was made up of quartz, mica, chlorite and feldspars. There was no evidence that any clays were present.

4.8.3 SIZE DISTRIBUTION

The size distribution of the wetland soil mineral fraction was determined according to the Pipette Analysis Method described by Head (1980). This method is similar to the Hydrometer tests typically used to determine the size distribution of fine grained soils. The

advantage of using the pipette method is that as little as 6 g of soil can be used for the test, and since there was only a small amount of mineral soil available for size distribution analysis, the pipette method was used.

The size distribution of the wetland soil mineral fraction is shown in Figure 4.15 for duplicate tests. The particle sizes ranged from 0.02 to 0.002 mm. These sizes fall into the coarse to fine silt category. This corresponds with the mineralogy results, which showed that no clays were present in this soil.

4.9 REFERENCES

The Book of ASTM Standards, Part 19. D854: 1987.

The Book of ASTM Standards, Part 19. D2974: 1987.

The Book of ASTM Standards, Part 19. D4427: 1987.

The Book of ASTM Standards, Part 19. D1587: 1994.

Becker, D. E., Crooks, J. H. A., Been, K., Jefferies, M. G., *Work as a Criterion for Determining in situ and Yield Stresses in Clays*. Canadian Geotechnical Journal, 24.4, November 1987: 549-564.

Bialon, J.L. *Characterization of the Physical and Engineering Properties of the Aberjona Wetland Sediment*. M.S. Thesis. Massachusetts Institute of Technology, Cambridge, MA, 1995.

Head, K.H. Manual of Soil Laboratory Testing. Volume 1: Soil Classification and Compaction Tests. Pentech Press, London, 1980

Mitchell, J.K. Fundamentals of Soil Behavior. 2nd Edition, John Wiley and Sons, Inc., New York, 1993

Mitsch, W. J., Gosselink, J. G., *Biogeochemistry of Wetlands*. Wetlands, 2nd Edition. Van Nostrand Reinhold, New York, 1993: 114-188.

Radforth, N.W., *Classification of Muskeg*. Muskeg Engineering Handbook. I.C. MacFarlane, Ed. Muskeg Subcommittee of the NRC Associate Committee on Geotechnical Research, 1969: 31-52.

Ratnam, S., *Geotechnical Centrifuge Modeling of the Behavior of Light Nonaqueous Phase Liquids (LNAPLs) in Sand Samples Under Hydraulic Flushing*. M.S. Thesis, Massachusetts Institute of Technology, Cambridge, MA. 1996.

Rycroft, D.W., Williams, J.A., and Ingram, H.A.P. *The Transmission of Water Through Peat: I. Review*. Journal of Ecology, 63, 1975a: 535-556.

Wissa, E. Z., Christian, J. T., Davis, E. H., and Heiberg, S. (1971), *Consolidation at Constant Rate of Strain*. Journal of Soil Mechanics and Foundation Division, ASCE, 97.SM10, October 1971: 1393-1413

Table 4.1: Type and number of tests conducted on (a) re-sedimented and (b) undisturbed wetland samples

Batch No.	1		2		3		4		5				
	S1	S2	S3	S4	S5	S6	R	S7	S8	R	S9	S10	R
Gs	1	1		1	1	1	1	1		1			1
Ash Content				1	1			1	1		1		
Size Distribution													1
Salt-Peat Interaction		1					1						1
CRS	2	2	2	1	1	2		1	1	1	1	1	1
Colomn Experiment				1	1			1	1		1	1	1

(a)

Sample Name	N1	R	N2	R	N3	R
Gs	1		1		1	
Ash Content	1		1		1	
Size Distribution		1				
Salt-Peat Interaction		1				
CRS	1		1		1	
Colomn Experiment	1		1		1	

(b)

R = Peat remaining after batching or after cutting sampels from tube

Table 4.2: Summary of Specific Gravity values for wetland soil samples

Sample Name	Specific Gravity	
	Average	Error
Unprocessed*	1.97	1.6%
B1	1.95	3.4%
B1	1.97	1.0%
B2	2.03	5.8%
B3, S5	2.17	2.8%
B3, S6	2.08	7.2%
B3	2.09	0.9%
B4	1.98	2.3%
B5	2.14	1.0%
Average G_s	2.04	4.0%

N**	1.93	5.1%
N1	1.7	0.8%
N2	1.41	2.6%
N3	1.67	4.5%
Average G_s	1.68	12.7%

* Sample taken from re-sedimented soil stock, before processing

** Sample taken from undisturbed Core 1

Note: Error is associated with values of G_s at different temperatures

Table 4.3: Summary of Ash Content values for wetland soil samples

Sample Name	Ash Content	
	440 °C	750 °C
S1	-	-
S2	-	-
S3	-	-
S4	56.9%	55.5%
S5	57.7%	56.1%
S6	57.8%	56.1%
S7	58.7%	57.1%
S8	59.0%	57.3%
S9	59.7%	58.0%
S10	58.0%	56.4%
Average	58.3%	56.6%
Error	1.6%	1.5%

N1	43.5%	41.0%
N2	39.4%	37.5%
N3	47.0%	45.9%
N4	57.8%	56.3%
Average	46.9%	45.2%
Error	16.8%	18.1%

Table 4.4: Size Distribution data for re-sedimented specimens S4 and S5 and undisturbed specimen N1

Grain Diameter (mm)	% Passing		
	Batch 4	Batch 5	Undisturbed, N1
13.38	100.0%	100.0%	89.9%
4.7	100.0%	99.6%	85.1%
2	99.2%	92.4%	82.0%
0.85	85.3%	83.8%	76.1%
0.25	61.9%	58.1%	50.5%
0.15	54.3%	49.5%	40.2%
0	0.0%	0.0%	0.0%

Property	Batch 4	Batch 5	Undisturbed, N1
e_{average}	5.465	5.97	9.17
D_{10} (mm)	0.025	0.03	0.04
D_{50} (mm)	0.14	0.16	0.25
D_{60} (mm)	0.22	0.28	0.4
Uniformity Coef.	8.80	9.33	10.00

Table 4.5: Ash Content for the different particle size classes in re-sedimented specimens S4 and S5 and undisturbed specimen N1

Grain Diameter (mm)	Batch 4		Batch 5		Undisturbed, N1	
	440 °C	750 °C	440 °C	750 °C	440 °C	750 °C
13.38	-	-	-	-	23.8%	19.9%
4.7	-	-	26.7%	26.7%	16.5%	14.2%
2	38.5%	38.5%	34.8%	32.6%	32.2%	30.4%
0.85	46.3%	44.1%	40.8%	38.8%	39.6%	37.6%
0.25	54.4%	52.3%	49.4%	47.7%	42.1%	41.0%
0.15	59.8%	57.5%	53.8%	51.8%	40.6%	38.7%
0	66.1%	63.6%	58.5%	57.0%	44.4%	42.4%
Total Ash Content	58.9%	57.2%	59.7%	58.0%	43.5%	41.0%

Table 4.6: CRS data for re-sedimented specimens S1 to S10 (except S2 and S6)

Property	S1a	S1b	S3a	S3b	S4	S5	S7	S8	S9	S10	Averages
CR	0.331	0.348	0.342	0.325	0.341	0.357	0.362	0.329	0.319	0.322	0.338 +/- 4.4%
RR	-	-	0.162	-	0.171	0.155	0.184	0.031	0.025	0.020	0.025 +/- 22.5%
RR/CR	-	-	47.3%	-	50.1%	43.3%	50.7%	9.5%	7.8%	6.2%	7.8% +/- 21.3%
C _k	1.05	0.91	1.15	1.10	1.29	1.11	1.09	1.28	1.89	1.69	1.26 +/- 24.3%
e _o	5.89	5.84	5.44	5.73	5.75	5.79	5.10	5.83	5.80	6.14	5.73 +/- 4.9%
W _c	285%	278%	256%	261%	267%	271%	251%	272%	264%	279%	268% +/- 4.0%
S _o	95.3%	93.7%	95.5%	92.5%	94.1%	97.9%	97.6%	92.1%	97.3%	97.1%	95.3% +/- 2.2%
σ' _p (kPa)	30	37	55	30	34	47	64	52	76	68	49.3 +/- 33.5%
σ' (kPa, applied)	55										-
	48										-

Table 4.7: CRS data for undisturbed specimens N1 to N3

Property	N1	N2	N3	Averages
CR	0.240	0.299	0.293	0.277 +/- 11.6%
RR	0.179	0.197	0.030	0.135 +/- 67.4%
RR/CR	74.5%	65.8%	10.4%	0.502 +/- 69.2%
C_k	1.56	1.09	2.02	1.556 +/- 29.7%
e_o	9.17	8.66	11.04	9.62 +/- 13.0%
W_c	384%	380%	484%	4.16 +/- 14.1%
S_o	89%	90%	90%	0.90 +/- 0.8%
σ'_p (kPa, measured)	24	14.5	20	19.5 +/- 24.5%

Table 4.8: Age of soil after re-sedimentation and during testing, and duration of final batching increment

Sample	σ' (kPa)	σ'_p (kPa)	e_o	S_o	Final Incr. Duration (days)	Age of Soil at Batching (days)	Age of Sample (days)	Total Age of Soil at Testing (days)
1a	55	30	5.89	95.3%	2 to 5	74	12	86
1b	"	37	5.84	93.7%	2 to 5	74	19	93
3a	48	44	5.44	95.5%	2 to 8	117	15	132
3b	"	30	5.73	92.5%	2 to 8	117	18	135
4	"	34	5.75	94.1%	2 to 8	117	40	157
5	"	47	5.79	97.9%	2	157	9	166
7	"	64	5.10	97.6%	5	194	12	206
8*	"	52	5.83	92.1%	36	194	207	401
9	"	76	5.80	97.3%	2	396	63	459
10	"	68	6.14	97.1%	2	396	146	542

* Batch apparatus standpipe was leaking.

Figure 4.1: Sample locations at the Wells G and H Site, Woburn, MA (Bialon, 1995)

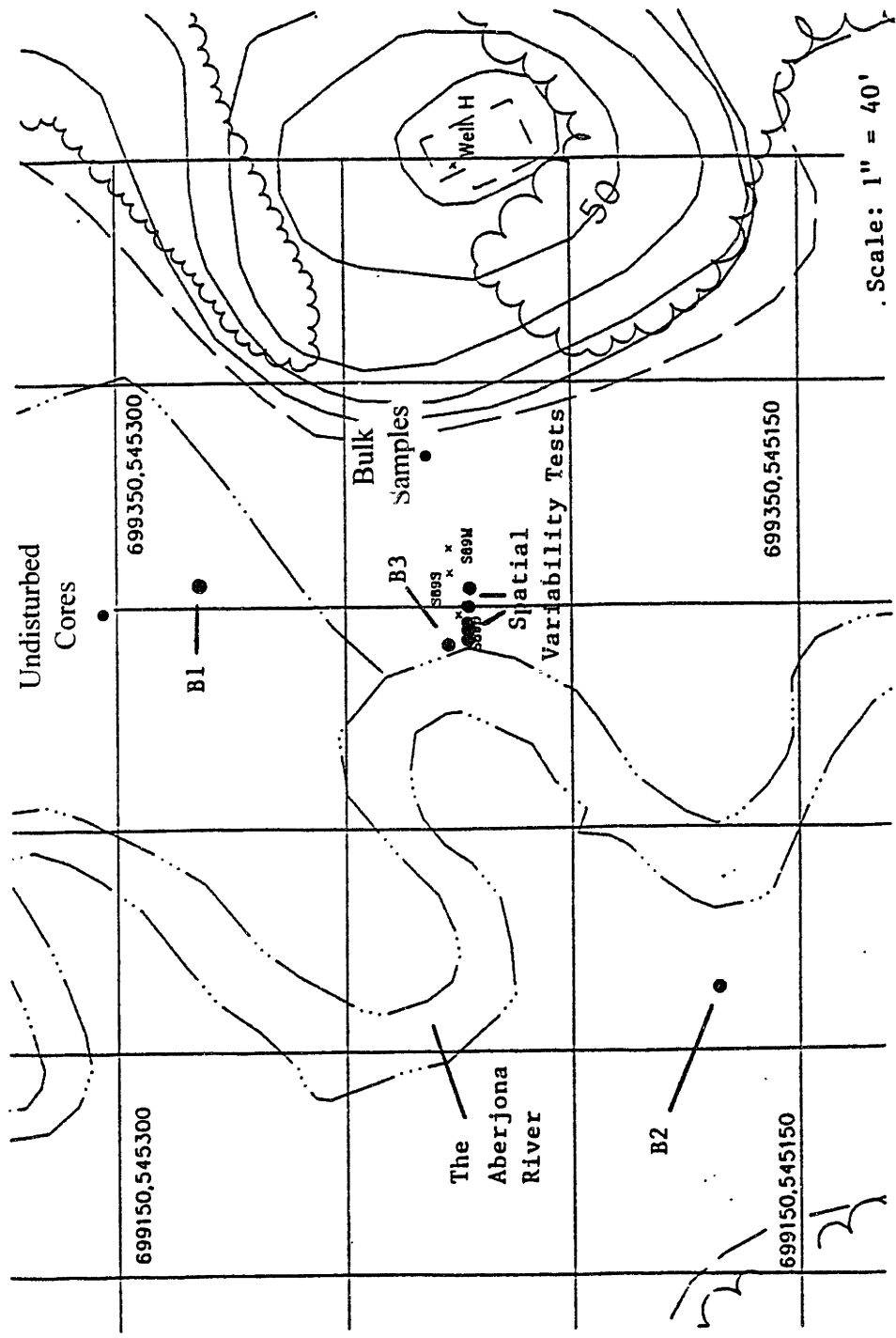


Figure 4.2: Manually operated, portable Piston Sampler. (a) Piston and threaded rod. (b) Shelby Tube connected to Steel Tube and Handle Bars.

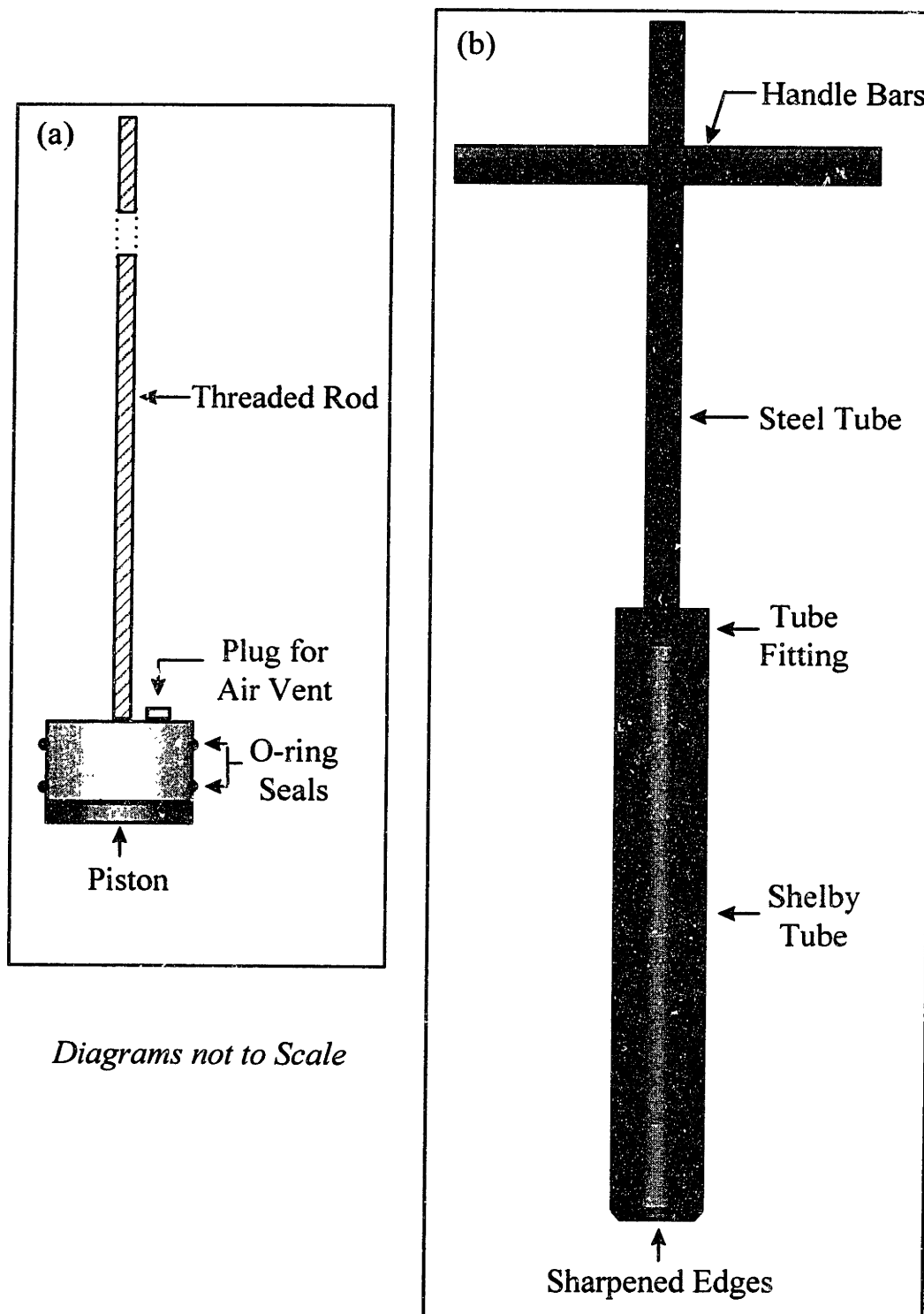


Figure 4.3: Example of Sample X-ray (Cores taken 4/96)

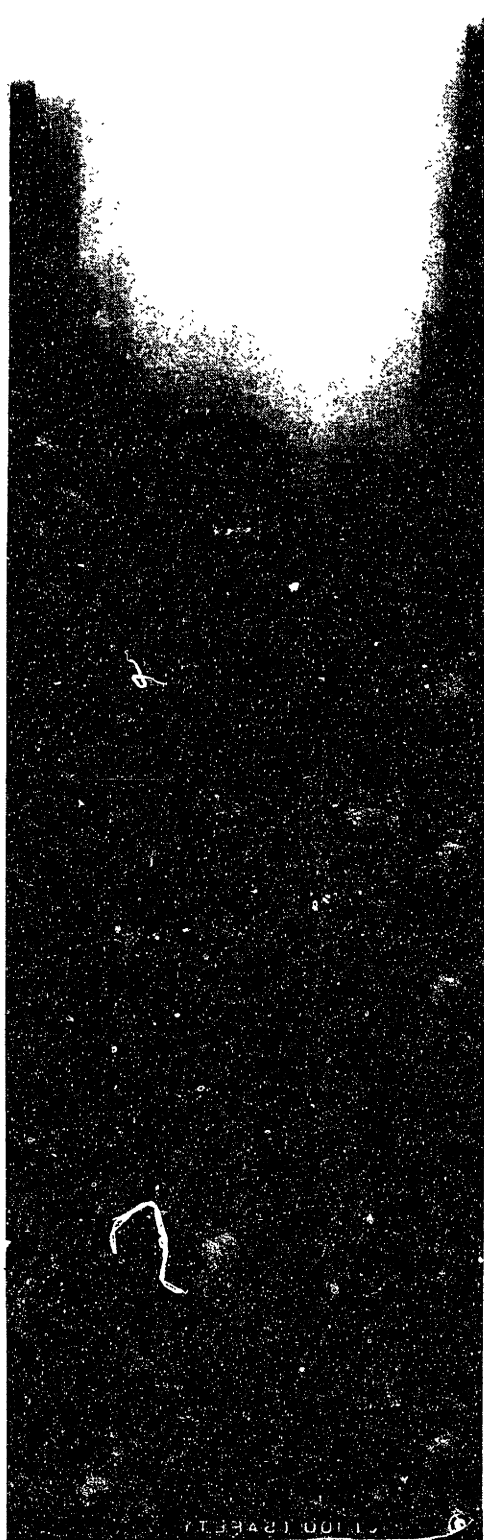


Figure 4.4: Organization of re-sedimentation batches and samples.

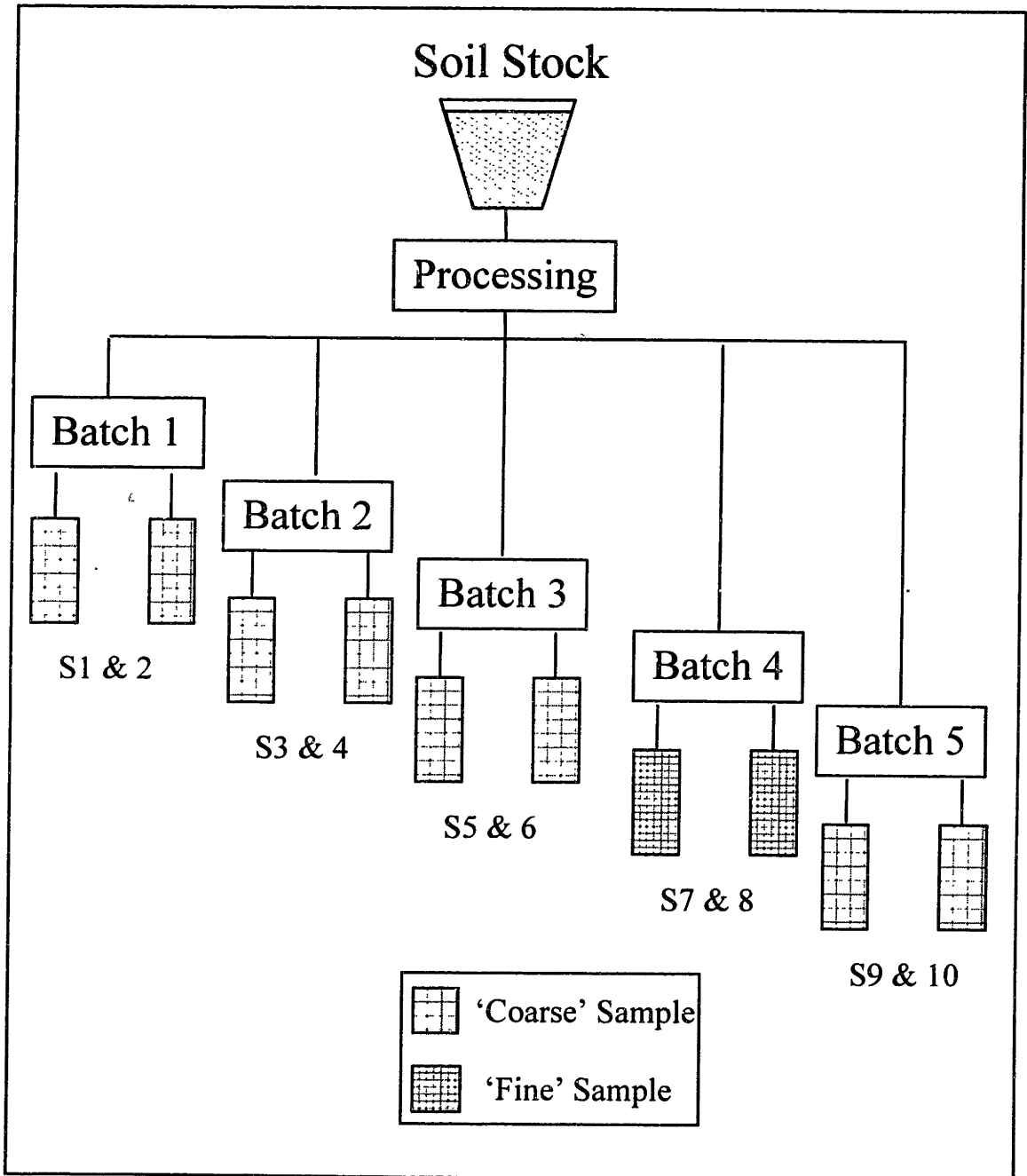


Figure 4.5: Particle Size Distribution for Batches 4 and 5, and Natural Sample N1.

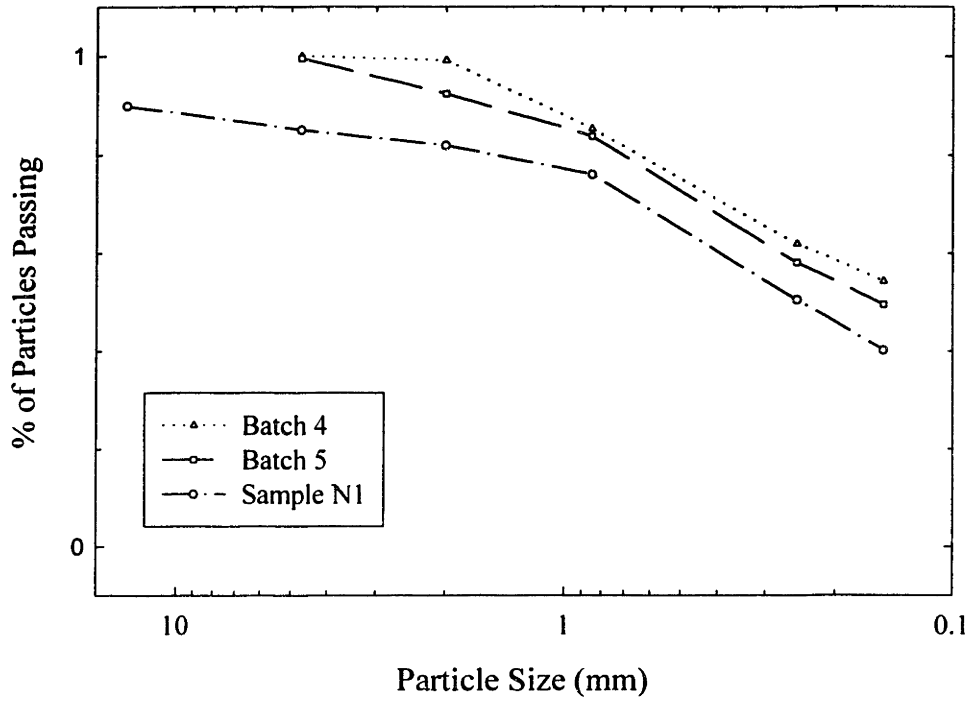


Figure 4.6: Ash Content vs. Particle Size Fraction: Batches 4 and 5, and Natural Sample N1.

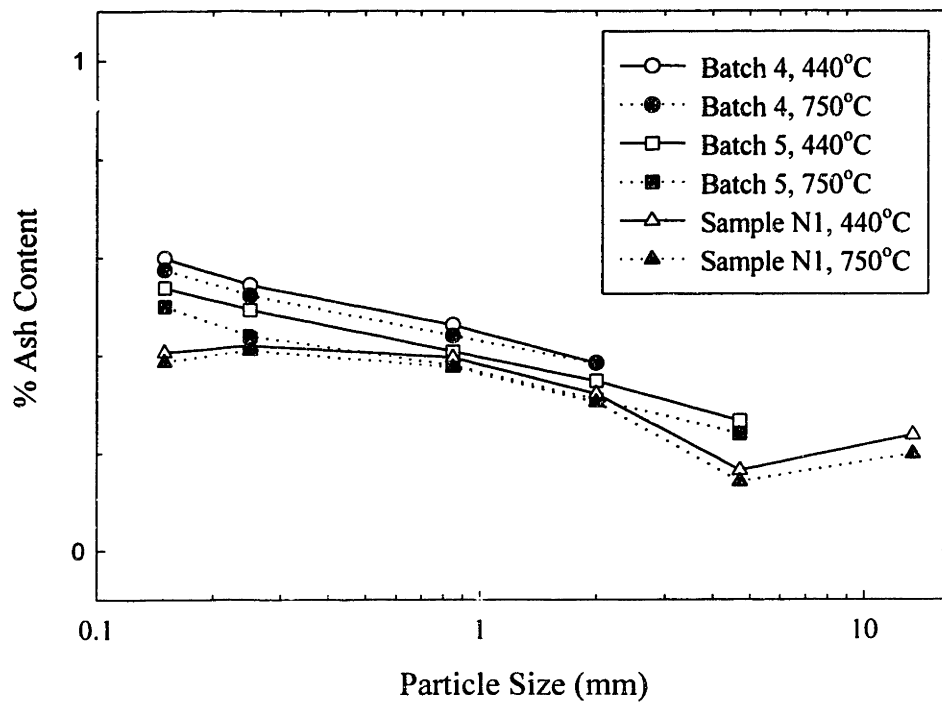


Figure 4.7: Schematic of Wissa CRS Device (Wissa et al., 1971)

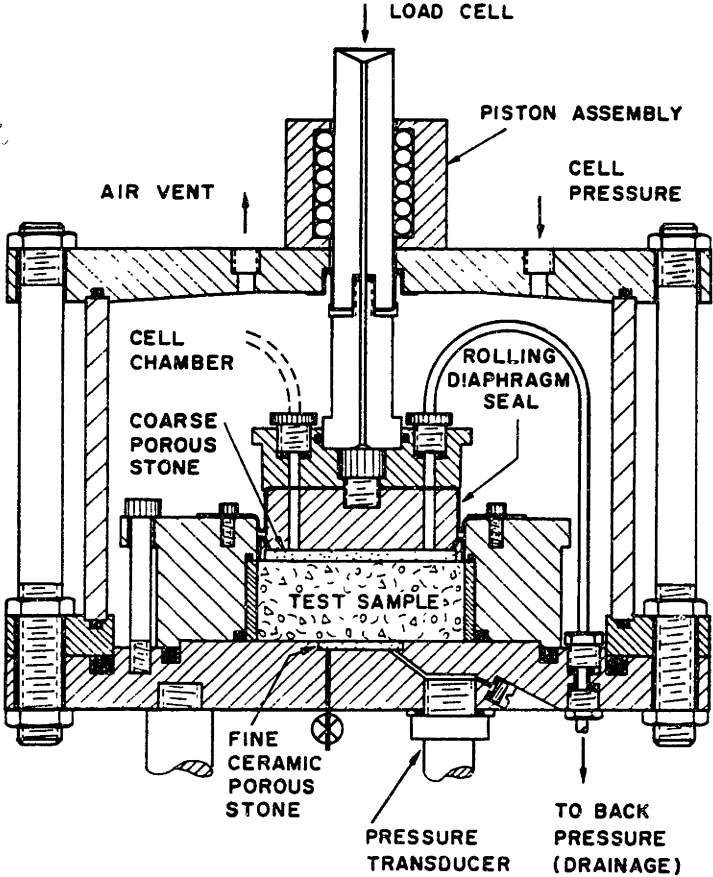


Figure 4.8: (a) Example of CRS data and constructions: re-settled Sample 9) STRAIN VS. STRESS

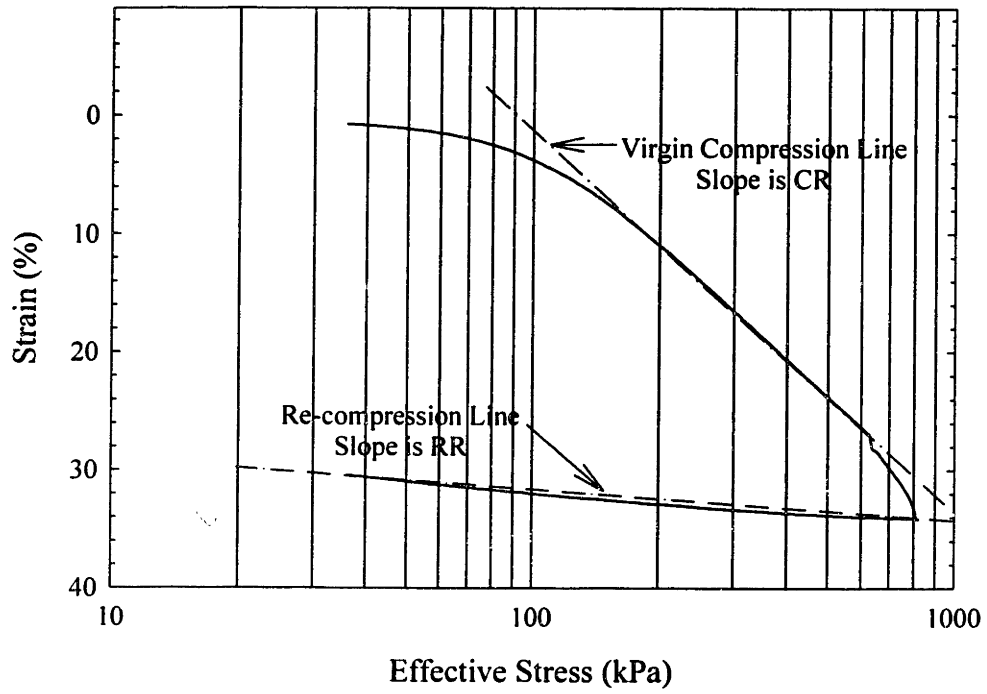


Figure 4.8: (b) Example of CRS data and constructions: re-sedimented Sample 9)
VOID RATIO VS. HYDRAULIC CONDUCTIVITY

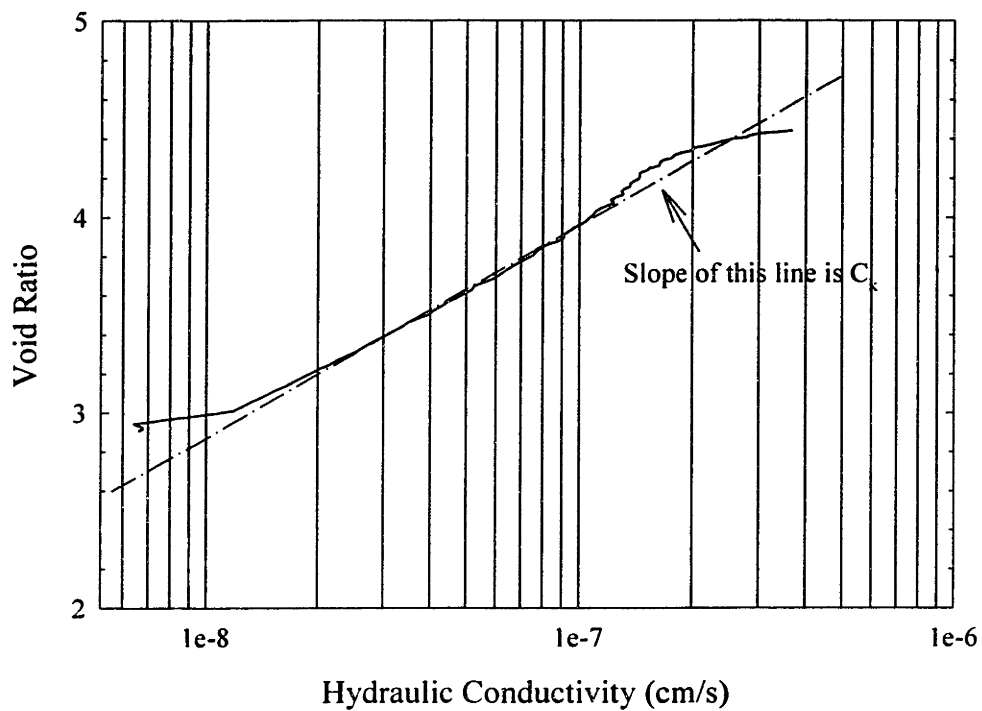


Figure 4.8: (c) Example of CRS data and constructions: re-sedimented Sample 9)
TOTAL WORK VS. STRESS

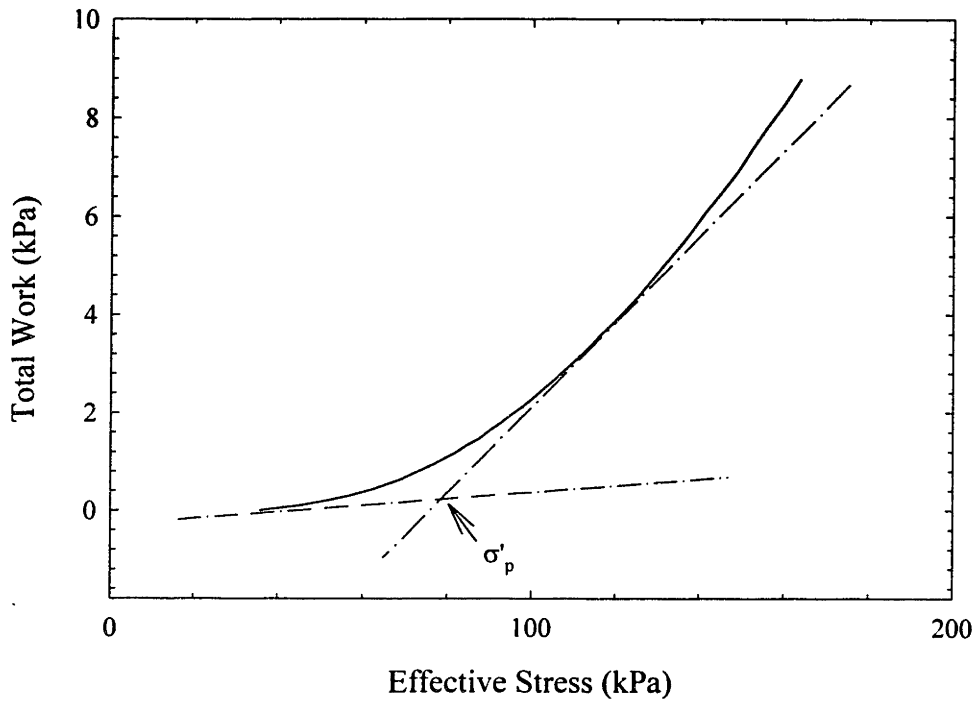


Figure 4.9: Summary of Void Ratio vs. Effective Stress data from CRS tests on Samples 1 to 10 (except 2 and 6).

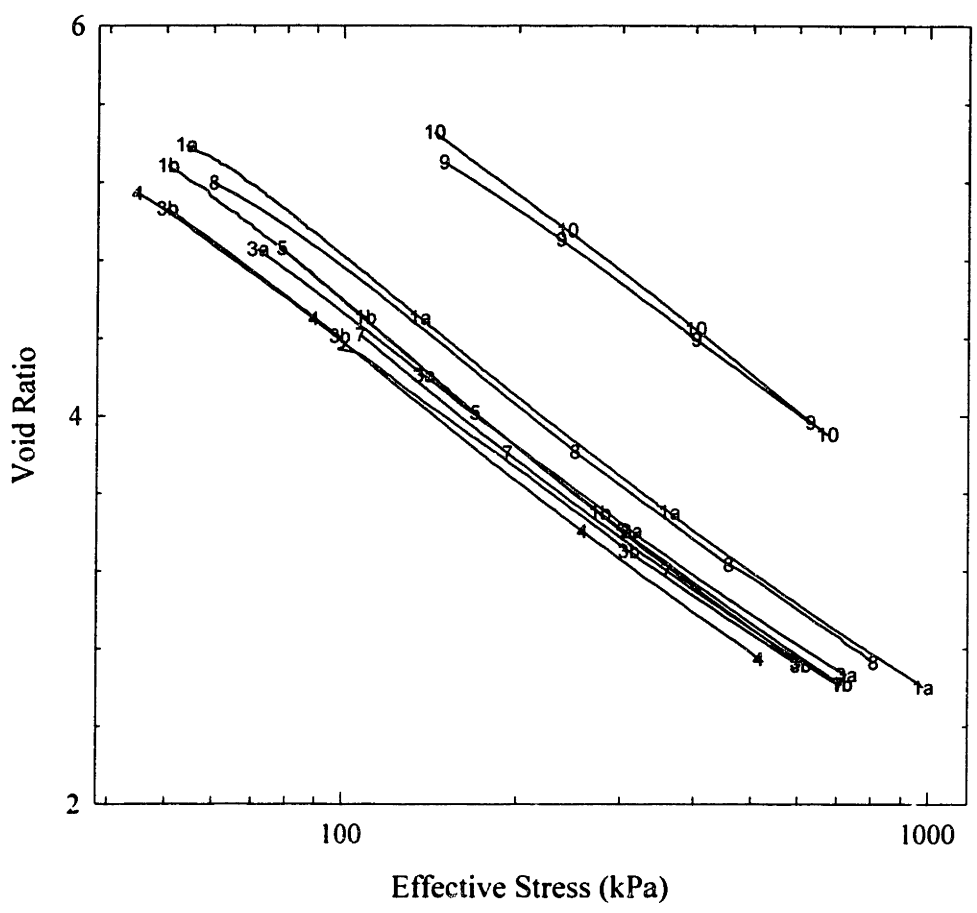


Figure 4.10: Summary of Void Ratio normalized to $e_{1.5}$ vs. Effective Stress data from CRS tests on Samples 1 to 10 (except 2 and 6).

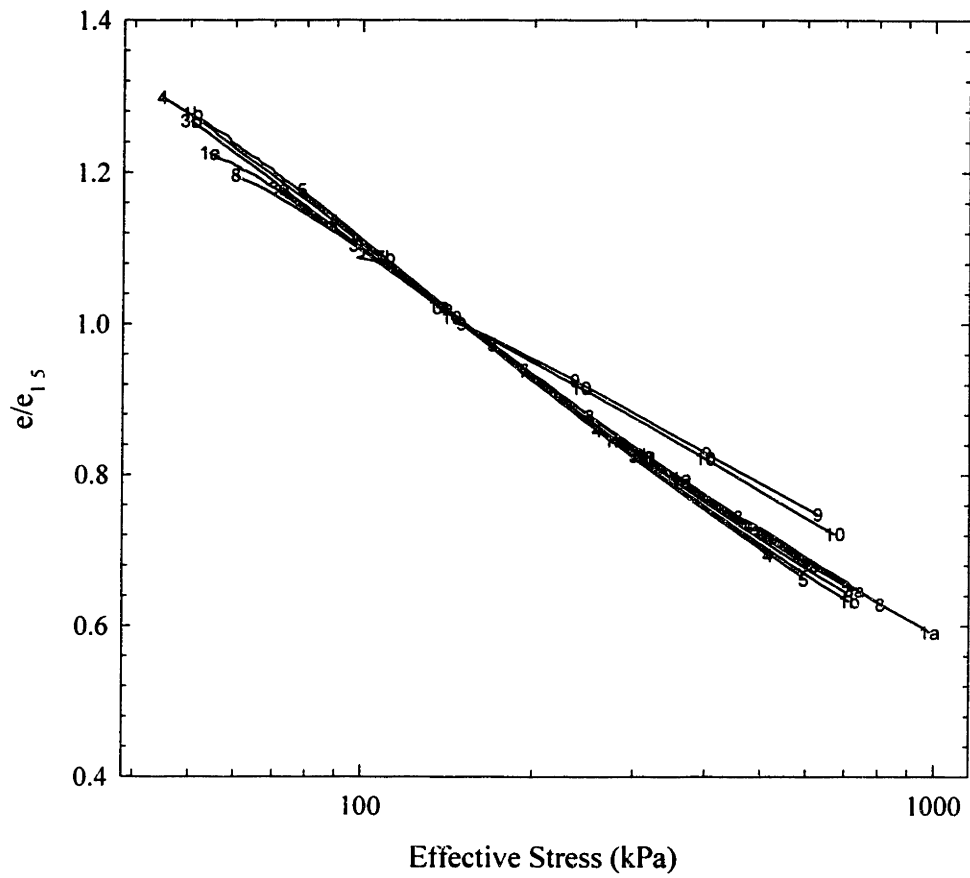


Figure 4.11: Summary of Void Ratio vs. Hydraulic Conductivity data from CRS tests on Samples 1 to 10 (except 2 and 6).

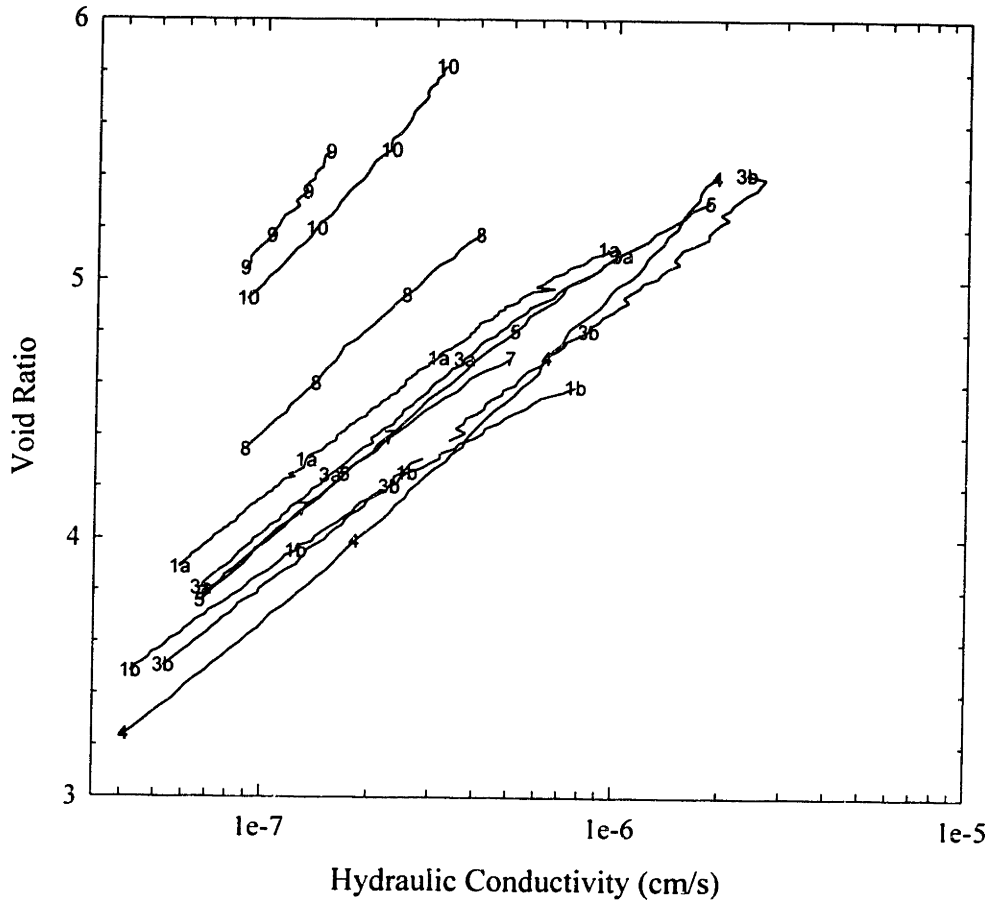


Figure 4.12: Summary of Void Ratio vs. Effective Stress data from CRS tests on Samples N1, N2, and N3 compared to tests on Samples 3 to 10 (except 6).

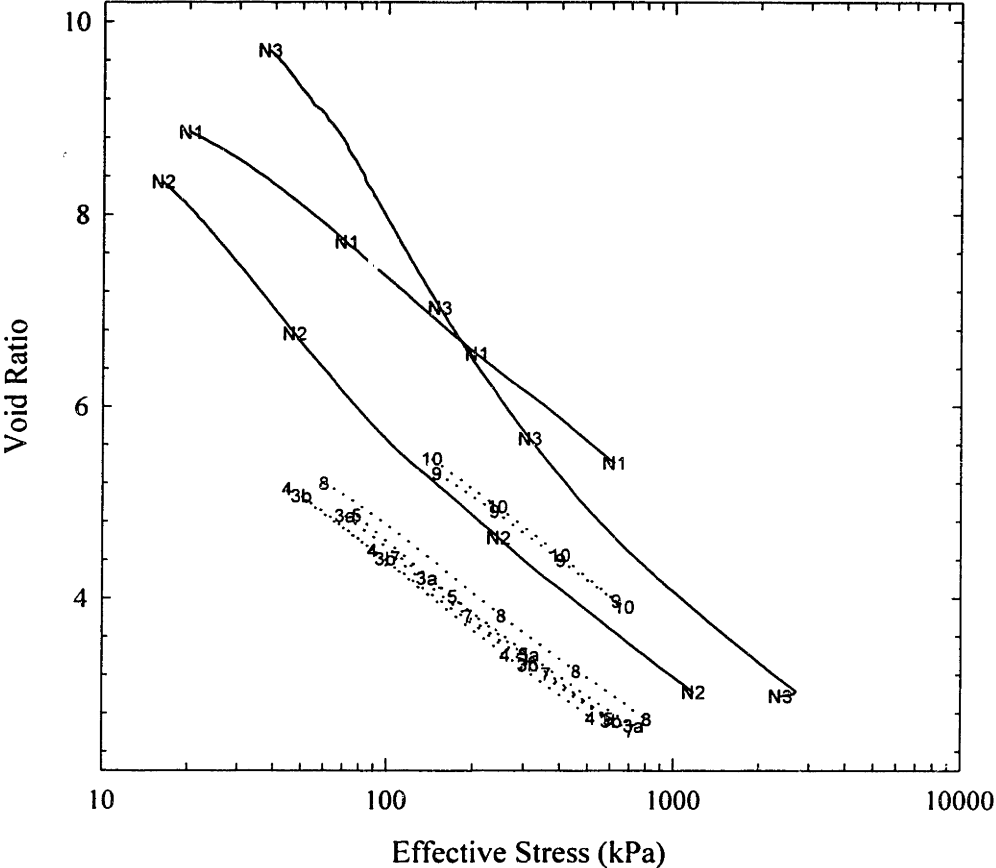


Figure 4.13: Summary of Void Ratio normalized to $e_{1.5}$ vs. Effective Stress data from CRS tests on Samples S7, S10, N1, N2, and N3.

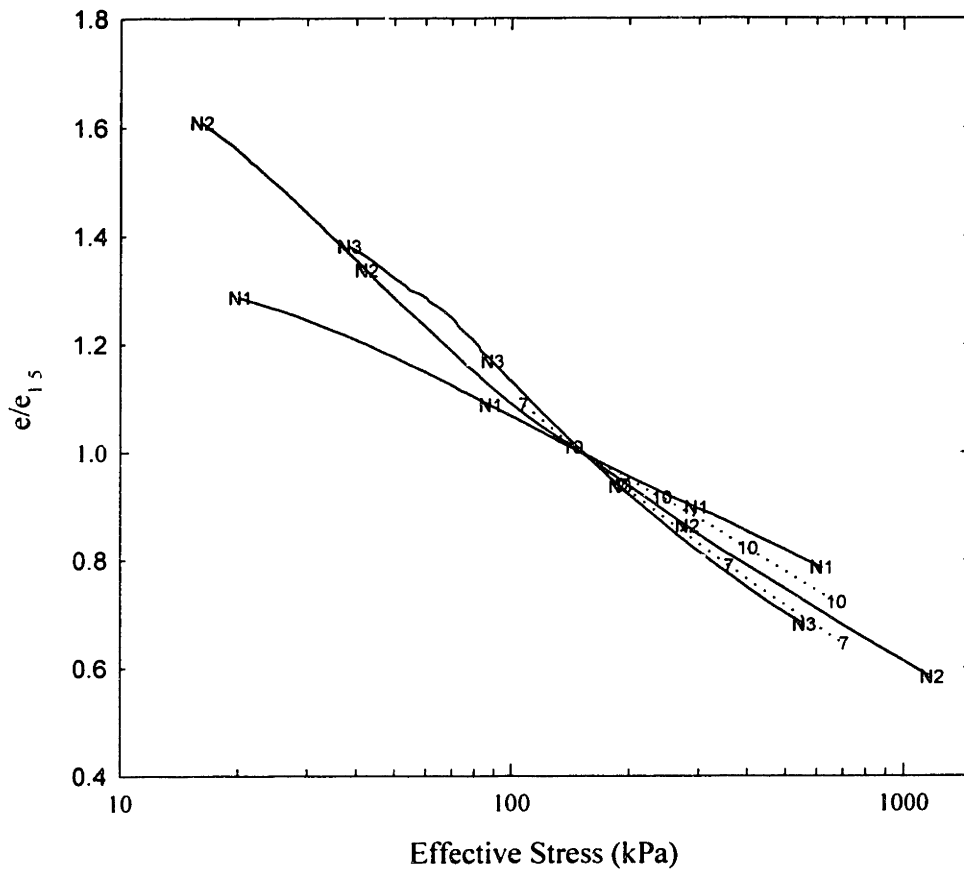


Figure 4.14: Summary of Void Ratio vs. Hydraulic Conductivity data from CRS tests on Samples N1, N2, and N3 compared to tests on Samples 3 to 10 (except 6).

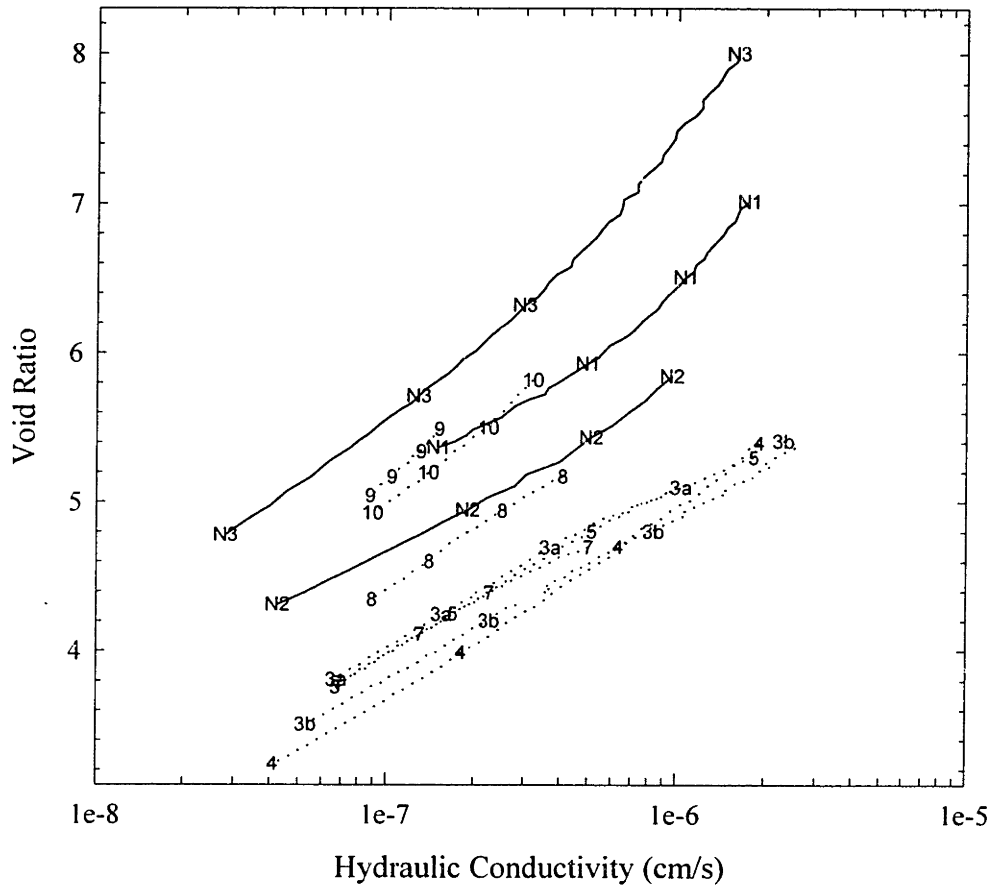
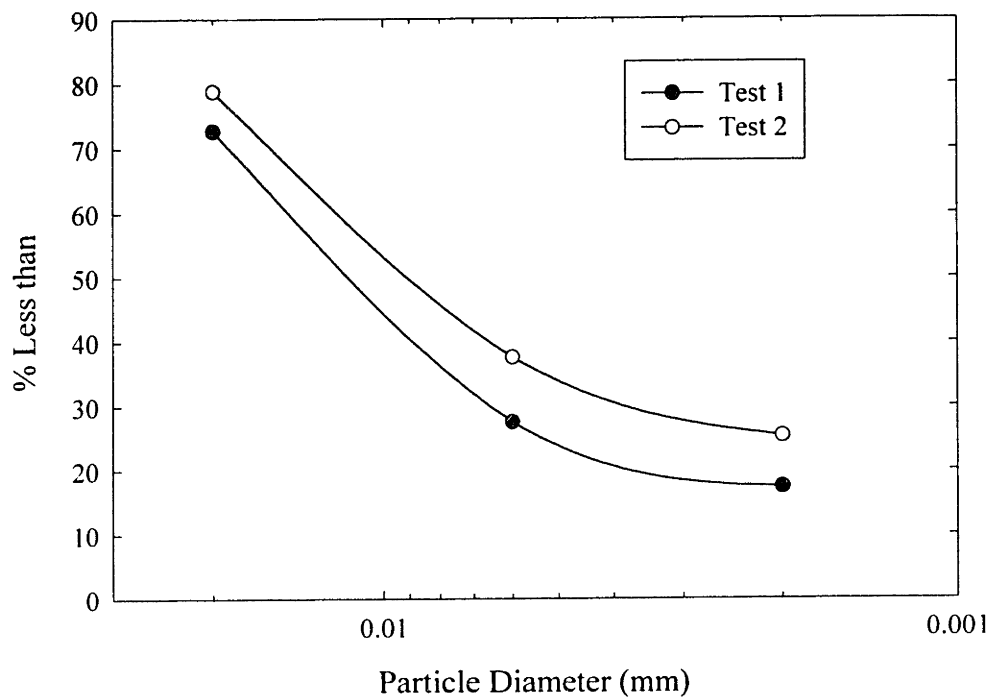


Figure 4.15: Size Distribution of wetland soil mineral fraction determined by the Pipette Analysis Method



5. COLUMN EXPERIMENTS: PROCEDURES AND DATA ANALYSES

5.1 INTRODUCTION

Column Experiments, set up on the modified permeameter described in Chapter 3, were conducted on re-sedimented and undisturbed wetland soil specimens. The goals of these experiments were twofold: first, to measure the hydraulic conductivity, k , of the soil at various effective stresses, and second, to measure the breakthrough of a sodium chloride tracer through the specimen.

Similar Column Experiments were also conducted on a uniform sand so that a comparison could be made between the tests on wetland deposits, which are considered dual porosity media, and uniform sands, which are not.

In this chapter, the testing procedures and the data analysis are discussed. Section 5.2. includes a detailed description of specimen setup and testing sequence. Section 5.3 includes an explanation of the spreadsheet used to manipulate the electronically acquired data, and, finally, Section 5.4 includes an explanation of how the breakthrough curves are fitted using CXTFIT (See Section 2.3.1). The results of the Column Experiments and a discussion of all the data are included in Chapter 6.

5.2 EXPERIMENTAL PROCEDURE

5.2.1 SPECIMEN PREPARATION AND SETUP

The Column Experiment procedure is similar for re-sedimented wetland soils, undisturbed wetland soils, and sands, the only significant difference being in specimen preparation and setup. A detailed description of the specimen preparation, and the specimen setup are included below. The Procedure and Data Sheet for these experiments are included in Appendix B8.

5.2.1.1 RE-SEDIMENTED SOIL

5.2.1.1.1 Obtaining the soil for trimming.

After batching, a re-sedimented sample, which is cylindrical with a 6.35 cm diameter, is stored in a hollow brass cylinder having a 6.4 cm inner diameter (See Section 3.3.2.1). The brass cylinder is sealed with wax at top and bottom and kept in a humid room until the sample is ready to be tested. Cylindrical sub-samples, 2.54 cm high, are then taken, as needed, for either the CRS tests (See Section 4.7) or for the Column Experiments. The sub-samples are taken as follows:

1. Any wax lining the inner walls of the cylinder is scraped off.
2. The sample is *partially* extruded from the cylinder using a piston having a 6.35 cm diameter.
3. A stainless steel ring used in CRS testing (inner diameter: 6.35 cm, height: 2.54 cm) is placed around the partially extruded sample, and the sample is pushed out until the wax cap is completely clear of the ring.
4. The wax cap is cut away using a sharp textile-cutting blade (30 cm long). The blade is kept flush against the top edge of the ring, and firm, clean cuts are made into the peat. The blade is wiped clean with a moist towel in between each cut.
5. A similar cut is made at the bottom edge of the ring, and the 2.54 cm high sub-sample removed.
6. If either top or bottom face of the sub-sampled soil is not even, a recess tool, also used in trimming CRS specimens (See Appendix B6), is used to push the soil from the ring about 2 mm. Then, the excess, uneven soil is cut away.
7. Any un-sampled soil remaining in the brass cylinder is re-sealed with wax and put back into storage.

5.2.1.1.2 Trimming the specimen

The sub-sampling procedure described above determines the specimen height, which is between 2.34 and 2.54 cm. Then, the sub-sample is also trimmed from its original diameter of 6.35 cm to 3.56 cm. This is done as follows:

1. The stainless steel ring is removed from the sub-sample, which has been placed on a plexi-glass plate.
2. The plexi-glass plate is placed in a trimming jig, which consists of a stainless steel, square base with a steel rod at two corners (Figure 5.1). These rods are used as guides to keep the cutting blade at a constant distance from the specimen as it is being trimmed.
3. A 3.56cm diameter cylinder is placed on the sub-sample. This cylinder determines the specimen diameter.
4. The plexi-glass plate is moved such that the edge of the sub-sample is overhanging the base of the trimming jig, and a cut is made using the textile-cutting blade which is kept flush against the steel rods. The blade is wiped clean with a moist towel between each cut.
5. The plexi-glass plate is rotated, and another cut is made.
6. The initial cuts are made at the outer edges of the sub-sample, and the plate rotated at large angles. However, as the trimming proceeds and the cuts are closer to the final diameter of the specimen, the cuts are smaller, and the plate is rotated at smaller angles.
7. The 3.56 cm diameter cylinder placed on the sub-sample is used as a guide when the final, fine cuts are made.
8. Once the trimming is done, the specimen mass is determined. The trimmings are used for water content measurements.

5.2.1.1.3 Column setup

Once the specimen has been trimmed and massed, it is ready to be setup in the permeameter, according to the following steps (Refer to Figure 5.2):

1. All permeameter lines are cleaned, then filled with appropriate fluid, that is, the fresh water pot and lines are filled with fresh water, and the salt-water pot and lines are filled with salt water.
2. The Pedestal Pressure transducer zero is taken.
3. The porous stones, filter paper and distribution caps are sonicated in distilled water for half an hour.
4. One porous stone is placed on the pedestal followed by filter paper and one distribution cap. These are secured in place with a rubber membrane protector.
5. The top cap is unscrewed from the influent line, and one porous stone is placed on its bottom face, followed by filter paper and one distribution cap. These are secured to the top cap with a rubber membrane protector.
6. The specimen is placed on the pedestal.
7. One prophylactic membrane is placed on the membrane stretcher (Figure 5.3), which is a hollow cylinder with a side vent. A vacuum is applied through the side vent to keep the membrane flush against the stretcher sides.
8. The membrane and stretcher are slipped over the sample, and the bottom end of the membrane released from the stretcher onto the specimen and pedestal.
9. The top cap is then placed on the sample, and the top end of the membrane released from the stretcher onto the specimen and top cap.
10. The membrane is secured with a rubber o-ring at the top cap and the pedestal.
11. A second membrane is placed over the specimen in the same way as the first, and secured with two o-rings at the pedestal and two at the top cap.
12. The top cap is re-attached to the influent line.
13. The permeameter cell is screwed tightly to the cell base and is filled with distilled water.

14. The Cell Pressure transducer zero is taken, when the cell fluid is halfway up the specimen.
15. The specimen is back-pressure saturated to 400 kPa in 50 kPa increments. Each increment is applied as soon as the pore pressure has dissipated, and care is taken to maintain the effective stress on the specimen below 5 kPa.
16. The drainage lines are closed, and saturation is confirmed by measuring the B-value for a 25 kPa increase in cell pressure (ASTM D5048). B-values greater than 98% are acceptable.
17. The two Top Cap Pressure transducer zeroes are calculated from their voltage output at a back-pressure of 400 kPa.
18. The specimen is consolidated to the desired effective stress.
19. The effluent line is attached to the pedestal, and the flow pump, with the proper worm attached, is screwed into proper gears in the volume change device. The volume change device can be hand cranked before the flow pump is inserted into the gears such that the pressure is built up in the effluent line to a level equal to, or slightly greater than, the pore pressure in the pedestal.
20. The flow pump is switched on at a low speed. When the pressure in the effluent line is exactly the same as that in the pedestal, the flow lines are opened. This starts the flow of distilled water into the specimen and allows the specimen to be rinsed of any salts already present in the soil.
21. The flow rate is observed and increased until there is at least a 5 kPa difference between the pore pressure at the top cap and pedestal.

5.2.1.2 UNDISTURBED SOIL

5.2.1.2.1 Obtaining the soil for trimming.

The undisturbed soil, which is stored in the Shelby tube it was sampled with, is x-rayed to determine which portion of the sample is usable (See Section 4.3.1). Once the portion of the core to be tested is chosen, the following steps are taken:

1. The section of the Shelby tube where the sub-sample is desired is marked, and then cut using a band saw. The un-sampled portion is sealed with wax and returned to storage.
2. The cut faces of the sub-sampled soil are scraped clean to remove any soil contaminated with steel shavings from the cutting process.
3. The soil is removed from the steel tube. This is done by, first, breaking the contact between the soil and the tube wall using a steel wire, and by then using a piston, which has the same diameter as the tube, to push the sub-sample out.
4. The sub-sample is placed on the CRS trimming jig and trimmed into the same stainless steel ring (height: 2.54 cm, diameter: 6.35 cm) used for cutting re-sedimented sub-samples. A razor blade, and not a textile-cutting blade is used for this step.
5. The sub-sample is removed from the CRS trimming jig, and cut to the height of the stainless steel ring using the textile-cutting blade.

5.2.1.2.2 Trimming the specimen and column setup

The same procedure is used for trimming and setting up the undisturbed specimen as is used for the re-sedimented specimen. However, great care must be taken not to pull out large organic fragments with the blade while trimming the specimen, and to not compress it while cutting and handling it.

5.2.1.3 SAND

The sand specimen is prepared on the pedestal itself according to the following steps:

1. All permeameter lines are filled with appropriate fluid; that is, the fresh water pot and lines are filled with fresh water, and the salt-water pot and lines with salt water.
2. The Pedestal Pressure transducer zero is taken.
3. The porous stones, filter paper and distribution caps are sonicated in distilled water for half an hour.
4. One porous stone is placed on the pedestal followed by filter paper and one distribution cap.
5. A rubber membrane that is at least 16 cm long is placed on the pedestal and secured with a rubber o-ring.
6. A prophylactic membrane is also placed on the pedestal and secured with two rubber o-rings.
7. A triaxial sand mold is assembled on the pedestal and a vacuum is applied to it so that the membranes are flush with the mold wall. The mold inner dimensions are measured.
8. Sand is rained into the mold using the pepper shaker method (Reference).
9. When the mold is full and the top of the sand specimen has been smoothed over with a straight edge, the top cap is placed on the sand, and the membranes are released from the sand mold one at a time, each being secured with o-rings.
10. The sand mold is disassembled, and the pedestal base is cleared of any sand grains.
11. The sand mass is determined by subtracting the sand container mass before and after the specimen is setup.
12. The permeameter cell is screwed tightly to the cell base and is filled with distilled water.
13. From this point onward, the same steps for column setup are taken for sand as for wetland deposits.

5.2.2 TRACER TESTING PROCEDURE & SPECIMENS TESTED

5.2.2.1 TRACER TESTS

After flow of distilled water through the specimen is started, the electrical conductivity probe readings at the pedestal and the flow rate itself are monitored until they become steady.

When these outputs have come to equilibrium, the tracer experiments are begun. The tracer test consists of first, injecting a known concentration of NaCl solution for a known time interval, and then monitoring of the influent and effluent until the sodium chloride solution completely breaks through the specimen. The effluent is also sub-sampled throughout the test. The sub-samples are then diluted, and their electric conductivity, chloride, and sodium concentrations are measured using a conductivity probe, a chloride specific probe, and a sodium specific probe, respectively. The sub-sample concentrations are then compared to the effluent conductivity probe output to see if the probes are reading correctly.

The number of tracer tests on each specimen, the length of the tracer injection pulse, and the tracer concentration varied during the testing program as more was learned about the equipment and the optimal testing procedure. The evolution of the final testing procedure is detailed below.

5.2.2.1.1 Number of tests per specimen

For the initial tests (Specimens S4, 5, 7 and 8), four tracer tests or less were conducted on each specimen (See Table 5.1). None of the tests gave data that were usable for curve fits using CXTFIT. In most cases (Specimens S4, 5 and 8), the poor data was a result of the desensitizing of the effluent conductivity probe (See Section 3.3.1). In some cases (Specimen S4), the sample became impermeable, and recovery of the tracer was very slow (on the order of 3 weeks). For tests on Specimen S7, breakthrough curves were collected with full recovery of tracer. However, these BTCs were not useable since the distribution caps (See Section 3.3.3) were not used, and it would have been impossible to separate the Two-Region behavior of the porous stones, from the Two-Region behavior of the specimen.

For tests on Specimens S9, S10, and N1, six or more tracer tests were conducted. The first tracer test on S9 and the first four tests on N1 were not useable because the specimen had not been rinsed sufficiently.

All tests on S10 were fully recovered, since the specimen was sufficiently rinsed, and enough time was given for each tracer pulse to breakthrough. It was found that the higher number of tracer tests on each specimen (6 or more), at a wide range of flow rates and effective stresses were more useful for making comparisons between effective stress, hydraulic conductivity and effective porosity.

5.2.2.1.2 Tracer concentration

For tracer tests on Specimens S4, 5, and 7 through 9, the Sodium Chloride tracer concentration was 0.1 M. In the case of tests on S9, which was not sufficiently rinsed, the first breakthrough curves were superimposed on the tail end breakthrough of salt already in the specimen (Figure 5.4), and it was difficult to separate the breakthrough of one tracer injection from the other. For subsequent tracer tests, with the exception of the first four on N1, which were lost, the Sodium Chloride tracer concentration was 0.5 M. All these tests were usable for fitting.

5.2.2.1.3 Length of tracer injection pulse

In most cases, the length of the tracer injection pulse was 10 minutes. The fourth tracer test on S7 was 20 minutes long, and was used to determine whether pulse the length altered test results. Also, the fourth and fifth tracer tests on S9 were 30 minutes long. This was done to increase the input of salt into the system, with the hope that the breakthrough curves would be more pronounced. Changing the pulse length had no significant effect on breakthrough except to make it take longer, so it was kept at 10 minutes.

5.2.2.2 CONTINUOUS TRACER INJECTION

For each specimen tested, with the exception of S5, whose results were completely lost, and S7, tracer was injected continuously into the specimen, until a steady output was obtained. The data collected from the continuous injection was used as a check of the electrical

conductivity probe output. In most cases, the probe readings were off by a certain percentage. This percentage was used to scale the breakthrough curves collected for each specimen.

For experiments on S4, 8 and 9, the continuous injection was run before the tracer tests. However, due to the long time required to rinse the specimen after it has become saturated with salt, the continuous injections for S10, and N1, were run after the tracer tests.

5.2.2.3 SUMMARY OF TESTING SEQUENCE FOR ALL SPECIMENS

Column Experiments on wetland deposit samples were conducted as follows. After a specimen was setup on the permeameter and back pressure saturated, it was consolidated to some low effective stress between 5 and 10 kPa. The flow pump was turned on, which induced the flow of distilled water through the specimen. After several days of fresh water flow, the tracer tests were begun.

Tests on Specimens S4, 5 and 8, were lost due to excessive consolidation of the specimen, or the desensitizing of the effluent electrical conductivity probes. The four tracer tests on Specimen S7, were used to evaluate the effluent electrical conductivity probes (See Section 3.3.1.3.2). For these tests, the electrical conductivity of effluent sub-samples were compared to the effluent concentration value as determined by the pedestal probes. The BTCs from these tests were not usable for CXTFIT analysis, since the distribution caps discussed in Section 3.3.3 were not used.

In the case of specimen S9, 0.1 M sodium chloride solution was injected continuously for 8 days at the beginning of the Column Experiment. Then, the specimen was rinsed for 4 days (See Table 5.2a). Subsequently, six 10 minute tracer pulses were injected, and their breakthrough measured. The effective stress on the sample, as well as tracer flow velocity were varied from pulse to pulse, and the tracer recovery took on the order of 2 to 3 days. The first of the six tracer tests was not useable.

In the case of specimens S10 and N1, 0.5 M sodium chloride solution was used as a tracer, and more than nine 10 minute tracer pulses were injected into the specimen. Effective stress and tracer flow velocity were also varied from pulse to pulse. The tracer breakthrough was

monitored over 4 to 6 days (See Tables 5.3 and 4). After all the 10 minute pulses were injected and recovered, tracer was injected continuously into the specimens.

For the continuous injection on specimen S10, first 0.01 M sodium chloride solution was injected for 5 days, at which point a 0.5 M, 10 minute pulse was injected, and the pulse breakthrough was monitored over 4 days. Then, 0.5 M sodium chloride solution was injected continuously into the specimen for 7 days. The data from this step injection, and from the intermediate pulse were used to determine how salt concentration influenced hydraulic conductivity and tracer breakthrough. This is discussed in Section 6.2.1 and again in Section 6.4.

For specimen N1, 0.5 M sodium chloride solution was injected continuously for 3 days, after which the specimen was rinsed for 1 day. Subsequently, the salt solution was again injected continuously into the specimen for 3 days.

5.2.3 CONTROL COLUMN EXPERIMENTS

Five types of control experiments were conducted. These special experiments were designed to address specific ambiguities found during the principal Column Experiments testing. These ambiguities are discussed in Chapter 6. The control experiments are outlined briefly below.

1. Six tracer tests were conducted on sand Specimen 2. The breakthrough curves for these tests were used to determine whether CXTFIT analysis differentiates between One-Region and Two-Region Soils (See Section 6.3.1).
2. Specimen N2 was setup according to the procedures outlined above, but no tracer tests were conducted on it. Instead, for this specimen, the hydraulic conductivity was measured as the specimen was consolidated to different effective stress levels. This Column Experiment was used to determine how well the k vs. σ' relationship for this stress controlled test compared to that of the strain controlled Constant Rate of Strain (CRS) tests.

3. Since it had been observed that k decreased for the wetland deposit specimens as soon as salt solution was injected into the specimen, the Column Experiment on Specimen N3 was used simply to determine if the hydraulic conductivity of the specimen changed if only fresh water was injected into the system. For this experiment, k was monitored as fresh water was injected into the soil for over 10 days.
4. To determine whether the transport behavior of the NaCl tracer was affected by ion exclusion, a special tracer made with deuterium oxide (D_2O) and NaCl was pulsed through undisturbed wetland specimen N4. For this tracer test, the effluent was sub-sampled at 5 to 12 hour intervals. These sub-samples were sent to NuMega Resonance Labs, Inc. and analyzed for D_2O . The D_2O and NaCl breakthrough curves were compared to see how a non-reactive tracer behaved in this soil.
5. The final Column Experiment was conducted on undisturbed Specimen N5. For this experiment, tracer tests were run at different background levels of NaCl. The first tracer pulse was injected after the specimen was flushed with distilled water until the effluent electrical conductivity probe read a constant effluent concentration. The second tracer pulse was injected after the specimen was saturated with 0.01 M NaCl, and the third pulse was injected after the specimen was saturated with 0.05 M NaCl. However, due to the extremely high hydraulic conductivity of the specimen, no k value was measured for the first tracer test. The flow velocity and effective stresses on the specimen had to be increased between the first and second tracer tests in order to create a pressure gradient across the specimen.

5.3 PROCESSING OF DATA ACQUISITION FILES

5.3.1 LIST OF DATA COLLECTED

From the beginning of the rinsing phase, and throughout the tracer and the continuous injection tests, data from the permeameter were acquired using ten separate data acquisition channels (Refer to Section 2.2 for equipment description and Figure 2.5 for acquisition point location). The data are collected at constant time intervals, which range from 10 to 30 minutes depending on the length of the test. The ten data sources are listed below:

1. Displacement of the Volume Change Device Piston (LVDT).
2. The Cell, Pedestal, Fresh Water and Tracer Reservoir pressures (4 Pressure Transducers)
3. The Electrical Conductivity of the Influent and Effluent (2 Two-Pin Probes).
4. The Effluent Temperature (Pedestal Temperature Probe).
5. The Input Voltage, or voltage powering the system (Taken in two locations).

5.3.2 DESCRIPTION OF SPREADSHEET CALCULATIONS

The data acquired for the rinsing phase, each of the tracer tests, and the continuous injection tests were input into a spreadsheet to be analyzed. First, each probe or transducer reading was normalized to the Input Voltage value. Then, the readings were further manipulated to obtain the parameters detailed below. An example spreadsheet is included in Appendix D.

5.3.2.1 FLOW RATE, EFFECTIVE STRESS, AND K

The LVDT data, which correspond to the displacement of the Volume Change Device piston, were converted to their appropriate displacement value using the LVDT Calibration Factor and Zero. The displacement data are used to calculate the *flow rate* of the effluent for a given test. This was done by finding the slope of displacement vs. time. This slope value was multiplied by the ratio of the piston diameter to sample diameter, giving the value of the flow rate through the specimen.

The *effective stress* on the specimen during a given test was calculated by subtracting the average pore pressure at the center of the specimen, which is the average of the pore pressures at the top cap and pedestal, from the average cell pressure. Note: all pressure transducer data were converted to pressure values using the appropriate transducer Calibration Factor and Zero.

The *hydraulic conductivity*, k , of the specimen during a given tested was calculated in two parts. First, the gradient across the specimen was calculated from the pressure difference across the specimen (top cap to pedestal) and the specimen height. Then, using Darcy's Law, k was calculated from the ratio of flow rate to gradient. The value of k was plotted vs. time

to see how much it varies throughout the test. However, the average k value was also calculated, and it is this value that is used for comparisons between tracer tests.

5.3.2.2 INFLUENT AND EFFLUENT CONCENTRATION

5.3.2.2.1 Temperature Correction

Before the data from the influent and effluent probes were converted to concentration data, they were adjusted for temperature variations during testing (Figure 5.6c). The corrections were made using Hewitt's equation as cited by Head (1983), which converts a conductivity value at any temperature to a conductivity value at a reference temperature of 18 °C:

$$\frac{\sigma(T)}{\sigma(18)} = 1 + b(T - 18) \quad (5.1)$$

$$\text{Where } b = \sum_{N=0}^4 a_N T^N,$$

$$a_0 = 2.1179818 \times 10^{-2},$$

$$a_1 = 7.8601061 \times 10^{-5},$$

$$a_2 = 1.5439826 \times 10^{-7},$$

$$a_3 = -6.2634979 \times 10^{-9},$$

$$a_4 = 2.2794885 \times 10^{-11}$$

5.3.2.2.2 Electrical Conductivity to Concentration

The temperature-adjusted electrical conductivity values were converted to concentration data using calibration curves, which were developed for both the influent and effluent electrical conductivity probes. This was done by setting the permeameter up without a specimen and then measuring the probe output for solutions having 0.001, 0.05, 0.1, 0.15 and 0.5 M concentrations.

It was necessary to re-calibrate the electrical conductivity probes after each Column Experiment on a wetland deposit specimen. It was also necessary to scale the influent and

effluent conductivity values by a factor, which is given by the results of the continuous injection test that is run on each specimen. This factor is the ratio between the probe readings and the actual concentration input into the system during the continuous injection experiment, and it varied from experiment to experiment.

5.3.2.2.3 % Recovery

After the electrical conductivity data were converted to concentration data, the areas under the influent and effluent curves were calculated and compared. Ideally, the ratio between the influent and effluent areas, which reflects the proportion of NaCl recovered, is unity. This was not always the case. Recoveries greater than unity were measured when the specimen was not sufficiently rinsed of salts, and recoveries less than unity were measured when the breakthrough of NaCl was not complete. In some cases, high or low recoveries were due to inaccurate readings of the probes. Tracer recovery will be discussed in detail in Section 6.3.2.

5.3.2.3 EFFLUENT SAMPLE CONCENTRATION

The effluent sub-sample data were input into the spreadsheet and converted to concentration data. The total salt concentration, as measured by the conductivity probe, as well as the chloride and sodium concentrations, were compared to the breakthrough data measured by the electrical conductivity probe in the permeameter pedestal.

5.3.2.4 BREAKTHROUGH CURVES (BTCs) FOR CXTFIT

5.3.2.4.1 Normalizing the BTCs

The CXTFIT model requires that all concentration data be normalized to the tracer concentration. Therefore, the first step in preparing the breakthrough data for input into the model is to divide the effluent concentration by 0.1 or 0.5 M.

5.3.2.4.2 De-sloping and zeroing the BTCs

It was found that, for some of the tracer tests, the concentration at the tail of the breakthrough curve was lower than the initial concentration (Figure 5.5). This sloping of the curves was

attributed to insufficient rinsing of the specimen, which results in the superposition of one, shorter, breakthrough curve on the tail of another longer breakthrough curve.

The sloping had to be removed from the breakthrough curves in order to properly fit them. This was done by finding the equation of the line formed by the slope in the curve. This line was subtracted from the curve, effectively de-sloping and zeroing it (Figures 5.5).

5.3.2.4.3 Adjusting the BTCs for travel time

The initial part of the breakthrough curves includes the time it takes for the tracer to travel from the tracer reservoir to the top cap and through the porous stones and distribution caps. This travel time must be removed from each breakthrough curve in order to fit it properly. The equation describing travel time vs. flow velocity, outlined in Section 3.3.4, was used to determine the travel time for each tracer test. This travel time was removed from the time column for breakthrough curves, which resulted in shifting each curve to the left, towards the origin (Again, See Figure 5.5).

5.4 CXTFIT CURVE-FITS

After each breakthrough curve that is collected from the tracer test is processed into the proper format, it is fit using CXTFIT. This computer model can apply either the One-Region Model (ORM) or Two-Region Model (TRM) to estimate values for the Diffusion Coefficient and the Retardation Factor. In the Two-Region mode, the model also estimates β and ω , dimensionless variables describing the ratio of mobile to immobile pore space and the transfer rate between each region, respectively (See Section 2.2 for a discussion of these variables).

The variables and data entered into the model must follow the specific format outlined by the CXTFIT User's Manual written by Toride, et al. (1995). Below is a modified version of the this manual.

5.4.1 INPUT PARAMETERS

An ASCII input file, consisting of the breakthrough curve (BTC) data and a series of descriptive parameters, is written for each breakthrough curve being fit. This file is divided into eight blocks.

Each block is discussed below. The parameter names, descriptions, and typical values for TRM (wetland deposits) and ORM (sand) cases are included in the discussion. Refer to Figure 5.6 for an input file typical of a tracer test on wetland deposits and Figure 5.7 for an input file typical of a tracer test on sand. See Appendix C2 for the text of the CXTFIT program.

5.4.1.1 BLOCK A: MODEL DESCRIPTION

Block A includes five parameters. These define the type of problem to be solved:

1. **NCASE:** TRM/ORM = 1. How many cases are being considered? In all case, only 1.
2. **INVERSE:** TRM/ORM = 1. The model can solve the *direct* problem by formulating a BTC for a given set of conditions (V , D , R , β , and ω), or it can solve the *inverse* problem by finding V , D , R , β , and ω for a given BTC. The latter is desired in this case.
3. **MODE:** ORM = 1, TRM = 2. The model has 7 modes, which include the *deterministic* equilibrium and non-equilibrium convection-dispersion equations as well as the *stochastic* equilibrium and non-equilibrium convection-dispersion equations. The deterministic equilibrium Convection Dispersion Equation (CDE) is used for sand and the deterministic non-equilibrium CDE is used for wetland deposits.
4. **NREDU:** ORM/TRM = 1. This parameter defines which input variables (time, position, or concentrations) are dimensional or not. In this case, time and position are dimensional, and concentration is dimensionless.
5. **MODC:** ORM/TRM = 1. What is the concentration mode? In this case, it is flux averaged.
6. **ZL:** ORM/TRM = characteristic length of dimensionless parameters.

5.4.1.2 BLOCK B: INVERSE PROBLEM PARAMETERS

Block B contains five parameters, which define the estimation procedure. The last two parameters are omitted for the ORM case.

MIT: $ORM/TRM = 50$. The user is given the option to define the maximum number of iterations in which the program can estimate the desired parameters. The User's Manual recommends 30 to 50 iterations.

ILMT: $ORM/TRM = 0$. The user can choose to place minimum or maximum constraints on the parameters being estimated. No constraints are given in this case.

MASS: $ORM/TRM = 0$. The program can estimate the total mass of tracer from the BTC. This option is not used.

MNEQ: $TRM = 0$. The user can choose which of the Two Region mechanisms, either physical or chemical, that the program solves for. For this case, the physical TRM is used.

MDEG: $TRM = 0$. This parameter is used if any degradation of the tracer occurs. For this case it does not.

5.4.1.3 BLOCK C: TRANSPORT PARAMETERS

In this block, the transport parameters are defined. The user inputs known or estimated values of V , D , R , β and ω , and marks which of these parameters the program should estimate.

1. V : This value of flow velocity, q , which is measured during testing is input as a starting value, but V is estimated. The values of θ_m , the effective porosity, is taken from the ratio of flow velocity, q , to the estimated tracer velocity, V .
2. D : The value that is input is the molecular diffusion coefficient of NaCl, which is $1.5 \times 10^{-5} \text{ cm}^2/\text{s}$ at 25°C . The program estimates this parameter.
3. R : For both the ORM and TRM case, the value for R that is measured in the Sorption Experiments (Section 2.3.1.1) is input. However, the model also estimates this value, and a comparison is made between the experimental value and the calculated value.

4. β : For the ORM case, this value is not considered. For the TRM case, this value is input as 0.5, but is estimated.
5. ω : For the ORM case, this value is not considered. For the TRM case, this value is input as 1, but is estimated.

5.4.1.4 BLOCK D: BOUNDARY VALUE PROBLEM

In this block, the user inputs the method in which the tracer was injected into the column as a function of time. The program provides seven options, which include: no tracer, Dirac Delta input, step input, pulse input of application time, T, multiple pulse input, exponential input, and an arbitrary function input.

MODB: ORM/TRM = 3. The choice of the seven options mentioned above is input here. For this case, the input is a pulse of a finite length.

PULSE(1): ORM/TRM = % Recovery.

TPULSE(2): ORM/TRM = 600. This is the pulse length in seconds.

5.4.1.5 BLOCK E: INITIAL VALUE PROBLEM

In this block, the user quantifies the initial concentration input into the system. The program provides five options, which include zero initial concentration, constant initial concentration, stepwise initial distribution, exponential initial distribution, and Dirac Delta initial condition.

MOD1: ORM/TRM = 0. The choice of the five options mentioned above is input here. For this case, the initial input concentration is zero.

5.4.1.6 BLOCK F: PRODUCTION VALUE PROBLEM

In this block, the user defines the tracer production term. The program provides four options, which include no production, constant production, stepwise production, and exponential production.

MODP: ORM/TRM = 0. The choice of the four options mentioned above is input here. For this case, there is no production term.

5.4.1.7 BLOCK G: OBSERVED DATA FOR INVERSE PROBLEM

This is the block where the BTC data is input.

INPUTM: ORM/TRM = 1. This parameter describes the form that the data is in. In this case, the observation point is fixed, and the data is given time vs. normalized concentration.

DUMTZ: ORM/TRM = Specimen length.

T: Time column **C:** Concentration Column

5.4.1.8 BLOCK H: POSITION AND TIME FOR A DIRECT PROBLEM

This block is only used for the direct type of problem. It is not used in this case.

5.4.2 OUTPUT DATA

The CXTFIT program writes all its results to an ASCII output file. This file includes the input BTC data as well as the fitted data. It also includes estimated values for V , D , β , and ω . This file is imported into a spreadsheet, where a comparison of the experimental and fitted curves is made, and where the estimated parameters are tabulated and analyzed. See Figure 5.8 for a typical output file. See Sections 6.3 and 6.4 for a discussion of the output data.

5.5 REFERENCES

The Book of ASTM Standards, Part 19. D5084: 1993.

Head, J.L., *The Use of Miniature Four-Electrode Conductivity Probes for High Resolution Measurement of Turbulent Density or Temperature Variations in Salt Stratified Water Flows*. PhD Thesis. University of California, San Diego, CA, 1983.

Toride, N., Leij, F.J., van Genuchten, M.T. *The CXTFIT Code for Estimating Transport Parameters from Laboratory or Field Tracer Experiments, Version 2.0*. U.S. Salinity Laboratory, Agricultural Research Service, U.S. Department of Agriculture, Research Report 137, August 1995.

Table 5.1: Summary of Column Experiments on wetland deposit specimens

Specimen No.	S4	S5	S7	S8	S9	S10	N1
Specimen Type	Coarse	Coarse	Fine	Fine	Coarse	Coarse	Undisturbed
NaCl Conc. (M)	0.1	0.1	0.1	0.1	0.1	0.5	0.5
Cotinus Injection	Yes*	-	No	Yes*	Yes*	Yes	Yes
Pulses Injected	3	-	4	2	6	10	10
Pulses Recovered	1	-	4		6	10	10
Pulses Usable for Analysis	-	-	-	-	3	10	6

* Indicates that Continuous Injection was run before pulses were begun

Table 5.1: Summary of Column Experiments on wetland deposit specimens

Test Sequence	Duration (days)	Injection Time	Tracer Conc. (M)	q (cm/s)	σ' (kPa)	Data Usable?
Rinse	2	-	-	1.19E-05	7.41	-
Continuous Injection	8	8 days	0.1	1.19E-05	8.14	-
Rinse	4	-	-	1.19E-05	8.14	-
Tracer Test 1	6	10 min	0.1	1.13E-05	10.28	No
2	3	30 min	0.1	1.17E-05	10.49	Yes
3	2	30 min	0.1	1.63E-05	1.58	Yes
4	2	30 min	0.1	2.21E-05	6.01	Yes
5	3	10 min	0.1	2.78E-05	12.45	Yes
6	3	10 min	0.1	2.70E-05	25.87	Yes

Table 5.3: Test sequence and testing parameters for Column Experiments on specimen S10

Test Sequence	Duration (days)	Injection Time	Tracer Conc. (M)	q (cm/s)	σ' (kPa)	Data Usable?
Tracer Test 1	4	10 min	0.5	1.10E-04	7.72	Yes
2	4	"	"	1.23E-04	7.97	Yes
3	4	"	"	1.32E-04	13.37	Yes
4	5	"	"	1.50E-04	14.68	Yes
5	5	"	"	1.33E-04	19.29	Yes
6	6	"	"	1.37E-04	19.54	Yes
7	4	"	"	1.53E-04	20.12	Yes
8	6	"	"	1.21E-04	25.41	Yes
9	4	"	"	1.79E-04	10.91	Yes
Continuous Injection 1	5	5 days	0.01	1.79E-04	11.16	-
Tracer Test 10	4	10 min	0.5	1.79E-04	10.33	Yes
Continuous Injection 2	7	7 days	"	1.79E-04	10.33	-

Table 5.4: Test sequence and testing parameters for Column Experiments on specimen N1

Test Sequence	Duration (days)	Injection Time	Tracer Conc. (M)	q (cm/s)	σ' (kPa)	Data Usable?
Tracer Test 1	2	30 min	0.1	9.74E-05	0.03	No
2	2	10 min	"	1.23E-04	0.03	"
3	3	"	"	1.37E-04	0.03	"
4	4	81 min	0.1 to 0.5	9.74E-05	0.03	"
5	3	10 min	0.5	1.11E-04	0.04	Yes
6	5	"	"	1.23E-04	0.04	"
7	5	"	"	1.37E-04	0.08	"
8	4	"	"	1.80E-04	0.08	"
9	3	"	"	2.09E-04	0.03	"
10	3	"	"	2.16E-04	0.11	"
Continuous Injection 1	3	3 days	"	2.14E-04	0.07	-
Rinse	1	-	-	"	"	-
Continuous Injection 2	3	3 days	0.5	"	"	-

Figure 5.1: Trimming jig used for preparing wetland deposit specimens for Column Experiments

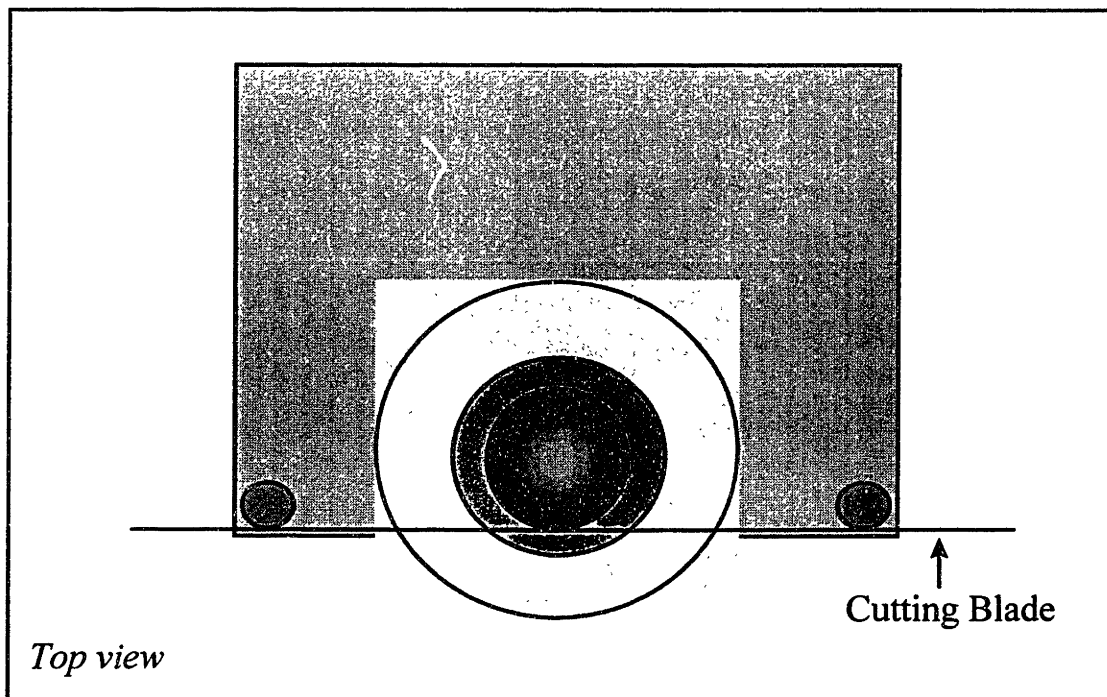
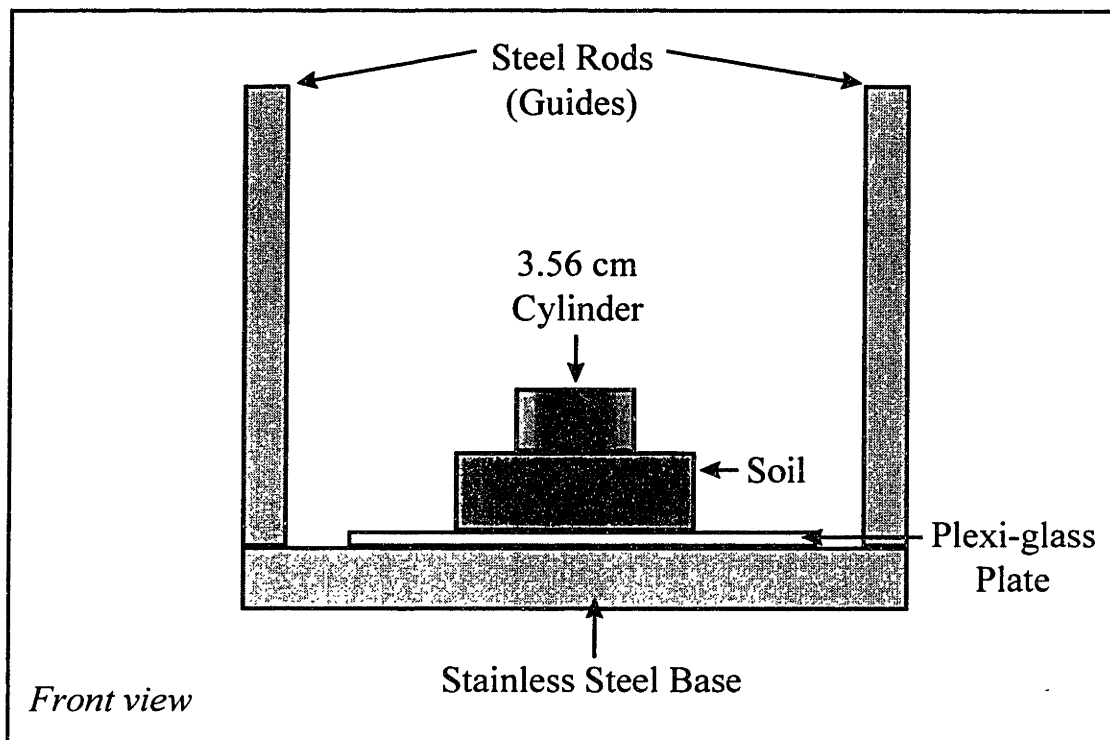


Figure 5.2: Specimen setup on permeameter (Cross Section)

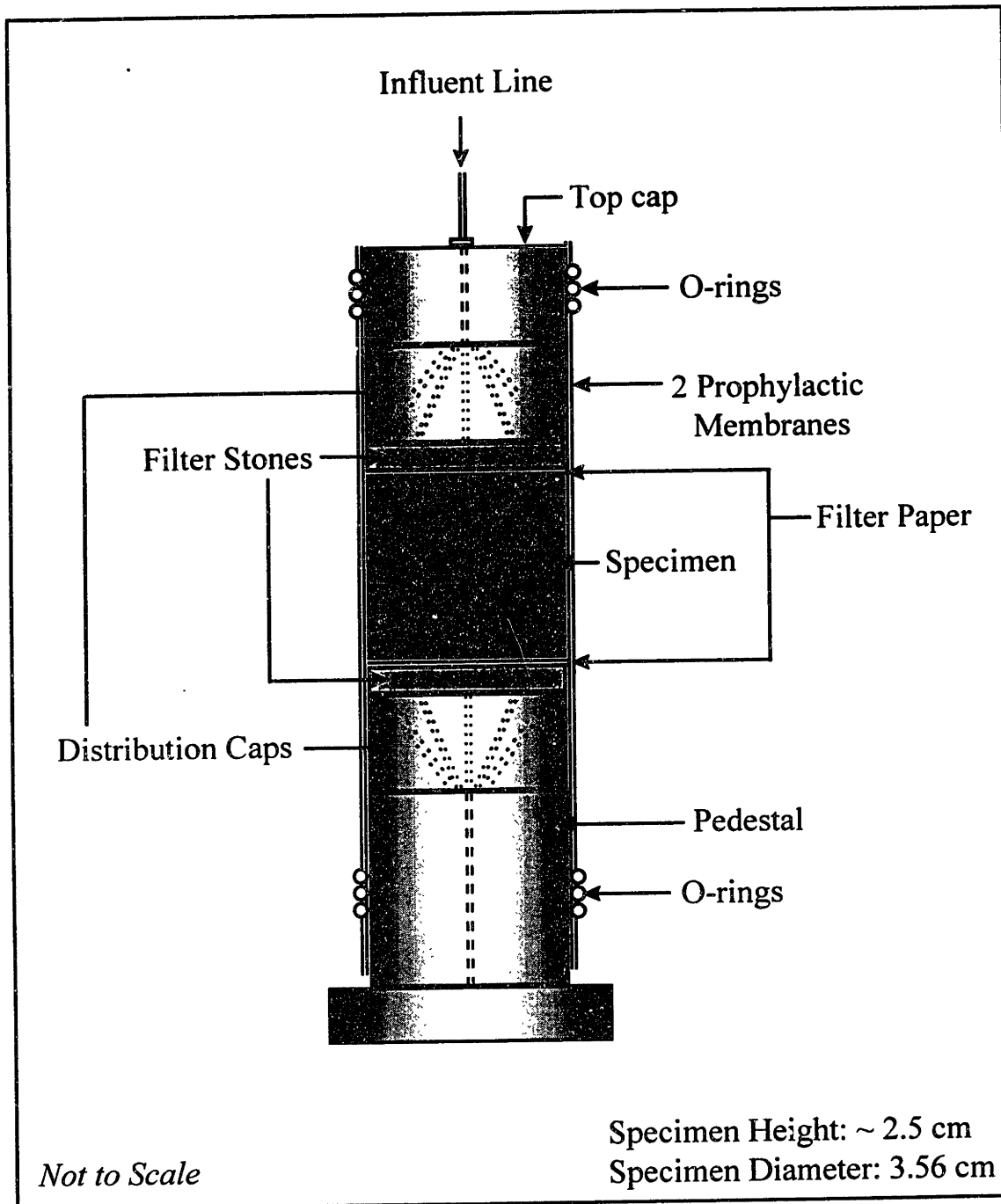


Figure 5.3: Membrane stretcher used for Column Experiment specimen setup.

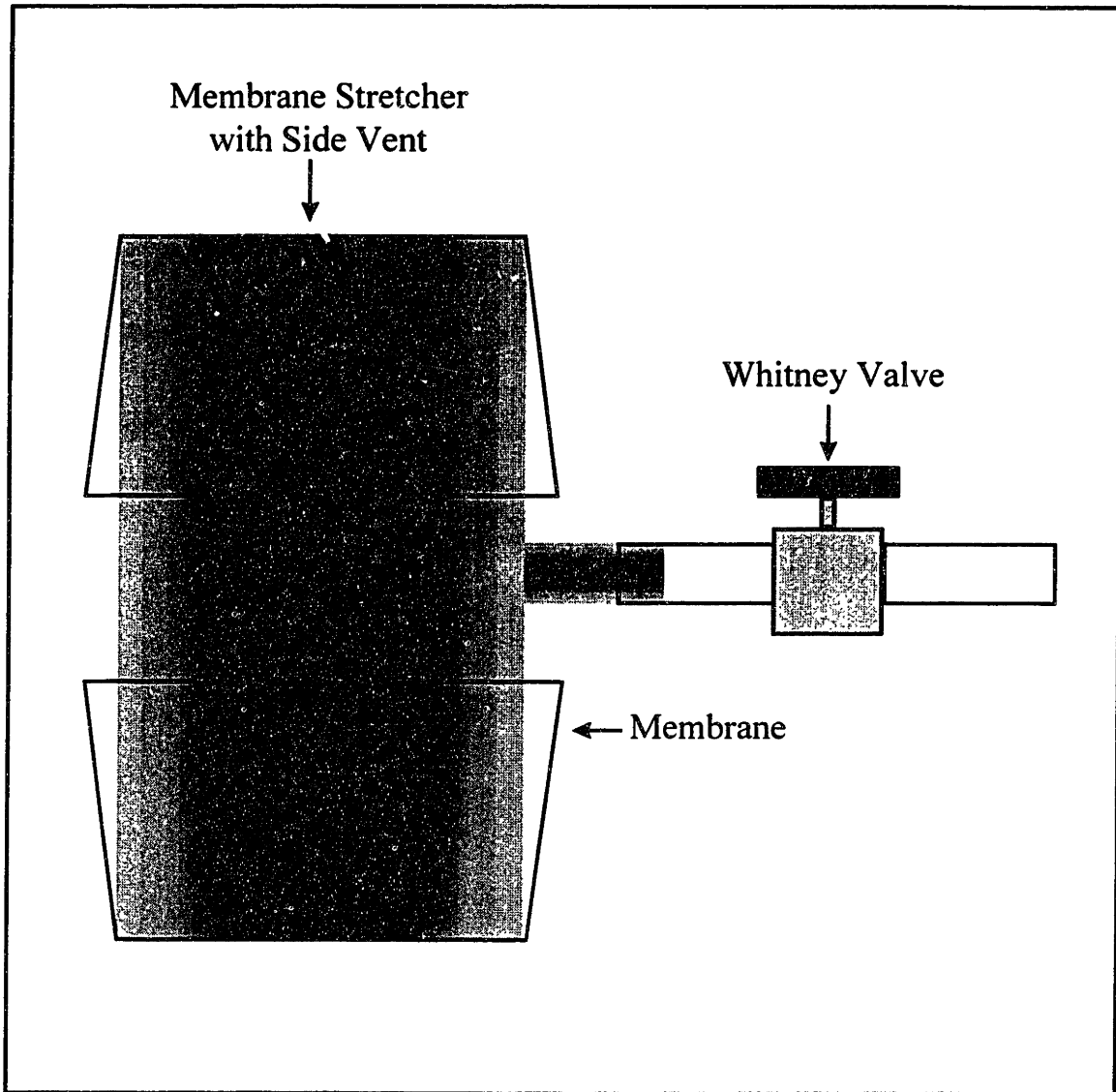


Figure 5.4: Breakthrough Curves (BTCs) for 6 consecutive Tracer Tests on Wetland Deposit Specimen S9

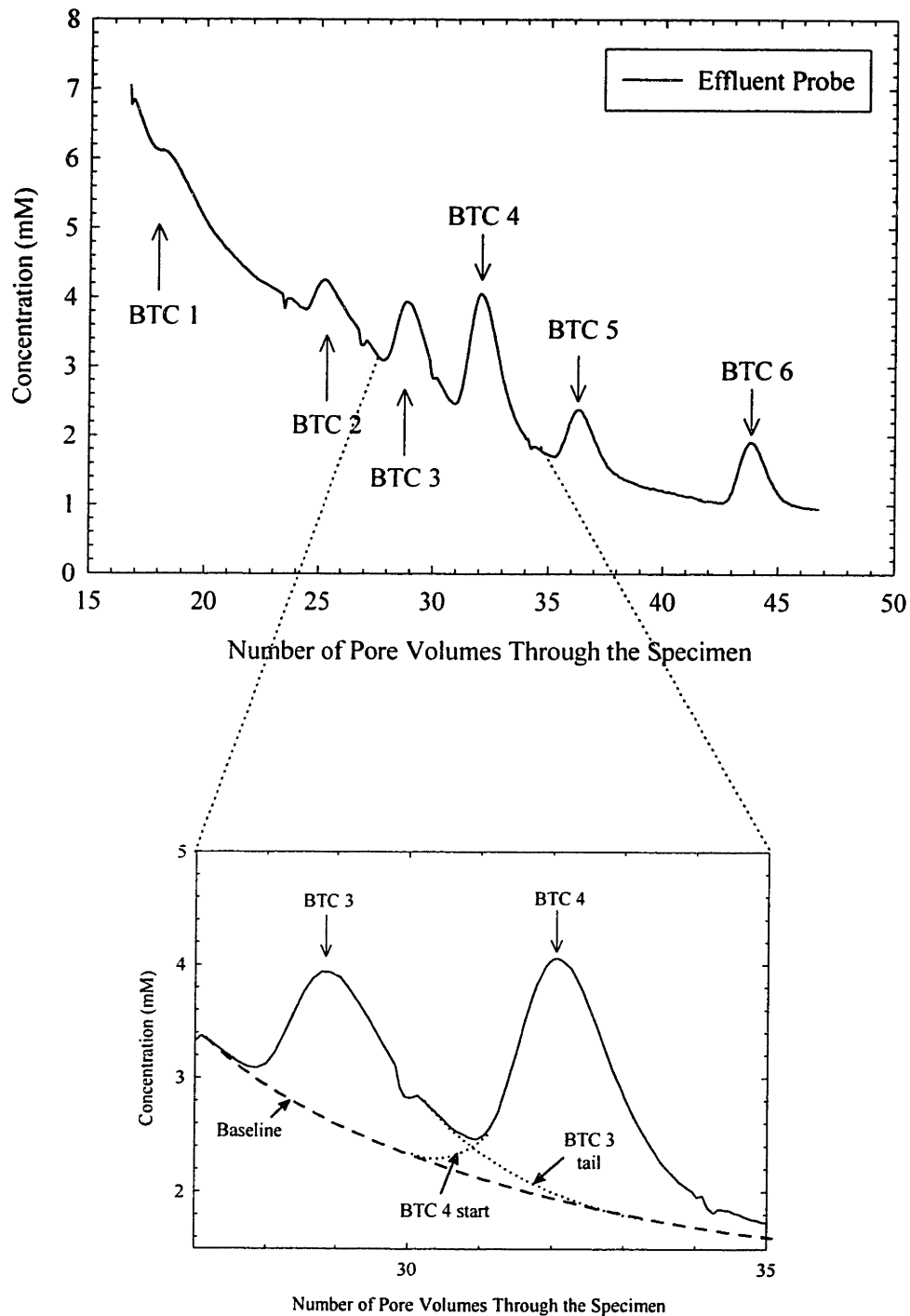


Figure 5.5: Breakthrough Curve (BTC) 4 for Tracer Test on Specimen S10. Experimental BTC, Line defining BTC slope, and De-sloped, Zeroed BTC.

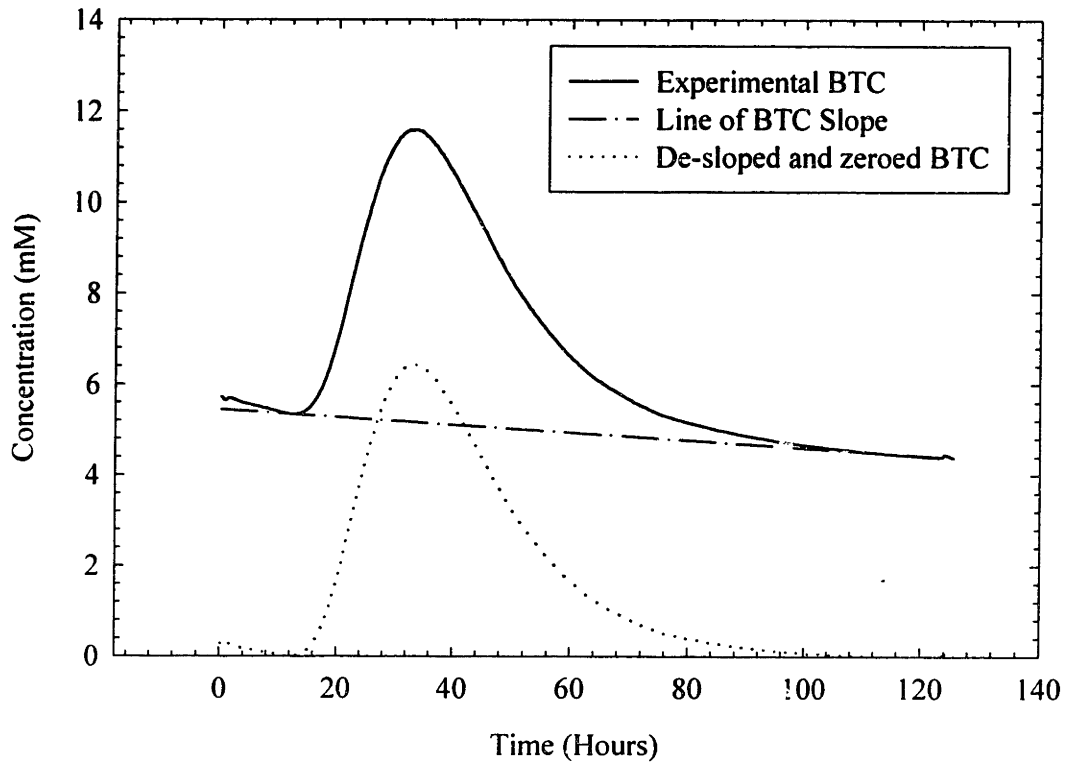


Figure 5.6: Typical CXTFIT Input file for Tracer Test on Wetland Deposit.

```

1
*** BLOCK A: MODEL DESCRIPTION *****
Peat: P10p1 5%, 2, d low
(UNITS: cm, s, concentratin dimensionless)
INVERSE MODE NREDU
  1  2  1
MODC  ZL
1
2.34
*** BLOCK B: INVERSE PROBLEM *****
MIT  ILMT  MASS
50  0  0
MNEQ  MDEG
0  0
*** BLOCK C: TRANSPORT PARAMETERS *****
  V    D    R    Beta  omega  Mu1  Mu2
1.27425E-05  0.000004  1.5  0.5  .01  0.  0.
  0    0    0    1    1    0
0
*** BLOCK D: BVP; MODB=0 ZERO; =1 Dirac.; =2 STEP; =3 A PULSE *****
MODB (Reduced Conc.& time) =4 MULTIPLE; =5 EXPONENTIAL; =6 ARBITRARY
  3
1.868  600
*** BLOCK E: IVP; MODI=0 ZERO; =1 CONSTANT; =2 STEPWISE; =3 EXPONENTIAL **
MODI
  0
*** BLOCK F: PVP; MODP=0 ZERO; =1 CONSTANT; =2 STEPWISE; =3 EXPONENTIAL **
MODP
  0
*** BLOCK G: DATA FOR INVERSE PROBLEM *****
INPUTM =0; Z,T,C =1; T,C FOR SAME Z =2; Z,C FOR SAME T
  1
  2.5
TIME      CONC  (Give "0 0 0" after last data set.)
1022.082  0.00015
2222.082  0.000123
3422.082  0.000119
4622.082  0.000102
5822.082  7.91E-05
7022.082  7.12E-05
8222.082  5.21E-05
9422.082  8.22E-05
10622.08  4.90E-05
11822.08  4.04E-05
13022.08  2.46E-05
14222.08  1.50E-05
15422.08  7.39E-06

```

Figure 5.7: Typical CXTFIT Input file for Tracer Test on Sand.

```

1
*** BLOCK A: MODEL DESCRIPTION *****
PSand2: 1 RM, 6,50%,v
(UNITS: cm, s, normalized concentration)
INVERSE MODE NREDU
  1  1  1
MODC  ZL
  1  5.18
*** BLOCK B: INVERSE PROBLEM *****
MIT  ILMT  MASS
  50  0  0
*** BLOCK C: TRANSPORT PARAMETERS *****
  V  D  R  Mu1  Mu2
0.009053014  0.000002  1.0  0.  0.
  0  1  0  0  0
*** BLOCK D: BVP; MODB=0 ZERO; =1 Dirac.; =2 STEP; =3 A PULSE *****
MODB (Reduced Conc.& time) =4 MULTIPLE; =5 EXPONENTIAL; =6 ARBITRARY
  3
  1  600
*** BLOCK E: IVP; MODI=0 ZERO; =1 CONSTANT; =2 STEPWISE; =3 EXPONENTIAL **
MODI
  0
*** BLOCK F: PVP; MODP=0 ZERO; =1 CONSTANT; =2 STEPWISE; =3 EXPONENTIAL **
MODP
  0
*** BLOCK G: DATA FOR INVERSE PROBLEM *****
INPUTM =0; Z,T,C =1; T,C FOR SAME Z =2; Z,C FOR SAME T
  1
  5.18
TIME      CONC  (Give "0 0 0" after last data set.)
29.39623  0.000832
59.39623  0.000827
89.39623  0.000843
119.3962  0.002287
149.3962  0.013963
179.3962  0.044278
209.3962  0.08838
239.3962  0.157254

```

Figure 5.8: Typical CXTFIT Output file for Tracer Test on Sand.

```

*****
*
* CXTFIT VERSION 2.0 (1/2/95)
* ANALYTICAL SOLUTIONS FOR ONE-DIMENSIONAL CDE
* NON-LINEAR LEAST-SQUARES ANALYSIS
*
* PSand2: 1 RM, 6,50%,v
* (UNITS: cm, s, normalized concentration)
*
* DATA INPUT FILE: s2 6.in
*
*****
MODEL DESCRIPTION
=====
DETERMINISTIC EQUILIBRIUM CDE (MODE=1)
FLUX-AVERAGED CONCENTRATION
REAL TIME (t), POSITION(x)
(D,V,mu, AND gamma ARE ALSO DIMENSIONAL)
INITIAL VALUES OF COEFFICIENTS
=====
NAME INITIAL VALUE FITTING
V..... .9053E-02 N D..... .2000E-05 Y R..... .1000E+01 Y mu..... .0000E+00 N
BOUNDARY, INITIAL, AND PRODUCTION CONDITIONS
=====
SINGLE PULSE OF CONC. = 1.0000 & DURATION = 600.0000
SOLUTE FREE INITIAL CONDITION NO PRODUCTION TERM
PARAMETER ESTIMATION MODE
=====
MAXIMUM NUMBER OF ITERATIONS = 50
ITER SSQ D... R...
0 .6607E+01 .200E-05 .100E+01
1 .6136E+01 .781E-05 .990E+00
COVARIANCE MATRIX FOR FITTED PARAMETERS
=====
D... 1.000
R... .325 1.000
RSQUARE FOR REGRESSION OF OBSERVED VS PREDICTED = .95362403
(COEFFICIENT OF DETERMINATION)
NON-LINEAR LEAST SQUARES ANALYSIS, FINAL RESULTS
=====
95% CONFIDENCE LIMITS
NAME VALUE S.E.COEFF. T-VALUE LOWER UPPER
D... .4449E-02 .7970E-01 .5582E-01 -.1554E+00 .1643E+00
R... .7613E+00 .7970E-01 .9551E+01 .6014E+00 .9212E+00
-----ORDERED BY COMPUTER INPUT-----
CONCENTRATION RESI-
$ NO DISTANCE TIME OBS FITTED DUAL
1 5.1800 29.3962 .0008 .0000 .0008
2 5.1800 59.3962 .0008 .0000 .0008
3 5.1800 89.3962 .0008 .0000 .0008

```


6. COLUMN EXPERIMENT RESULTS

6.1 INTRODUCTION

Column Experiments were conducted on undisturbed and re-sedimented wetland deposit specimens as well as on one sand specimen. The data from these experiments were analyzed according to the procedures outlined in Chapter 5. The results of these analyses are given in this chapter and are organized as follows. First, in Section 6.2, the results of the CXTFIT analysis on the Column Experiment breakthrough curves are presented. Second, in Section 6.3, an interpretation of these results is given and the influence of effective stress, tracer concentration, and specimen age on the specimen hydraulic conductivity, k , is evaluated. Third, in Section 6.4, a conceptual model that takes into account the results of the analyses is developed and the significance of the results are discussed. In Section 6.5, Nuclear Magnetic Resonance (NMR) imaging is presented as a means of validating the Column Experiment findings, and finally, in Section 6.6, future goals are listed.

6.2 CXTFIT ANALYSIS

The CXTFIT computer program, written by Parker and Van Genuchten (1986), and updated by Toride, et al (1995), was used to process a number of breakthrough curves (BTCs) collected during the Column Experiments run on wetland deposits and sand. See Section 2.2.3 for an overview of the program, Section 5.2.2 for a description of the specimens tested and the testing sequence, and Section 5.4 for a description of the input and output parameters used for the fitting process. The program was used to fit breakthrough data using both the One-Region Model (ORM) and the Two-Region Model (TRM), which are discussed in Section 2.2. The results of these fits are compared below.

As discussed in Chapter 5, only the breakthrough curves (BTCs) collected in Column Experiments on wetland deposit specimens S9, S10, and N1 were useable for the fitting analysis. The results of the final fits for all three Column Experiments are included in

Section 6.2.2.2. BTCs from the Column Experiment on sand specimen Sand 2 were also fitted. The results of the final fits for this experiment are discussed directly below.

6.2.1 FITS FOR ONE-REGION SOILS (SANDS)

The One-Region Model was used to fit all six of the BTCs collected for specimen Sand 2. These fits were used to determine whether the ORM is adequate in describing the flow of the sodium chloride tracer through this type of one-region soil. For the ORM fits, the program can be used to fit the tracer flow velocity, V , the dispersion coefficient, D , and the retardation factor, R , or any subset of the three. In this case, the six BTCs were fitted with R fixed at unity, and V and D were left for the model to interpret.

The results of these fits were relatively good for Tracer Test 1, 3, 4 and 5, with R^2 values equaling 98.6% or higher (See Table 6.1a). The poor fits for Tracer Tests 2 and 6 are probably due to the fact that the BTCs retrieved for these tests were almost square (See Figures 6.1b and 1f), and CXTFIT is unable to interpret step functions. For Tracer Test 2, the BTC is square because, for this test, the tracer was injected for a duration of 20 minutes, allowing the tracer concentration to reach a maximum and to plateau. The tracer concentration also reached a maximum during Tracer Test 6, because this test was run at a relatively high pore water velocity of 0.0104 cm/s.

It was found that the fitted values for the tracer velocity, V_m , were higher than the pore water velocity values, V_c (See Table 6.1a), that were calculated by dividing the Darcy Velocity, q , by the measured total porosity of the sand ($\theta = 0.39$). The ratio of V_c to V_m averaged at $0.906 \pm 3.2\%$. This means that this sand has a mobile region that is 90.6% of the total porosity, or an effective porosity of $0.906 \times 0.39 = 0.35$.

To see whether the Two-Region model would better fit these breakthrough curves, the BTC for Tracer Test 3 was fit in the TRM mode (See Table 6.1b). The quality of the fit ($R^2_{\text{ORM}} = 98.6\%$ vs. $R^2_{\text{TRM}} = 99.2\%$) and the value of effective porosity ($\theta_{m,\text{ORM}} = 0.88$ vs. $\theta_{m,\text{TRM}} = 0.85$) for both fits were similar. However, the value of the Diffusion Coefficient, D , for the ORM fit was considerably higher than for the TRM fit ($D_{\text{ORM}} = 1.8 \times 10^{-3}$ vs. $D_{\text{TRM}} = 1.0 \times 10^{-7}$).

When the values of D were normalized to the free diffusion coefficient, D^* , and plotted on the D/D^* vs. The Peclet Number curve discussed in Section 2.2.2, the D/D^* ratio for the ORM fits fall in the zone where mechanical dispersion dominates (See Figure 6.2). Although the D/D^* values are a little high for the corresponding Peclet Numbers of 4 to 10, they seem reasonable for flow through sand. The D/D^* value for the TRM fit on the Tracer Test 3 BTC falls in the zone where diffusion dominates, which is too low for the corresponding Peclet Number of 6.7, and which does not seem reasonable for sand. The implausible TRM value for D is probably due to the fact that there are too many unconstrained variables in this fitting mode and suggests that the ORM should be used to fit these BTCs, even though the soil seems to possess a mobile and an immobile region.

However, that the ORM is adequate in describing flow through this sand despite the fact that the effective porosity for this soil is less than the total porosity suggests that, though there is an immobile region in the soil, the tracer does not interact with it. Two region behavior has been observed previously in sands by Holmen, 1995, who hypothesized that small fissures in the sand grain surface act as immobile pore spaces and are inaccessible.

6.2.2 FITS FOR TWO REGION SOILS (WETLAND SOILS)

Breakthrough curves collected from Tracer Tests 2 through 6 on re-sedimented specimen 9, Tracer Tests 1 through 10 on re-sedimented specimen 10, and Tracer Tests 5 through 10 for un-disturbed specimen N1 were fit using both CXTFIT's One-Region and Two-Region modes. A comparison between the two modes is included in Section 6.2.2.1. The final fit results are presented in Section 6.2.2.2, and a verification of these results using the Method of Moments is included in Section 6.2.2.3.

6.2.2.1 ONE VS. TWO-REGION MODELS

Initially, the breakthrough curves for this two region soil were fit with the TRM form of CXTFIT. However, it was found that good fits were possible for a range of values of V , D , β , and ω . That is to say, no unique set of parameters were found that corresponded to these breakthrough data. This suggests that there were too many degrees of freedom to allow for the TRM fit. On the other hand, unique, good ($R^2 > 98.8\%$) fits were possible using the ORM

form of CXTFIT (See Figure 6.3 for a typical fit). Therefore, it appears that the tracer broke through the wetland deposit specimens as if it were a one region soil, meaning that the tracer only interacted with the mobile region of the soil.

The One-Region model fits do show that there are two regions in this soil. As for the sand fits, the tracer velocity, V_m , calculated by the model was larger than the pore water velocity, V_c , calculated from the ratio of Darcy Flux, q , divided by the total porosity of the specimen, θ . The fact that the tracer velocity was faster than q/θ indicates that flow occurred through a subset of pore space in the soil. That is, the effective porosity of these specimens is significantly less than the total porosity (See below).

6.2.2.2 FIT RESULTS

The results of the final, fits on specimens S9, S10 and PN1 are listed in Tables 6.2, 3, and 4, respectively. The values of D averaged at $6.72 \times 10^{-6} \pm 6.0\%$ cm^2/s , $6.55 \times 10^{-6} \text{ cm}^2/\text{s} \pm 8.4\%$, and $7.79 \times 10^{-6} \pm 26.1\%$ cm^2/s for specimens S9, S10, and N1, respectively. The ratio of D/D^* vs. Pe is plotted in Figure 6.4. The D/D^* values plot in the diffusion dominated region of the compiled graph in Figure 6.2.

Effective porosity was plotted against effective stress, number of pore volumes through the specimen, and hydraulic conductivity in Figures 6.5, 6, and 7, respectively. No trends appear between θ_m and any of these parameters. In fact, for each Column Experiment θ_m does not vary much at all. For S9, θ_m averaged $0.531 \pm 4.9\%$. For S10 the average θ_m value for BTCs 1 to 9 was $0.550 \pm 3.95\%$. For N1, θ_m averaged $0.596 \pm 1.9\%$. The effective porosity average across all three specimens is $0.559 \pm 5.8\%$, which shows that the effective porosity of the re-sedimented and undisturbed soils are very similar. It should be noted that the value of θ_m calculated from BTC 10, from the experiment on specimen S10, was excluded from all averages. This is because, for this tracer test, the background salt concentration was increased, which led to a higher value of k and θ_m (See Section 6.3.2 for an explanation).

The question remains whether it is possible that the effective porosity for one specimen does not change with a sixteen fold increase in σ' , with a tenfold decrease in k , and over the course of the one or two month long experiments, or whether, in fact, the model is not sensitive

enough to detect whatever changes are occurring in the specimen. It would seem, in observing that the specimen appears to be 5 or 10% smaller in size at the end of each experiment, that effective porosity would decrease significantly. Nonetheless, it is possible that other mechanisms are at work during the course of the experiment that affect hydraulic conductivity without changing the overall mobile porosity in the specimen. This is considered in Section 6.4. However, it was important to verify the CXTFIT results with an independent method for calculating D and θ_m . The Method of Moments was used for this verification and is discussed directly below.

6.2.2.3 VERIFICATION OF FIT VALUES

Since CXTFIT results indicated that θ_m did not change even though the measured value of k varied, it was necessary to check the validity of the model with respect to θ_m trends with k . To that end, the CXTFIT model was evaluated by comparing its results to the results of the Method of Moments calculations.

The Method of Moments, developed by Aris (1959) and updated by Goltz and Roberts (1987), uses the Two-Region model, and the temporal moments of BTCs, to determine the values of the transport parameters, D , θ_m , and α . This method is outlined below.

1. The three moments, m_0 , m_1 , and m_2 , for a given BTC are calculated using the following:

$$m_j = \int_0^{\infty} t^j C dt \quad (6.1)$$

Where t is time (T), and C is concentration (M/L^3)

2. The ratio of m_1 to m_0 , μ_1 , is given by

$$\mu_1 = \frac{m_1}{m_0} = \frac{L}{V_R} + \frac{2D_R}{V_R^2} \quad (6.2)$$

Where L is specimen length (L), V_R is V/R (LT^{-1}), and D_R is D/R (L^2T^{-1})

3. The ratio of m_2 to m_0 , μ_2 , is given by

$$\mu_2 = \frac{m_2}{m_0} = \frac{L^2}{V_R^2} + \frac{6D_R L}{V_R^3} + \frac{12D_R^2}{V_R^4} \quad (6.3)$$

4. μ_1 and μ_2 are manipulated such that:

$$\mu_2 - \mu_1^2 = \frac{2D_R L}{V_R^3} + \frac{8D_R^2}{V_R^4} \quad (6.4)$$

5. The two unknowns, V_R and D_R are solved for using Equations 6.2 and 6.4.

6. θ_m is calculated from the ratio of q to V .

The values for D and θ_m calculated by the Method of Moments for the ten BTCs collected for specimen S10 are given in Table 6.4. It was found that the values of D , according to the Method of Moments, were within 15% of the values of D , found using CXTFIT, and followed the same trend in k (See Figure 6.8). The values of θ_m were almost exactly 48.5% higher for the Method of Moments calculation, but also followed the exact same trend in k that the CXTFIT values exhibited (See Figure 6.9).

These findings indicate that, although the values of θ_m are offset by some constant, the trends with k according to the two methods are the same. Since it is the lack of variability of θ_m , given large changes in k , that is in question, it would appear that both methods show that θ_m is, in fact, not significantly varying. Thus, the observed changes in k are the result of physical mechanisms, unrelated to effective pore size. These mechanisms are discussed in Section 6.4.

6.3 INTERPRETATION OF FIT RESULTS AND OTHER COLUMN EXPERIMENT DATA

The CXTFIT results discussed above were unexpected in two significant ways. First, the breakthrough of NaCl tracer through wetland deposits was easily described using the One, not the Two, Region model, and, second, no changes in effective porosity were calculated despite large changes in hydraulic conductivity. To understand how this is possible, a broader analysis of the Column Experiment data is necessary for both the tests on specimens mentioned above, as well as for subsequent tests on Specimens N4 and N5.

6.3.1 THE ONE-REGION BEHAVIOR OF THE NaCl TRACER

The breakthrough of NaCl tracer through wetland soil specimens can be described by the ORM, yet these specimens were calculated to have an effective porosity that was roughly 66% of the total porosity. This means that the NaCl tracer was not interacting with the immobile region of the soil. One possible reason for this is that ion exclusion was not allowing the NaCl to travel from the principal flow channels into the dead (i.e. immobile) pore space.

To test this hypothesis, a special tracer test was conducted on undisturbed Specimen N4 (See Section 5.2.2). For this test, the NaCl tracer was made with heavy water, deuterium oxide (D_2O). The test was run as all other tracer tests, and the effluent was sampled at regular intervals. The effluent samples were then analyzed for D_2O concentration, and the breakthrough curve for the D_2O tracer was constructed. In Figure 6.10, the breakthrough curve for the D_2O tracer is superimposed on the breakthrough for the NaCl tracer. By comparing the two BTCs, it was observed that the D_2O tracer breaks through 3 to 4 hours earlier than the NaCl tracer and then takes an additional 6 to 8 hours to clear the specimen. However, the reasons for the different breakthroughs is unclear, since the ORM was able to also fit the breakthrough of D_2O through the specimen. This means that, the D_2O does not seem to be diffusing in and out of any 'immobile' pore space.

Also, although the fit was a good one ($R^2 = 98.9\%$), a correct calculation for the tracer flow velocity, V , was not possible since no sorption tests had been conducted for D_2O and the value of R was unknown. When R for D_2O was assumed to be unity (meaning that D_2O is non-sorbing), the value calculated for the tracer velocity was slower than the Darcy velocity divided by the total porosity, which is not possible. In fact, for the D_2O velocity to equal to, or to be faster than, q/θ , R would have to be 1.33 or greater. For the D_2O velocity to equal the NaCl velocity (q/θ_m), R would have to be 1.45. That is, for the model to calculate any immobile pore space with respect to the D_2O tracer, R would have to be higher than 1.33. For it to calculate an effective porosity that is higher than 0.78, the effective porosity calculated for the NaCl BTC, R would have to be between 1.33 and 1.45. At any rate, the retardation of D_2O in the soil is responsible for the lag in the breakthrough of the tracer.

Also, if R is anything less than 1.67 for this tracer, the value of the diffusion coefficient, D , is less than that of NaCl. That is, D_2O diffuses less in this soil, and this implies that D_2O is flowing at higher velocity than the NaCl tracer is, and that the D_2O is traveling through less of the soil! The significance of this is that the value of effective porosity measured is different for the different tracers. That is, for these wetland soils, effective porosity is not only a soil-dependent property, but a solute-dependent property.

6.3.2 RELATIONSHIP BETWEEN θ_m AND K

As mentioned in Section 6.2, there does not seem to be any clear relationship between effective porosity and the hydraulic conductivity of the wetland deposit specimens tested. For example, although k decreased up to tenfold in the column experiment on S10, θ_m did not deviate by more than 4% from the average value. This suggests that some mechanism was affecting the measured k values without affecting the calculated θ_m values. One plausible explanation for this could be that k decreased as point constrictions developed along the flow channels. These constrictions would have caused the measured head drop across the specimen to increase, leading to a lower value of k for the same flow rate; however, they would not have altered the overall pore volume of the specimen. To explore how these constrictions might have developed, it is important to understand which experimental parameters were responsible for changes in k . These parameters are discussed directly below.

6.3.2.1 EFFECTIVE STRESS

The relationship of k vs. σ'_p for these specimens is known from compression tests run on nearest-neighbor specimens. These tests were discussed in Section 4.7. These tests showed that this soil is highly compressible material and that, in the normally consolidated region, a threefold change in effective stress could lead to a tenfold change in k . However, for the tracer tests on specimens S9, S10, and N1, effective stress levels were maintained at or below the pre-consolidation pressure, σ'_p to avoid any extreme compression of the specimens during testing that would cause the specimen to become almost impermeable.

Nonetheless, it was observed, visually, that the specimen volume decreased by 5 to 10% during the course of the Column Experiments. This volume change was probably due to the secondary compression of the specimen, which can be significant for these soil types (Mesri et al, 1997). It was not possible to measure the actual volume change of the specimen, because the volume change equipment that was hooked up to the permeameter was not sensitive enough to measure small increments of volume change over long periods of time.

Nonetheless, it is believed that some compression did occur, even though the imposed effective stresses were not high enough to consolidate the specimen. However, the test data suggest that if compression was responsible for some decrease in hydraulic conductivity, it did not affect the value of effective porosity of the specimen.

6.3.2.2 SALT CONCENTRATION

It was observed that there was a significant and repeatable relationship between hydraulic conductivity and the pore water salt concentration. However, this relationship is a complex one. To simplify the discussion of the findings, the experimental observations are discussed first. Then, the mechanisms that might have been responsible for these observations are presented in the following section.

6.3.2.2.1 Decreasing Background Concentration

In order to decipher the connections between hydraulic conductivity and pore water salt concentration, the results of the Column Experiment on specimen S10 were examined. A summary of the tracer breakthrough for all tracer tests conducted on this specimen is given below and is shown in Figure 6.11.

Initially, only fresh water was injected into the specimen, and the resulting effluent concentration started at 4 mM salt according to the electrical conductivity probe in the permeameter pedestal. The first tracer test was run by injecting a 10 minute pulse of 500 mM NaCl solution. It was observed that the concentration of the effluent after the first tracer test had completely broken through the specimen was 3 mM salt, 25% lower than the initial concentration. This indicated that the specimen's native salt was being rinsed out during the

tracer tests. This rinsing out process continued for the 8 subsequent tracer tests, but became less dramatic with time. After the first 9 tracer tests were completed, 10 mM NaCl solution was injected continuously into the specimen until the effluent concentration became constant. At that point, the 10th tracer test was run by injecting the same 10 minute pulse of 500 mM NaCl solution into the specimen, which was then rinsed out with the 10 mM NaCl solution.

6.3.2.2.2 10 Minute Salt Injections

A comparison of the behavior of hydraulic conductivity with respect to the breakthrough of salt (Figure 6.12), shows that, during the first 9 tracer tests, k drops significantly from 1.8×10^{-6} to 2.3×10^{-7} cm/s. It is also observed that, for an individual tracer test (See Figure 6.13), k also increases as salt breaks through. For the case of Tracer Test 7, k increased by 10% as the salt concentration came to a maximum in the soil. Note, however, that k at the beginning of that tracer test is 18% higher than at the end, even though the background concentration did not decrease significantly.

6.3.2.2.3 Continuous Salt Injections

It was also observed that, during the Continuous Injection test, as the effluent concentration increased from 1.5 mM to 10 mM, k increased by 30 %, from 2.3×10^{-7} to 3×10^{-7} cm/s (See Figure 6.14). This is a significant increase, but, interestingly, k does not increase up to or more than its initial value of 1.8×10^{-6} cm/s, when the background pore water concentration was only 4 mM salt (Again, see Figure 6.12). At this stage in the experiment, there appears to have been an irreversible change in k .

This plastic change in k was also observed in the continuous injection test on specimen N1 (Figure 6.15). For this test, 500 mM NaCl solute was injected into the specimen till equilibrium was reached. Then, fresh water was injected into the specimen, before 500 mM NaCl solute was injected another time. Although k did increase with the initial increase in salt concentration and decreased when it was flushed with water, it did not increase again, when the 500 mM NaCl was injected the second time.

6.3.2.2.4 Constant Salt Concentration

Another, final Continuous Injection test was conducted on P10 after the one discussed above. For this test, the injected salt water concentration was increased from 10 mM to 500 mM (See Figure 6.16), and although the hydraulic conductivity increased initially, as was expected, it began to decrease again, gradually, even though the effluent NaCl concentration remained constant. This was observed again for the special tests on specimen N5, during which Tracer Tests were conducted at different background salt concentrations (See Figure 6.17 and discussion below). For this test, k even when the effluent salt concentration was held constant at 10 mM, and later at 50 mM. It should be noted that k decreased at the same rate for both concentration levels ($\sim 6\%$ per pore volume). On the other hand, when fresh water was continuously injected after the 50 mM salt water, the rate at which k decreased doubled ($\sim 12\%$ per pore volume). This shows that some factor other than salt addition or removal is causing changes in hydraulic conductivity.

6.3.2.2.5 Background Concentration Effect on θ_m

When CXTFIT results for Tracer Test 10, which was run at a background pore water concentration of 10 mM NaCl, were compared to the CXTFIT results for the other tracer tests on that specimen, it was observed that, for Tracer Test 10, θ_m equaled 0.611, which is 10% higher than the average θ_m of $0.556 \pm 4\%$ calculated for the first 9 pulses. Therefore, even though there was no observable change in θ_m when k changed by an order of magnitude during the first 9 tracer tests, θ_m did increase when the background pore water salt concentration was increased.

This increase in θ_m was verified when the results of the tracer tests on specimen N5 were analyzed. For this Column Experiment, Tracer Tests were run at background pore water concentrations of 10 mM, then 50 mM, and then at the minimum concentration of 1 mM. When the three resultant BTCs were fit (See Table 6.7), it was found that θ_m , which was 0.78 for the background pore water concentration for 10 mM, increased by 11% to 0.91, when the background pore water concentration was increased to 50 mM. What was most surprising

was that this change in θ_m was irreversible, since its calculated value remained at 0.90 even when the background pore water concentration was decreased to 1 mM.

6.3.2.2.6 Summary

The effects of pore water salt concentration on k and q_m are summarized as follows (See Table 6.6). For small increases in pore water salt concentration, there is a small increase in k . For small decreases in salt concentration, there is a small decrease in k . In most cases, the decrease in k is larger than the increase in k for a change in salt concentration of the same magnitude. In these cases, θ_m is not affected.

For large increases in pore water salt concentration, there is a significant increase in k . There is also a significant difference in θ_m . However, when k decreases with large decreases in pore water salt concentration, θ_m does not decrease.

When the pore water salt concentration remains constant, there is still a gradual decrease in k . It appears that there is an irreversible decrease in k that occurs over time. Also, there appears to be a connection between the flushing of the specimen with water and an irreversible decrease in k .

6.3.2.3 POSSIBLE MECHANISMS AT WORK

6.3.2.3.1 Salt Concentration Related

The observations listed above pose several important questions. First, what are the possible mechanisms that might cause the hydraulic conductivity of the soil to change when pore water salt concentration changes? Moreover, what are the possible mechanisms that might cause k to change when pore water salt concentration changes, but that do not affect the effective porosity of the specimen? And conversely, what other mechanisms might cause k and θ_m to increase when high concentrations high concentration salt solution is injected into the specimen?

Two salt-hydraulic conductivity connections are known. The first is a connection between salt concentration and organic fiber coiling, and the second is a connection between salt concentration and the mobilization of mineral fines. These are discussed individually below.

6.3.2.3.1.1 Organic Coiling

Pore water salt concentration can effect the organic portion of wetland soils. Specifically, increases in salt concentration can cause k to increase by increasing the coiling or compaction of organic fibers in peats (Chin and Gschwend, 1991, Ghosh and Scnitzer, 1980, and Ours et al, 1997). Ours et al (1997) observed a reduction in peat hydraulic conductivity during rigid wall permeameter tests conducted with NaCl tracer. They proposed that this was due to the flocculation of organic acids in saline water seen by Gosh and Schmitzen (1980) and by Chin and Gschwend (1991). Although the reason for this flocculation is not yet clear, this mechanism could explain how k can vary with changes in pore water concentrations while θ_m remains constant.

This can be explained as follows (See Figure 6.19). As salt travels through the specimen flow channels, it causes any organic fibers lining the channel walls to coil. This causes the reduction of point constrictions along the flow channel, which increases k . Conversely, when the salt is flushed out of the specimen, the organic fibers uncoil once again, enlarging the point constrictions along the flow channel and increasing k . And although the number and magnitude of the constrictions lining the flow channel walls would affect the hydraulic gradient across the specimen and k , it would not affect the speed with which the tracer was traveling, that is, it would not alter θ_m .

6.3.2.3.1.2 Colloid Mobilization

It has been observed that there is a connection between decreased pore water salt concentration and the mobilization of mineral colloids, which results in the clogging of flow channel pore throats (Goldenberg et al, 1983, Khilar and Fogler, 1984, Cerda, 1987). It has been proposed that, as pore water salt concentration decreases, minerals can spall off the flow channel walls and then collect at narrow pore throats (See Figure 6.20), increasing the hydraulic gradient across the specimen. This would reduce the hydraulic conductivity of the soil without reducing its effective porosity. However, this k -reducing mechanism would not be a reversible one, since an increase in salt concentration would not necessarily cause the mineral particles to move from the pore throats back onto the channel walls.

6.3.2.3.1.3 High Salt Concentrations

For small changes in pore water salt concentrations, no changes in effective porosity were observed. This is probably so because organic coiling and colloid mobilization occur at small levels. However, when pore water salt concentrations are increased significantly, it is likely that extreme decoiling of organics and mobilization of particles results in the flushing out of a significant amount of material. This would result in the irreversible increase in θ_m that was observed in Column Experiments on specimens S10 and N5.

6.3.2.3.2 Additional Factors

As was mentioned in Section 6.3.2.2.4, it was observed, even in the cases when pore water salt concentration remained constant, that hydraulic conductivity decreased. This was seen in the last Continuous Injection test on specimen S10 and for the special Tracer Tests on specimen N5. Since no factors such as flow velocity, effective stress, or salt concentration, were varied during these tests, it appears that there was an ongoing k -reducing mechanism that underlay all others. Like two of the three salt-related mechanisms cited above, this mechanism affects k but not θ_m . That is, this mechanism involves the increase of point constrictions or the clogging of pore throats in the flow channels.

What mechanism unrelated to pore water salt concentration can do this? Well, it was observed that, throughout all the Column Experiments, the effluent was discolored and brown. In fact, there were so many suspended solids in the effluent that the Teflon tubing that connected the permeameter pedestal to the flow pump became lined with a brown, flaking residue. These suspended solids, probably mobilized by the flow of water in the specimen, could very likely clog the pore throats of the flow channels. Of course, the extent to which flow velocity, pore water chemistry, and time affect the magnitude of particle discharge and therefore the subsequent reduction in k is still unclear.

Are there any other mechanisms that might be causing these gradual changes in k ? It is possible that the soil, which exists under reduced conditions in the field, undergoes changes when it is re-oxidized as aerated water travels through it. These changes could include the oxidation and precipitation of metals such as iron, arsenic, chromium, and zinc that are found

in abundance in these soils (See Appendix D for the types and concentrations of metals found in these specimens). Re-oxidation of the specimen could also cause the growth of bacteria and mio-fauna such as nematodes (Poltz, 1999). Both metal precipitation and biological growth could lead to clogging of the flow channels accessed by water. This would lead to an increase in the gradient across the specimen without affecting effective porosity. Tests would have to be conducted to confirm whether these mechanisms are occurring or if they are significant since there was no confirmation found in the literature.

6.4 DISCUSSION OF FINDINGS

As the experimental data show, the flow and transport behavior of NaCl tracer and water in wetland deposits is a complex matter. As listed above, there are several factors that can affect the hydrogeology of this soil, and these factors can work together or against each other in influencing k and θ_m . Therefore, it becomes necessary to assimilate our findings and to attribute the different k and θ_m changes observed during the Column Experiments to the mechanisms that are responsible for them. In doing this, the significance of this research becomes clearer.

6.4.1 CONNECTING CAUSE AND EFFECT

Changes in wetland deposit hydraulic conductivity and effective porosity occur at different levels. The mechanisms that induce these changes are superimposed one over the other and can be separated as follows.

Level 1: The continual decrease in k throughout each Column Experiment. This occurs when flow of water mobilizes soil particles. This causes an irreversible decrease in k as the mobilized particles collect at flow channel pore throats. This mechanism was illustrated in all tests during which flow velocity, effective stress, and pore water salt concentration were constant: the Continuous Injection test on S10 (Again see Figure 6.16), and special Tracer Tests on N5 (Again see Figure 6.17).

Level 2: The step decrease in k when salt is flushed out of the specimen. This occurs fine mineral particles spall off the flow channel walls, which results in an irreversible

decrease in k as mineral particles collect at flow channel pore throats. This mechanism explains the following: (1) How in the Continuous Injection test on PN1 (Again see Figure 6.15), k , which decreased after the pore water salt concentration was decreased from 500 mM to 10 mM, did not increase again when the concentration was increased back from 10 mM to 500 mM; (2) how k decreases during the initial Tracer Tests on each specimen (Again see Figure 6.12 for an example) as the background pore water salt concentration decreases; and (3) how, even when the background salt concentration was the same, k at the end of a Tracer Test was less than the k at the beginning of the Tracer Test (Again see Figure 6.13 for an example). In all three cases, the *rinsing* out of salt was responsible for the net decrease in k (minus, of course, the background decrease occurring at Level 1).

Level 3: The pulsing of k as low salt concentration pulses through the specimen. This occurs when the organic fibers lining the flow channel walls coil as salt passes through the specimen and then de-coil as salt exits the specimen. This mechanism appears to be reversible and effects k by decreasing or increasing point constrictions along the flow channel. This mechanism was made visible during the latter Tracer Tests in the Column Experiment on S9, S10 and N2 when the background pore water concentration was no longer decreasing (See Figures 6.12 and 6.13).

Level 4: The step increase in k and θ_m as salt concentration is stepped up. This occurs when extreme decoiling of organics and mobilization of particles results in the flushing out of a significant amount of material. This would result in the irreversible increase in θ_m that was observed in Column Experiments on specimens S10 and N5 (Again see Figure 6.17 and Table 6.7).

There are additional dynamics that may or may not be significant in changing k and possibly θ_m . First, it is possible that biological activity and metal precipitation might compound the continual decrease in k occurring throughout the experiments. Second, since it is not clear how the continual loss of particles due to flow does not significantly alter flow channel diameter, it is possible that 2° compression (See Section 6.3.2.1) might offset any increase in effective porosity due to the washing out of particles that occurs throughout the experiment.

Recall, that although it was not measured, the volume of the soil specimens tested appeared to decrease by 5 to 10% throughout the Column Experiments.

6.4.2 SIGNIFICANCE OF FINDINGS

6.4.2.1 FLOW AND TRANSPORT MODELING

Although, both NaCl and D₂O breakthrough could be modeled using the One Region flow and transport model, flow and transport through wetland soils is a complicated and dynamic process. There is interaction between the tracer and the flow channels, and different tracers affect flow channel structure differently. This has important implications for the modeling of solute transport through wetland soils, since knowing parameters such as Darcy flux, hydraulic conductivity, and the sorption coefficient are not enough to describe how fast a given solute will travel through a given soil. In fact, large changes in hydraulic conductivity, caused by flow, solute breakthrough or oxidation, do not necessarily mean that solute flow velocity is changing. On the other hand, tracer concentration can effect flow channel size and distribution. Furthermore, some physio-chemical processes in the soil are irreversible while others are not and each is triggered by different factors. This makes the net effect on tracer breakthrough hard to predict.

6.4.2.2 REAL WORLD APPLICATIONS

The findings of this work are not only important in understanding how contaminated water moved from the Aberjona River into Woburn's municipal water supply (See Section 1.1), they have important implications for the use of wetlands as waste repositories, and for the reclamation of wetlands for agricultural use.

First, the value of the hydraulic conductivity of wetland soils has no bearing on how solute moves through the soils. For example, the hydraulic conductivity of a certain deposit may be low, but solute can still travel relatively quickly through that soil. This means that an 'impermeable' wetland deposit layer is not necessarily impermeable to hazardous chemicals.

Second, solute type and concentration can affect flow channel structure and distribution, and therefore, solute flow velocity. This means that even though the transport of water can be

slow, the number of flow channels can be increased when a solute is introduced into the soil. In the case of using wetlands as waste repositories, great care must be taken to understand and limit the effect of the buried waste on increased solute transport.

Third, since solute type and concentration can affect flow channel structure and distribution, it is possible to open up and expose once immobile regions, which can re-introduce dangerous chemicals back into the environment. For example, the use of road salt close to a contaminated region like in the Aberjona watershed, could re-mobilize heavy metals by changing the oxidation levels in heretofore unexposed regions of the soil.

6.5 VERIFICATION OF FINDINGS USING NMR

Currently, the use of Nuclear Magnetic Resonance (NMR) imaging is being investigated as a new method to investigate flow and transport in wetland deposits (Sinfield, 1998). The goal of this study, is to get an exact measure of effective porosity for a given wetland deposit specimen, and to link pore space distribution to hydraulic conductivity. A secondary goal of this study is to evaluate whether the Two Region model adequately describes flow and transport through these types of soils. This work is in its preliminary stages. Nonetheless, the initial experiments show promise and give results that are similar to those discussed above. A summary of the testing procedures and preliminary results are given below.

A preliminary Column Experiment was conducted by Sinfield (1998) in an NMR device on the organic portion of the soil used in this work. These organics were hand packed into a quartz tube, and placed into the NMR device where the soil was back-pressure saturated to 400 kPa. Subsequently, 0.1mM Gadolinium solution was injected into the specimen, as cross-sectional images were taken at regular intervals along its length. Since Gadolinium and water have different imaging properties, they can be distinguished from each other, and the pore space into which the Gadolinium flows can be quantified. This pore space, in effect, is the mobile pore space.

According to the images in this experiment, the effective porosity of the organic portion of this soil changed from 0.32 to 0.39 as the Gadolinium broke through the specimen (See Figure 6.21). These values for θ_m are a little low, but that is probably due to low resolution

and the exclusion of water filled pores during the imaging process. The Gadolinium breakthrough did show the same change in k that was observed during the breakthrough of sodium chloride tracer in the Column Experiments.

NMR technology has some limitations where wetland soils are concerned. Since wetland deposits contain both organic material and mineral particles, and since this particular soil contains a wide range of metals like iron, arsenic, cadmium and cesium, the NMR signal is often scrambled due to the interference of these magnetic and non-magnetic elements. Once this limitation is overcome, NMR technology might be very useful in exploring the mechanisms by which k decreases.

6.6 FUTURE TESTS

This work has brought to light several interesting characteristics of wetland soils. However, as in all experimental work, each answer is met with numerous questions. This seems to be particularly true of these highly variable and heterogeneous soils. There are many experiments that would be helpful in the understanding of flow and transport through these soils, and although not all of them are possible at the moment, a few of them are listed below.

6.6.1 THE NEXT STEPS

The following are suggestions for short term goals for this project.

1. To understand how D_2O tracer breakthrough is different from NaCl breakthrough. First, sorption of D_2O in wetland deposits has to be quantified, but these tests need to be limited since sampling is labor intensive, and since D_2O detection is expensive.
2. To evaluate how variable measured θ_m is for different solutes by running Column Experiments with salt, organic, and metal tracers. Again detection would be a limitation in these tests.
3. To explore the mechanisms that affect k by:
 - Evaluating organic coating using NMR techniques
 - Evaluating how colloid mobilization affects k when salt concentration is increased with column experiments run on the mineral fraction of the soil.

- Evaluating if biological activity does affect k with column experiments run with a tracer that is made with a bacteria killing agent.
 - Evaluating the redox and pH of the soil to see if metal precipitation is significant.
4. To verify that high levels of NaCl do create additional pore space through extreme mobilization of organic and mineral particles using NMR techniques.
 5. To assess the effect of elevated effective stress on k and θ_m by running tracer tests at effective stresses that are higher than the pre-consolidation pressure.
 6. To examine the significance of 2° compression on k and θ_m by measuring volume change in the specimen.
 7. To compare the results of compression tests on the permeameter with CRS results by running tests on re-sedimented soil.

Since the results of the three Column Experiments discussed in Section 6.2 show that data from tests on undisturbed and re-sedimented specimens are comparable, and that re-sedimented soils are good models for undisturbed soils, all future tests should be conducted on re-sedimented wetland soil samples only. This would help to eliminate the variability in compressibility, hydraulic conductivity, and pore water concentration that was found in undisturbed samples.

6.6.2 LONG TERM GOALS

The long term goals of this project are still the same. The first is to understand the chemical transport in the Aberjona wetland soils and to model this effectively. The second is to learn how to translate this knowledge to other wetland soils and environments. Similar tests should be run for soils with higher and lower organic fractions and with increased and decreased levels of humification.

6.7 REFERENCES

Ceride, C.M. *Mobilization of Kaolinite Fines in Porous Media*. Colloids and Surfaces, 27, 1987: 219-241.

- Fried, J.J. Groundwater Pollution, Elsevier Scientific Publishing Co.: NY. 1975.
- Goldenberg, L.C., Magaritz, M., Mandel, S. *Experimental Investigation on Irreversible Changes of Hydraulic Conductivity on the Seawater-Freshwater Interface in Coastal Aquifers*. Water Resources Research, 19.1, 1983: 77-85.
- Khilar, K.C., Fogler, H.S., *The Existence of a Critical Salt Concentration for Particle Release*. Journal of Colloid and Interface Science, 101.1, September 1984: 214-224.
- Ladd, C.C. MIT Course 1.322: Soil Behavior, classroom notes. Spring, 1996.
- Mesri, G., Stark, T.D., Ajlouni, M.A., Chen, C.S., *Secondary Compression of Peat with or without Surcharging*. Journal of Geotechnical and Geoenvironmental Engineering, May 1997: 411-421.
- Ours, D.P., Siegel, D.I., Glaser, P.H. *Chemical Dilation and the Dual Porosity of Humified Bog Peat*. Journal of Hydrology, 196, 1997: 348-360.
- Parker, J.C., van Genuchten, M.T. *Determining Transport Parameters from Laboratory and Field Tracer Experiments*. Virginia Agricultural Experiment Station Bulletin 84-3, 1984.
- Poltz, M., Personal communication, April, 1999.
- Shackelford, C.D., *Waste-Soil Interactions that Alter Hydraulic Conductivity*. Hydraulic Conductivity and Waste Contaminant Transport in Soil. ASTM STP 1142, David E. Daniel and Stephen J. Trautwein, Eds., American Society of Testing Materials, Philadelphia, 1994: 111-168.
- Sinfield, unpublished data 1998.
- Toide, N., Leij, F.J., van Genuchten, M.T. *The CXTFIT Code for Estimating Transport Parameters from Laboratory or Field Tracer Experiments, Version 2.0*. U.S. Salinity Laboratory, Agricultural Research Service, U.S. Department of Agriculture, Research Report 137, August 1995.

Table 6.1: (a) Results of One-Region Model fits for Tracer Tests on Sand Specimen 2 (b) Comparison of One and Two Region Model fits for Tracer Test 3 on Sand Specimen 2

Table 6.1a

BTC	Inj. Length (s)	q (cm/s)	V _c (cm/s)	R ²	V _m (cm/s)	D (cm ² /s)	R	θ _m	D/D*	Pe
1	600	1.43E-03	3.66E-03	98.9%	4.1E-03	8.72E-04	1	0.902	58.2	4.3
2	1200	1.52E-03	3.90E-03	73.3%	1.9E-03	6.67E-03	1	2.087	444.3	2.0
3	600	2.10E-03	5.39E-03	98.6%	6.1E-03	1.80E-03	1	0.877	120.1	6.6
4	600	2.83E-03	7.26E-03	98.6%	7.9E-03	2.36E-03	1	0.918	157.1	8.4
5	600	3.51E-03	8.99E-03	98.7%	9.5E-03	2.13E-03	1	0.949	142.2	10.1
6	600	4.07E-03	1.04E-02	95.4%	1.2E-02	6.26E-03	1	0.885	417.5	12.6

Table 6.1b:

Fit	Inj. Length (s)	q (cm/s)	V _c (cm/s)	R ²	V _m (cm/s)	D (cm ² /s)	R	θ _m	D/D*	Pe
ORM	600	2.10E-03	5.39E-03	98.6%	6.1E-03	1.80E-03	1	0.877	120.1	6.6
TRM	600	2.10E-03	5.39E-03	99.2%	6.3E-03	1.02E-07	1	0.853	0.0068	6.7

Table 6.2: Results of One-Region Model fits for Specimen S9

BTC	q (cm/s)	V_c (cm/s)	R²	V_m (cm/s)	D (cm²/s)	R	θ_m	D/D*	Pe
2	1.17E-05	1.42E-05	98.7%	2.05E-05	6.09E-06	1.39	0.571	0.41	0.068
3	1.63E-05	2.01E-05	98.8%	3.06E-05	6.71E-06	1.39	0.532	0.45	0.102
4	2.21E-05	2.72E-05	99.6%	4.13E-05	6.63E-06	1.39	0.536	0.44	0.138
5	2.78E-05	3.44E-05	99.7%	5.44E-05	7.08E-06	1.39	0.511	0.47	0.181
6	2.70E-05	3.39E-05	99.5%	5.34E-05	7.07E-06	1.39	0.505	0.47	0.178

Table 6.3: Results of One-Region Model fits for Specimen S10

BTC	q (cm/s)	V_c (cm/s)	R²	V_m (cm/s)	D (cm²/s)	R	θ_m	D/D*	Pe
1	1.11E-05	1.27E-05	98.9%	1.99E-05	5.96E-06	1.35	0.557	0.40	0.066
2	1.24E-05	1.43E-05	99.7%	2.25E-05	6.56E-06	1.35	0.549	0.44	0.075
3	1.33E-05	1.54E-05	99.6%	2.25E-05	5.77E-06	1.35	0.549	0.38	0.075
4	1.51E-05	1.76E-05	99.9%	2.77E-05	7.35E-06	1.35	0.546	0.49	0.092
5	1.34E-05	1.57E-05	99.8%	2.42E-05	7.16E-06	1.35	0.556	0.48	0.081
6	1.38E-05	1.61E-05	99.1%	2.31E-05	6.94E-06	1.35	0.597	0.46	0.077
7	1.54E-05	1.81E-05	99.9%	2.95E-05	6.87E-06	1.35	0.522	0.46	0.098
8	1.21E-05	1.43E-05	99.8%	2.32E-05	5.82E-06	1.35	0.525	0.39	0.077
9	1.81E-05	2.13E-05	99.8%	3.30E-05	6.52E-06	1.35	0.548	0.43	0.110
10	1.81E-05	2.20E-05	99.6%	3.07E-05	6.55E-06	1.35	0.611	0.44	0.102

Table 6.4: Results of One-Region Model fits for Specimen N1

BTC	q (cm/s)	V_c (cm/s)	R²	V_m (cm/s)	D (cm²/s)	R	θ_m	D/D*	Pe
5	1.12E-05	1.27E-05	99.0%	1.87E-05	5.95E-06	1.16	0.601	0.40	0.062
6	1.24E-05	1.41E-05	99.7%	2.04E-05	5.57E-06	1.16	0.607	0.37	0.068
7	1.38E-05	1.59E-05	99.6%	2.29E-05	6.77E-06	1.16	0.603	0.45	0.076
8	1.82E-05	2.09E-05	99.8%	3.15E-05	8.21E-06	1.16	0.577	0.55	0.105
9	2.10E-05	2.43E-05	99.5%	3.57E-05	1.04E-05	1.16	0.589	0.69	0.119
10	2.17E-05	2.51E-05	99.7%	3.64E-05	9.84E-06	1.16	0.597	0.66	0.121

Table 6.5: Comparison of CXTFIT and Method of Moments results

BTC	D_c (cm²/s)	D_m (cm²/s)	D_c/D_m	θ_{m,c}	θ_{m,m}	θ_{m,c}/θ_{m,m}
1	5.96E-06	3.11E-06	1.92	0.557	0.465	1.20
2	6.56E-06	3.58E-06	1.83	0.549	0.444	1.24
3	5.77E-06	3.03E-06	1.91	0.549	0.486	1.13
4	7.35E-06	5.10E-06	1.44	0.546	0.464	1.18
5	7.16E-06	4.80E-06	1.49	0.556	0.466	1.19
6	6.94E-06	5.14E-06	1.35	0.597	0.501	1.19
7	6.87E-06	4.43E-06	1.55	0.522	0.446	1.17
8	5.82E-06	3.69E-06	1.58	0.525	0.445	1.18
9	6.52E-06	4.63E-06	1.41	0.548	0.479	1.15
10	6.55E-06	5.24E-06	1.25	0.611	0.521	1.17
Average	6.55E-06	4.27E-06	1.6	0.556	0.472	1.18
Error	8.4%	19.9%	15.1%	5.1%	5.4%	2.5%

Table 6.6: Summary of relationships between pore water salt concentration, hydraulic conductivity, and effective porosity

Change in pore fluid salt concentration	Corresponding change in k	Corresponding change in θ_m	Reference Figure
+ ΔC small	+ Δk small	-	6.13 region (a)
- ΔC small	- Δk small	-	6.13 region (b)
+ ΔC large	+ Δk	+ $\Delta\theta_m$	6.14
$\Delta C = 0$	- Δk gradual	-	6.16 and 6.17
- ΔC large	- Δk	-	6.18

Table 6.7: Results of One-Region Model fits for Specimen N5

BTC	[salt] mM	q (cm/s)	R²	V_m (cm/s)	D (cm²/s)	R	θ_m	D/D*	Pe
1	10	6.08E-05	97.1%	7.71E-05	2.41E-05	1.20	0.788	1.61	0.257
2	50	6.18E-05	97.7%	6.79E-05	2.57E-05	1.20	0.909	1.71	0.226
3	1	6.10E-05	98.0%	6.81E-05	2.48E-05	1.20	0.896	1.65	0.227

Figure 6.1: Breakthrough curves and CXTFIT fits for 6 Tracer Tests on Sand Specimen 2.

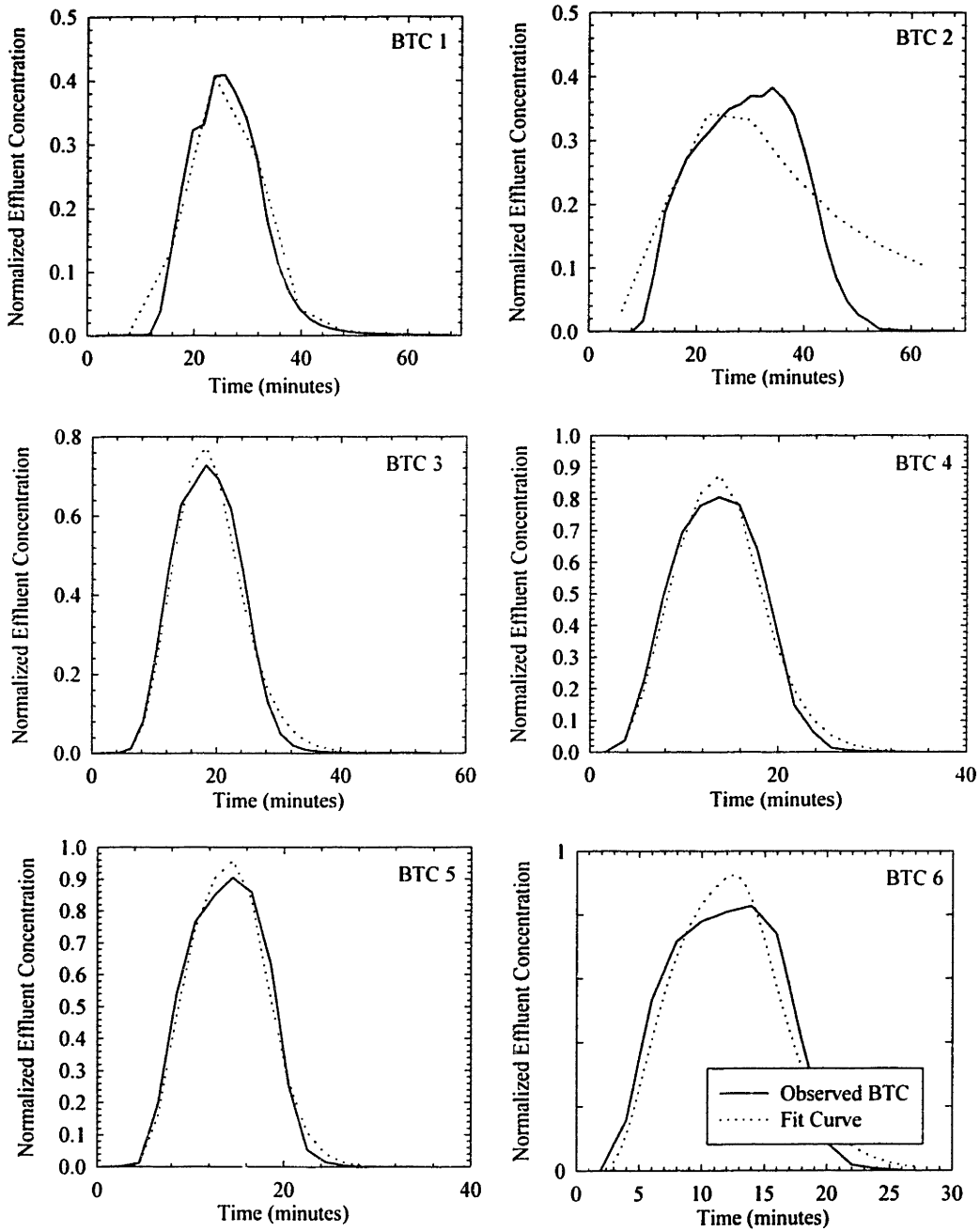


Figure 6.2: D/D^* vs. Peclet number from literature (Freeze and Cherry, 1979)

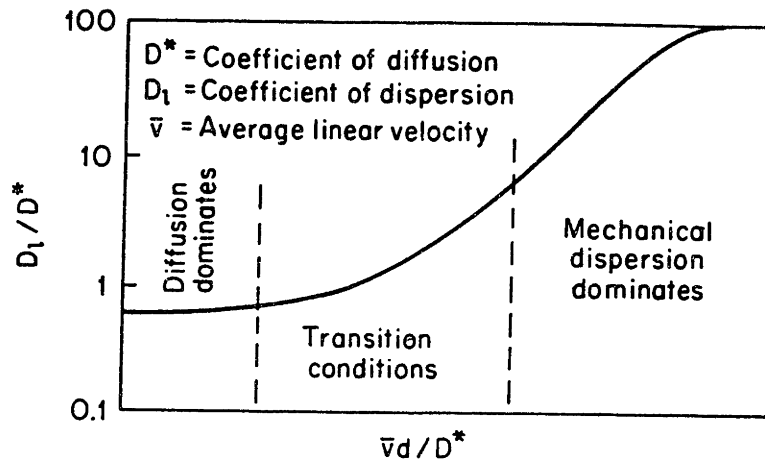


Figure 6.3: An example of the One Region Model Fit for Tracer Test 4 on specimen S10

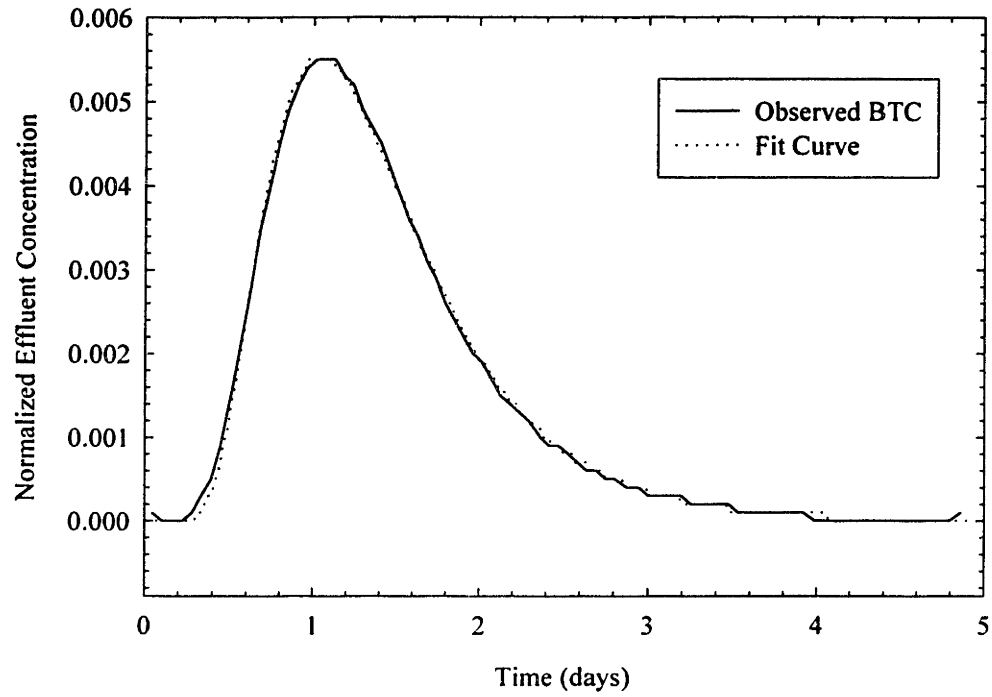


Figure 6.4: D/D^* vs. Peclet number from results of CXTFIT analysis on Tracer Tests run on specimens S9, S10, and N1

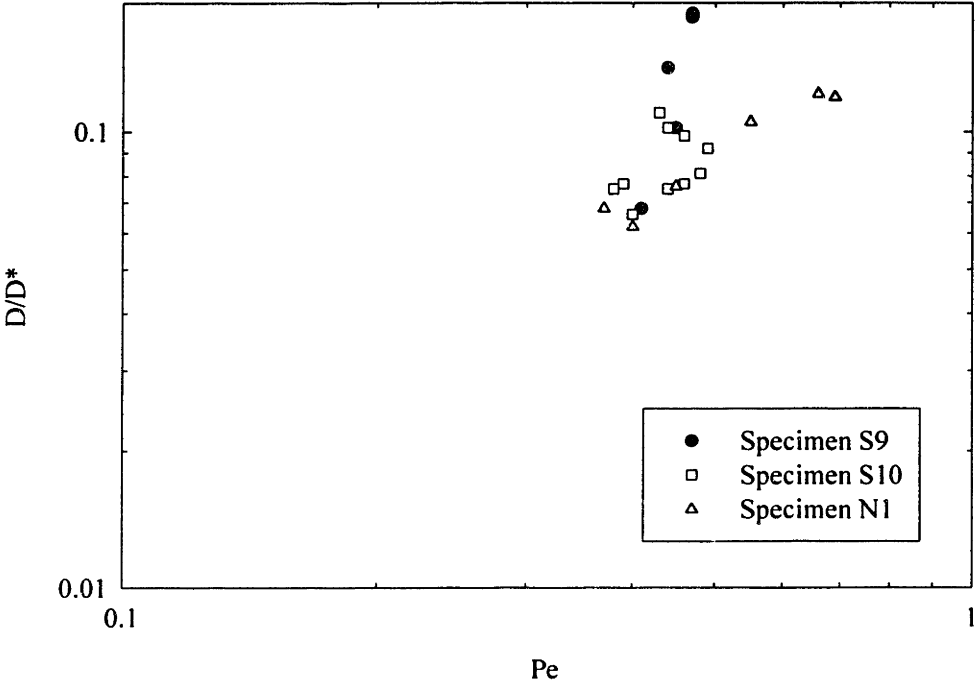


Figure 6.5: Effective porosity vs. Effective stress for Tracer Tests run on specimens S9, S10, and N1

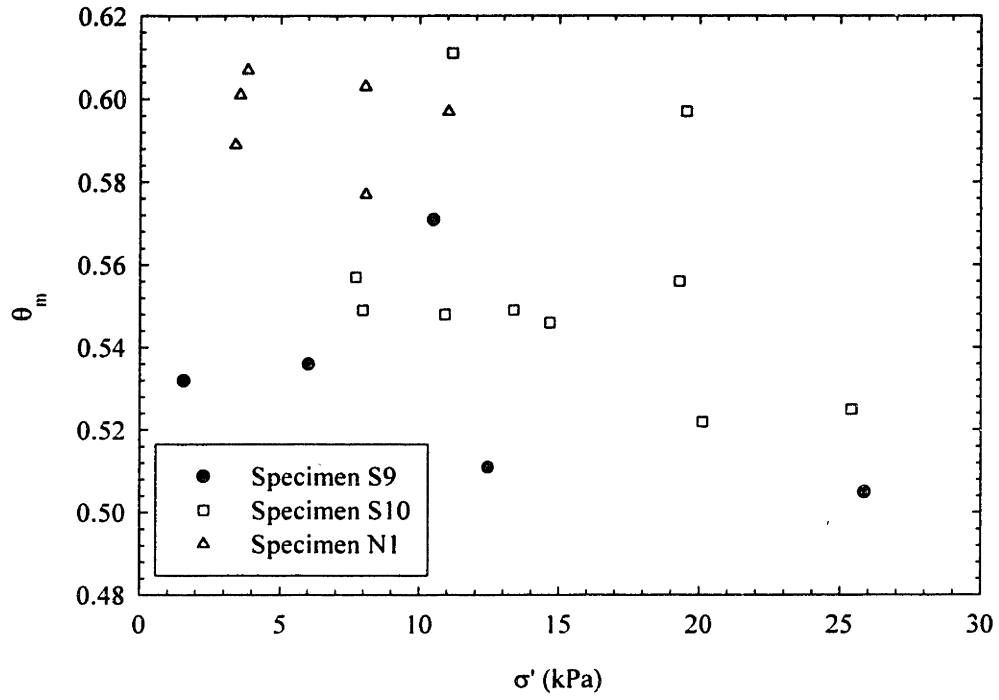


Figure 6.6: Effective porosity vs. Pore volume for Tracer Tests run on specimens S9, S10, and N1

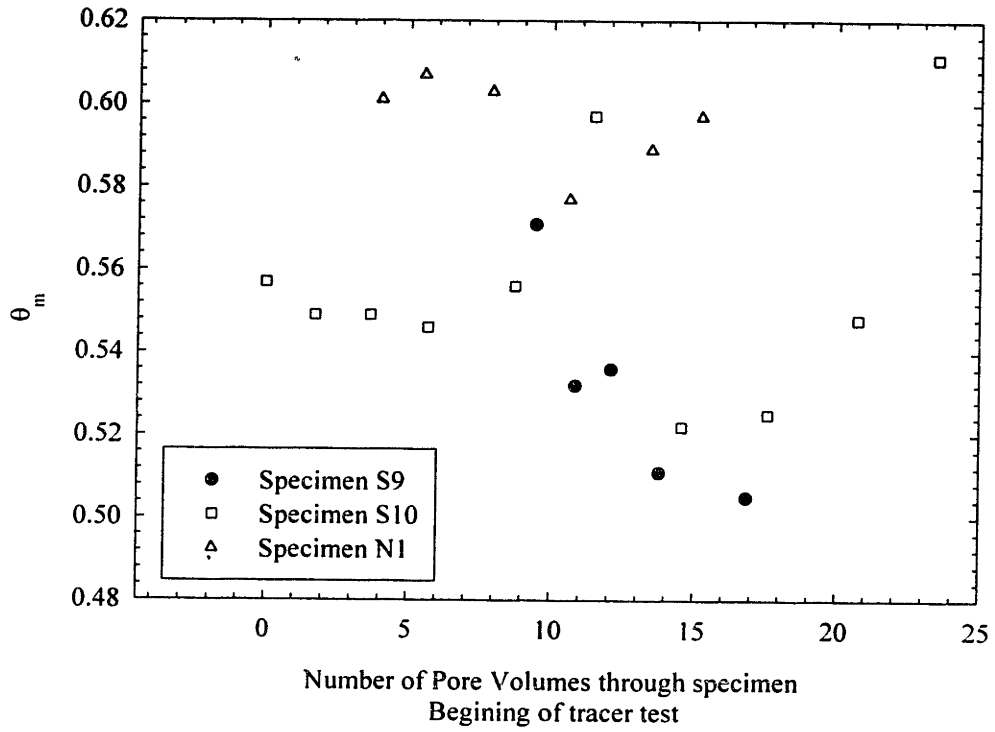


Figure 6.7: Effective porosity vs. Hydraulic conductivity for Tracer Tests run on specimens S9, S10, and N1

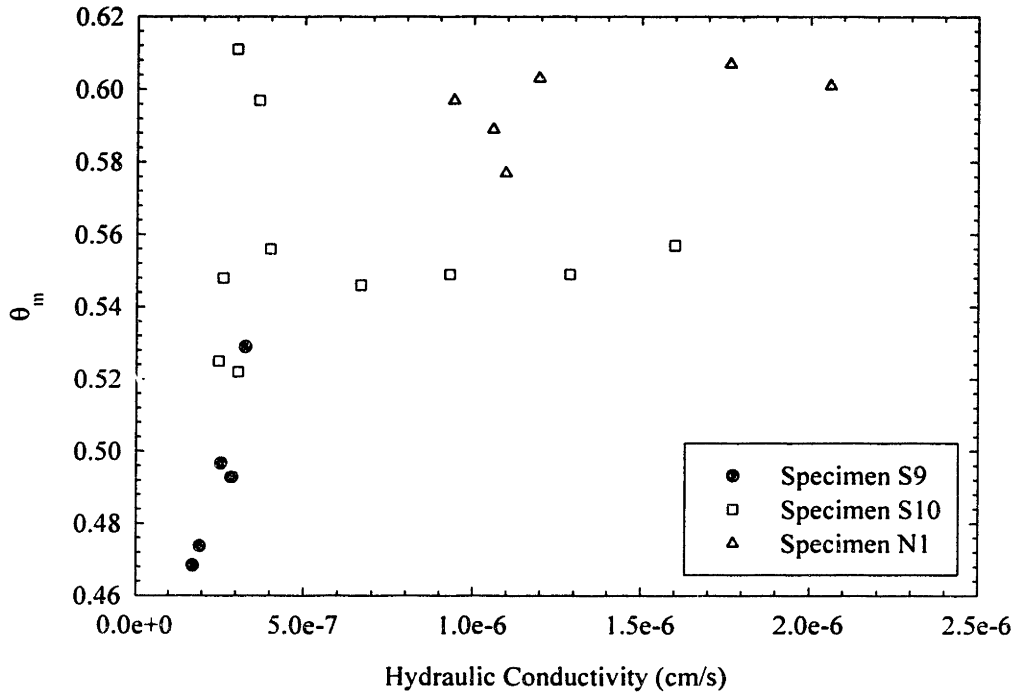


Figure 6.8: D calculated for Tracer Tests on specimen S10 using CXTFIT and the Method of Moments vs. Hydraulic conductivity

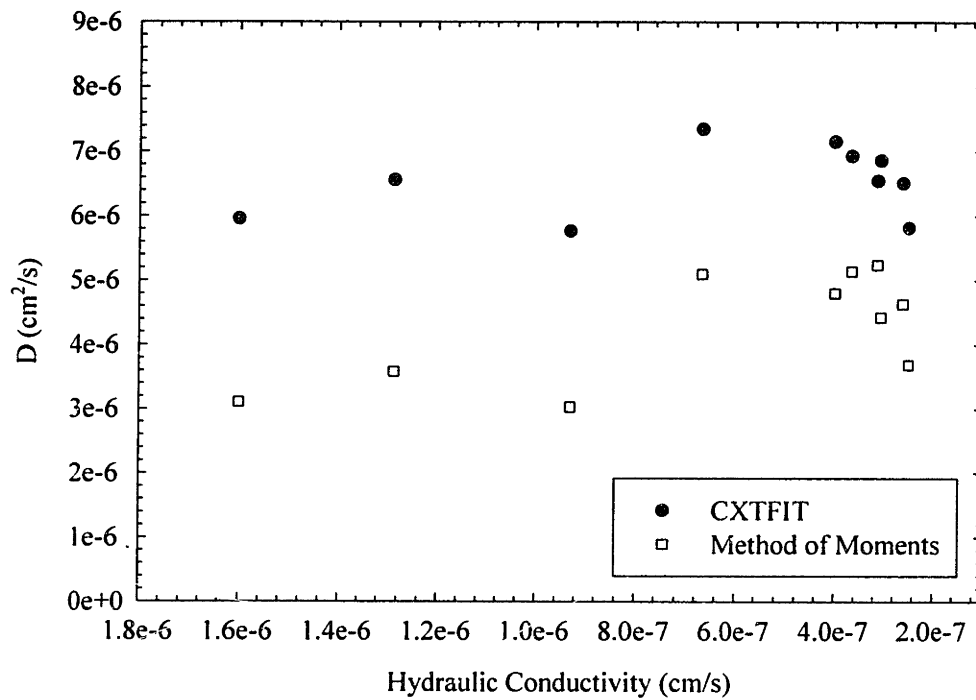


Figure 6.9: θ_m calculated for Tracer Tests on specimen S10 using CXTFIT and the Method of Moments vs. Hydraulic conductivity

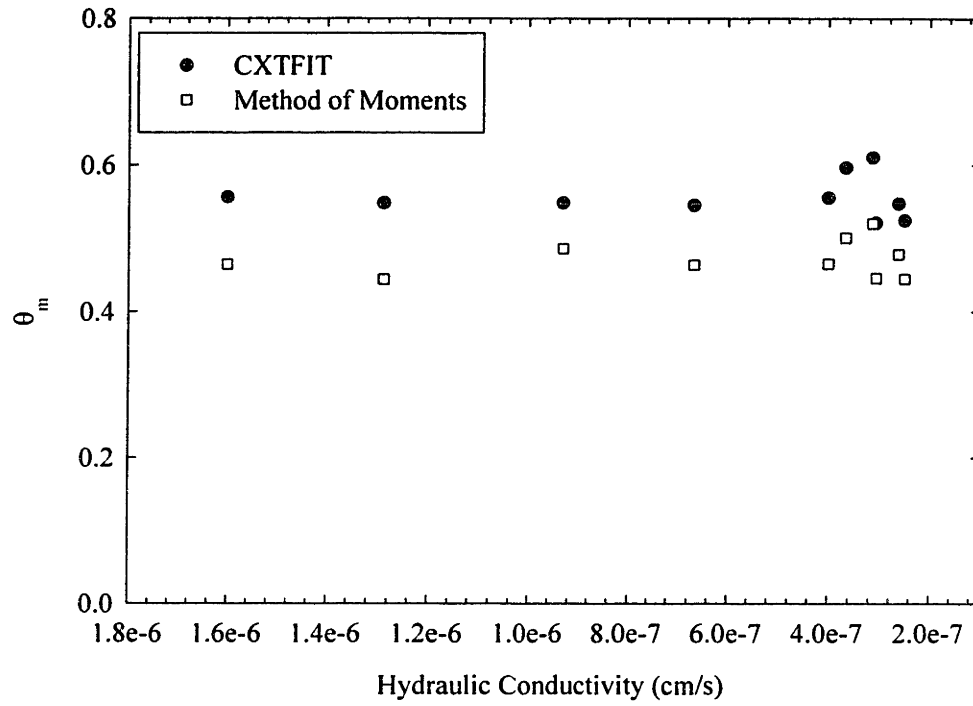


Figure 6.10: D₂O and NaCl breakthrough in Column Experiment on specimen N4

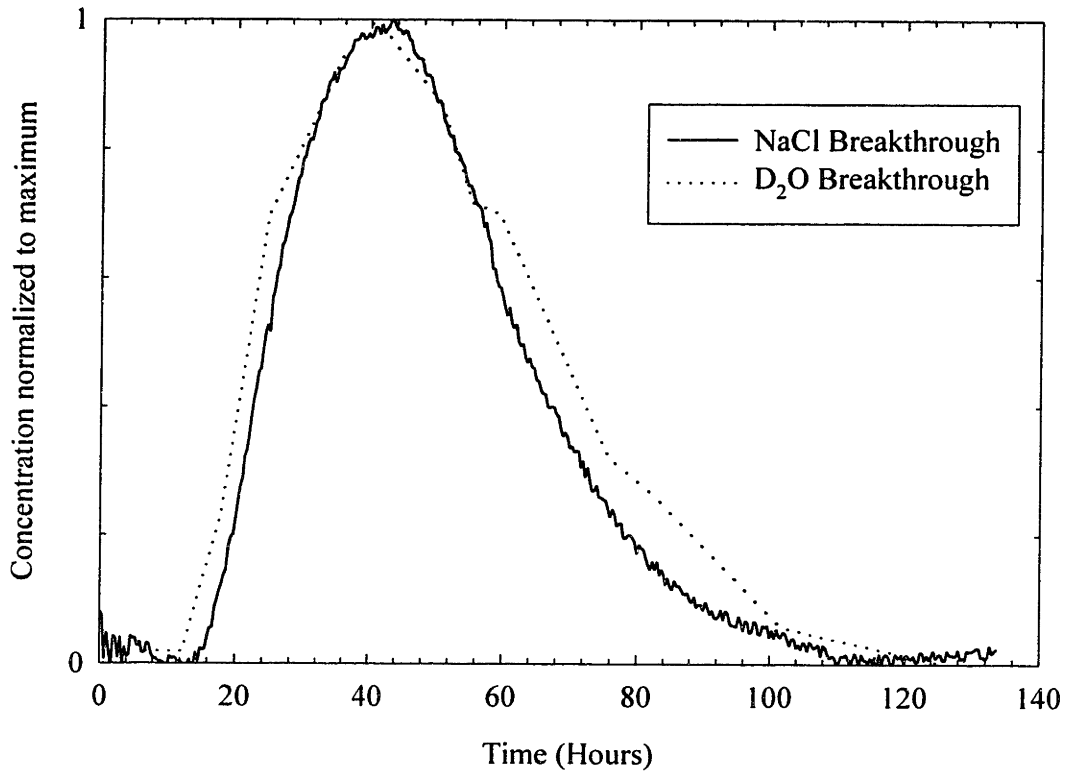


Figure 6.11: Breakthrough summary for Column Experiment on specimen S10

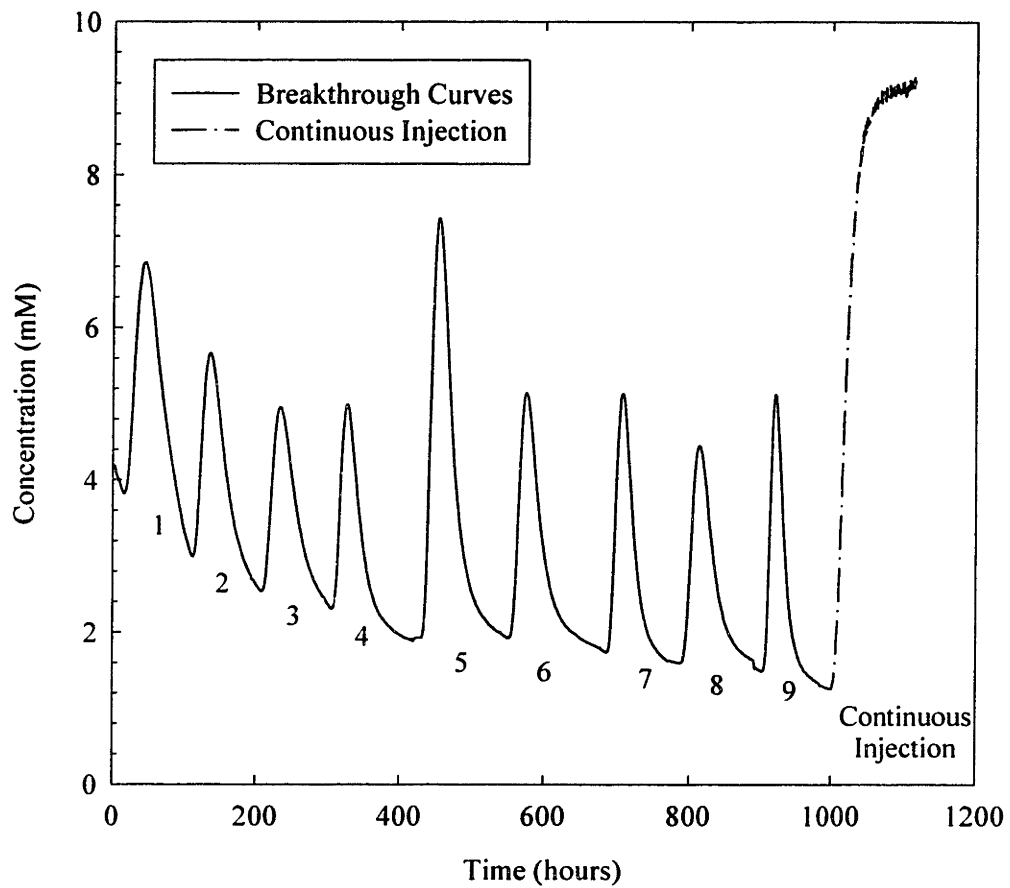


Figure 6.12: Breakthrough and hydraulic conductivity summary for Column Experiment on specimen S10

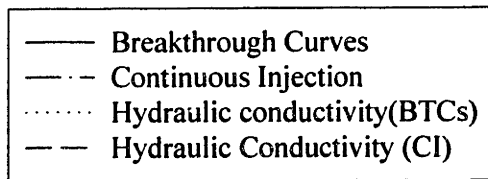
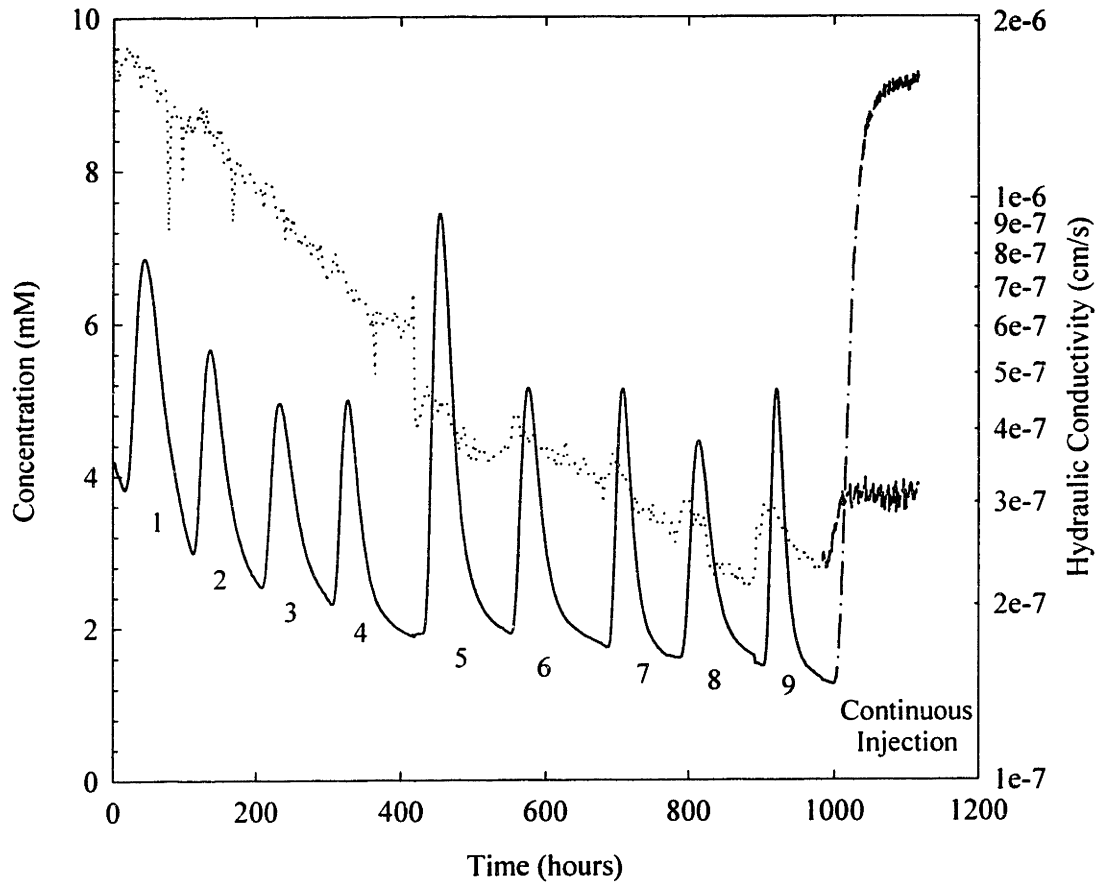


Figure 6.13: Hydraulic Conductivity variations for specimen S10 during Tracer Test 7

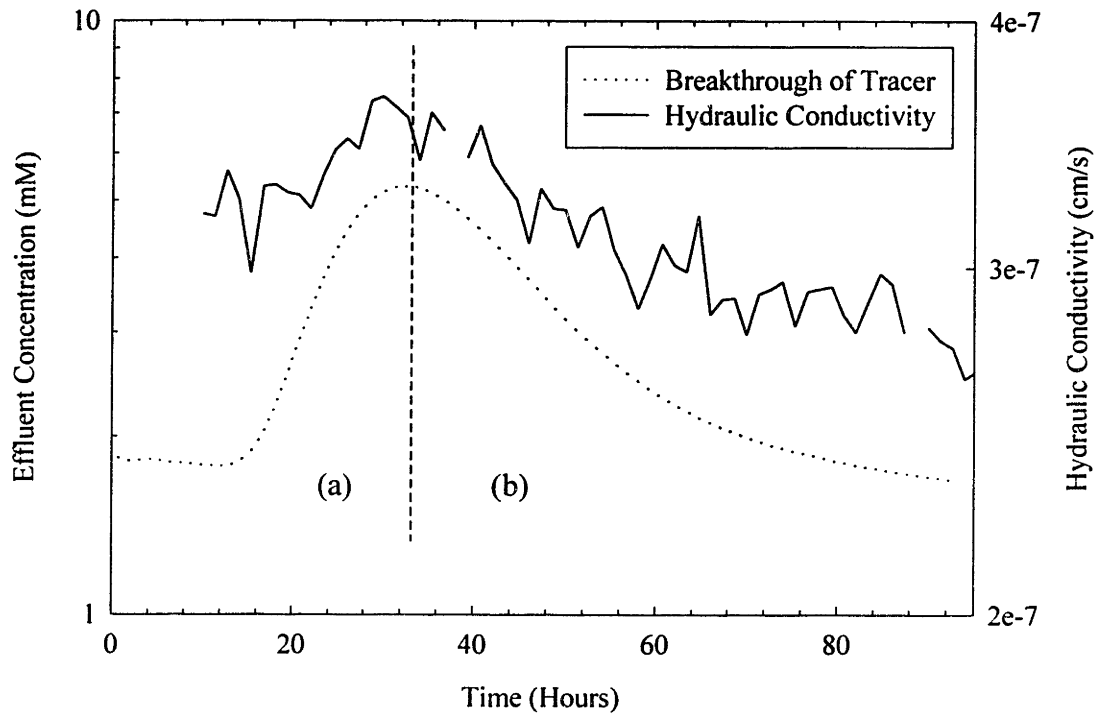


Figure 6.14: Hydraulic Conductivity of specimen S10 at a steady state effluent concentration of 10 mM NaCl

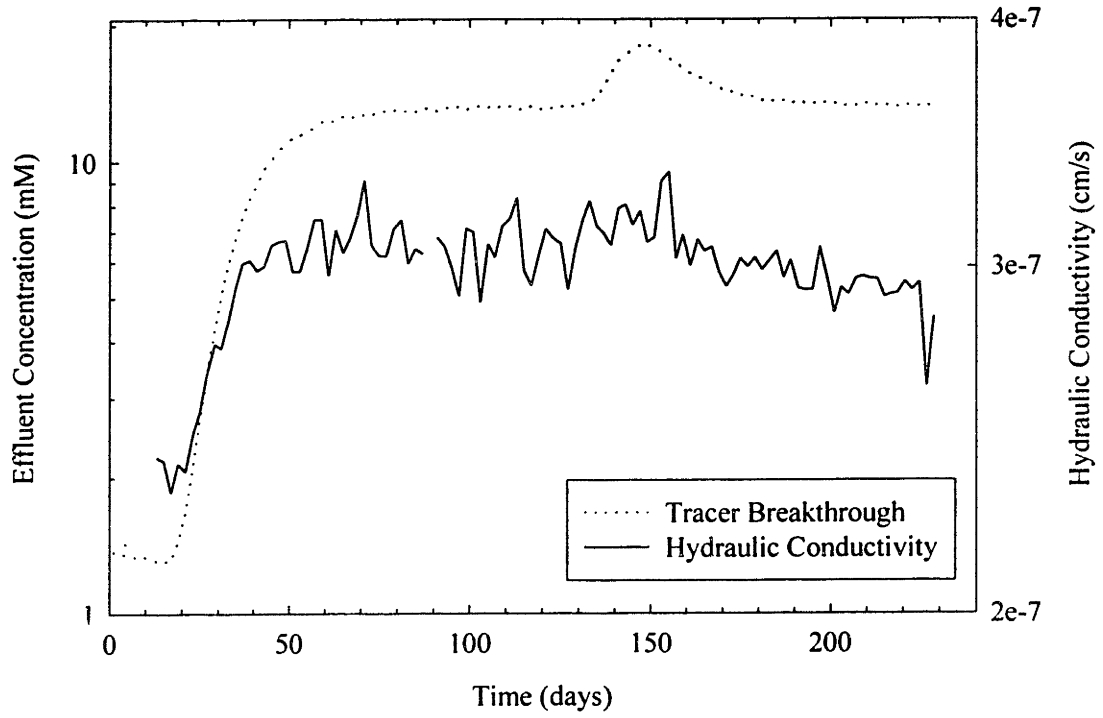


Figure 6.15: Hydraulic Conductivity of specimen N1 relative to variations in pore water salt concentration

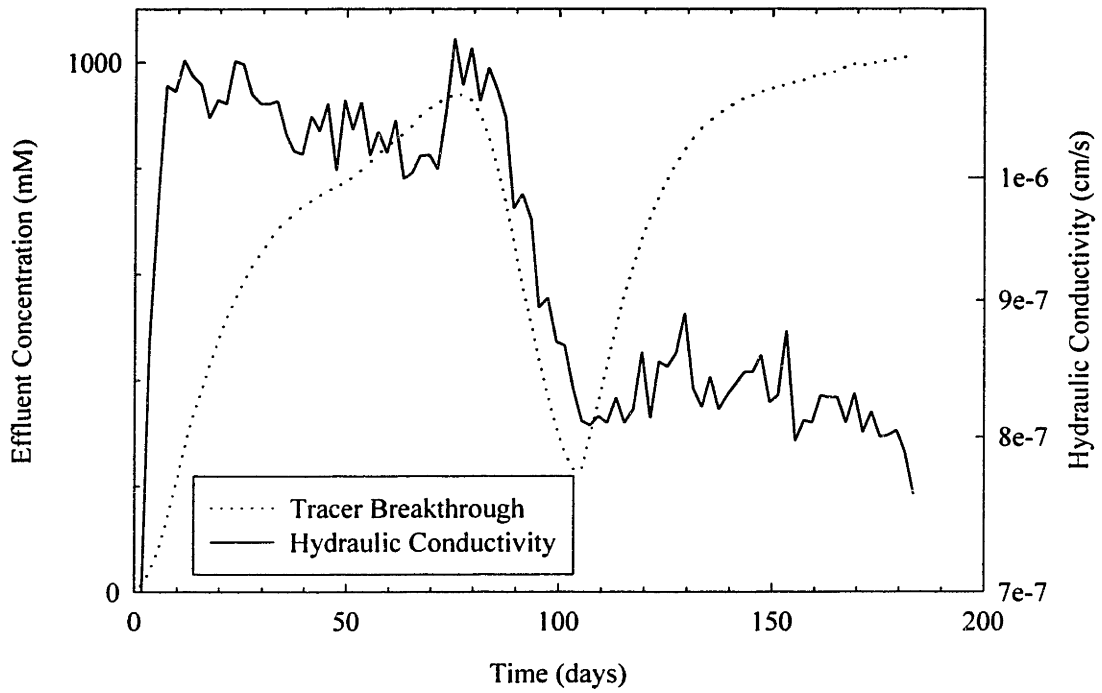


Figure 6.16: Hydraulic Conductivity of specimen S10 at a steady state effluent concentration of 50 mM NaCl

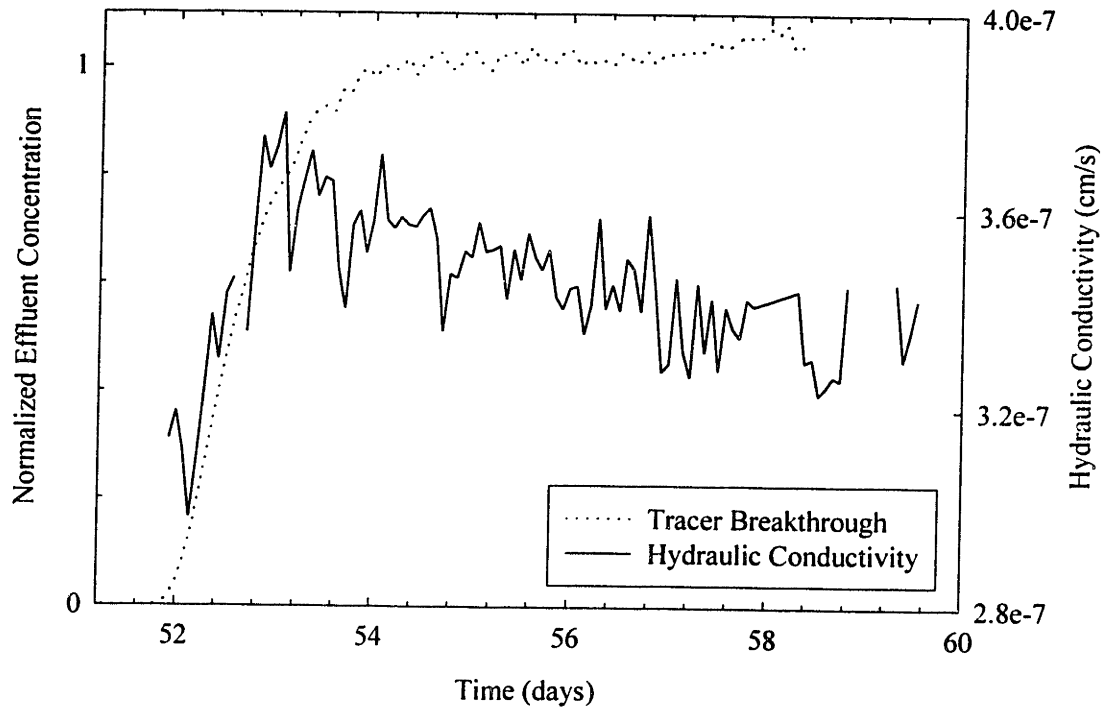


Figure 6.17: Hydraulic Conductivity variations for specimen N5 relative to variations in pore water salt concentration

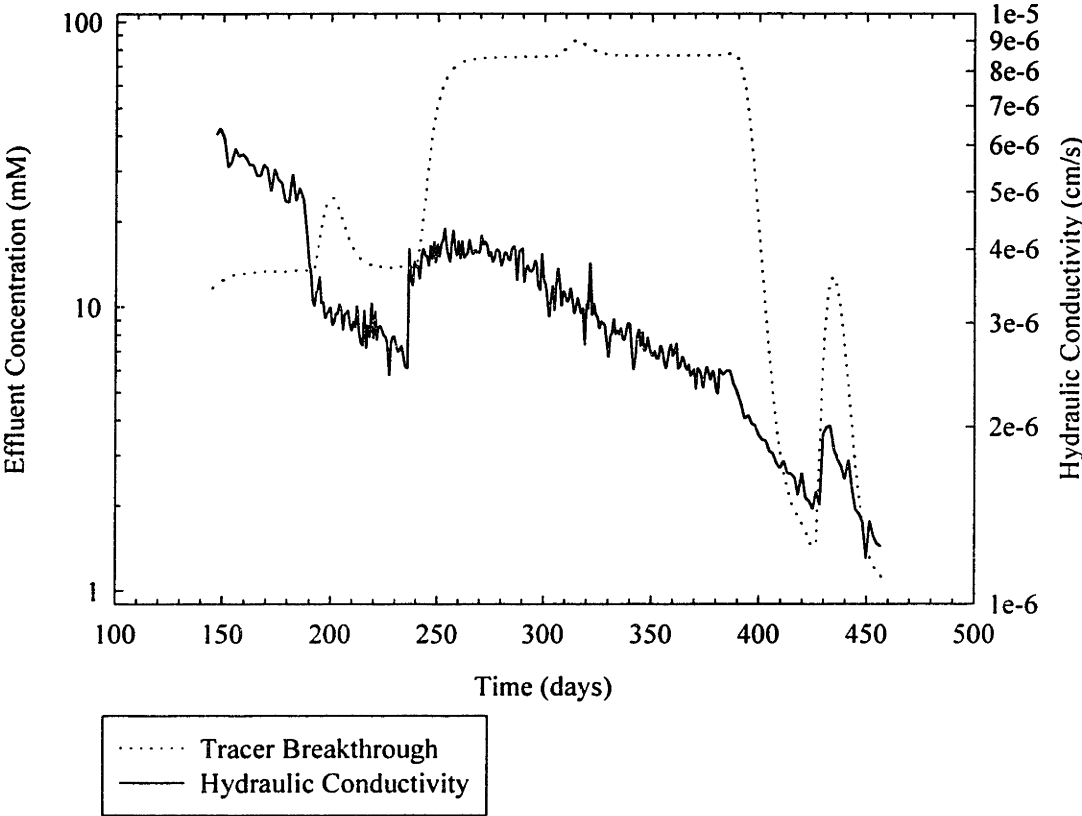


Figure 6.18: Effect of large decrease in pore water salt concentration on k (Specimen N5)

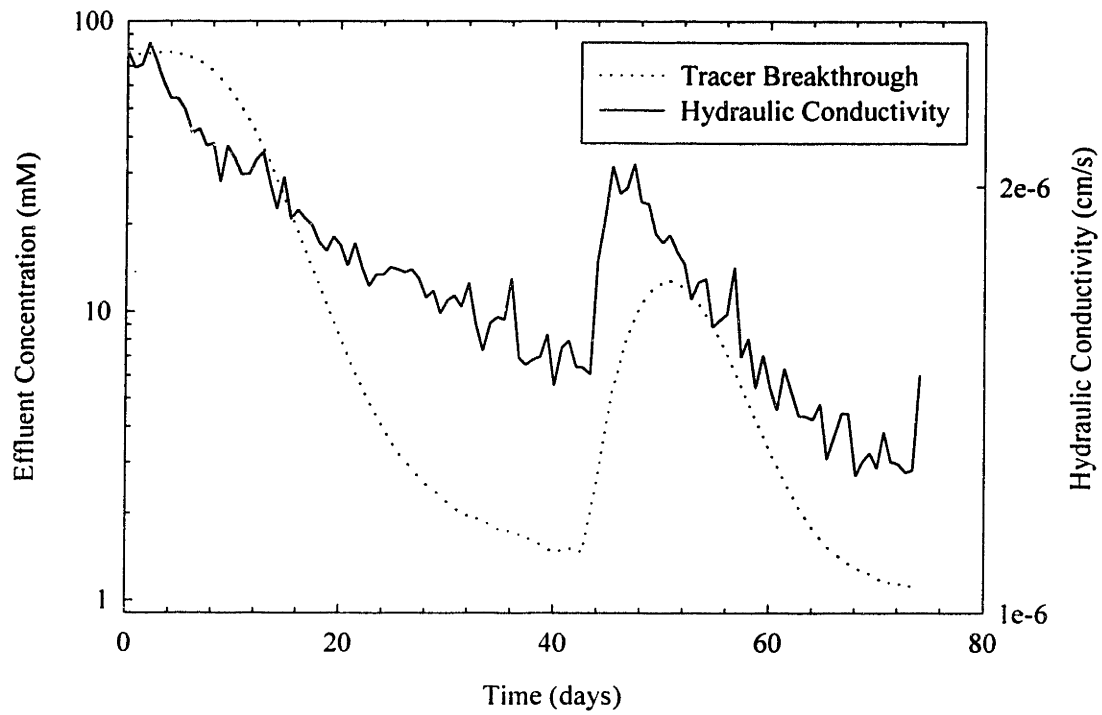


Figure 6.19: The influence of tracer salt concentration on organic fiber coiling in wetland soil flow channels

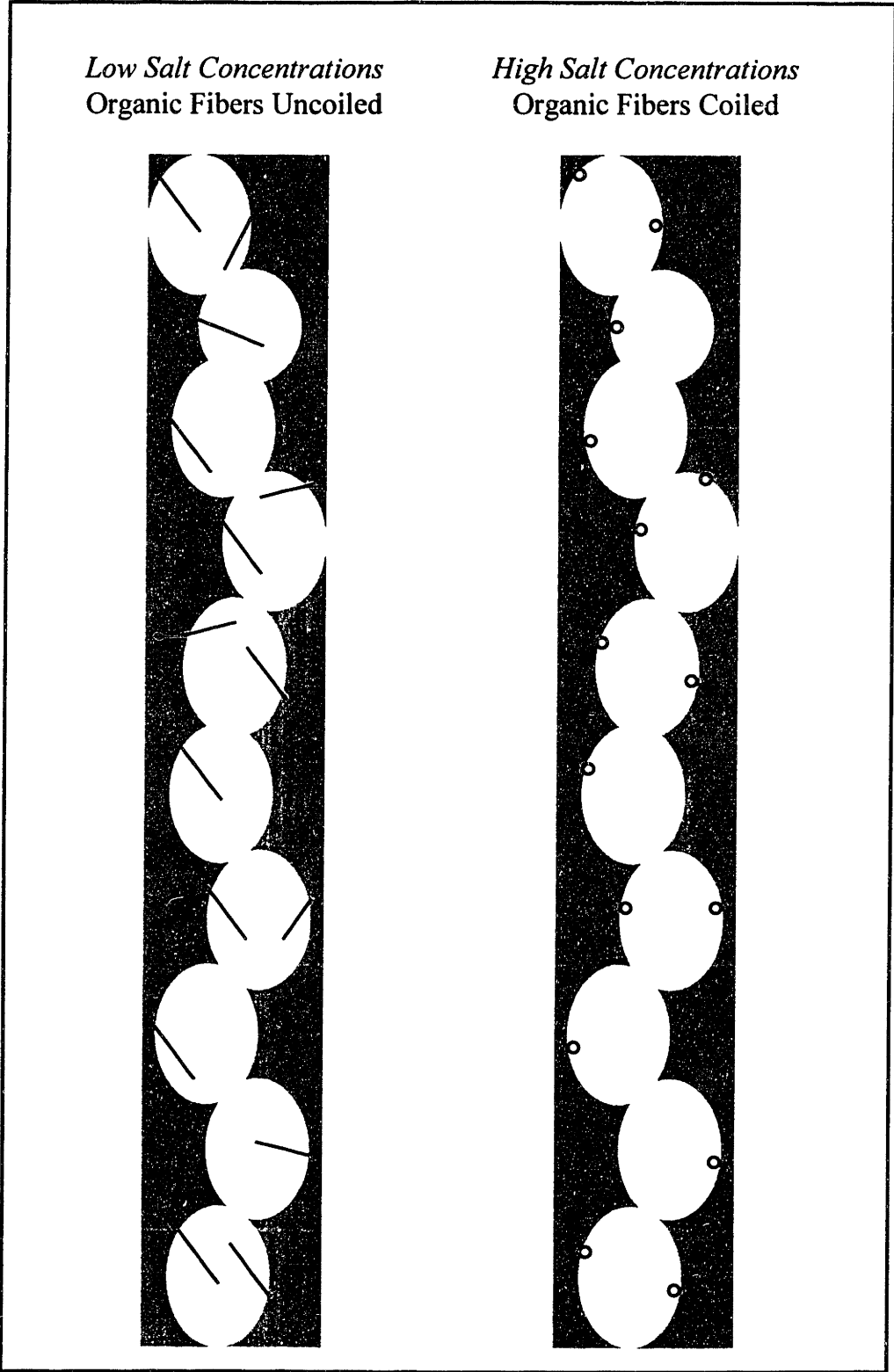


Figure 6.20: Schematic of colloid mobilization of clays in wetland soil flow channels

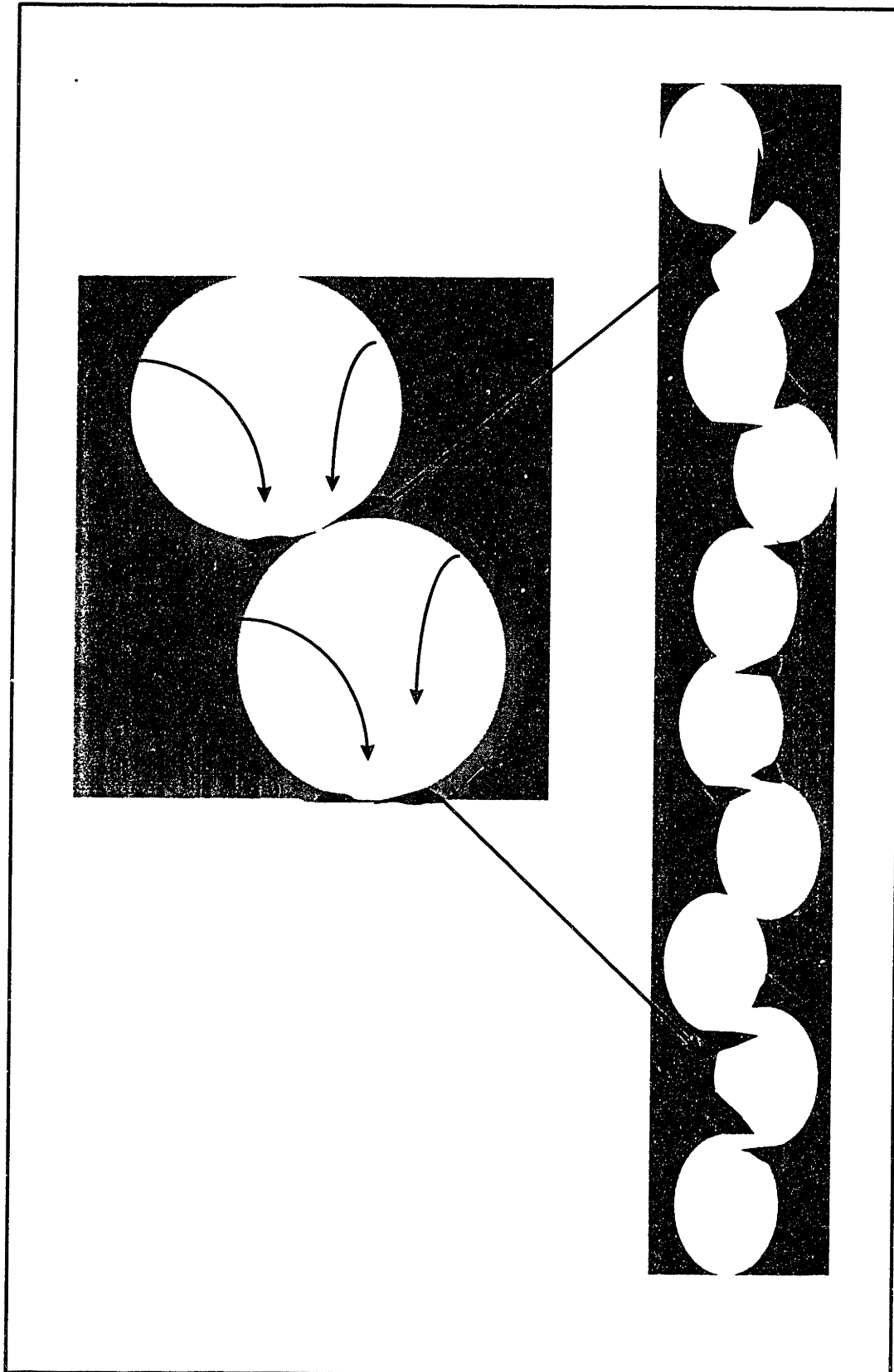
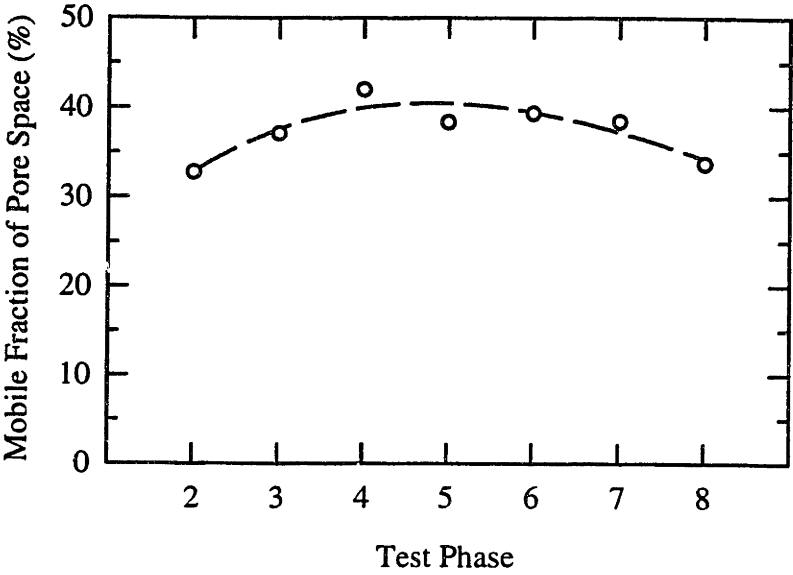


Figure 6.21: Measurements of the mobile fraction of the pore space in the peat specimen obtained through NMR imaging (Sinfield, 1998)



7. CONCLUSIONS AND RECOMMENDATIONS

Industrial contaminants, consisting of heavy metals and organic solvents, can be found throughout the Aberjona watershed, which comprises most of the city of Woburn, Massachusetts. In the late 1970s, high doses of Volatile Organic Compounds were found in Woburn's municipal drinking Wells G and H. Apparently, these potentially carcinogenic materials had moved from the Aberjona river, which drains the watershed, through a deposit of wetland soils that comprise the riverbed, and into the sand and gravel aquifer, which supplied the drinking wells. It is the goal of this thesis to present some insight into what controls flow and transport of water and solutes through wetland soils. These insights will hopefully contribute to the umbrella study organized by the Center of Environmental Sciences at MIT. The overall objective of this study is to understand what risks the industrial contaminants posed and still pose to human health.

7.1 SUMMARY OF FINDINGS

As stated above, the primary goal of this work was to assess the hydro-geologic properties of wetland soils. However, to optimize this research, it was necessary to take two additional steps.

First, it was important to evaluate how the testing apparatus worked, and to improve both the equipment and testing procedures. The results of this evaluation and of the equipment and procedural modifications are discussed in Chapter 3 and are highlighted below in Section 7.2.1.

Second, it was important to characterize the geotechnical properties of the wetland soils being tested. The geotechnical tests that were conducted, their procedures, and their results are given in Chapter 4. They are also summarized in Section 7.2.2.

These two investigations were run prior to and in conjunction with the principal investigation, which consisted of Column Experiments on undisturbed and re-sedimented

wetland soils. The experimental procedures used in these Column Experiments are outlined in Chapter 5. Their results are discussed in Chapter 6 and again in Section 7.2.3.

7.1.1 EQUIPMENT AND PROCEDURE DEVELOPMENT

The Column Experiments were conducted on a permeameter which was built from a modified triaxial cell by Ramsay (1996). The flexible-wall permeameter were built with several distinctive features. First, electrical conductivity probes, which allowed for the measurement of influent and effluent salt concentration, were built into the influent line and the permeameter pedestal. Temperature, pH, and eH probes was also built in to the pedestal, and were intended to give more information about the effluent properties.

Second, two influent reservoirs, each with air-water interfaces, were hooked into the permeameter. This made it possible to alternately inject saline tracer then fresh water into the specimen. The tracer flow rate was controlled by a flow pump, which, in turn, was controlled by a manual rheostat. Both the flow rate, which was set, and the hydraulic gradient, which resulted, were used to calculate the hydraulic conductivity of the specimen, using Darcy's Law.

The third distinctive feature of the permeameter was that the electrical conductivity and temperature probes, the displacement transducer, which measures flow rate in the specimen, as well as the pressure transducers, which measure the cell and pore pressures, were all monitored using a central data acquisition system. This system collected and stored the electronic output of the probes and transducers at regular intervals during the week long Tracer Tests, facilitating what might have been very labor intensive experiments.

Some modifications were made in the testing equipment as well as some of the testing and analysis procedures that were proposed by Ramsay. These helped to optimize the Column Experiment results, and are outlined below.

7.1.1.1 ELECTRICAL CONDUCTIVITY PROBES

Preliminary Column Experiments to evaluate the equipment were conducted by Ramsay. To ascertain that the mass of NaCl tracer injected into the system was fully recovered, he

conducted a mass balance calculation, which compared the mass of salt injected, according to the influent probe, to the mass of salt recovered, according to the effluent probe. He found, for some Tracer Tests, that up to 50% of NaCl mass could not be accounted for.

To understand why NaCl recovery was considerably less than 100% in the tests conducted by Ramsay, a Column Experiment was conducted on a sand specimen. Twenty two Tracer Tests were run on the specimen. Between tests, flow velocity and effective stress were varied, and the mass injected was compared to the mass recovered. It was observed that the relative amount of mass recovered decreased for the later Tracer Tests. This implied that the electrical conductivity probe at the pedestal was becoming less sensitive with time. This was verified in two ways. First, soap was injected into and rinsed out of the system, and it was found that salt recovery was improved. Second, effluent samples were taken and their electrical conductivity measured by an independent electrical conductivity probe. It was found that the tracer was indeed conserved, and that the effluent electrical conductivity probe was reading too low.

It was also found that, if the effluent electrical conductivity signal was scaled by the ratio of mass injected to mass recovered, the probe readings matched the effluent sample concentrations. Therefore, the low recovery issue was resolved by incorporating the effluent electrical conductivity probe scaling factor in the analysis of Tracer Test breakthrough.

7.1.1.2 RE-SEDIMENTED SOIL SPECIMENS

Undisturbed wetland deposit specimens can be difficult to test for several reasons. Extreme variability in properties such as water content, ash (mineral) content, hydraulic conductivity, stress history, and compressibility, can exist from specimen to specimen (Bailon, 1995). As a result, it is difficult to evaluate the effect of different physical features on the hydrogeology of the different soils. Second, the sometimes low maximum past pressure of a given specimen can make it difficult to conduct Column Experiments on those specimens, since they compress easily and become relatively impermeable during testing (Ramsay, 1996). Finally, some organic macro-features, such as reeds and twigs, create short circuits in some specimens, causing the hydraulic conductivity to be unmeasurably high.

To avoid such problems, wetland soil was collected from the field, processed, then re-sedimented according to the procedure described in Section 2.3.2.1. During re-sedimentation, large (> 2 cm) features were removed, then the soil was ground such that the maximum particle size was controlled. The soil was then placed in a mold, loaded and allowed to consolidate to the desired stress level. As a result, not only was variability between specimens reduced, but the stress history of the soil was known.

To evaluate the properties of the re-sedimented specimens, Constant Rate of Strain (CRS) tests were conducted on specimens taken from the same re-sedimented sample, and on specimens from different re-sedimented samples. The results of those tests showed that, not only were the properties of the re-sedimented soils similar, but that they compared very well to the results of tests on undisturbed specimens.

Column Experiments were conducted on both re-sedimented and undisturbed specimens. The results of these are discussed in Chapter 6 and below in Section 7.2.3.

7.1.1.3 THE LIMITING OF END EFFECTS

To see if solute breakthrough in the Tracer Tests was affected by the equipment itself, a Column Experiment was setup without any specimen. It was found that, even with no soil in the column, the solute, which was injected as a square, ten minute pulse, broke through in a diffused, asymmetrical bell shaped fashion.

Since this system effect would obscure the true solute breakthrough in a Tracer Test on soil, A Column Experiment was setup without the filter stones that are placed at the top and bottom of the specimen and which are used to distribute the tracer at the top of the specimen and to collect it at the bottom. From the tracer tests conducted in this Column Experiment, the tracer was injected and recovered as a square pulse. It became clear that the filter stones were not distributing and collecting the tracer effectively.

To help eliminate this problem, distribution caps, plexi-glass cylinders with radially distributed holes drilled into them, were constructed (See Section 2.2.3.2). These caps were effective in reducing the filter stone end effects by distributing the influent evenly across the

top of the filter stone at the top, and then by redirecting the effluent front at the bottom of the pedestal filter stone.

7.1.2 GEOTECHNICAL ANALYSIS

Several geotechnical tests were conducted on both the undisturbed and re-sedimented samples to characterize the wetland soils being tested. The tests and their results are summarized below.

1. **Specific Gravity (G_s):** The average specific gravity for the five re-sedimented batches was $2.04 \pm 4.0\%$. The average specific gravity for four undisturbed specimens was $1.68 \pm 12.7\%$. The average was lower than the re-sedimented value because the re-sedimented samples had less organic material in them as a result of the processing step in the re-sedimentation procedure. The undisturbed soil G_s values were also more spread out than the values of the re-sedimented values due to the variability found in natural wetland deposits.
2. **Ash Content:** The average Ash content for the five re-sedimented batches was $58.3 \pm 1.6\%$ (Ashing Temperature = 450°C). The average specific gravity for four undisturbed specimens was $46.9 \pm 16.8\%$. As for the specific gravity measurements, the average was lower than the re-sedimented value because the re-sedimented samples had less organic material in them, and the undisturbed soil ash content values were more spread out due to the variability found in natural wetland deposits.
3. **Soil Size Distribution:** Three size distribution experiments were conducted, the first, on soil processed on the 'fine' setting, that is, with a maximum particle size of 0.4 cm, the second, on soil processed on the 'coarse' setting, that is, with a maximum particle size of 1 cm, and third, on a sub-sample of the undisturbed cores. As expected, the unprocessed, natural soil had larger particles and more particles in the large size fractions. On the other hand, the 'finely' processed soil had a narrower range of particle size with the maximum particle size, as designed, being 4mm. The Size Distribution Curve for the 'coarsely' processed soil fell in between those of the unprocessed and fine soils.

4. **Soil Compressibility:** Constant Rate of Strain (CRS) tests were conducted to better understand the compressibility behavior and the stress history of the soil samples. For the re-sedimented specimens, the values for the compression ratio, CR, were consistent for all the specimens, ranging from 0.319 to 0.362, with an average value of $0.338 \pm 4.4\%$. The values for CR measured for the undisturbed specimens were over 20% lower than was measured for the re-sedimented specimens, and they ranged from 0.240 to 0.299, with an average value of $0.277 \pm 11.6\%$. A discussion of these findings as well as the values of the re-compression ratio, RR, maximum past pressure, σ'_p , and other properties are included in Section 4.7.
5. **Mineral Fraction Characteristics:** The mineral fraction of the soil was separated from the organic fraction. Then its mineralogy and size distribution was assessed. It was found that the soil consisted primarily of fine to coarse silts, which were made up of quartz, mica, chlorite, and feldspars.

7.1.3 FLOW AND TRANSPORT IN WETLAND SOILS

Tracer tests were run on Column Experiments conducted on two re-sedimented specimens (S9 and S10) and on one undisturbed specimen (N1). Between 6 and 10 Tracer Tests were run on each specimen, and tracer flow velocity and effective stress were varied between Tracer Tests.

For each Tracer Test, 100 or 500 mM NaCl tracer was injected for 10 or 20 minutes. The effluent breakthrough was monitored using the pedestal electrical conductivity, its flow velocity was measured using the displacement transducer attached to the flow pump piston, and the hydraulic gradient across the specimen was measured via the pressure transducers linked to the top cap, pedestal, and permeameter cell.

For each Tracer Test, hydraulic conductivity was calculated from the flow velocity and gradient data and Darcy's law, while the effective porosity, θ_m , and Diffusion coefficient, D , were calculated using the breakthrough data and the CXTFIT package. The CXTFIT program, which was written by Parker and van Genuchten (1986) and updated by Toride, et al (1995), uses the One-Region model and a nonlinear least squares inversion method to find

values for flow and transport parameters such as tracer flow velocity, D , and the retardation factor, R . CXTFIT can also be run in the Two-Region model mode. In this mode CXTFIT calculates additional parameters called β , a dimensionless ratio relating θ_m and the fraction of sorbing sites to total porosity and total number of sorption sites, as well as ω , a dimensionless ratio relating the mass transfer rate to total porosity and average pore water velocity.

Two additional Column Experiments were run on undisturbed specimens N4 and N5. Special Tracer Tests were run on each specimen. For the Column Experiment on specimen N4, the 500 mM NaCl tracer was made with heavy water, or deuterium oxide (D_2O). This test was meant to verify that ion exclusion was preventing the NaCl from moving into immobile regions of the soil. For the Column Experiment on specimen N5, three Tracer Tests were run, each at a different pore water salt concentration. These tests were meant to show that high levels of pore water salt affected the effective porosity of the specimen.

An analysis of the Tracer Test data for all the column experiments led to the following conclusions:

1. Flow of NaCl and D_2O tracer can be described using the One-Region model, even though peat has both a mobile and an immobile region.
2. According to the NaCl Tracer Tests, order of magnitude decreases in k were observed during the course of each column experiment, yet there was no observable change in θ_m . This probably occurred as a result of several actions.
 - a. First, particles that were mobilized by flow of water collected at flow channel pore throats. This occurred throughout each column experiment and resulted in the gradual, continual decrease in k .
 - b. Second, large decreases in k occurred when fresh water was flushed through the specimen. The flushing of the specimen removed salts from the pore water and, subsequently, mobilized mineral colloids, which moved through the flow channels and clogged narrow pore openings. This increased the hydraulic gradient across the specimen, and decreased k . The clogging of small pores does not affect the overall size of the flow channels through which

the NaCl tracer moves, and therefore, θ_m according to the NaCl tracer tests does not change.

- c. Additional decreases in k could occur as more point obstructions develop due to the aerated tracer re-oxidizing the specimen. The presence of oxygen can cause the large mass of metals in the specimen to precipitate, and it can cause biological activity to resume. The metal precipitate as well as dead bacteria and mia-fauna could deposit in and obstruct the flow channels.
3. Some increases in k were also observed during the course of each column experiment, in some cases irreversible increases in θ_m were also observed. This can be explained by the following two mechanisms.
- a. Increases in k during the Tracer Tests, occurred as the low NaCl concentration increased in the specimen. This increase in k occurred, in part, when organic fibers lining the specimen flow channel walls, coiled in the presence of soil. This like the other mechanisms, caused the hydraulic gradient across the specimen to decrease but did not effect the overall size of the flow channels.
 - b. Increases in k also occurred during the Continuous Injection tests, as NaCl solution saturated the specimen. This resulted in significant increases in k as well as θ_m . This was probably due to extreme organic coiling and colloid mobilization, which flushed out a significant amount of material from the pore channel walls

These conclusions illustrate the complexity of flow and transport in wetland soils, and although they are very revealing, they have exposed interesting questions that need to be answered before flow and transport of pollutants can be well understood and modeled. Several tests and the specific questions they address are suggested below.

7.2 RECOMMENDATIONS FOR FUTURE RESEARCH

7.2.1 RECOMMENDATIONS

The following steps would be necessary to improving our understanding of flow and transport through wetland soils.

1. To understand how D_2O tracer breakthrough is different from NaCl breakthrough. First, sorption of D_2O in wetland deposits has to be quantified, but these tests need to be limited since sampling is labor intensive, and since D_2O detection is expensive.
2. To evaluate how variable measured θ_m is for different solutes by running Column Experiments with salt, organic, and metal tracers. Again detection would be a limitation in these tests.
3. To explore the mechanisms that affect k by:
 - Evaluating organic coiling using NMR techniques
 - Evaluating how colloid mobilization affects k when salt concentration is increased with column experiments run on the mineral fraction of the soil.
 - Evaluating if biological activity does affect k with column experiments run with an tracer that is made with a bacteria killing agent.
 - Evaluating the redox and pH of the soil to see if metal precipitation is significant.
4. To verify that high levels of NaCl do create additional pore space through extreme mobilization of organic and mineral particles using NMR techniques.
5. To assess the effect of elevated effective stress on k and θ_m by running tracer tests at effective stresses that are higher than the pre-consolidation pressure.
6. To examine the significance of 2^o compression on k and θ_m by measuring volume change in the specimen.
7. To compare the results of compression tests on the permeameter with CRS results by running tests on re-sedimented soil.

Since the results of the three Column Experiments discussed in Section 6.2 show that data from tests on undisturbed and re-sedimented specimens are comparable, and that re-

sedimented soils are good models for undisturbed soils, all future tests should be conducted on re-sedimented wetland soil samples only. This would help to eliminate the variability in compressibility, hydraulic conductivity, and pore water concentration that was found in undisturbed samples.

7.2.2 LONG TERM GOALS

The long term goals of this project are still the same. The first is to understand the chemical transport in the Aberjona wetland soils and to model this effectively. The second is to learn how to translate this knowledge to other wetland soils and environments. Similar tests should be run for soils with higher and lower organic fractions and with increased and decreased levels of humification. This would help in defining which solute/soil interaction is most important when soil characteristics change.

7.3 REFERENCES

- Bialon, J.L. *Characterization of the Physical and Engineering Properties of the Aberjona Wetland Sediment*. M.S. Thesis. Massachusetts Institute of Technology, Cambridge, MA, 1995.
- Ramsay, W. B., *A Modified Triaxial Permeameter for Physical Characterization of Parameters Affecting Contaminant Transport Through Wetland Deposits*. M.S. Thesis, Massachusetts Institute of Technology, Cambridge, MA. 1996.
- Parker, J.C., van Genuchten, M.T. *Determining Transport Parameters from Laboratory and Field Tracer Experiments*. Virginia Agricultural Experiment Station Bulletin 84-3, 1984.
- Toride, N., Leij, F.J., van Genuchten, M.T. *The CXTFIT Code for Estimating Transport Parameters from Laboratory or Field Tracer Experiments, Version 2.0*. U.S. Salinity Laboratory, Agricultural Research Service, U.S. Department of Agriculture, Research Report 137, August 1995.

APPENDIX A: SOIL PROPERTIES

Appendix A: SAND TYPE 90P PROPERTIES

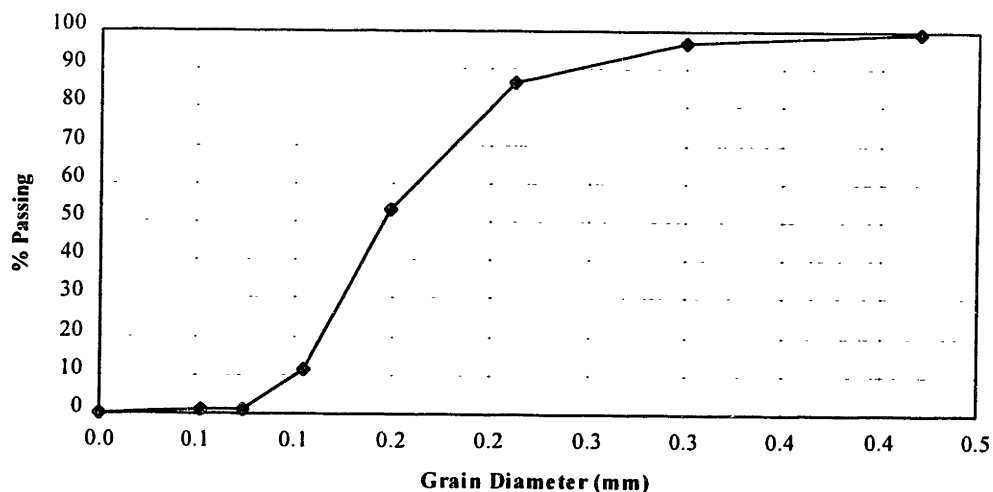
This sand (Type 90P), used in the hydraulic conductivity experiments in this work, was acquired commercially from WHIBCO Inc., NJ by Mr. S. Ratnam for his work. Its particle size distribution and other geotechnical properties were determined by Ratnam at the MIT laboratories (1996). A summary of these properties is given below.

Size Distribution	
Grain Diameter (mm)	% Passing
0.420	99.65
0.300	97.11
0.212	86.38
0.149	52.99
0.106	11.21
0.074	0.88
0.053	0.81
0.000	0.00

D_{10}	0.10 mm
D_{50}	0.16 mm
D_{60}	0.17 mm
Uniformity Coef.	1.6

Other properties	
e_{max}	0.97
e_{min}	0.73
$e_{average}$	0.78 - 0.84
Relative Density (%)	54.2 - 79.2
Specific Gravity	2.66
k_{min} (cm/s)	0.015
k_{max} (cm/s)	0.019
$k_{average}$ (cm/s)	0.016

Grain Size Distribution (Sand Type 90P)



APPENDIX B: LABORATORY PROCEDURES AND DATA SHEETS

Appendix B1: PROCEDURE FOR TESTING SALT-SOIL SORPTION

Materials & Equipment

- 10 1L bottles (with wide mouth)
- 40 3cc syringes
- 40 0.45mm syringe filters
- 40 2ml centrifuge tubes
- 44 50ml centrifuge tubes
- 25ml pipettes
- 44 1ml pipettes
- Pipetter
- 4 Liter shallow container and lid
- evaporating dish
- ~1kg of soil ($w_c=400\%$)
- Distilled water
- Sodium Chloride
- 10 % micro solution
- Conductivity Probe
- Chloride specific probe
- Sodium specific probe (and all necessary solutions, see manual)
- Scales
- Vacuum pump
- Thermometer
- pH meter able to read mV
- Conductance meter

Procedure

Use the data sheets prepared for this experiment.

Sources of Error:

Steps in this procedure where care must be taken in order to minimize error are *starred. It was found that any carelessness in these particular steps was especially likely to cause error that rendered the results of the experiment** or parts of the experiment* useless.

Preparing Soil:

The soil needs to be washed of all native salts and metals.

1. Place ~1kg processed¹ soil in 4 Liter shallow container and fill with distilled water.
2. Stir soil and water well, then let soil settle (2 to 3 days).
3. Siphon off water above soil (use vacuum pump).
4. Repeat steps 1-3.
5. If there is water above soil that was not siphoned off, let it evaporate overnight.

¹ See Processing Procedure

Preparing the bottles:

1. Wash bottles.
 - Soak overnight in 10% Micro solution.
 - Rinse 6 times with tap water, then 6 times with distilled water.
 - Allow to dry completely.
2. Add 750g of distilled water to each bottle.

3. *Add NaCl to each bottle to desired concentration (e.g. 1.5, 1.75, 2.0, 2.25, 2.5 M).
(There should be duplicate bottles for each concentration.)
4. Shake bottles well.
5. Sample each bottle (see below) before adding soil.
6. Measure and record the mass of each bottle.

Sampling:

The bottles are sampled once right before the soil is added, once right after it is added, once an hour afterwards, and finally, after 24 hours.

1. To expedite sampling, make sure all 2ml centrifuge tubes are labeled, and that all syringes and syringe filters are laid out.
2. Shake bottle well
3. **Using 3cc syringe, draw 2cc of fluid from the bottle, making sure that there is no air trapped in the syringe.
4. Screw on the syringe filter and slowly squeeze the sample out into the 2ml centrifuge tube.
5. **Do not let the sample overflow the centrifuge tube as any overflow will leave salt residue on the rim and cap.
6. Make sure the cap on the 2ml centrifuge tube is secure.
7. Measure and record the temperature of the bottle.
8. Repeat steps 2 to 6 for each bottle.
9. Record the time when sampling started and the time when it was finished.

Adding soil:

1. Measure and record the mass of the washed soil.
2. Mix the soil well.
3. Add one spoonful of soil to each bottle.
4. Add one spoonful to an evaporating dish.
5. Repeat steps 3 to 4 until soil runs out. Each bottle and the evaporating dish should have ~100g of soil.
6. Measure and record the mass of the bottles and evaporating dish.
7. Sample the bottles (see above) directly after adding soil.
8. Sample one or two hours after soil is added and then one last time, 24 hours after soil is added.
9. Measure and record the mass of the evaporating dish when the soil has completely air dried.

Preparing samples for measurement:

1. *Add 40ml of distilled water to each of 40 50ml centrifuge tubes using 25ml pipette and pipetter.
2. Label each of these tubes to correspond to the sample labels (e.g. Bottle 2, Sample b)
3. *Add 0.5ml from each sample into the corresponding 50ml centrifuge tube using a 1ml pipette and pipetter.
4. Secure cap and shake well.

Measuring the concentrations of the samples:

1. Prepare 50, 100, 150 and 200 ppm NaCl standards.
2. Calibrate the conductivity probe using these standards at the beginning, during, and after measuring samples.
3. Measure and record the conductivity of the samples using the probe and a conductance meter, making sure to rinse the probe with distilled water and then dry it in between each measurement.
4. Prepare Chloride specific probe according to manual (Orion 96B-11). Use a pH meter set to read mV instead of the conductance meter with this probe.
5. Repeat steps 2 to 3 for the Chloride specific probe.
6. Prepare Sodium specific probe according to manual (Orion 86B-11). Use a pH meter set to read mV instead of the conductance meter with this probe.
7. Add Orion Sodium ISA to all the samples (including standards).
8. Repeat steps 2 to 3 for the Sodium specific probe. **IMPORTANT.** Rinse with special ISA solution (see manual). Distilled water alone will damage this probe, and samples without ISA added will also damage the probe.

Data Analysis:

Analyze data using spreadsheet template.

Example Calculation for K_s and R are below.

Summary of Porcedure:

Wash soil.

Wash bottles.

Add NaCl solution to the bottles. making sure to have duplicate bottles for each concentration.

Sample each of the bottles.

Mass each bottle

Add soil.

Reserve a portion of the soil in an evaporating dish (to determine water content).

Mass each bottle and the evaporating dish (before and after the soil dries).

Sample each of the bottles at three different times after adding soil.

Dilute samples (0.5ml sample into 40ml of distilled water).

Measure the Conductivity, the Chloride activity and the Sodium activity with the appropriate probes.

Analyze the data.

Sample Calculation of Freundlich Isotherms to find K_d and R:

(Directly from Roy et al., 1991)

The distribution ratio, K_d is defined as:

$$K_d = dS/dC \text{ (mol/kg)/mol/L} \quad (1)$$

where S and C are the concentration of sorbent in the solid phase and the equilibrium concentration of sorbent in solution, respectively.

The Freundlich Equation defines an empirical relationship between S and C :

$$S = x/m = K_f C^{1/n} \quad (2)$$

where x is the concentration of solute adsorbed, m is the mass of the adsorbent, and K_f and $1/n$ are constants. By taking the logarithms of both sides of equation 2, K_f and $1/n$ can be solved for using a linear regression:

$$\log(x/m) = 1/n \log C + \log K_f \quad (3)$$

When $1/n$ equals 1, in the case of a Linear Isotherm, the proportion of sorbent in the solid phase is the same no matter what the ambient concentration of sorbent in solution. At low concentrations of sorbent in solution, most sorbents behave in this linear fashion (Scharzenbach, et al. 1993).

The retardation factor, R , can be defined as the ratio of the velocity of the sorbent to that of the water and is given by:

$$R = 1 + \rho_b(K_d)/\theta$$

Where ρ_b is the dry bulk density of the soil, K_d equals K_f , and θ is the volumetric water content of the soil.

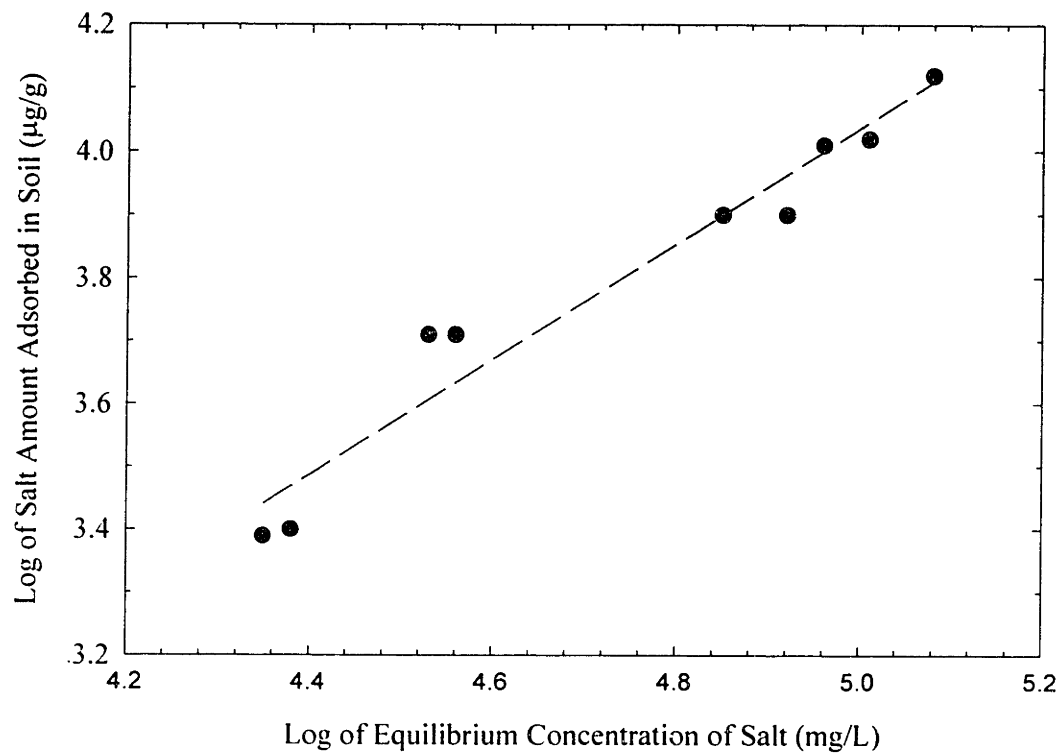
Below is a portion of a spreadsheet used to calculate K_f and R for a fine grained soil:

NaCl mw	58.4428	g/mol				
Initial C (M)	Equil. C (M)	Adst wt (g)	Total water (mL)	Amt. Adsorb. ($\mu\text{g/g}$)	Log Amt. Ad. $\log(\mu\text{g/g})$	Log Equil C $\log(\text{mg/L})$
0.0480	0.0433	9.48	823.40	23863.72	4.38	3.40
0.0461	0.0416	9.57	824.07	22528.90	4.35	3.39
0.0949	0.0879	9.25	821.58	36028.71	4.56	3.71
0.0942	0.0875	9.56	824.02	33803.35	4.53	3.71
0.1510	0.1344	9.56	824.02	83603.83	4.92	3.90
0.1489	0.1349	9.51	823.63	71134.72	4.85	3.90
0.1951	0.1771	9.46	823.20	91927.90	4.96	4.01
0.2001	0.1803	9.26	821.68	102375.55	5.01	4.02
0.2500	0.2266	9.44	823.10	119094.19	5.08	4.12
0.2500	0.2261	9.54	823.86	120377.57	5.08	4.12

Intercept =	0.7887	= $\log K_f$
X Variable =	1.0405	= $1/n$
R^2 =	0.9537	

K_f =	6.15
ρ =	0.33
θ =	4.75
R =	1.43

Figure B1: Example Freundlich Isotherm Construction and Regression
(Soil-Salt Sorption Experiment)



PS Experiment No.: _____
 Process Batch Nos.: _____

SALT-SOIL SORPTION DATA SHEET

Date: _____

Bottle #	[NaCl] (M)	g NaCl to add to 750mls	Mass of Bottle	Mass of Bottle + Water	Mass of Bottle, Water, Salt - Sample	Mass of Bottle + Soil	Mass of Soil
1							
2							
3							
4							
5							
6							
7							
8							
9							
10							

	Sampling 1	Sampling 2	Sampling 3	Sampling 4
Date:				
Time started:				
Time ended:				

Mass of Soil + Container: _____
 Mass of Container: _____
 Mass of Soil: _____
 Mass of Soil / 11: _____
 Mass of Soil + Cont. (after sampling): _____
 Mass of dry Soil + Container: _____
 Water Content W_w/W_{soil} : _____

Bottle #	Temperature
1	
2	
3	
4	
5	
6	
7	
8	
9	
10	

Appendix B2: WETLAND SOIL PROCESSING PROCEDURE AND DATA

Date: _____
 Procedure #: _____
 Maximum Pore Size: _____
 (Setting on meat grinder)

Procedure

Label and tare 4 containers
 Remove roughly 1kg of wet soil from stock
 Take two samples for water content
 Assuming water content from previous process,
 add necessary water to bring batch to 400% water content

Use: $W_{\text{solid}} = W_{\text{total}} / (W_c + 1)$

$$W_{\text{to add}} = 4/W_{\text{solid}} - (W_{\text{total}} - W_{\text{solid}})$$

Mix soil well, and pass through meat grinder
 Take two samples for water content

<i>Water contents</i>	Unprocessed		Processed	
Container Name				
Container Mass				
Mass of container + wet soil				
Mass of container + dry soil				
Water content				

For soil

Mass of container: _____
 Mass of container + unprocessed soil: _____
 Mass of water to be added: _____
 Mass of container + processed soil: _____

Appendix B3: WETLAND DEPOSIT RE-SEDIMENTING PROCEDURE

Materials and Equipment

- Oedometer, with long collar and extended stand pipes
- Triaxial cell with piston and piston end caps (known mass)
- Displacement transducer
- Brass top cap (known mass)
- Various weights
- Container for soil
- Spoon
- Scale
- Sonicator

Procedure

Use Data Table for Batching to record data

1. Prepare soil according to Processing Procedure
2. Sonicate filter stones and paper for 0.5 hours
3. Grease batching ring
4. Mass batching ring and record
5. Measure diameter and height of ring, record
6. Assemble oedometer with saturated filter stone and paper at the base
7. Spoon soil into ring, tamping spoon to clear large air bubbles
8. Once ring is full, place filter paper, then filter stone on the soil
9. Use left over soil to make water content measurements
10. When the soil has settled enough for the filter stone to enter the ring (usually 1 hour), place brass top cap on soil, making sure it is level.
11. Fill stand pipes with distilled water
12. Leave the batch until the top of the top cap is flush with the edge of the oedometer ring (usually overnight), making sure that it is level.
13. Place the oedometer in a triaxial cell frame, centering the triaxial piston over the top cap
14. Screw the base and top of the triaxial cell to insure that the piston is vertical
15. Zero displacement transducer
16. Set timer and a data acquisition file, then add first mass
17. Repeat previous step every two days with additional mass at a load increment ratio of 1
18. Two days after the last mass has been added, remove triaxial cell and disassemble oedometer
19. Measure the distance from the top of the batching ring to the top of the batch, record
20. Mass the batching ring with the soil
21. Extrude the soil carefully into a storage ring
22. Seal the ring with wax and then plastic wrap
23. Store in a dark and humid room

Batch No.: _____
 Process No.: _____

WETLAND DEPOSIT RE-SEDIMENTING DATA SHEET

Tested By: _____

Batching Station: _____
 Mass of piston and ends: _____
 DCDT CF: _____
 Data Acq Channels monitored: _____

DATE	TIME	INC. No.	MASS ADDED	DATA AQ. FILE	DCDT READING	Vin	COMMENTS
		1					
		2	~1 kg				
		3	~2.25 kg				
		4	~4 kg				
		5	~7.25 kg				

Which batching ring is it? _____
 Height = _____ = _____
 Diameter = _____ = _____

How much does the batch weigh at the end?
 Mass of Tare: _____
 Mass of Tare and Soil: _____
 Mass of Soil: _____

How tall is it?
 Depth of recess: _____ = _____
 Filter stone thickness: _____ = _____
 Filter paper thickness: _____ = _____

Sample Height = Batching ring Height - Recess-Filter Stone and Paper thickness: _____
 What is its density? _____

Some useful info:

	Station 1	Station 2
Top Cap	0.566	0.577
Filter Stone&Paper	0.09646	0.0966
Piston&ends	0.301	0.32
Increment #		
1	0.923 (2)	0.994
2	2.256	2.256
3	3.98	3.979 (2)
4	7.062 (2)	7.23 (2)

DCDT CF (cm/V/V)	2.171732	2.444179
------------------	----------	----------

Appendix B4: PROCEDURE FOR SPECIFIC GRAVITY EXPERIMENT

Equipment & Materials

- Pycnometer with cap
- Digital scale
- Knife
- Spatula
- Laminar flow tube (close-ended tube with a slit on one side)
- Wash bottle
- Digital thermometer
- Cooler
- Paper towels
- 1cc syringe
- 3cc syringe
- Rubber stopper with tubing attached (see Figure B4.1)
- Vacuum pump
- Ultrasonic cleaner
- Metal support with base and clamps
- Side-arm flask
- At most 2 pyrex flasks or bottles to withstand vacuum
- Soil
- Kerosene

Procedure

The Specific Gravity Experiment:

1. Mass labeled pycnometer and matching lid on digital scale and record.
2. Classify peat sample (as processed, batched, ground, etc.) and describe.
3. If necessary, cut the sample with knife.
4. Place the cut peat into the massed pycnometer.
5. Mass pycnometer, lid, and peat and record.
6. Calculate mass of the peat (see Equation 1).
7. Fill the pycnometer with kerosene up to 1/3 full.
8. In order to de-air the peat slurry, place the rubber stopper with attachments into the side arm-flask, and plug into the pycnometer; all extensions should be plugged into a closed vessel (See Figure B.1).
9. Clamp pycnometer in place such that it is at least half-way submerged into the ultrasonic cleaner.
10. Using a rubber hose, connect the arm-side flask to the vacuum pump system (See Figure B.2).
11. Turn on two black valves immediately to the left of the pump.
12. Turn on the switch of motor "M" (make sure there are no air bubbles in connected tank).
13. Turn valve 3 on.
14. Turn valve 1 or 2 on (depending on where the side-arm flask is connected), the vacuum should reach about 28 psi.
15. Turn the ultrasonic cleaner on.
16. De-air the sample for about an hour.
17. Stop the vacuum, remove the sample from the tank of the ultrasonic cleaner, and disassemble vacuum setup.

18. Add kerosene to the pycnometer using the laminar flow tube and the wash bottle. Make sure that the peat slurry is not disturbed, and fill pycnometer almost to the rim.
19. Carefully place the lid on top of the pycnometer at an angle, propping it on the rim so that it leaves the bottle half-open.
20. Place the pycnometer, wash bottle filled with kerosene, and digital thermometer in a covered cooler, and leave it to equilibrate to room temperature (at least 12 hours).
21. Bring the cooler to the digital scale, and remove the pycnometer, the kerosene-filled wash bottle, and the digital thermometer. *Make sure to handle the pycnometer by its rim only.*
22. Next, start sliding the lid into the pycnometer, carefully, so as not to introduce any air bubbles under the lid, and using a 3 cc syringe to extract the displaced kerosene. *Kerosene should not overflow and wet the outside of the pycnometer walls.*
23. With the lid precisely in place, use a 1 cc syringe and paper towels to completely remove any kerosene in the area around and above the lid.
24. Mass the pycnometer, and record the reading as "Mass of pycnometer + kerosene + peat," together with date and time at which the measurement was taken.
25. Next, open the pycnometer and, using digital thermometer, measure the temperature inside it.
26. If there are several pycnometers, repeat steps 22 through 25 for each of them. *However, as readings from one pycnometer are being taken, the rest of samples should stay in covered cooler.*
27. When done with taking measurements for all pycnometers, carefully, using the wash bottle, add kerosene almost to the rim.
28. Repeat steps 19 through 27 two more times, leaving the cooler overnight in places with lower temperature than the day before.

Calibrating the Pycnometer:

The pycnometer must be calibrated before the specific gravity calculations can be made. To do this, fill the bottle with kerosene only and then perform steps 19 to 28. Then, plot the mass of the pycnometer and kerosene vs. Temperature. A linear regression of this line can be used in calculating the mass of the pycnometer and kerosene at any Temperature.

Calculations

1. Mass of peat:

$$M_{\text{peat}} = M_{\text{pycnometer+peat}} - M_{\text{pycnometer}} \quad (1)$$

2. Specific gravity:

$$G_s = (M_p * \gamma_{k(T)}) / [\gamma_{w(T)} * (M_2 + M_p - M_1)] \quad (2)$$

where,

M_p = mass of peat

M_1 = mass of pycnometer + kerosene + soil (taken in step 24)

M_2 = mass of pycnometer + kerosene specific to pycnometer (from the pycnometer calibration)

For pycnometer SG-4 $M_2 = -0.1766(T) + 376.13$

 M-6 $M_2 = -0.1905(T) + 386.40$

 M-8 $M_2 = -0.1861(T) + 392.83$

$\gamma_{w(T)}$ = unit weight of water values (from CRC Handbook of Chemistry and Physics, 74th edition)

$\gamma_{k(T)}$ = unit weight of kerosene found during calibration to equal to $-0.0007(T) + 0.8236$

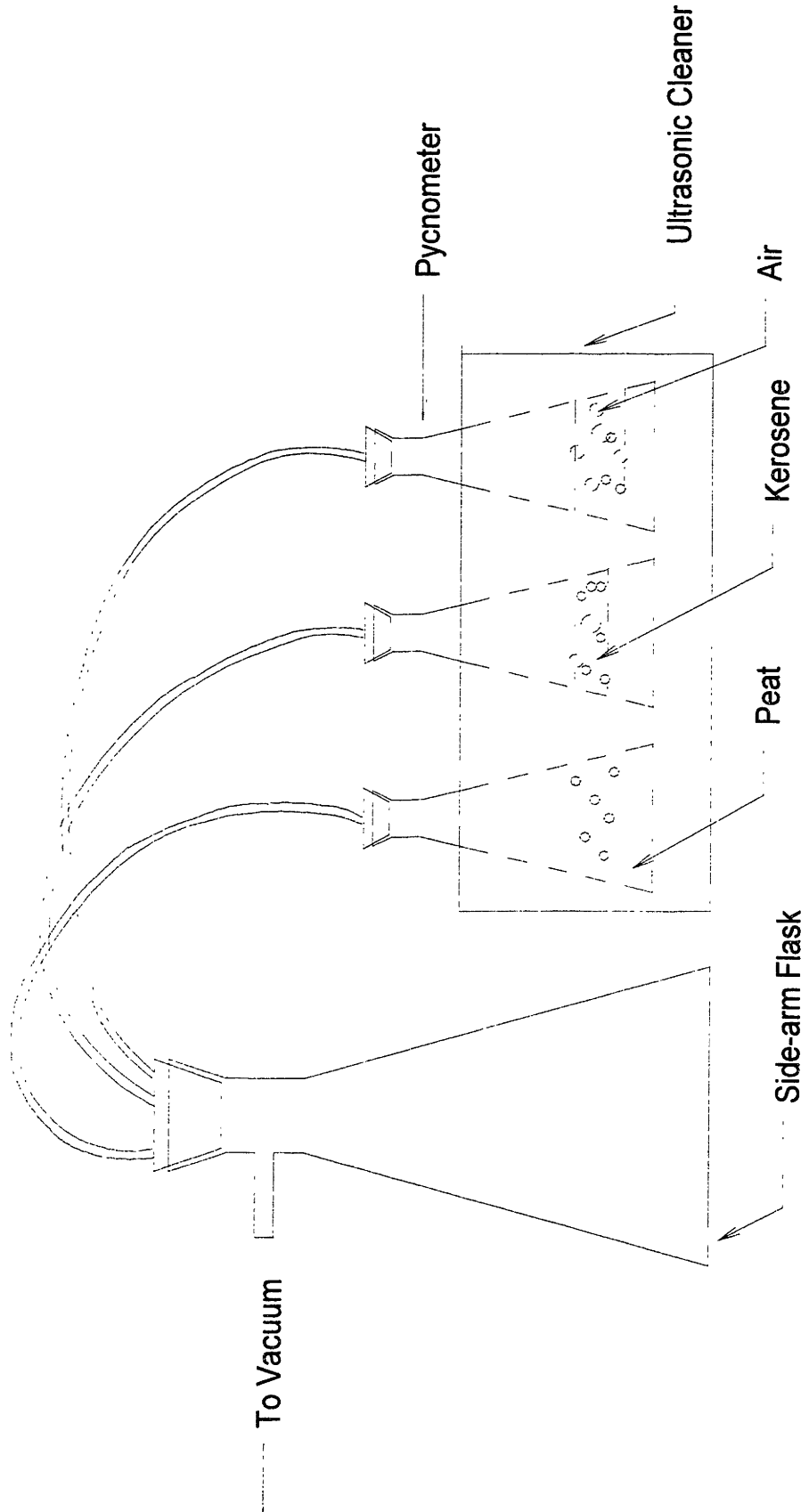


Figure B4.1

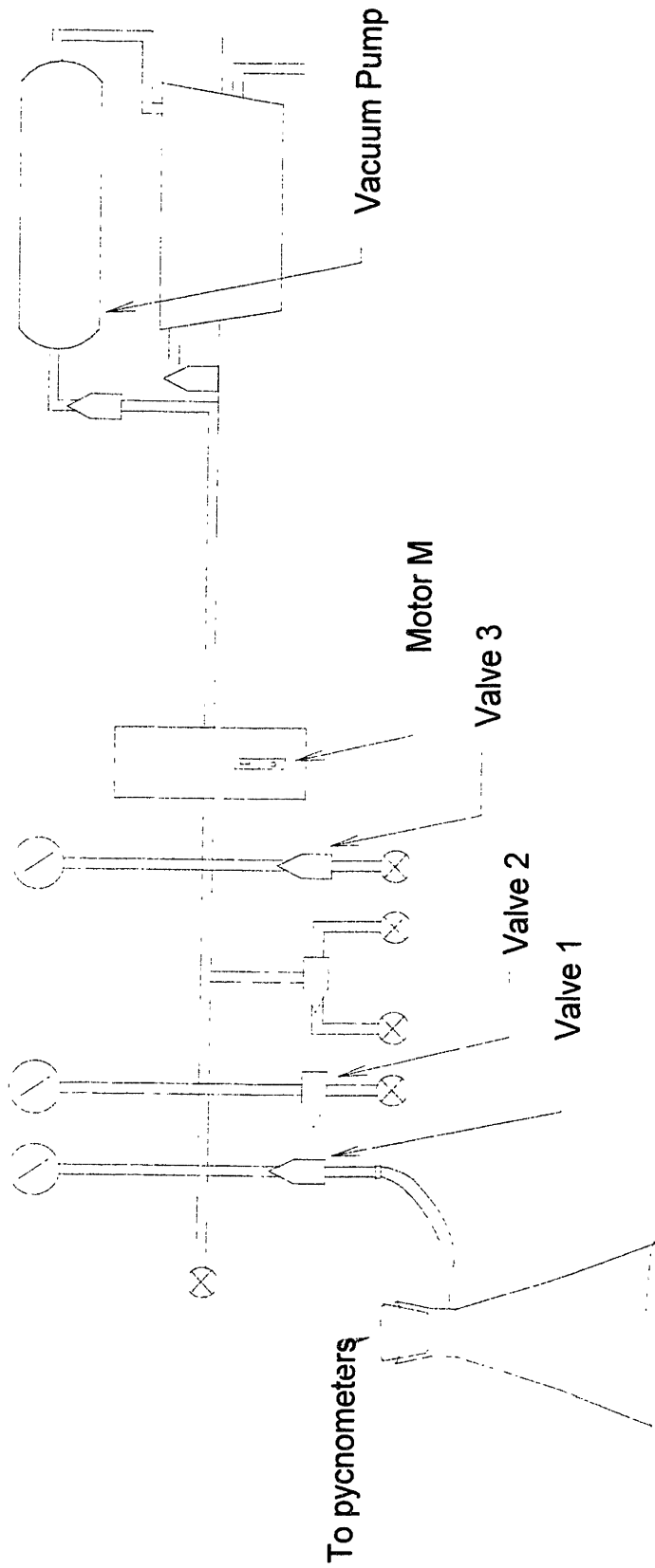


Figure B4.2

SPECIFIC GRAVITY DATA SHEET

Sample Number: _____ Date: _____
 Soil Description: _____ Tested by: _____

Pycnometer Number: _____
 Mass of Pycnometer: _____
 Mass of Pycnometer + Peat: _____
 Mass of Peat: _____

Reading No.	1	2	3
Date			
Time			
Mass of Bottle + Kersoene + Soil			
Temperature			
Mass of Bottle + Kerosene (calibrated)			
Specific Gravity of Kerosene			
Specific Gravity of Peat			

Comments:

Appendix B5: PROCEDURE AND DATA SHEET FOR ASH CONTENT TEST

Procedure: (Follow ASTM standard D 2974-87)

1. Allow peat to air dry completely.
2. Dry in 60 °C oven.
3. Dry in 105 °C oven.
4. Set temperature on kiln to 440 °C.
(This may take some time.
Make sure the kiln has reached an equilibrium Temperature
- give it at least an hour).
5. Mass dry, clean crucibles.
(As the crucibles can't be marked, keep a track of their relative positions)
6. Mass the crucibles with peat.
7. Place the peat in the kiln for at least 24 hours.
8. Before massing, allow crucibles to cool in a dessicator.
9. Return samples to kiln for at least an hour.
10. Cool and remass. If mass is not constant, repeat step 7.
11. Repeat steps 7 to 10 at 750 °C
12. Turn off kiln.

Materials: (per test)

Crucibles
Scale
60-110 °C oven
High Temperature Kiln

Data Table:

Sample Name (Process or Batch Number)				
Tare Number				
Tare Mass				
Tare Mass + Air Dried Peat				
Tare Mass + 110oC Oven Dried Peat				
Tare Mass + 60oC Oven Dried Peat				
Crucible Position (See grid below)				
Crucible Mass				
Crucible Mass + Oven Dried Peat				
Crucible Mass + 440oC Kiln Dried Peat				
Crucible Mass + 750oC Kiln Dried Peat				

Plan view of kiln

A	B
C	D

Appendix B6:
PROCEDURE AND DATA SHEET FOR SIZE DISTRIBUTION TESTS

Procedure:

1. Mass sieves, then stack in descending order of size with one pan at the bottom. Keep second pan in reserve.
2. Mix peat well.
3. Mass tares, subsample peat for water content measurement, Mass tares and peat, place tares in 60oC oven. ReMass when dry.
4. Mass peat container.
5. Spoon 150 to 200 g of peat into top sieve.
6. ReMass peat container to determine exact Mass of peat sampled.
7. Using Wash bottle wash peat throughtop sieve with distilled water
8. Once the top sieve is washed of all particles finer, place it on the second pan to continue draining.
9. Repeat steps 7-8 for each of the sieves, placing the top sieve in the first stack under the top sieve in the second, draining stack.
10. Let the sieves air dry in two stacks (untill they stop dripping).
11. Place the sieves in the 60°C oven.
12. Mass them when dry.
13. Place the sieves in a 110°C oven, and repeat step 12.

Materials: (per test)

Sieves # 4, 10, 20, 60, 100	Spatula/Spoon	Distilled Water
Hydrated peat (Wc = 400%)	Tares	Wash bottle
2 Pans	Scale	60-110 °C oven

Data Tables:

Water Content:

Container No.		
Mass of Container		
Mass of Cont. + wet Soil		
Mass of Cont. + dry Soil		
Mass of Water		
Mass of dry Soil		
WATER CONTENT		
Average Water Content		

Mass of Container and Peat:

Before Sampling: _____
 After Sampling: _____
 Mass of Peat Sampled: _____

Sieve Mass:

Sieve#	Mass	Mass + Wet Peat	Mass + 60° Oven Dried Peat	Mass + 110° Oven Dried Peat
4				
10				
20				
60				
100				
Pan 1				
Pan 2				

Appendix B7: PROCEDURE FOR RUNNING CONSTANT RATE OF STRAIN TEST ON PEAT (WISSA DEVICE)

Use data sheet that corresponds to this experiment.

Trimming the sample (<1 hour)

Batched samples are easy to trim since they are the exact diameter of the CRS ring - only two cuts are required.

1. Grease the inside of the CRS testing ring.
2. Mass the ring and measure its height and diameter using calipers.
3. Measure the height of the recess tool platform using a depth micrometer.
4. Measure the thickness of the filter paper that goes on top of the sample.
5. Push part of the sample out of the batching or storage ring using a solid cylinder with the same diameter as the sample.
6. Slide the sample into the greased CRS ring until it's flush with the top.
7. Leave a small gap between the CRS and batching rings so that some peat is showing in between.
8. Using a sharp textile cutting blade (it is about a foot long), slice firmly through the peat, keeping the blade up against the bottom edge of the CRS ring.
9. Turn the rings 45 degrees, clean off the blade and take another slice.
10. Repeat this until the cut is complete.
11. Great care must be taken not to let the sample slip in the CRS ring as you are cutting.
12. Fit the recess tool against the fresh cut face of the sample and push the peat sample out at the other end.
13. Cut the excess peat with the textile knife, setting the knife at 45° angle plane of the sample.
14. Mass the sample with the ring.
15. Mass the trimmings, let them air dry completely, then reMass them. Calculate the water content of the sample.
16. The CRS ring has a groove running along its outer diameter on one side. This is the bottom of the ring. The sample should be flush with the bottom edge of the CRS ring. There is a space between the top of the sample and the top edge of the CRS ring. This space is as high as the recess tool platform

Setting up the sample (30 min)

1. Sonicate the filter stone and paper for half an hour.
2. Grease and place the two large o-rings at the base of the CRS cell.
3. With a 'puddle' of water on the porous ceramic base, take the pore pressure transducer ZERO (~ -3.2 mV).
4. Grease and place the 6.4 cm o-ring around the middle of the CRS ring.
5. Carefully remove the water from the 'puddle' on the base, being careful not to dry the porous ceramic.
6. Place the sample in the center of the cell base, directly on top of the porous ceramic center.

7. Place the large brass ring around the CRS ring and push down. The o-ring around the CRS ring will be pushed to the bottom to fit into the groove.
8. Screw in the three Allan screws tightly to secure the brass ring.
9. Place the filter paper and then the filter stone gently, on top of the sample.
10. Using vacuum, make sure to suck up the piston and its diaphragm of the cell cover into place.
11. Secure the DCDT around the very bottom of the piston so as to prevent the piston from sliding down when the cell cover is in the vertical.
12. Place the cell cover so that the placement bolts fit into the cell base.
13. Screw in the cell bolts tightly.
14. Screw threaded rod into the load cell.
15. Seat the piston (i.e. loosen the DCDT clamp and let the piston sit on top of the sample. Make sure to refasten the DCDT).
16. Take the DCDT ZERO (~ -2.8 V).
17. Place the small metal piece that transfers the load from the piston to the threaded rod screwed into the load cell on the piston.
18. Move the platform so that the metal piece is touching the threaded rod. Use the 'fine' knob on the platform crank.
19. Take the load cell ZERO (~ -48.6 mV).
20. Make sure the air jack on top of the loading frame is open.
21. Fill up the cell with distilled water.
22. Close the cell vent.
23. Measure the cell pressure transducer Zero, by closing the line in the manifold that leads to the cell pressure pots and by opening one of the lines in the manifold to the atmosphere. Line up the phreatic surface in this line with the center of the cell. This gives you the cell pressure transducer ZERO (~ -0.5 mV).
24. Close this line off, then open the line that goes into the cell. Make sure water is flowing before attaching it into the base of the cell.
25. Re-open the line that links the pressure pots to the cell.

Pressuring up the Cell (30 min)

1. Using the Calibration Factors and the zeros for both the cell and pore pressure transducers, calculate the milli-voltage that corresponds to a 0.5 ksc increment.
2. The cell pressure is increased by turning the crank to the mercury pots to the right of the setup in the clockwise direction. Before starting, make sure that the pots are filled halfway with mercury.
3. Increase the cell pressure in 0.5 ksc increments making sure that the pore pressure increases by 0.5 ksc increments also. The pore pressure response is usually immediate.
4. Take the cell pressure to 4 ksc.
5. It was found that any DCDT corrections for either the cell or the ---- are unnecessary for peat.

Loading (4-5 hours)

1. Make sure the motor gears are set to the correct strain rate (355 min/10 mm)
2. Set up a data acquisition file with a timed delay.

3. Release the clutch.
4. Move the motor switch to the forward position.
5. Check to see that the load cell is picking up load and that the pore pressure is increasing. The load will increase slowly at first, increasing at faster rate with time.
6. Take load to 4 to 8 ksc (usually 4 to 5 hours).

Maintaining a Constant Load (overnight)

1. Close the valve at the top of the air tank above the load frame.
2. Open the air line at the 2-way Whitney valve at the side of the CRS cabinet.
3. Turn motor off (the following 2 steps must be done as soon after this one as possible).
4. Disengage the clutch.
5. Begin increasing the air pressure while lowering the cell platform (use a socket wrench on the fine knob). Maintain the load within 0.5 mV.
6. Once the air jack has taken up all the load, keep lowering the cell platform until there is a visible gap between the load cell block and the load frame arm.
7. Let the pore water pressure dissipate over night.
8. The data acquisition interval can be increased for this portion of the test.

Unloading

1. Change the gears for a slower strain rate (2852.2 min/10 mm).
2. Reverse the steps above:
 - a. Move the cell platform up until the load cell block and the load frame arm touch.
 - b. Keep moving cell platform up while decreasing the air pressure, maintaining the load within 0.5 mV.
 - c. Release the clutch.
 - d. Move the motor switch to the backward position.
 - e. Close 2-way Whitney air valve.
 - f. Close the valve at the top of the air tank above the load frame.
3. Check to see that the load is decreasing. The load will decrease quickly at first, decreasing at slower rate with time. The unloading rate should be slow enough to maintain the pore pressure close to zero, but it might go below zero.
4. Take load to 0 (usually 4 to 5 hours).

Disassembling the equipment

1. Stop the motor.
2. Disengage the clutch.
3. Decrease the cell pressure by lowering the Mercury pots. Do it in 0.5 ksc increments, making sure that the pore pressure matches the cell pressure in absolute value.
4. Drain the cell.
5. Disassemble cell in reverse order of assembly.
6. Remove sample and extrude it from ring.
7. Mass sample for final water content measurement.
8. Scrub base, remove all o-rings and clean all soil thoroughly from base.
9. Leave reservoir of water on porous ceramic base.

Processing and Analyzing the Data:

1. Use the GWbasic program written by Dr. J. T. Germaine to process the raw data file. A copy of this program is included below.
2. Plot the following 3 graphs once the data is processed:
 - a. Strain vs. Effective Stress
 - b. Void Ratio vs. Hydraulic Conductivity
 - c. Effective Stress vs. Total Work
3. Find the compression ratio, CR, and the re-compression ratio, RR, by taking the slopes of the virgin compression line and the re-compression line (graph a), respectively.
4. Find the Hydraulic Conductivity Index, C_k , by taking the slope of the line in graph b.
5. Use the Strain Energy method to find the Pre-consolidation Pressure, σ_p . Draw a line tangent to the initial points in graph c and a line tangent to the subsequent points. The pressure corresponding to the intersection of these two lines is the pre-consolidation pressure.

CRS DATA SHEET

Test No.: _____
 Batch No.: _____, Process No.: _____
 Sample No.: _____

Date Started: _____
 Date Ended: _____
 Tested by: _____

SAMPLE DIMENSIONS:

Height of Sample ring: _____, _____, _____ = _____
 Height of recess tool platform: _____, _____, _____ = _____
 Total Height of Sample: _____

Diameter of Sample ring: _____, _____, _____ = _____
 Area of Sample (A_s): _____

Total Volume of Sample: _____

SAMPLE Mass:

Mass of ring w/ grease: _____
 Mass of ring w/ grease & SAMPLE: _____
 Mass of SAMPLE: _____

WATER CONTENTS:

	Trimmings	Trimmings		Hockey Puck
Container No.				
Mass of Container				
Mass of Cont. + wet Soil				
Mass of Cont. + dry Soil				
Mass of Water				
Mass of dry Soil				
WATER CONTENT				
Average Water Content				

HEIGHT OF SOLIDS:

Specific Gravity (G_s): _____
 $V_{solids} = M_{solids}/G_s$: _____ $M_{solids} = M_{sample}/(w_c + 1)$
 $H_{solids} = V_{solids}/A_s$: _____

DATA ACQUISITION FILE INFO:

Name: _____
 Increment Length-
 Loading: _____
 Constant Load: _____
 Unloading: _____
 Number of Readings: _____ (Should not exceed 500)

ADDITIONAL COMMENTS (CHRONOLOGY, ETC.)

TRANSDUCER INFORMATION:

	Channel No.	CF	CF units	Zero @ Start	Zero @ Finish	Norm. Zero(V/V _{in})
Cell Pressure	5	-707.824	ksc/(V/V)			
Pore Pressure	6	-700.075	ksc/(V/V)			
DCDT	7	2.548751	cm/(V/V)			
Vertical Load	8	26987.236	kg/(V/V)			
V _{in}	9	5.506	-			

CELL PRESSURE UP SEQUENCE:

Time of pressure up:

σ_c (ksc)	Typical Pore P. (mV)	Typical Cell P. (mV)
0	-3.1	-0.4
0.25	-5.07	-2.37
0.5	-7.03	-4.33
0.75	-9.00	-6.30
1	-10.96	-8.26
1.5	-14.90	-12.20
2	-18.83	-16.13
2.5	-22.76	-20.06
3	-26.69	-23.99
4	-34.56	-31.86

Pore and Cell Pressure values vary depending on the Zero. Pore pressure goes down -4.01mV for every 0.5 ksc. and Cell Pressure goes down -3.93mV for every 0.5 ksc.

SOME IMPORTANT READINGS:

	Channel No.	End Pressure Up	End of Loading	End of 2° Comp.	End of Unloading
Date					
Time					
Cell Pressure	5				
Pore Pressure	6				
DCDT	7				
Vertical Load	8				
V _{in}	9				

ADDITIONAL READINGS FOR THE ANXIOUS TESTER:

	Channel No.					
Cell Pressure	5					
Pore Pressure	6					
DCDT	7					
Vertical Load	8					
V _{in}	9					

NOTES:

Appendix B8: COLUMN EXPERIMENT PROCEDURE AND DATA SHEET

TEST #:

PAGE 1

DATE:

Setup

- Fill all lines with appropriate fluid (don't forget line between pedestal and top cap and pH reference).
- Grease o-rings and membranes and put on stretchers.
- Sonicate filter stones and paper (30 min).
- Trim sample.

Height of sample = Height of CRS ring = _____
 Diameter of sample = Diameter of cylinder = _____
 Weight of sample = _____

Water Contents:

	Top and Bottom		Edges	
Name of (C)ontainer				
Weight of C				
Weight of C & <i>wet</i> peat				
Weight of C & <i>dry</i> peat				
Water content:				

Average: _____

- Take pedestal transducer zero (with puddle of water on pedestal).
Zero = _____

- Unscrew top cap from influent line.
- Place membrane protectors on pedestal and top cap.
- Place stone, paper, sample on pedestal.
- Release 1st condom from stretcher, around sample, secure with o-rings at top and bottom.
- Release 2nd condom from stretcher, around sample, secure with o-rings at top and bottom.
- Re-attach top cap is to influent line.
- Screw on cell tightly to pedestal.
- Fill cell with distilled water.
- Take cell transducer zero when cell fluid is half way up sample.
Zero = _____

TEST #:

PAGE 2

DATE:

Back Pressure Saturation

- Close cell valve .
- Close top cap valve.
- Increase pressure in cell pot and FW pot to 0.5 ksc.
- Open Cell valve and Top cap valve at the same time.
- Link pedestal line to Top cap line and open Pedestal PT to pedestal
- Increase pressure in cell pot and FW pot by 0.5 ksc increments, making sure the cell pressure is between 0 and 0.1 ksc higher than the pore pressure.

Follow these guidelines:

Cell PT CF = -701.822 ksc/V/V

Ped PT CF = -701.741 ksc/V/V

V in = _____ V

Cell P increment = _____ V

(for 0.5 ksc increment:

PP increment = _____ V

Dmv = 0.5*Vin/CF)

σ_t (ksc)	σ_t (mv)	u (mv)
0		
0.5		
1		
1.5		
2		
2.5		
3		
3.5		
4		

(zeros from previous page)

- Pore Pressures should equilibrate immediately, otherwise, wait until they do before increasing pressures.

- Check B-value:

Close drainage lines (Top Cap and Pedestal)

Increase cell pressure by 0.25 ksc:

Increment = Cell Increment/2 = _____

Total voltage = _____

Record PP value = _____

dPP value (mV) = _____

B value = dPP value/0.25ksc in mV = _____

(Should = 1)

- Open Top Cap line.

- Calculate FW and SW transducer zeros

Vin = _____ V

FW @ 4ksc = _____ mV

CF = -701.7594

Zero = _____ mV

SW @ 4ksc = _____ mV

CF = -703.5676

Zero = _____ mV

Zero = V @ 4ksc - 4ksc(Vin)/CF

APPENDIX C: COMPUTER CODE

Appendix C1: CONSTANT RATE OF STRAIN DATA REDUCTION PROGRAM

```

10 '*****
15 ' Rev 1.05 programmed by jtg 8/01/97: apparatus compr. option for new
    device
20 ' Rev 1.04 programmed by jtg 3/10/97: apparatus compr. equation update
30 ' Rev 1.03 programmed by DFC 1/28/96: apparatus compr. equation
40 ' Rev 1.02 programmed by JTG 9/02/94: make output compatable with 123
50 ' Rev 1.02 programmed by MPW 2/15/94: dU/T.Str and Total Work
60 ' Rev 1.01 programmed by JVS 1/13/94: regression analysis for Cv and k
70 '                                     revised k equation
80 ' Rev 1.0 programmed by JTG rev date 6/27/90
90 '*****
100 ' v(i,j) is data reading array;i=1 time;=2 disp;=3 vert sts
110 '      =4 pore pressure;=5 cell pressure ;=6 input voltage
120 ' r(i,j) is results file
130 'REM $DYNAMIC: V, R
135 REV$="CRS-1.05"
140 DIM V(7, 500), R(6, 500), V.L(5, 30), A.D(5, 30), H$(30), ZERO(6),
    CF(6), ES(500), A.DEFL(500), AC(4,2)
150 FOR I = 1 TO 30: H$(I) = "": NEXT I
160 FOR I = 1 TO 7: P(I) = 1: NEXT I
170 CLS : PRINT
180 PRINT "      **** This Program is part of the ****"
190 PRINT "      *                MIT/WCC                *"
200 PRINT "      *                GEOTECHNICAL                *"
210 PRINT "      *                DATA ACQUISITION                *"
220 PRINT "      *                SYSTEM                *"
230 PRINT "      *****"
240 PRINT " This is the CRS TEST REDUCTION PROGRAM rev ";REV$
250 PRINT "      (last revised in June 1997)": PRINT
260 PRINT "Please select from the following options"
270 PRINT "      1...Create NEW Reduction File"
280 PRINT "      2...Input Reduction data from disc"
290 PRINT "      3...Edit Reduction File in Memory"
300 PRINT "      4...Store Reduction File"
310 PRINT "      5...Compute and Store Results"
320 PRINT "      6...Print Headings, Data and Results (*)"
330 PRINT "      7...Print Headings and Results (*)"
340 PRINT "      8...Print Headings (*)"
350 PRINT "      9...Read Program Notes                (* = not completed)"
360 PRINT "      10...End Program"
370 PRINT : INPUT "enter option:", X
380 ON X GOTO 1450, 2970, 940, 2800, 3120, 170, 170, 170, 410, 400, 370
390 GOTO 170
400 END
410 REM
420 REM program notes section
430 REM
440 CLS : PRINT : PRINT
450 PRINT "-This program computes STRESS,STRAIN,K ETC."
460 PRINT "-Apparatus deflection last performed August 1997"

```

```

461 PRINT "      -Data are corrected for cell pressure and axial force"
470 PRINT "-Data are smoothed for computation of Cv and Kv using selected
      strain range"
480 PRINT "      -This moving average does not adjust for load reversals"
490 PRINT "          therefore results should be ignored for half the
      strain"
500 PRINT "          window prior to reaching the hold stress point or"
501 PRINT "          load reversal points."
502 PRINT "-The format of the stored reduction file created by Revision
      1.05"
503 PRINT "          is not compatible with previous revisions. "
510 PRINT ""
520 INPUT "press 'Enter' to continue", ANS$
530 GOTO 170
540 REM
550 REM this routine is to be used to input data from a data acq file
560 REM
570 OPEN "I", #1, IFIL$(K)
580 INPUT #1, X1$, X2$, NCH, X3$, X4$, X1, X2, X5$
590 FOR I = 1 TO NCH + 1
600 INPUT #1, HED$(P(I))
610 NEXT I
620 FOR I = 1 TO NCH + 1
630 INPUT #1, UTS$(P(I))
640 NEXT I
650 FOR I = 1 TO NCH + 1
660 INPUT #1, DUM(P(I))
670 NEXT I
680 FOR I = 1 TO NCH + 1
690 INPUT #1, REF(P(I))
700 NEXT I
710 FOR I = 1 TO NCH + 1
720 INPUT #1, DUM(P(I))
730 NEXT I
740 INPUT #1, X$, X$
750 FOR I = 2 TO NCH + 1
760 INPUT #1, DUM(P(I))
770 NEXT I
780 FOR I = 1 TO NCH + 1
790 INPUT #1, RUTS$(P(I))
800 NEXT I
810 ON ERROR GOTO 880
820 I = 0
830 I = I + 1
840 FOR J = 1 TO NCH + 1
850 INPUT #1, V(J, I)
860 NEXT J
870 GOTO 830
880 RESUME 890
890 ON ERROR GOTO 0
900 CLOSE #1
910 NR = I - 1
920 PRINT "Data file "; IFIL$(K); " contains "; NR; " readings"
930 GOTO 3390

```

```

940 REM
950 REM this section creates and edits the reduction file
960 REM
970 CLS : EDT$ = "on"
980 PRINT " *** REDUCTION DATA ***"
990 PRINT ""
1000 PRINT " 1. TEST NAME : "; TESTN$
1010 PRINT " 2. DATE      : "; DR$
1020 PRINT " 3. YOUR NAME : "; OPR$
1030 PRINT " 4. INITIAL SPECIMEN HEIGHT (cm) : "; H.INIT
1040 PRINT "    HEIGHT OF SOLIDS      (cm) : "; HS
1060 PRINT " 5. SPECIMEN AREA (sqr cm)      : "; AREA
1070 PRINT " 6. APPATATUS INFORMATION "
1074 PRINT "     Device name: "; DEVICE$
1075 PRINT "     Seating Load (kgs): "; SLOAD
1080 PRINT
1090 PRINT " 7. VERTICAL HEIGHT TRANSDUCER, Z:"
1100 PRINT "     ZERO(volts/volt): "; ZERO(2)
1110 PRINT "     CF (cm/(v/v)): "; CF(2)
1120 PRINT " VERT. STRESS TRANSDUCER : "
1130 PRINT "     ZERO(volts/volt): "; ZERO(3)
1140 PRINT "     CF (kg/(v/v)): "; CF(3)
1150 PRINT " PORE PRESSURE "
1160 PRINT "     ZERO(volts/volt): "; ZERO(4)
1170 PRINT "     CF (ksc/(v/v)): "; CF(4)
1180 PRINT " CELL PRESSURE"
1190 PRINT "     ZERO(volts/volt): "; ZERO(5)
1200 PRINT "     CF (ksc/(v/v)): "; CF(5)
1210 INPUT "press 'Enter' for more"; ANS$
1220 CLS
1230 PRINT
1240 PRINT " 8. DATA POSITION IN FILE : "
1250 PRINT "     TIME.....column "; P(1)
1260 PRINT "     DISPLACEMENT...column "; P(2); "...channel "; X(2)
1270 PRINT "     VERTICAL STRESScolumn "; P(3); "...channel "; X(3)
1280 PRINT "     PORE PRESSURE .column "; P(4); "...channel "; X(4)
1290 PRINT "     CELL PRESSURE. column "; P(5); "...channel "; X(5)
1300 PRINT "     VOLTS IN.....column "; P(6); "...channel "; X(6)
1310 PRINT
1320 PRINT ""
1330 PRINT " 9.DAT FILE NAME"
1340 FOR I = 1 TO FILS
1350 PRINT "     "; IFIL$(I)
1360 NEXT I
1370 PRINT
1380 INPUT " *** ARE THERE ANY CORRECTIONS (N or Item Number) "; M$
1390 IF M$ = "N" OR M$ = "n" OR M$ = "" GOTO 170
1400 ITNUM = VAL(M$)
1410 IF ITNUM > 11 THEN 1380
1420 CLS
1430 PRINT "": PRINT ""
1440 ON ITNUM GOTO 1490, 1510, 1530, 1550, 1590, 1610, 1670, 2290, 1960,
    2800, 2970
1450 REM following lines used only to create new reduction file

```

```

1460 CLS : PRINT "Enter the following information"
1470 PRINT "units must be in the kg and cm system"
1480 EDT$ = "off"
1490 INPUT " 1. TEST NAME : "; TESTN$
1500 IF EDT$ = "on" THEN GOTO 970
1510 INPUT " 2. DATE : "; DR$
1520 IF EDT$ = "on" THEN GOTO 970
1530 INPUT " 3. YOUR NAME : "; OPR$
1540 IF EDT$ = "on" THEN GOTO 970
1550 INPUT " 4. INITIAL SPECIMEN HEIGHT (cm) : "; H.INIT
1560 INPUT " HEIGHT OF SOLIDS (cm) : "; HS
1580 IF EDT$ = "on" THEN GOTO 970
1590 INPUT " 5. SPECIMEN AREA (cm^2 ) : "; AREA
1600 IF EDT$ = "on" THEN GOTO 970
1610 PRINT " 6. SELECT THE TEST DEVICE FROM THE FOLLOWING : "
1620 PRINT " 1...Wissa Device"
1621 PRINT " 2...Trautwein Device"
1622 PRINT: INPUT " ";D
1640 IF D = 1 THEN DEVICE$="Wissa" : GOTO 1660
1642 IF D = 2 THEN DEVICE$= "Trautwein" : GOTO 1660
1650 GOTO 1622
1660 PRINT " Enter the seating load (kgs): "
1661 PRINT " This is the load on the specimen when the zero value of
the"
1662 PRINT " vertical height transducer is recorded. It includes the
"
1663 PRINT " load cell force plus the weight of the top cap and
piston"
1664 INPUT " Value = ";SLOAD
1668 IF EDT$ = "on" THEN GOTO 970
1669 CLS
1670 PRINT " 7. VERTICAL HEIGHT TRANSDUCER, Z:"
1680 PRINT " ZERO(volts/volt): "; ZERO(2)
1690 INPUT " value or <enter> to keep current value" ;A$
1700 IF A$="" THEN GOTO 1710 ELSE ZERO(2)=VAL(A$)
1710 PRINT " CF (cm/(v/v)): "; CF(2)
1720 INPUT " value or <enter> to keep current value" ;A$
1730 IF A$="" THEN GOTO 1740 ELSE CF(2)=VAL(A$)
1740 PRINT " VERT. STRESS TRANSDUCER : "
1750 PRINT " ZERO(volts/volt): "; ZERO(3)
1760 INPUT " value or <enter> to keep current value" ;A$
1770 IF A$="" THEN GOTO 1780 ELSE ZERO(3)=VAL(A$)
1780 PRINT " CF (kg/(v/v)): "; CF(3)
1790 INPUT " value or <enter> to keep current value" ;A$
1800 IF A$="" THEN GOTO 1810 ELSE CF(3)=VAL(A$)
1810 PRINT " PORE PRESSURE "
1820 PRINT " ZERO(volts/volt): "; ZERO(4)
1830 INPUT " value or <enter> to keep current value" ;A$
1840 IF A$="" THEN GOTO 1850 ELSE ZERO(4)=VAL(A$)
1850 PRINT " CF (ksc/(v/v)): "; CF(4)
1860 INPUT " value or <enter> to keep current value" ;A$
1870 IF A$="" THEN GOTO 1880 ELSE CF(4)=VAL(A$)
1880 PRINT " CELL PRESSURE"
1890 PRINT " ZERO(volts/volt): "; ZERO(5)

```

```

1900 INPUT " value or <enter> to keep current value" ;A$
1910 IF A$="" THEN GOTO 1920 ELSE ZERO(5)=VAL(A$)
1920 PRINT "          CF (ksc/(v/v)): "; CF(5)
1930 INPUT " value or <enter> to keep current value" ;A$
1940 IF A$="" THEN GOTO 1950 ELSE CF(5)=VAL(A$)
1950 IF EDT$ = "on" THEN GOTO 970
1960 PRINT "          DATA INPUT FILES AND VERTICAL STRESS"
1970 CLS : PRINT
1980 PRINT "          two file input modes are available"
1990 PRINT "          1...enter first file name and program will
          increment"
2000 PRINT "          automatically (format yxx.dat)"
2010 PRINT "          y-name up to 6 characters"
2020 PRINT "          xx-sequence number entered separately"
2030 PRINT "          .dat-extension ,added automatically"
2040 PRINT "          NOTE..end sequence with stress =-1"
2050 PRINT "          2...enter each file separately ,end with 'Enter'"
2060 PRINT : INPUT "Please make selection "; S
2070 PRINT
2080 X = 1
2090 IF S = 1 THEN GOTO 2110
2100 IF S = 2 THEN GOTO 2140 ELSE GOTO 2060
2110 INPUT "enter the file name : "; F$
2120 INPUT "enter the starting sequence number : "; X
2130 EXT$ = ".dat"
2140 ON ERROR GOTO 2250
2150 I = 1
2160 IF X < 10 THEN X$ = "0" + RIGHT$(STR$(X), 1)
2170 IF X > 9 THEN X$ = RIGHT$(STR$(X), 2)
2180 IF S = 1 THEN IFIL$(I) = F$ + X$ + EXT$: GOTO 2210
2190 PRINT "enter the name for file number "; I; " : ";
2200 INPUT IFIL$(I)
2210 OPEN "i", #1, IFIL$(I)
2220 CLOSE #1
2230 I = I + 1: X = X + 1
2240 GOTO 2160
2250 FILS = I - 1
2260 RESUME 2270
2270 ON ERROR GOTO 0
2280 IF EDT$ = "on" THEN GOTO 970
2290 REM
2300 REM this routine is to be used to select sorting sequence
2310 REM programed by jtjg 1/30/89
2320 REM
2330 OPEN "I", #1, IFIL$(1)
2340 INPUT #1, X$, IFIL$, NCH, T$, D$, SC, UC, X$
2350 PRINT X$, IFIL$, NCH, T$, D$, SC, UC, X$
2360 CLS : PRINT "YOU must select the proper channels for each reading"
2370 PRINT "          EVERY file must have the same format"
2380 PRINT "          The following inforamtion is based only on the first file"
2390 PRINT
2400 PRINT "This file was created under the name "; IFIL$
2410 PRINT "at "; T$; "on "; D$; " ";
2420 PRINT "by user number "; UC

```

```

2440 PRINT "using computer code number "; SC
2470 PRINT : PRINT "THE FILE CONTAINS THE FOLOWING CHANNELS"
2480 FOR I = 1 TO NCH + 1
2481 INPUT #1, X$
2482 PRINT X$;
2483 NEXT I
2484 PRINT
2490 FOR I = 1 TO NCH + 1
2491 INPUT #1, X$
2492 PRINT X$;
2493 NEXT I
2500 FOR I = 1 TO 4
2501 INPUT #1, X$
2502 PRINT X$
2503 NEXT I
2505 PRINT
2510 INPUT #1, X$
2511 PRINT X$;
2520 FOR I = 2 TO NCH + 1
2530 INPUT #1, CH(I)
2540 PRINT CH(I);
2550 NEXT I
2560 CLOSE #1: C = 0
2570 'PRINT : INPUT "Hit <Enter> to Continue..."; ZZ$
2580 'CLS
2590 REM
2600 REM the following lines are TEST specific
2610 EN$(1) = "TIME      ": EN$(2) = "VERT DISP": EN$(6) = "VOLTS IN "
2620 EN$(3) = "VERT.STRESS": EN$(4) = "PORE PRESSURE": EN$(5) = "CELL
      PRESSURE"
2630 PRINT : PRINT "Select the channel number for.."
2640 INPUT "The vertical displacement ", X(2)
2650 INPUT "The vertical stress      ", X(3)
2660 INPUT "The Pore Pressure          ", X(4)
2670 INPUT "The Cell Pressure          ", X(5)
2680 INPUT "The input voltage (-1 if not recorded) ", X(6)
2690 REM
2700 REM sort channels by function
2710 P(1) = 1
2720 FOR I = 2 TO NCH + 1
2730 FOR J = 2 TO NCH + 1
2740 IF X(I) = CH(J) THEN P(I) = J: C = C + 1
2750 NEXT J
2760 NEXT I
2770 IF X(6) = -1 THEN P(6) = -1
2780 IF C <> 5 THEN PRINT "YOU HAVE A MISMATCH.. TRY AGAIN": C = 0: GOTO
      2630
2790 IF EDT$ = "on" THEN GOTO 970 ELSE GOTO 170
2800 REM
2810 REM this section stores the reduction data
2820 REM
2830 CLS : PRINT : PRINT
2840 PRINT "This section stores the reduction data on disc"
2850 PRINT "the resulting file can be used for subsequent tests"

```

```

2860 PRINT "or be recalled during batch calculation"
2870 PRINT "note: the extension '.red' will be added to the file name"
2880 INPUT "enter the file name (8 character max) ", RFIL$
2890 RFIL$ = RFIL$ + ".red"
2900 OPEN "o", #1, RFIL$
2910 WRITE #1, REV$, ,RFIL$, DR$, TME$, OPR$, TESTN$, H.INIT, HS, SR, AREA,
    D, SLOAD, ZERO(2), CF(2), ZERO(3), CF(3), ZERO(4), CF(4), ZERO(5),
    CF(5), FILS, P(1), P(2), P(3), P(4), P(5), P(6), X(2), X(3), X(4), X(5),
    X(6)
2920 FOR I = 1 TO FILS
2930 WRITE #1, IFIL$(I)
2940 NEXT I
2950 CLOSE #1
2960 GOTO 170
2970 REM
2980 REM this section retrieves the reduction file from disc
2990 REM
3000 CLS : PRINT "This section retrieves a reduction file from disc"
3010 INPUT RFIL$
3020 RFIL$ = RFIL$ + ".red"
3030 OPEN "i", #1, RFIL$
3040 INPUT #1, REV$, , RFIL$, DR$, TME$, OPR$, TESTN$, H.INIT, HS, SR
3050 INPUT #1, AREA, D, SLOAD, ZERO(2), CF(2), ZERO(3), CF(3), ZERO(4),
    CF(4), ZERO(5), CF(5), FILS, P(1), P(2), P(3), P(4), P(5), P(6), X(2),
    X(3), X(4), X(5), X(6)
3060 FOR I = 1 TO FILS
3070 INPUT #1, IFIL$(I)
3080 NEXT I
3090 CLOSE #1
3091 IF D=1 THEN DEVICE$="Wissa "
3092 IF D=2 THEN DEVICE$="Trautwein"
3110 GOTO 170
3120 REM
3130 REM this routine computes values for consolidation tests
3140 REM
3150 CLS
3160 OPEN "O", #2, TESTN$ + ".res"
3170 RESTORE
3180 NR.MAX = 1
3190 '
3200 '*****COMPUTATIONS SECTION
3210 '
3220 CLS
3230 PRINT "This program uses a moving linear regression analysis in an "
3240 PRINT "attempt to provide representative values of Cv and k without "
3250 PRINT "being hindered by the problems associated with a high "
3260 PRINT "frequency of data acquisition."
3270 PRINT : PRINT
3280 PRINT " ENTER THE STRAIN INCREMENT TO BE USED FOR THE REGRESSION
    ANALYSIS."
3290 PRINT "      Input it as a percentage, i.e. input '1.0' for 1% ."
3300 PRINT "      NOTE: 1.0 is usually a good value. Use a larger value to
    "
3310 PRINT "      'smooth out' your curves."

```

```

3320 INPUT " ENTER THE VALUE YOU CHOOSE "; INC
3330 CLS
3340 LOCATE 10, 15: PRINT "PERFORMING CALCULATIONS"
3350 '
3351     REM compute compressibility
3352 GOSUB 5000     'get apparatus values
3353     REF.APP=AC(1,D)*SLOAD^AC(2,D)
3360 '
3370 FOR K = 1 TO FILS'loop over each file
3380     GOTO 540         'input data into v(1,m)
3390     PRINT "Data retrieval complete for "; IFIL$(K)
3410 '
3420     IF NR < NR.MAX THEN GOTO 3430 ELSE L.NR = NR.MAX: C = 1'all ok
3470     REM compute strains
3480         FOR I = 1 TO NR
3490             M = 2
3500             FOR J = 2 TO 5
3510                 V(P(J), I) = ((V(P(J), I) / V(P(6), I)) - ZERO(J)) *
CF(J)
3520                 NEXT J
3530                 V(P(3), I) = ((V(P(3), I)) - V(P(5), I) * AP(D))+WP(D)
3540                 IF V(P(3), I) <= 0 THEN A.DEFL=REF.APP : GOTO 3565
3560                 A.DEFL = AC(1,D)* (V(P(3), I))^AC(2,D)
3565                 C.DEFL = AC(4,D)* V(P(5), I)
3566                 T.DEFL = REF.APP-A.DEFL-C.DEFL
3580                 V(P(2), I) = (V(P(2), I) + T.DEFL) / H.INIT * 100
3590                 V(P(3), I) = V(P(3), I) / AREA
3600             NEXT I
3610             CLS
3620             CLS : LOCATE 10, 15: PRINT "STORING RESULTS AND PERFORMING
REGRESSION ANALYSIS"
3630             REM data storage
3640             WRITE #2, DATE$, TIME$, OPR$
3650             WRITE #2, IFIL$(K)
3660             WRITE #2, "      "
3670             WRITE #2, TESTN$, " CONSOLIDATION TEST RESULTS
Page"
3680             WRITE #2, "      "
3690             WRITE #2, " Time ", " Strain ", "Vert.Sts", " Pore ", "
Cell ", "Eff.Sts.", "Void Rto", " dU ", " K ", " Cv ",
"dU/TVSts", "Tot.Work"
3700             WRITE #2, " (sec) ", " (% ) ", " (ksc) ", " (ksc) ", "
(ksc) ", " (ksc) ", "      ", " (ksc) ", " (cm/sec)", " (cm2/sec)", "
", "      "
3710             WRITE #2, "      "
3720             TOTWORK = 0
3730 '
3740 '***** DETERMINE BEGINNING AND ENDING POINTS FOR FULL WINDOW PROCEDURE
3750 '
3760 FOR I = 1 TO NR
3770     IF (ABS(V(P(2), I) - V(P(2), 1))) > INC / 2 THEN BEGIN = I: GOTO
3790
3780 NEXT I
3790 FOR I = NR TO 1 STEP -1

```



```

3800     IF (ABS(V(P(2), NR) - V(P(2), I))) > INC / 2 THEN ND = I: GOTO 3820
3810 NEXT I
3820 '
3830         FOR I = 1 TO NR
3840             FLAG = 0
3850             E = (H.INIT - V(P(2), I) * H.INIT / 100 - HS) / HS
3860             U = (V(P(4), I) - V(P(5), I))
3870             ES(I) = V(P(3), I) - ((2 / 3) * U)
3880 '
3890             IF I = 1 THEN DT = 0: DK = 0: CV = 0: GOTO 4010
3900             IF I < BEGIN OR I > ND THEN FLAG = 1
3910 '
3920             GOSUB 4070
3930             LOCATE 12, 20: PRINT "Finished line "; I; " out of
"; NR; "      "
3940 '
3950             UTVS = U / V(P(3), I)
3960             AVESTS = (ES(I) + ES(I - 1)) / 2
3970             DELSTRN = LOG((1 - (V(P(2), I - 1) / 100)) / (1 -
(V(P(2), I) / 100)))
3980             INCWORK = AVESTS * DELSTRN
3990             TOTWORK = TOTWORK + INCWORK
4000 '
4010             WRITE #2, V(1, I), V(P(2), I), V(P(3), I), V(P(4),
I), V(P(5), I), ES(I), E, U, DK, CV, UTVS, TOTWORK
4020             NEXT I
4030 NEXT K
4040 CLOSE #2
4050 GOTO 170
4060 '
4070 '***** REGRESSION SUBROUTINE
4080 '
4090 '
4100 '***** DETERMINE LOCAL REGRESSION WINDOW LIMITS
4110 '
4120 '*****LIMITS FOR MAIN BODY OF DATA
4130 IF FLAG = 1 THEN GOTO 4270
4140         STRT = 0: FINISH = 0
4150         FOR BEFORE = I TO 1 STEP -1
4160             IF ABS(V(P(2), BEFORE) - V(P(2), I)) > INC / 2 THEN STRT =
BEFORE + 1: GOTO 4180
4170         NEXT BEFORE
4180         FOR AFTER = I TO NR
4190             IF ABS(V(P(2), AFTER) - V(P(2), I)) > INC / 2 THEN FINISH =
AFTER - 1: GOTO 4210
4200         NEXT AFTER
4210 '
4220             IF STRT = 0 THEN STRT = 1
4230             IF FINISH = NR + 1 THEN FINISH = NR
4240             IF STRT = FINISH THEN FINISH = STRT + 1
4250 GOTO 4410
4260 '
4270 '*****LIMITS FOR BEGINNING AND END OF DATA SET

```

```

4280          STRT = 0: FINISH = 0 'HALFINC=increment at start or end of
      data set
4290          IF I < BEGIN THEN STRT = 1 : HALFINC = ABS(V(P(2), I) -
      V(P(2), 1)) ELSE GOTO 4340
4300          FOR AFTER = I TO NR
4310              IF ABS(V(P(2), AFTER) - V(P(2), I)) > HALFINC THEN
      FINISH = AFTER - 1: GOTO 4380
4320          NEXT AFTER
4330 '
4340          IF I > ND THEN FINISH = NR: HALFINC = ABS(V(P(2), NR) -
      V(P(2), I))
4350          FOR BEFORE = I TO 1 STEP -1
4360              IF ABS(V(P(2), BEFORE) - V(P(2), I)) > HALFINC THEN
      STRT = I + 1: GOTO 4380
4370          NEXT BEFORE
4380          IF STRT = FINISH OR STRT >= NR AND I > ND THEN STRT =
      FINISH - 1
4390          IF STRT = FINISH AND I < BEGIN THEN FINISH = STRT + 1
4400 '
4410          WR = 0
4420 ' ***** DETERMINE LOCAL REGRESSION EQUATION
4430 '          WR=number of window readings
4440 '          TI=time, EI=strain, VSI=vertical stress, SUM before a
      variable indicates sum over window range
4450 '
4460 '          TI2=TI^2
4470          WR = FINISH - STRT + 1
4480          AVGTI = 0: AVGEI = 0: SUMEI = 0: SUMTI = 0: SUMTIEI = 0:
      SUMTI2 = 0
4490          AVGVSI = 0: SUMVSI = 0: SUMTIVSI = 0
4500 '
4510          FOR CALC = STRT TO FINISH
4520              SUMTI = SUMTI + V(P(1), CALC)
4530              SUMEI = SUMEI + V(P(2), CALC)
4540              SUMVSI = SUMVSI + V(P(3), CALC)
4550              SUMTI2 = SUMTI2 + (V(P(1), CALC) * V(P(1), CALC))
4560              SUMTIEI = SUMTIEI + (V(P(1), CALC) * V(P(2), CALC))
4570              SUMTIVSI = SUMTIVSI + (V(P(1), CALC) * V(P(3), CALC))
4580          NEXT CALC
4590          AVGTI = SUMTI / WR
4600          AVGEI = SUMEI / WR
4610          AVGVSI = SUMVSI / WR
4620 '
4630 '
4640          BETA = 0
4650 ' *****SLOPE OF REGRESSION LINE GIVEN BT BETA
4660 '          BETAE=strain rate, BETAVS=stress rate
4670          IF (SUMTI2 - WR * (AVGTI) ^ 2) = 0 THEN BETAE = 1E+15:
      BETAVS = 1E+15: GOTO 4700
4680          BETAE = (SUMTIEI - WR * AVGTI * AVGEI) / (SUMTI2 - WR *
      (AVGTI) ^ 2)
4690          BETAVS = (SUMTIVSI - WR * AVGTI * AVGVSI) / (SUMTI2 - WR *
      (AVGTI) ^ 2)
4700 '

```

```

4710 '
4720      DT = V(P(1), I) - V(P(1), I - 1)
4730      DK = BETAE * (((1 - V(P(2), I) / 100) * H.INIT) ^ 2) / U /
      200000!
4740      CV = BETAVS * (((1 - V(P(2), I) / 100) * H.INIT) ^ 2) / 2 /
      U
4750 RETURN
4760 END
4999 '
5000 REM apparatus compressibility parameters
5010 '
5015 'FOR THE WISSA DEVICE
5020      AC(1,1)=.0031      ' /
5030      AC(2,1)=.2351      ' / COMPRESSIBILITY
5040      AC(3,1)= 0!      ' / FACTORS
5050      AC(4,1)= .001      ' /
5060      AP(1)=3.37      ' PISTON AREA
5070      WP(1)=2.04      ' PISTON WEIGHT
5115 'FOR THE TRAUTWEIN DEVICE
5120      AC(1,2)=.0408
5130      AC(2,2)=.0578
5140      AC(3,2)=0
5150      AC(4,2)= .0002
5160      AP(2)=3.56
5170      WP(2)=1!
5180 RETURN

```


Appendix C2: CXTFIT MODEL COMPUTER PROGRAM

```

C CXTFIT2.FOR 3/3/95
C
C *****
C *
C *   CXTFIT VERSION 2.0
C *
C *   LAST MODIFIED:           JAN 2 1994
C *
C *   NON-LINEAR LEAST-SQUARES ANALYSIS OF C(X,T) DATA
C *   FOR ONE-DIMENSIONAL DETERMINISTIC OR STOCHASTIC
C *   EQUILIBRIUM AND NONEQUILIBRIUM CONVECTIVE DISPERSIVE
C *   EQUATION
C *
C *
C *   NOBUO TORIDE
C *   U.S. SALINITY LABORATORY
C *   4500 GLENWOOD DRIVE
C *   RIVERSIDE CA 92501
C *
C *   TEL.909/369-4853
C *   FAX.909/369-4818
C *   E-MAIL NOBUO@UCRAC1.UCR.EDU
C *****
C
C   IMPLICIT REAL*8 (A-H, O-Z)
C   MAXOB; No. OF OBSERVATION.
C   PARAMETER (MAXOB=405)
C
C   DIMENSION T (MAXOB), Z (MAXOB), C (MAXOB), C1 (MAXOB), C2 (MAXOB),
C   & VAR1 (MAXOB), VAR2 (MAXOB), F (MAXOB), R (MAXOB), DELZ (MAXOB, 15), B (30),
C   & E (15), TH (30), P (15), PHI (15), Q (15), LSORT (MAXOB), TB (30), A (15, 15),
C   & D (15, 15), BMAX (15), BMIN (15), DERL (30)
C   CHARACTER BI (15) *6
C   CHARACTER FILEIN*15, FILEOUT*15
C   COMMON MODC, MM, AA, BB, DA, CX, PEC, BETA, BETR, OMEGA, RE, DMU1, DMU2,
C   & MODE, MCON, TT, ZZ, STOPPER, LEVEL, ICHEB
C   COMMON/MODAT/INDEX (15), INVERSE, NREDU, NVAR, ZL, MIT, MDEG, MASS,
C   & DUMTP (10), DUMGAL (10), MNEQ, ISKIP, PHIM, PHIIM
C   COMMON/STOCH/MODD, MODK, MODS, MSTOCH, CORR, M CORR, MSD, SDLNK,
C   & V, SDLNV, VMAX, VMIN, DIS, AVEY, SDLNY, YMAX, YMIN, ALPHA, SDLND
C   & , DK, RHOTH, MD56, MK34, MAL8
C   COMMON/BOUN/MODB, NPULSE, TPULSE (10), PULSE (10), MASSST
C   COMMON/INITI/MODI, NINI, CINI (10), ZINI (10)
C   COMMON/PROD/MODP, NPRO1, NPRO2, GAMMA1 (10), ZPRO1 (10), GAMMA2 (10),
C   & ZPRO2 (10)
C
C   ----- OPEN I/O FILES -----
C   KP=7
C   WRITE (*, 1000)
C   READ (*, 1001) FILEIN
C   IF (FILEIN.EQ. ' ') FILEIN='CXTFIT2.IN'
C   OPEN (5, FILE = FILEIN, STATUS = 'OLD')
C
C   WRITE (*, 1002)
C   READ (*, 1001) FILEOUT
C   IF (FILEOUT.EQ. ' ') FILEOUT='CXTFIT2.OUT'
C   OPEN (KP, FILE = FILEOUT, STATUS = 'UNKNOWN')

```

```

C
C ----- READ NUMBER OF CASES -----
READ(5,*) NC
DO 155 NCASE=1,NC
  ISKIP=0
C ----- READ, CHECK, AND WRITE DATA -----
C
  CALL DATAIN(NOB, NU1, NU2, T, Z, C, B, BMAX, BMIN, BI, ILMT,
  & KP, MAXOB, MPRINT, DT, DZ, NT, NZ, FILEIN, INRHO)
C
  CALL CONST1(MAXTRY, STOPCR, GA, GD, DERL, STSQ, MM, ICHEB, NU1, NU2, OMMAX,
  & MIT)
C
C ----- DIRECT PROBLEM -----
IF(INVERSE.LE.0) THEN
  CALL DIRECT(T, Z, B, C1, C2, VAR1, VAR2, MPRINT, DT, DZ, NT, NZ, MAXOB, KP)
  GOTO 154
END IF
C
C ----- PREPARE INVERSE PROBLEM -----
C
C
C WRITE EXPERIMENTAL DATA
C   WRITE(KP,1009)
C   DO 14 I=1,NOB
C     WRITE(KP,1010) I,C(I),Z(I),T(I)
C 14 CONTINUE
C
C
C TWO-SITE MODEL; BETA SHOULD BE LARGER THAN 1/R
C   (MODE=2, MNEQ=2, R=B(NVAR+3),BETA=B(NVAR+4))
C
C TWO-REGION MODEL; PHIM/R < BETA < (PHIM+R-1)/R
C   (MODE=2, MNEQ=3, R=B(NVAR+3),BETA=B(NVAR+4))
C
C BMINTS; INITIAL VALUE OF A MINIMUM CONSTRAINT FOR BETA
C BMAXTS; INITIAL VALUE OF A MINIMUM CONSTRAINT FOR BETA
  IF(MNEQ.LE.1.OR.ILMT.NE.1) GOTO 210
  BMINTS=BMIN(4)
  BMAXTS=BMAX(4)
C
C BETA SHOULD BE LESS THAN 1 FOR THE NONEQUILIBRIUM CDE
C OMEGA SHOULD BE LESS THAN OMMAX
C   (DEFAULT VALUE IS 100, SEE CONST1)
210  NB=0
     NR=0
     NOMEQ=0
     IF(MODE.EQ.2) THEN
       NB=INDEX(1)+INDEX(2)+INDEX(3)+INDEX(4)
       NR=INDEX(1)+INDEX(2)+INDEX(3)
       NOMEQ=INDEX(1)+INDEX(2)+INDEX(3)+INDEX(4)+INDEX(5)
     END IF
     IF(MODE.LE.2) GOTO 212
C
C   IF(MOD(MODE,2).EQ.1) GOTO 212
     NOMEQ=INDEX(1)+INDEX(2)+INDEX(3)+INDEX(4)
C
C ----- REARRANGE VARIABLE ARRAYS -----
212 NP=0
   DO 20 I=NU1,NU2
     TB(I)=B(I)

```

```

        IF(INDEX(I-NVAR).EQ.0) GO TO 20
        NP=NP+1
        DERL(NP)=DERL(I)
        BI(NP)=BI(I-NVAR)
        B(NP)=B(I)
        TB(NP)=B(I)
        TH(NP)=B(NP)
        IF(ILMT.NE.0) BMIN(NP)=BMIN(I-NVAR)
        IF(ILMT.NE.0) BMAX(NP)=BMAX(I-NVAR)
20    TH(I)=B(I)
C
C    ALL PARAMETERS SHOULD BE POSITIVE (EXCEPT RHO FOR MODE>=3).
C    [MODE=1]>1.D-10 [MODE>=2] > 1.D-7
C    [MODE>=3] RHO < -1.D5, RHO > 1.D5
        DO 22 I=1, NP
        IF(I.EQ.NP.AND.INRHO.EQ.1) THEN
            IF(TH(I).LT.-1.0) TH(I)=-1.D+00
            IF(TH(I).GT.1.0) TH(I)=1.D+00
            IF(DABS(TH(I)).LT.1.D-05) THEN
                IF((TH(I)-1.D-30).GT.0.D+00) THEN
                    TH(I)=1.D-05
                ELSE
                    TH(I)=-1.D-05
                END IF
            END IF
            GOTO 22
        END IF
        IF(MODE.EQ.1.AND.DABS(TH(I)).LT.1.D-10) TH(I)=1.D-10
        IF(MODE.GE.2.AND.DABS(TH(I)).LT.1.D-07) TH(I)=1.D-07
22    CONTINUE
C
C    ----- START INVERSE PROBLEM -----
        NIT=0
        NP2=2*NP
        ISKIP=0
        DO 200 I=1, NOB
        TT=T(I)
        ZZ=Z(I)
        CALL MODEL(TH, TT, ZZ, CXT1, CXT2, DUM1, DUM2)
        ISKIP=1
        F(I)=CXT1
C    TOTAL RESIDANT CONCENTRATIONS FOR THE NONEQUILIBRIUM TRANSPORT
        IF(MODE.EQ.2.AND.(MODC.EQ.4.OR.MODC.EQ.6)) THEN
            F(I)=F(I)+CXT2
        END IF
200    CONTINUE
        IF (MIT.EQ.0) GO TO 140
        SSQ=0.
        DO 32 I=1, NOB
        R(I)=C(I)-F(I)
32    SSQ=SSQ+R(I)*R(I)
        WRITE(KP,1011) (BI(I), I=1, NP)
        WRITE(KP,1012) NIT, SSQ, (B(I), I=1, NP)
        IF(MODE.GE.2) THEN
            WRITE(*,1011) (BI(I), I=1, NP)
            WRITE(*,1012) NIT, SSQ, (B(I), I=1, NP)
        END IF
C
C    ----- BEGIN ITERATION -----FOR NIT=1 GA=GA/GD (=0.001)
        MFINAL=0
34    NIT=NIT+1

```

```

ISIG=1
NTRIAL=0
GA=GA/GD
DO 38 J=1, NP
  IF (J.EQ.NP.AND.INRHO.EQ.1) THEN
    IF (DABS (TH (J) * (1+DERL (J))) .GT.1.0D+00) ISIG=-1
  END IF
  IF (MODE.EQ.2.AND.INDEX (4) .EQ.1) THEN
    IF ((TH (J) * (1+DERL (J))) .GE.1.0D+00) ISIG=-1
  END IF
  TEMP=TH (J)
C
  TH (J) = (1.0+ISIG*DERL (J)) * TH (J)
C
  Q (J) = 0.
C
  ISKIP=0
  DO 201 I=1, NOB
    TT=T (I)
    ZZ=Z (I)
    CALL MODEL (TH, TT, ZZ, CXT1, CXT2, DUM1, DUM2)
    ISKIP=1
    DELZ (I, J) = CXT1
    IF (MODE.EQ.2.AND. (MODC.EQ.4.OR.MODC.EQ.6)) THEN
      DELZ (I, J) = DELZ (I, J) + CXT2
    END IF
201 CONTINUE
  DO 36 I=1, NOB
    DELZ (I, J) = ISIG * (DELZ (I, J) - F (I))
  36 Q (J) = Q (J) + DELZ (I, J) * R (I)
  Q (J) = Q (J) / TH (J) / DERL (J)
C
  ----- Q=XT*R (STEEPEST DESCENT) -----
C
  (DERL (I) INCREMENT FOR PARAMETER I)
C
  38 TH (J) = TEMP
  DO 44 I=1, NP
    DO 42 J=1, I
      SUM=0.
      DO 40 K=1, NOB
        40 SUM=SUM+DELZ (K, I) * DELZ (K, J)
      D (I, J) = SUM / (TH (I) * TH (J)) / DERL (I) / DERL (J)
      42 D (J, I) = D (I, J)
      E (I) = DSQRT (D (I, I))
      44 E (I) = DMAX1 (E (I), 1.D-30)
      50 DO 52 I=1, NP
        DO 52 J=1, NP
          52 A (I, J) = D (I, J) / (E (I) * E (J))
C
  ----- A IS THE SCALED MOMENT MATRIX -----
C
  PHI IS THE SCALED VECOTR
  DO 54 I=1, NP
    P (I) = Q (I) / E (I)
    PHI (I) = P (I)
  54 IF (MFINAL.EQ.0) A (I, I) = A (I, I) + GA
  CALL MATINV (A, NP, P)
  IF (MFINAL.EQ.1) GOTO 97
C
  ----- P/E IS THE CORRECTION VECTOR -----
C
  A = THE INVERSE OF A (COVARIANCE MATRIX)
  STEP=1.0
56 CONTINUE

```



```

C
C TWO-SITE MODEL; BETA SHOULD BE LARGER THAN 1/R
C (MODE=2, MNEQ=2)
C
C TWO-REGION MODEL; PHIM/R < BETA < (PHIM+R-1)/R
C (MODE=2, MNEQ=3)
  IF(MNEQ.GE.2.AND.INDEX(4).EQ.1) THEN
    IF(INDEX(3).EQ.0) THEN
      CR=B(NVAR+3)
    ELSE
      TB(NR)=P(NR)*STEP/E(NR)+TH(NR)
      CR=TB(NR)
    END IF
  IF(ILMT.EQ.0) GOTO 255
  IF(MNEQ.EQ.2) THEN
    BMIN(NB)=1/CR
    IF(BMIN(NB).LT.BMINTS) BMIN(NB)=BMINTS
  ELSE IF(MNEQ.EQ.3) THEN
    BMIN(NB)=PHIM/CR
    IF(BMIN(NB).LT.BMINTS) BMIN(NB)=BMINTS
    BMAX(NB)=(PHIM+CR-1.0)/CR
    IF(BMAX(NB).GT.BMAXTS) BMAX(NB)=BMAXTS
  END IF
END IF
C
255 DO 59 I=1,NP
  TB(I)=P(I)*STEP/E(I)+TH(I)
C STOCHASTIC MODEL RHO CANNOT BE ZERO TO EVALUATE DERIVATIVES
  IF(I.EQ.NP.AND.INRHO.EQ.1) THEN
    IF(DABS(TB(I)).LT.1.D-05) THEN
      IF((TB(I)-1.D-30).GT.0.D+00) THEN

```

```

        TB(I)=1.D-05
    ELSE
        TB(I)=-1.D-05
    END IF
    GOTO 58
END IF
END IF
END IF
IF(ILMT.EQ.0) THEN
C   STOCHASTIC MODEL  -1=<RHO<=1
    IF(I.EQ.NP.AND.INRHO.EQ.1) THEN
        IF(TB(I).LE.-1.0) TB(I)=-1.D+00
        IF(TB(I).GE.1.0) TB(I)=1.D+00
        GOTO 58
    END IF
C   PARAMETERS SHOULD BE POSITIVE
    IF(MODE.EQ.1) THEN
        IF(TB(I).LT.1.D-10) THEN
            TB(I)=1.D-10
            GOTO 58
        ELSE
            GO TO 59
        END IF
    ELSE
        IF(TB(I).LT.1.D-07) THEN
            TB(I)=1.D-07

            GOTO 58
        ELSE
            GO TO 59
        END IF
    END IF
    IF(DABS(BMAX(I)-BMIN(I)).LT.1.D-10) GO TO 59
    IF((TB(I)-BMAX(I)).GT.1.D-20) GO TO 57
    IF((TB(I)-BMIN(I)).GT.1.D-20) GO TO 59
    TB(I)=BMIN(I)
    GO TO 58
57 TB(I)=BMAX(I)
58 P(I)=(TB(I)-TH(I))*E(I)/STEP
59 CONTINUE
C
C   BETA SHOULD BE LESS THAN ONE
    IF(MODE.EQ.2) THEN
        IF(INDEX(4).EQ.1.AND.TB(NB).GT.0.9999) THEN
            TB(NB)=0.9999
            P(NB)=(TB(NB)-TH(NB))*E(NB)/STEP
        END IF
        IF(INDEX(4).EQ.1.AND.TB(NB).LT.0.0001) THEN
            TB(NB)=0.0001
            P(NB)=(TB(NB)-TH(NB))*E(NB)/STEP
        END IF
        IF(ILMT.NE.0) GO TO 60
C
C   IF(MNEQ.GE.2.AND.INDEX(4).EQ.1) THEN
        IF(MNEQ.EQ.2) THEN
            IF(TB(NB).LE.1/CR) THEN
                TB(NB)=1/CR
                P(NB)=(TB(NB)-TH(NB))*E(NB)/STEP
            END IF
        ELSE IF(MNEQ.EQ.3) THEN
            IF(TB(NB).LE.PHIM/CR) THEN

```

```

        TB(NB)=PHIM/CR
        P(NB)=(TB(NB)-TH(NB))*E(NB)/STEP
    ELSE IF(TB(NB).GE.(PHIM+CR-1.0)/CR) THEN
        TB(NB)=(PHIM+CR-1.0)/CR
        P(NB)=(TB(NB)-TH(NB))*E(NB)/STEP
    END IF
    END IF
    END IF
C OMEGA IS LESS THAN OMMAX (=100)
    IF(INDEX(5).EQ.1.AND.TB(NOMEG).GT.OMMAX) THEN
        TB(NOMEG)=OMMAX
        P(NOMEG)=(TB(NOMEG)-TH(NOMEG))*E(NOMEG)/STEP
    END IF
    END IF
    IF(MODE.EQ.4.OR.MODE.EQ.6) THEN
        IF(INDEX(4).EQ.1.AND.TB(NOMEG).GT.1.E04) THEN
            TB(NOMEG)=OMMAX
            P(NOMEG)=(TB(NOMEG)-TH(NOMEG))*E(NOMEG)/STEP
        END IF
    END IF
    IF(MODE.EQ.8.AND.INDEX(4).EQ.1) THEN
        DOMECA=TB(NOMEG)*RHOTH*TB(NVAR+4)*ZL/TB(NVAR+1)
        IF(DOMECA.GT.OMMAX) THEN
            TB(NOMEG)=OMMAX/RHOTH/TB(NVAR+4)/ZL*TB(NVAR+1)
            P(NOMEG)=(TB(NOMEG)-TH(NOMEG))*E(NOMEG)/STEP
        END IF
    END IF
60 DO 62 I=1,NP
    IF(I.EQ.NP.AND.INRHO.EQ.1) GOTO 62
    IF(TH(I)*TB(I))66,66,62
62 CONTINUE
    SUMB=0.0
C
    ISKIP=0
    DO 205 I=1,NOB
        TT=T(I)
        ZZ=Z(I)
        CALL MODEL(TB,TT,ZZ,CXT1,CXT2,DUM1,DUM2)
        ISKIP=1
        F(I)=CXT1
        IF(MODE.EQ.2.AND.(MODC.EQ.4.OR.MODC.EQ.6)) THEN
            F(I)=F(I)+CXT2
        END IF
    205 CONTINUE
C ----- DEVIATION FROM THE STEEPEST DESCENT DIRECTION -----
C     ANGLE BETWEEN PHI AND P (CORRECTION VECTOR)
C     AND PHI (STEEPEST DECENT DIRECTION)
    DO 64 I=1,NOB
        R(I)=C(I)-F(I)
64 SUMB=SUMB+R(I)*R(I)
66 SUM1=0.0
        SUM2=0.0
        SUM3=0.0
        DO 68 I=1,NP
            SUM1=SUM1+P(I)*PHI(I)
            SUM2=SUM2+P(I)*P(I)
68 SUM3=SUM3+PHI(I)*PHI(I)
        ARG=SUM1/DSQRT(DMAX1(SUM2*SUM3,1D-20))
        ARG1=0.0D+00
        IF(NP.GT.1) ARG1=DSQRT(1.-ARG*ARG)
C     (57.29578=180/pi)

```

```

      ANGLE=57.29578*DATAN2(ARG1,ARG)
C
C -----
      DO 72 I=1,NP
          IF(I.EQ.NP.AND.INRHO.EQ.1) GOTO 72
          IF(TH(I)*TB(I))74,74,72
72 CONTINUE
          NTRIAL=NTRIAL+1
C          write(7,*) 'ntrial step ga ',ntrial,step,ga
C          write(7,*) 'ssq new/ssq angle',sumb/ssq,angle
C
C IF THE TRIAL SUCCEED, DECREASE GA.
C FAILURE, IF ANGLE < 30, DECREASE THE SCALE OF THE CORRECTION VECTOR.
C OTHERWISE, INCREASE GA.
          IF(NTRIAL.GT.MAXTRY) GO TO 95
          IF((SUMB/SSQ-1.0).LE.1.D-10.OR.STEP.LT.1.D-20) GOTO 80
74 IF(ANGLE-30.0)76,76,78
C IF
76 STEP=0.5*STEP
      GO TO 56
78 GA=GA*GD
      GO TO 50
C ----- PRINT COEFFICIENTS AFTER EACH ITERATION -----
80 CONTINUE
      DO 82 I=1,NP
82 TH(I)=TB(I)
      WRITE(KP,1012) NIT,SUMB,(TH(I),I=1,NP)
      IF(MODE.GE.2) THEN
          WRITE(*,1012) NIT,SUMB,(TH(I),I=1,NP)
      END IF
C IF CHANGES OF ALL PARAMETE VALUES < STOPCR, STOP THE ITERATION.
      DO 86 I=1,NP
          DUMX=DABS(P(I)*STEP/E(I))/DABS(1.0D-20+TH(I))
C          WRITE(*,*) 'I STOP',I,DUMX
          IF(DUMX-STOPCR) 86,86,94
86 CONTINUE
      GO TO 96
94 SSQ=SUMB
C STSQ=STOP CRITERIA TO EVALUATE THE IMPROVEMENT OF SSQ
          IF(NIT.EQ.1) SSQ3=SSQ
          IF(NIT.EQ.2) SSQ2=SSQ
          IF(NIT.EQ.3) SSQ1=SSQ
          IF(NIT.GE.4) THEN
              DSSQ1=1.0-SSQ/SSQ1
              DSSQ2=1.0-SSQ1/SSQ2
              DSSQ3=1.0-SSQ2/SSQ3
              IF(DSSQ3.LT.0.0) GOTO 91
              IF(DSSQ2.LT.0.0) GOTO 91
              IF(DSSQ1.LT.0.0) GOTO 91
              IF(DSSQ1.LT.STSQ.AND.DSSQ2.LT.STSQ.AND.DSSQ3.LT.STSQ) THEN
                  WRITE(KP,1035) NIT-3,NIT
                  GO TO 96
              END IF
91          SSQ3=SSQ2
              SSQ2=SSQ1
              SSQ1=SSQ
          END IF
          IF(NIT.LT.MIT) GO TO 34
          IF(NIT.EQ.MIT) WRITE(KP,1034) MIT
          GO TO 96
95 WRITE(KP,1038) MAXTRY

```

```

C
C   ----- END OF ITERATION LOOP -----
C   EVALUATE COVARIANCE MATRIX USING THE ESTIMATED PARAMETERS
96 MFINAL=1
   .GOTO 34
C
C   ----- WRITE COVARIANCE MATRIX -----
97 DO 98 I=1,NP
   IF(A(I,I).LT.0.0+00) THEN
       WRITE(KP,1020)
       GOTO 104
   END IF
   E(I)=DSQRT(A(I,I))
98 E(I)=DMAX1(E(I),1.D-30)
   IF(NP.EQ.1) GO TO 104
   WRITE(KP,1013) (BI(I),I=1,NP)
   DO 102 I=1,NP
   DO 100 J=1,I
100 A(J,I)=A(J,I)/(E(I)*E(J))
102 WRITE(KP,1014) BI(I),(A(J,I),J=1,I)
C   ----- COEFFICIENT OF DETERMINATION (r2) -----
104 SUMC=0.0
   DO 105 I=1,NOB
   SUMC=SUMC+C(I)
105 CONTINUE
   SUMC=SUMC/NOB
   SUMC2=0.0
   SUMCF=0.0
   DO 106 I=1,NOB
   SUMC2=SUMC2+(C(I)-SUMC)**2
   SUMCF=SUMCF+(C(I)-F(I))**2
106 CONTINUE
   RSQ=1.0-SUMCF/SUMC2
   WRITE(KP,1041) RSQ
C
C   ----- CALCULATE 95% CONFIDENCE INTERVAL -----
XZ=1./FLOAT(NOB-NP)
SDEV=DSQRT(XZ*SUMB)
TVAR=1.96+XZ*(2.3779+XZ*(2.7135+XZ*(3.187936+2.466666*XZ**2)))
IF(NP.EQ.1)WRITE(KP,1042)
IF(NP.GT.1)WRITE(KP,1015)
DO 108 I=1,NP
SECOEF=E(I)*SDEV
TVALUE=TH(I)/SECOEF
TSEC=TVAR*SECOEF
TMCOE=TH(I)-TSEC
TPCOE=TH(I)+TSEC
IF(NP.EQ.1) WRITE(KP,1043) BI(I),TH(I),SECOEF,TMCOE,TPCOE
IF(NP.GT.1) WRITE(KP,1016) BI(I),TH(I),SECOEF,TVALUE,TMCOE,TPCOE
108 CONTINUE
C
C   ----- COMMENT FOR THE NONEQUILIBRIUM CDE -----
C   FOR BETA = 0.9999
       IF(MODE.EQ.2) THEN
           IF(INDEX(4).EQ.1.AND.ABS(TB(NB)-0.9999).LT.1.E-5) THEN
               WRITE(KP,1045)
           END IF
       END IF
C   FOR OMEGA = OMMAX (=100)
       IF(ILMT.NE.0) GO TO 250
       IF(MODE.EQ.2) THEN

```

```

        IF(INDEX(5).EQ.1.AND.ABS(TB(NOMEG)-OMMAX).LT.
&          OMMAX*1.E-04) THEN
            WRITE(KP,1047)
            END IF
        END IF
    IF(MODE.EQ.4.OR.MODE.EQ.6) THEN
        IF(INDEX(4).EQ.1.AND.(TB(NOMEG)-OMMAX).LT.OMMAX*1.E-04) THEN
            WRITE(KP,1047)
            END IF
        END IF
    IF(MODE.EQ.8.AND.INDEX(4).EQ.1) THEN
        DOMECA=TB(NOMEG)*RHOTH*TB(NVAR+4)*ZL/TB(NVAR+1)
        IF((DOMECA-OMMAX).LT.OMMAX*1.E-04) THEN
            WRITE(KP,1049)
        END IF
    END IF
C  ----- PREPARE FINAL OUTPUT -----
250 LSORT(1)=1
    DO 115 J=2,NOB
        TEMP=R(J)
        K=J-1
        DO 111 L=1,K
            LL=LSORT(L)
            IF(TEMP-R(LL)) 112,112,111
111 CONTINUE
        LSORT(J)=J
        GO TO 115
112 KK=J
113 KK=KK-1
        LSORT(KK+1)=LSORT(KK)
        IF(KK-L) 114,114,113
114 LSORT(L)=J
115 CONTINUE
        WRITE(KP,1017)
        DO 116 I=1,NOB
116 WRITE(KP,1018) I,Z(I),T(I),C(I),F(I),R(I)
C        WRITE(KP,1019)
C        DO 117 I=1,NOB
C            J=LSORT(NOB+1-I)
C 117 WRITE(KP,1018) J,Z(J),T(J),C(J),F(J),R(J)
            GO TO 150
140 WRITE(KP,1030)
            DO 145 I=1,NOB
145 WRITE(KP,1033) I,Z(I),T(I),F(I)
150 CONTINUE
C        WRITE(KP,'(A)') CHAR(12)
154 CONTINUE
C
155 CONTINUE
C
C  ----- END OF PROBLEM -----
1000 FORMAT(' Enter input file name (default = CXTFIT2.IN)')
1001 FORMAT(A15)
1002 FORMAT(' Enter output file name (default = CXTFIT2.OUT)')
1011 FORMAT(//5X,'ITER',5X,'SSQ',3X,5(4X,A6))
1012 FORMAT(4X,I3,1X,E12.4,5(E10.3))
1013 FORMAT(///,5X,'COVARIANCE MATRIX FOR FITTED PARAMETERS'/5X,39(1H=)
&/15X,10(A6,1X))
1014 FORMAT(8X,A6,10(F7.3))
1015 FORMAT(5X,'NON-LINEAR LEAST SQUARES ANALYSIS, FINAL RESULTS'
1/5X,48(1H=)//48X,'95% CONFIDENCE LIMITS'/5X,1X,'NAME',6X,'VALUE',

```

```

25X, 'S.E.COEFF.', 1X, 'T-VALUE', 6X, 'LOWER', 8X, 'UPPER')
1016 FORMAT(5X, A6, E11.4, E12.4, 1X, E9.4, E12.4, E13.4)
1017 FORMAT(//5X, 18(1H-), 'ORDERED BY COMPUTER INPUT', 19(1H-)/40X,
1'CONCENTRATION', 9X, 'RESI-'/'$', 4X, 'NO', 4X, 'DISTANCE', 7X, 'TIME',
28X, 'OBS', 8X, 'FITTED', 7X, 'DUAL')
1018 FORMAT(4X, I3, F12.4, 4F12.4)
1019 FORMAT('$', //5X, 18(1H-), 'ORDERED BY RESIDUAL', 25(1H-)/40X,
1'CONCENTRATION', 9X, 'RESI-'/'$', 'NO', 4X, 'DISTANCE', 7X, 'TIME',
28X, 'OBS', 8X, 'FITTED', 7X, 'DUAL')
1020 FORMAT(///, 5X, 'COVARIANCE MATRIX FOR FITTED PARAMETERS'/5X, 39(1H=)
&/15X, ' OUT OF RANGE !!')
1030 FORMAT(//5X, 6(1H-), 'RESULTS FOR INITIAL COEFFICIENT VALUES', 6(1H-)
1/5X, 'NO', 8X, 'DISTANCE', 9X, 'TIME', 6X, 'CONCENTRATION')
1033 FORMAT(4X, I3, 3(3X, F12.4))
1034 FORMAT(/5X, 'CONVERGENCE CRITERIA NOT MET IN', I4, ' ITERATIONS')
1035 FORMAT(/5X, 'NO FURTHER DECREASE IN SSQ OBTAINED FROM ', I3, ' TO ',
&I3, ' ITERATIONS')
1038 FORMAT(/5X, 'NO FURTHER DECREASE IN SSQ OBTAINED AFTER ', I3, ' TRIAL
1S')
1041 FORMAT(/7X, 'RSQUARE FOR REGRESSION OF OBSERVED VS PREDICTED =',
1F10.8, /, 10X, '(COEFFICIENT OF DETERMINATION)'/)
1042 FORMAT(5X, 'NON-LINEAR LEAST SQUARES ANALYSIS, FINAL RESULTS'
1/5X, 48(1H=)//47X, '95% CONFIDENCE LIMITS'/5X, 'NAME', 8X, 'VALUE',
28X, 'S.E.COEFF.', 8X, 'LOWER', 10X, 'UPPER')
1043 FORMAT(5X, A6, 1X, E13.4, 3X, E13.4, 1X, E13.4, 2X, E13.4)
1045 FORMAT(/7X, 'BETA = 0.9999 THE EQUILIBRIUM CDE SHOULD BE USED ! ')
1047 FORMAT(/7X, 'OMEGA = 100 THE EQUILIBRIUM CDE SHOULD BE USED ! ')
1049 FORMAT(/7X, '<OMEGA> = 100 THE EQUILIBRIUM CDE SHOULD BE USED ! ')
C
C ----- CLOSE FILES -----
CLOSE(5)
STOP
END
C
-----
SUBROUTINE MATINV(A, NP, B)
C
C PURPOSE: PERFORM MATRIX INVERSION FOR PARAMETER ESTIMATION
C
IMPLICIT REAL*8(A-H, O-Z)
DIMENSION A(15, 15), B(15), INDEX(15, 2)
DO 2 J=1, 15
2 INDEX(J, 1)=0
I=0
4 AMAX=-1.0
DO 12 J=1, NP
IF(INDEX(J, 1)) 12, 6, 12
6 DO 10 K=1, NP
IF(INDEX(K, 1)) 10, 8, 10
8 P=DABS(A(J, K))
IF(P.LE.AMAX) GO TO 10
IR=J
IC=K
AMAX=P
10 CONTINUE
12 CONTINUE
IF(AMAX) 30, 30, 14
14 INDEX(IC, 1)=IR
IF(IR.EQ.IC) GO TO 18
DO 16 L=1, NP
P=A(IR, L)
A(IR, L)=A(IC, L)

```

```

16 A(IC,L)=P
   P=B(IR)
   B(IR)=B(IC)
   B(IC)=P
   I=I+1
   INDEX(I,2)=IC
18 P=1./A(IC,IC)
   A(IC,IC)=1.0
   DO 20 L=1,NP
20 A(IC,L)=A(IC,L)*P
   B(IC)=B(IC)*P
   DO 24 K=1,NP
   IF(K.EQ.IC) GO TO 24
   P=A(K,IC)
   A(K,IC)=0.0
   DO 22 L=1,NP
22 A(K,L)=A(K,L)-A(IC,L)*P
   B(K)=B(K)-B(IC)*P
24 CONTINUE
   GO TO 4
26 IC=INDEX(I,2)
   IR=INDEX(IC,1)
   DO 28 K=1,NP
   P=A(K,IR)
   A(K,IR)=A(K,IC)
28 A(K,IC)=P
   I=I-1
30 IF(I) 26,32,26
32 RETURN
   END

```

C

APPENDIX D: OUTSIDE TEST DATA

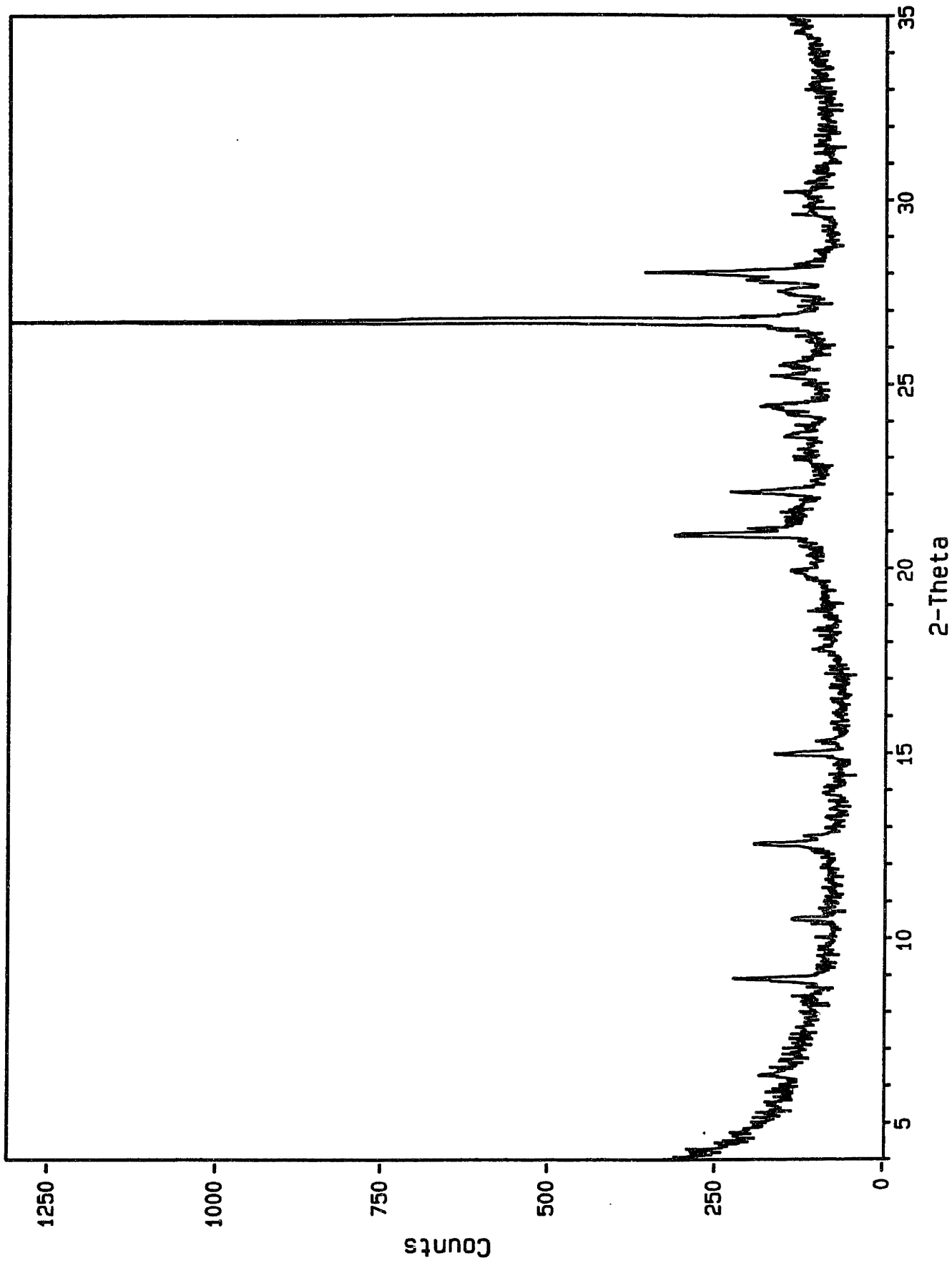
Xral Activation Services Confidential

ELEMENT	AG PPM	AS PPM	AU PPB	BA PPM	BR PPM	CA %	CD PPM	CO PPM	CR PPM	FE %
Detection Limit	2	1	1	100	1	0.5	2	1	1	0.05
S6	<2	1000	150	200	31	<0.5	15	47	2000	8.5
S6 -S8	<2	1000	130	300	28	<0.5	<10	47	2000	8.66
N1	<2	3500	<5	300	35	<0.5	<10	10	91	3.1

ELEMENT	MO PPM	NA PPM	NI PPM	RB PPM	SB PPM	SC PPM	SE PPM	TA PPM	TH PPM	U PPM
Detection Limit	0.5	100	20	20	0.1	0.2	2	0.5	0.5	0.1
S6	1.7	4500	30	30	26	4.4	7	0.8	4.3	14.3
S6 -S8	3.5	4500	40	30	26	4.5	8	0.7	4.6	14.8
N1	<0.5	3000	30	<20	51	2.7	5	<0.5	1.7	43.8

ELEMENT	W PPM	ZN PPM	LA PPM	CE PPM	SM PPM	IR PPB	HG PPM
Detection Limit	1	20	1	1	0.1	10	0.5
S6	<4	2000	61	94	7.2	<10	<0.5
S6 -S8	<4	2000	62	94	7.1	<10	<0.5
N1	<4	950	143	265	24.5	40	<0.5

ID: Y PASSING #3 / MINERALS FROM 4, 11-MAR-99@09:00
File: Z13210.RAW Scan: 4-35/.02/ 30/#1551, Anode: CU



THESIS PROCESSING SLIP

FIXED FIELD: ill. _____ name _____

index _____ biblio _____

► COPIES: Archives Aero Dewey Eng Hum
Lindgren Music Rotch Science

TITLE VARIES: ► _____

NAME VARIES: ► _____

IMPRINT: (COPYRIGHT) _____

► COLLATION: 361p

► ADD: DEGREE: _____ ► DEPT.: _____

SUPERVISORS: _____

NOTES:

cat'r: _____ date: _____

► DEPT: C.E.

page: J173

► YEAR: 1999 ► DEGREE: Sc.D.

► NAME: AREF, Lana A.